Phenotypic Investigation of Biofilm Formation and Transcriptional Analysis of Invasive Growth of Commercial Wine *Saccharomyces cerevisiae*

Ee Lin Tek

A thesis submitted for the degree of
Doctor of Philosophy

THE UNIVERSITY
of ADELAIDE

Department of Wine and Food Science
Faculty of Science
The University of Adelaide
September 2017

Contents

Nomenclature

Term	Description
Biofilm	Surface-attached multicellular communities with an extracellular matrix including any related biofilm-forming ability tests such as mat formation and plastic adhesion
Mat	Thin layer of yeast biomass on low-density agar that resembles a film
Filamentous growth	Interchangeable with pseudohyphal growth, a form of growth as a colony that has a filamentous shape, usually contains chains of elongated cells
Filamentous mat	A mat that has a filamentous periphery
Invasive growth	A form of growth that penetrates agar
'Hub and spokes' mat	A flat mat that has raised cables radiating from the hub

NB Filamentous growth and invasive growth are not ploidy-specific unless specified.

Abstract

This study investigated the morphological properties, environmental effects on and gene expression of biofilms, more specifically referred to as mats, formed by laboratory and commercial wine strains of *Saccharomyces cerevisiae*. Two morphological assays were conducted: mat formation and plastic adhesion. Mat features varied between strains and included various architectures, cellular morphologies, and incidence of invasive growth. One commercial strain, L2056, formed mats where a sector produced a distinctive mat morphology, which was retained when subcultured. In considering the role of biofilms in winery conditions, mat formation assays were also performed with grape pulp and adhesion to the soft plastic of common winery hoses. All strains grew invasively on all agar media and appeared to conduct fermentation on the grape-pulp mat assay. Some strains also had the ability to adhere to winery hose plastic. When only limited nitrogen was available, both laboratory and commercial wine strains formed mats with a subpopulation of cells that switched to filamentous and invasive growth. Such invasive growth was influenced by nitrogen concentration, the presence of a neighbouring mat, and by the addition of yeast metabolites. Ethanol and hydrogen sulfide were found to enhance invasive growth of cells within mats exposed to low levels of nitrogen whereas tryptophol and 2-phenylethanol suppressed this enhancement. Sulfite was found to delay overall mat growth. In an effort to understand the cellular decision to switch morphology, changes in the transcriptome of invasively growing cells were studied. In this analysis, 272 genes were identified to be upregulated and 84 genes were downregulated in invasively growing cells. Of the ten largest differentially expressed genes, four were genes encoding hexose transporters (*HXT3*, *HXT4*, *HXT6* and *HXT7*) which had an increase in transcript abundance up to 13-fold. One hypothetical gene (AWRI796_5153) with a 6-fold increase in transcript abundance, has translation sequence homologous to an amidase domain. Following differential expression and Gene Ontology analysis, five GO categories represented the 37 significantly enriched GO terms in the upregulated gene set of invasively growing cells, these being glucose import, carbohydrate metabolic process, fungal-type cell wall organisation, medium-chain fatty acid biosynthetic process and cellular water homeostasis. Since cellular water homeostasis has not previously been associated with invasive growth, and four out of five genes in this group were found to be significantly upregulated in the invasively growing cells, further analysis of deletion mutants of each of these confirmed that *FPS1*, encoding the glycerol export protein, is required for invasive growth of yeast mats in low nitrogen conditions. In summary, this work reports the phenotypic properties of commercial wine yeast biofilms in

environments of both rich nutrient and low nitrogen, either in typical laboratory type agar media or in conditions simulating that of a grape or wine hose. The ability of these yeasts to form complex morphologies, grow invasively into grape solids and attach to winery hose plastic may confer their residency and survival in the vineyard and winery. The influence of different yeast metabolites and transcriptional changes in invasively growing cells provide further understanding of this morphogenetic program.

Declaration statement

I certify that this work contains no material which has been accepted for the award of any other degree or diploma in my name, in any university or other tertiary institution and, to the best of my knowledge and belief, contains no material previously published or written by another person, except where due reference has been made in the text. In addition, I certify that no part of this work will, in the future, be used in a submission in my name, for any other degree or diploma in any university or other tertiary institution without the prior approval of the University of Adelaide and where applicable, any partner institution responsible for the joint-award of this degree.

I give consent to this copy of my thesis, when deposited in the University Library, being made available for loan and photocopying, subject to the provisions of the Copyright Act 1968.

I also give permission for the digital version of my thesis to be made available on the web, via the University's digital research repository, the Library Search and also through web search engines, unless permission has been granted by the University to restrict access for a period of time.

Ee Lin Tek

/ /

Acknowledgements

I would like to thank my supervisors, Prof Vladimir Jiranek, Dr Joanna Sundstrom and Dr Jennie Gardner, for their mentoring, guidance and encouragement throughout my candidature. Thanks to my independent advisor, Prof Steve Oliver, for the conceptual input and critiques for this project and the opportunity for me to undertake research at the University of Cambridge for 11 weeks. RNA-sequencing work would not be possible without Dr Andy Hesketh.

I wish to acknowledge the support from The University of Adelaide; scholarships and operating funds, these being the Adelaide Graduate Research Scholarship, the Research Abroad Scholarship, and the DR Stranks Travelling Fellowship provided by The University of Adelaide, and a Supplementary PhD Scholarship by Wine Australia. I would also like to acknowledge Dr Charles Boone (University of Toronto, Canada) for donating yeast strains in the Σ1278b background.

I am grateful to be part of the Wine Microbiology and Microbial Biotechnology research group where the staff and students offered generous assistance. Particularly, I would like to mention Nick, for solving many technical issues; Michelle, for providing yeast strain I1 and sharing knowledge on yeast metabolism; Tommaso, for helping to acquire winery hoses; and Jin, for giving advice on molecular biology techniques. I also thank Louise, Max, former students, Gang and Danfeng, former visitors, Marine, Sydney, and Helene for their companionship during my study.

Special thanks to Jess and Lisa for listening and sharing life journey and experiences, Alfredo for inspiring me to keep going when I was losing determination, Henry and Neesha for all the laughs, Christoph for the excitements, Thomas and Lenna for their moral support, friends and fellow dancers for keeping my life balance.

Finally, great appreciations to my beloved family for their support, respect, and love.

Thesis overview and structure

Purposefully inoculated fermentations using commercial wine yeast are broadly implemented due to their success in completing fermentation efficiently and producing quality wine. Many commercial wine strains, usually *Saccharomyces cerevisiae*, were originally isolated from indigenous microflora of successful fermentations. These strains are now produced commercially and are widely available. Evidence suggests that the use of commercial strains leads to their presence and survival in the vineyard and winery. This could potentially lead to an alteration in native microflora in must and subsequently influence the regional character of wine. The mechanism of how these commercial yeasts remain in the winery environment is barely understood.

Biofilm formation is considered a survival strategy for many fungi and bacteria under harsh conditions. *S. cerevisiae* has been reported to be able to form biofilms, evidenced by the ability to grow into a mat and to adhere to plastic. These abilities have been investigated in not only laboratory strains, but also some clinical yeasts and yeasts isolated from wine grapes and must. It is likely that commercial wine yeasts also possess the ability to form biofilms which could drive their residency in the wine making environment. Current knowledge on yeast biofilms has focussed on the laboratory strain Σ1278b which is not directly applicable to the understanding of wine yeast biofilms since they are substantially genetically different. The study of biofilm formation by commercial wine yeast and their characteristics is therefore warranted.

Given that biofilms are a multicellular growth form, and nitrogen is known to be essential for yeast proliferation, biofilm formation could be affected by nitrogen availability. Lack of nitrogen has been shown to induce a pseudohyphal (filamentous) and invasive growth response in yeast. Filamentous mats can be formed when cells are starved for glucose but the mat formation response to low nitrogen has not been reported. Filamentous and invasive growth responses can be manipulated by other environmental triggers and putative signalling molecules such as temperature, pH, atmosphere, preservatives and fusel alcohols. Studies have shown that cell-cell communication can occur in biofilm formation, but the involvement of this system in yeast, especially *S. cerevisiae* biofilms is poorly understood.

In a quest to understand wine yeast biofilms in greater details, the present study has three aims:

1. Investigation of commercial wine yeast biofilm-forming ability and characteristics;
2. Exploration of mat formation in low nitrogen conditions and the influence of putative quorum sensing or signalling molecules; and
3. Study the genetic regulation of wine yeast biofilms or related phenotypes.

This dissertation has been organised in several chapters to present background information, reports of studies to answer each of the aims, and a conclusion. Chapter 1 establishes the field of knowledge and summarises critical gaps for the present study. Areas of discussion include yeast biofilms and related morphological phenotypes, influence of nitrogen availability, and potential signalling molecules. Chapter 2 presents mat characteristics and plastic adhesion properties of commercial wine yeast strains which addresses Aim 1. Chapter 3 addresses Aim 2 where data involving mat formation of commercial wine yeast strains in a low nitrogen environment and the response to potential signalling molecules is presented. Based on the findings from Chapter 3 that describe invasive growth as the primary observation in low-nitrogen, Chapter 4 presents the investigation of transcriptional changes of invasively growing wine yeast. Chapter 5 is a summary of the main findings including how this work contributes to current knowledge, limitations and future directions of the work.

Chapters 2–4 are presented as unsubmitted work prepared in manuscript style. For consistency, the typing, format, and referencing styles have been adjusted. Numbering of figures and tables has also been modified according to the order in the dissertation. References from all chapters can be found in the Bibliography.

Chapter 1

Literature review

Contextual statement

This literature review was mostly written within the first six months of candidature and only covers the literature up to August 2014. The purpose of this literature review was to provide the background information and establish a theoretical framework for this PhD project. For a more updated literature, please refer to the introduction section in Chapters 2 to 4.

1.1 Commercial wine yeast in the vineyard and winery

Traditional wine production takes advantage of indigenous yeasts in grape must and on winery equipment to carry out fermentation, *i.e.* uninoculated or indigenous fermentation as opposed to the relatively modern practice of purposeful inoculation with commercial wine yeast strains. The surface of intact grapes is predominantly colonised with species of *Kloeckera*, *Hanseniaspora*, *Candida*, *Cryptococcus*, *Rhodotorula*, *Pichia*, *Kluyveromyces*, and *Hansenula*, which usually dominate the early stage of alcoholic fermentation (Fleet and Heard, 1993). The composition of microflora on grapes fluctuates depending on climatic influences, soil and viticulture practices, grape variety, the incidence of physical damage of grapes, and potential insect vectors (Mortimer and Polsinelli, 1999; Pretorius et al., 1999; Stefanini et al., 2012). The yeast flora of must is further influenced by harvest method, transport time, grape temperature, and must treatment (Pretorius et al., 1999). Yeasts resident on winery equipment are likely introduced through contact with grapes, use of commercial starter cultures, and use of oak barrels with the source varying depending on the surface nature of equipment and cleaning and sanitisation practices (Martini, 1993; Ciani et al., 2004; Goddard et al., 2010). As the fermentation progresses, conditions usually favour the growth of *Saccharomyces cerevisiae*, which often becomes predominant at the later stage of the process. Due to a variety of factors that influence the microflora in must, the microbial composition of an uninoculated fermentation is highly variable between fermentations, vintages and subsequently is unpredictable.

The capacity to control and predict fermentation aids winemakers to produce quality products. This has led to the common use of commercial starter culture preparations. A large selection of wine yeast is manufactured in an active dry form and is available to inoculate grape must. For large-scale wineries, this method is beneficial since the use of commercial cultures is more likely to produce consistent, reliable and predictable outcomes. In addition to ethanol and nutrient stress tolerance, commercial wine yeast are also selected based on organoleptic properties such as desirable concentrations of organic acids and volatile thiols and little to no production of compounds generally considered as faults, such as hydrogen sulfide.

The use of commercial wine yeast for inoculation has become common practice since the second half of the twentieth century, however, there are some wineries that continue to use the traditional uninoculated method. This is mainly a result of the belief that the regional character will be retained in the wine, due to the presence of indigenous microbes from the region specific to the grapes (rather than inoculation with a purchased commercial yeast). An alternative that some winemakers choose is to use a reduced amount of a single culture or perform mixed culture inoculation with non-*Saccharomyces* species. Some studies report benefits of this practice, such as enhancing wine quality and complexity (Comitini et al., 2011; Azzolini et al., 2012; Gobbi et al., 2013). More specifically, the

mixed culture fermentation of *Lachancea thermotolerans* and *S. cerevisiae* reduced pH and enhanced the production of 2-phenylethanol and glycerol, and the differences were also detected in sensory analysis (Gobbi et al., 2013). Also, the combination of *Metschnikowia pulcherrima* and *S. cerevisiae* enhanced medium-chain fatty acid, 2-phenylethanol and isoamyl acetate production and increased polysaccharide content in wine (Comitini et al., 2011). Furthermore, the use of *Torulaspora delbrueckii* with *S. cerevisiae* enhanced the aroma of Amarone wine by affecting alcohol, fermentative ester, fatty acid and lactone content (Azzolini et al., 2012).

The frequent use of commercial wine yeast in wineries may result in survival of residual yeast on winemaking equipment, or in wine lees (which is often disposed of in close proximity) even after sanitation. The impact of these yeast in the winery and vineyard ecosystem remains unknown. There is evidence that traces of commercial wine yeast are found in proximal vineyards. Three out of 13 such sites recovered commercial yeasts isolated from vineyards in the coastal regions of Western Cape, South Africa (Van der Westhuizen et al., 2000). A three-year study of Portuguese and French vineyards found that dissemination of commercial yeast was primarily restricted to short distances, with 94% of recovered commercial yeasts at 10 to 200 m from the winery (Valero et al., 2005). However, the population varied from year to year. Historical use of commercial yeast can also affect yeast microflora in uninoculated fermentation. For instance, a study spanning seven years of uninoculated fermentations in a winery that had routinely used commercial strains to inoculate fermentations reported that eight out of ten of the dominant yeasts isolated were commercial strains that had previously been used in the winery (Blanco et al., 2011). Furthermore, *S. cerevisiae*, the common commercial wine yeast, has been found inhabiting the winery surfaces prior to harvest (Bokulich et al., 2013). Residual commercial yeast can therefore survive in a winery or vineyard, and may consequently affect wine styles relying on fermentation with indigenous microflora. Information on how these yeast behave in a winery environment and mechanisms supporting their survival is limited.

1.2 Yeast's lifestyle as multicellular communities

Yeast cells experience many and varied nutritional challenges in both nature and industry where competition for nutrients leads to the selection of fitter individuals. For example, during alcoholic fermentation, nutrients are utilised and some, such as assimilable nitrogen, become limiting especially in high sugar and low nitrogen content grape juices. In other cases, yeast cells encounter physical or chemical stresses, such as high osmolarity, low pH and the presence of toxins (Bauer and Pretorius, 2000). In response to these environmental challenges, yeast often undergo morphological changes and develop diverse structured multicellular communities (Brückner and Mösch, 2012). The advantages of being in such a community are:

(a) having better protection from a harmful environment,

(b) having enhanced survival due to differentiation into specialised cell types, and

(c) the provision of nutrients to the surviving cells in the community when supplies are limited (Palková and Váchová, 2006).

The architecture of multicellular communities can be influenced by their environment. For example, some industrial yeast cells flocculate after completing alcoholic fermentation and they can either form a sediment as flocs or float on the liquid surface as flors (Martínez et al., 1997; Verstrepen et al., 2003). Yeast can also form biofilms, which can be defined as a structured cell aggregate that is attached to a solid or semisolid surface and is encased by an extracellular matrix (Ramage et al., 2005; Zara et al., 2005). Previous investigations of yeast biofilms focussed on clinical implications, such as biofilms of *Candida spp.*, due to their association with virulence, pathogenesis and impact on human infections. *S. cerevisiae* also possesses common features of yeast and bacterial biofilms (Parsek and Singh, 2003; Hasan et al., 2009; Bojsen et al., 2012). Since *S. cerevisiae* is both a key industrial organism and one of the standard models of eukaryotic cellular biology, due to its genomic tractability, it is the preferred model to study mechanisms underlying yeast biofilm formation.

1.3 Biofilm formation of *S. cerevisiae*

Biofilms are communities of microorganisms attached to a surface, surrounded by self-produced extracellular matrix, with the formation involving cell-surface and cell-cell interactions (O'Toole et al., 2000). The cycle of biofilm development consists of initial surface attachment, colonisation, biofilm maturation and cell detachment (Fig. 1.1; O'Toole et al., 2000).

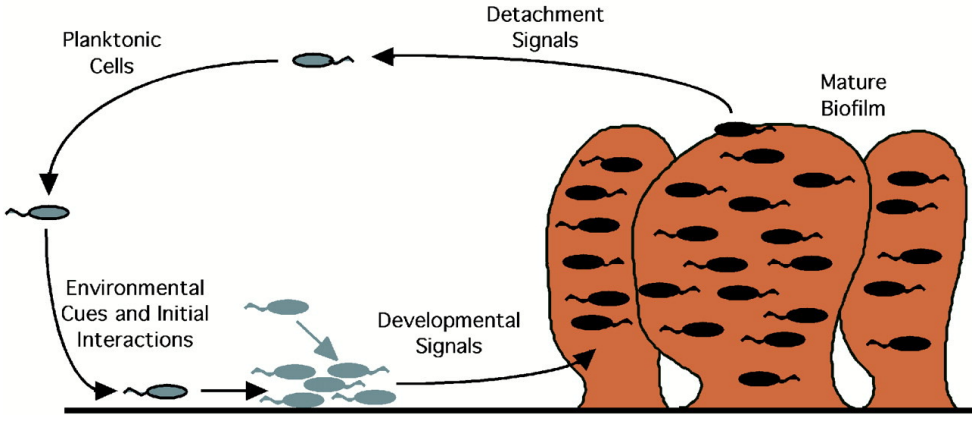

Figure 1.1: Model of biofilm development cycle. Figure adapted from O'Toole et al. (2000).

Biofilm forming ability of *S. cerevisiae* was first reported by Reynolds and Fink (2001) where they demonstrated that *S. cerevisiae* was able to form a flat mat with 'hub and spokes' structure covering a large area across the surface of a YPD low-density agar medium (Fig. 1.2; Reynolds and Fink, 2001).

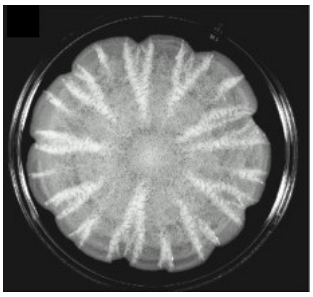

Figure 1.2: A mat formed by a haploid *S. cerevisiae* Σ1278b strain on a 0.3% agar YPD plate after 13 days at 25 °C. Figure adapted from Reynolds and Fink (2001).

The group also showed that *S. cerevisiae* was able to adhere to plastic and adhesion was enhanced when cells were grown in low glucose conditions, indicating a nutrient-mediated response (Reynolds and Fink, 2001). Adhesion is an indication of the first step in biofilm development in pathogenic yeast and bacteria (O'Toole et al., 2000). Mat formation is thought to be similar to the ability to 'slide' on a low-density agar medium observed in non-flagellated *Mycobacterium spp.* which has a close connection with biofilm formation (Martínez et al., 1999; Recht et al., 2000). This form of translocation requires cell surface glycopeptidolipids. Similarly, both structured mat formation and plastic adhesion require Flo11p, a yeast adhesion-related cell surface glycoprotein. When *FLO11* was deleted, yeast cells adhered poorly to plastic and formed a poorly spreading mass of cells without complex structure (Reynolds and Fink, 2001). In this report, the term "biofilm" will be used to describe all forms of surface-attached multicellular communities with extracellular matrix and any related biofilm-forming ability tests such as adhesion, whereas "mat" refers specifically to the thin layer of yeast biomass that resembles a film on low-density agar.

Following the discovery of *S. cerevisiae*'s ability to form biofilms, many studies have investigated genes affecting mat formation and the regulatory pathways involved. Numerous signalling pathways have been identified that regulate the expression of *FLO11* (Fig. 1.3; Brückner and Mösch, 2012). Briefly, these include the mitogen-activated protein kinase (MAPK) pathway, the cAMP-PKA pathway, the SNF pathway, and the RIM pathway. A handful of *FLO11*-independent pathways have also been reported, such as the multivesicular body protein sorting pathway, the cell wall integrity pathway that is not via MAPK cascade, and the molecular chaperone of 70 kDa heat shock proteins (Martineau et al., 2007; Sarode et al., 2011, 2014).

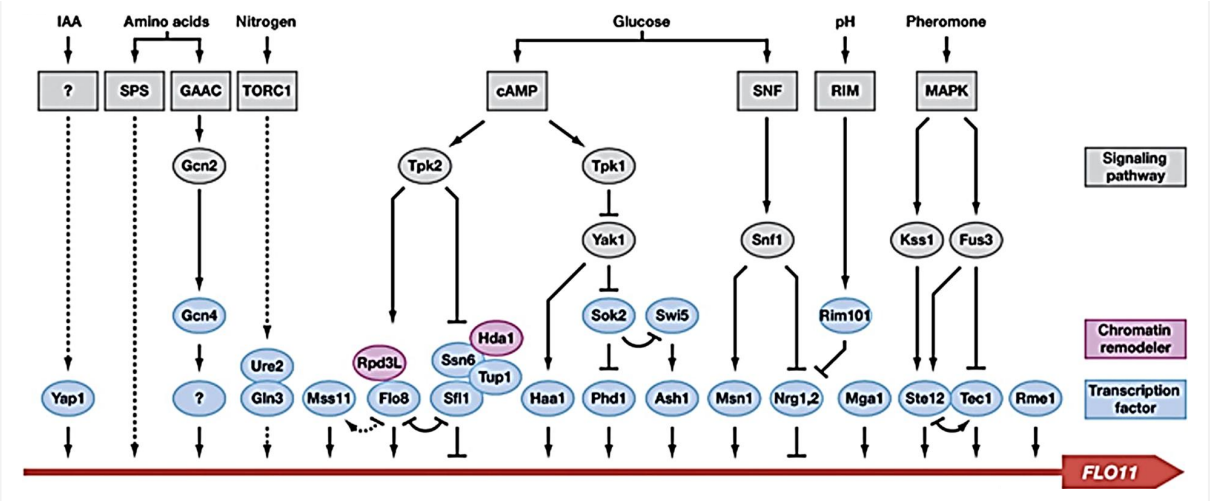

Figure 1.3: Regulation of *FLO11* expression. Arrows indicate positive regulation and inhibition is shown by bars. Figure adapted from Brückner and Mösch (2012).

So far, these *S. cerevisiae* biofilm studies have mainly been investigated in common laboratory strains. Wine strains of *S. cerevisiae* are known to be genetically different compared to laboratory strains, and this can affect their phenotypes (Borneman et al., 2008, 2011). The ability to form biofilms seems to be an inherent property for most microbes to survive in natural challenging environments (Costerton et al., 1995). Wine yeast are the dominant yeasts historically found in fermenting grape musts and where they have undergone natural selection driven by the conditions in grape juice fermentation (Querol et al., 1994). This may include the ability to form biofilms. Casalone and colleagues (2005) reported the ability of nine wine yeast isolates from grape and must to form mats that varied in size. *S. cerevisiae* has also been isolated from a mixed population biofilm developed on the rotating biological contactor disc in winery wastewater systems (Malandra et al., 2003). During the wastewater treatment process, industrial yeasts including *S. cerevisiae* adapted to the aerobic conditions in wastewater, combined with bacteria forming mixed population biofilms on the surface of the disc while degrading organic compounds (Malandra et al., 2003). This formation is beneficial because it can reduce the chemical oxygen demand of wastewater and bulking problems (Andreottola et al., 2005). The mechanism of this development is not completely understood. Therefore, an investigation of wine yeast biofilm formation is important within the context of the wine industry.

Biofilm formation might also serve as a model of survival to contribute to the understanding of how wine yeast respond to nutritional status such as during the course of fermentation. Even though *S. cerevisiae* is the principal organism for alcoholic fermentation, it is not usually prevalent on healthy intact grape berries, instead, it is commonly found on damaged grape berries and in the winery (Mortimer and Polsinelli, 1999; Bokulich et al., 2013). Damaged berries allow wine yeast to access rich nutrients from the semisolid grape interior, and hence encourage colonisation. An understanding of the successful yeast colonisation and behaviour on grapes would also be of great interest. More importantly,

the understanding of biofilm formation of commercial wine yeast could serve as the possible mechanisms for their residency and survival in the vineyard and winery.

1.4 Biofilm-related phenotypes in *S. cerevisiae*

In *S. cerevisiae*, the cell surface glycoprotein, Flo11p, required for mat formation and plastic adhesion, is also required for other phenotypes, such as invasive and filamentous growth (Lambrechts and Bauer, 1996; Lo and Dranginis, 1998). Invasive growth involves growing cells penetrating an agar medium. Haploid yeast cells have been shown to grow invasively in response to glucose depletion, which is termed haploid invasive growth (Cullen and Sprague, 2000). The authors also observed a filamentous morphology containing elongated cells that had a unipolar budding pattern associated with invasive growth (Fig. 1.4; Cullen and Sprague, 2000, 2002). Palecek and colleagues (2000) further showed that unipolar budding with or without cell elongation was sufficient to promote invasive growth.

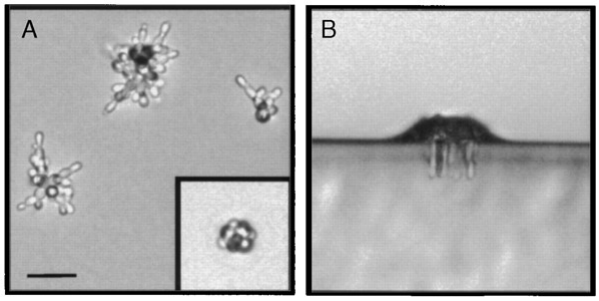

Figure 1.4: (A) Microcolonies forming from single cells of Σ1278b on Synthetic Complete medium lacking glucose after 24 h visualised by light microscopy at 200× magnification. Inset image represents an example of a microcolony formed in the presence of glucose. (B) A microcolony grown on SC medium lacking glucose visualised perpendicular to the plane of agar invasion by light microscopy. All images are at the same scale, with scale bar in (A) representing 40 μm. Figure adapted from Cullen and Sprague (2000).

Diploid cells have been shown to respond to nitrogen depletion, by growing into colonies with filamentous form where the filamentous regions contained chains of elongated cells growing away from the colony (Fig. 1.5; Gimeno et al., 1992). This morphology is similar to the hyphae formed by filamentous fungi, and therefore has been termed diploid pseudohyphal growth. The authors also reported that cells of diploid pseudohyphal growth can invade into agar.

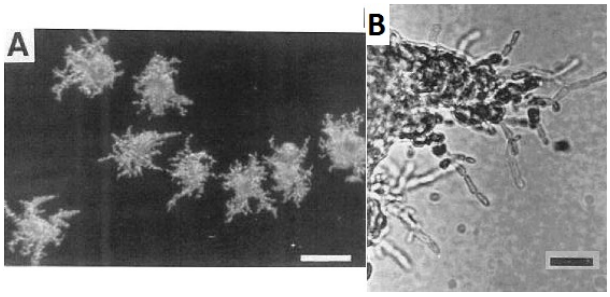

Figure 1.5: (A) Filamentous colonies formed by diploid cells of CGX19, a strain congenic to the Σ1278b genetic background, on a low nitrogen medium after 11 days of incubation. Scale bar, 0.2 mm. (B) A high magnification view of a filamentous colony of the same strain on a low nitrogen medium after 2 days of incubation. Scale bar, 30 μm. Figure adapted from Gimeno et al. (1992).

Filamentous growth (pseudohyphal growth) is a complex morphogenetic differentiation program that is tightly controlled with cell polarity, cell cycle and cell adhesion (Cullen and Sprague, 2012). At the start of a new cell cycle, G_1, cell polarity is determined by bud-site-selection proteins, which will direct bud growth (Park and Bi, 2007). Haploid cells bud in an axial pattern whereas diploid cells bud in a bipolar pattern (Chant and Pringle, 1995). When a cue to switch to filamentous growth is encountered, cells of both ploidy switch to a distal-unipolar budding pattern through Bud8p localisation (Gimeno et al., 1992; Harkins et al., 2001; Cullen and Sprague, 2002). When a bud emerges, actin cables extend into the bud and the bud grows apically (Pruyne and Bretscher, 2000). When nutrition is limiting, apical growth is prolonged at G_2 phase, resulting in elongated cells (Kron et al., 1994). At the end of the cell cycle, cell adhesion proteins, such as Flo11p, enable cells to remain attached (Guo et al., 2000; Halme et al., 2004). Given that this differentiation occurs in response to nutrient limitation, it is widely believed that this represents a nutrient foraging response. Since nutrient fluctuation occurs in the winery environment, filamentous growth may also be employed for persistence and nutrient search.

Another biofilm-related phenotype is complex colony morphology or structured morphology from fluffy colonies, which also requires Flo11p (Granek and Magwene, 2010; Štovíček et al., 2010). Fluffy colonies are raised but not smooth and have an aerial morphology. Colonies of such type produced a protective extracellular matrix, were more agar-adhesive, and may contain pseudohyphae and agar invasion ability (Štovíček et al., 2010; Váchová et al., 2011). The extracellular matrix contained a glycoprotein of molecular weight $>$ 200 kDa that is not related to flocculins (Kuthan et al., 2003). A genome-wide transcriptome analysis showed that the fluffy formation involved cell wall remodelling, secretion and modification of cell wall/membrane proteins, amino acid metabolism and nutrient transport (Štovíček et al., 2014). This formation that harbours multiple transcriptomic and phenotypic modulations is seen as a protective mechanism to survive in the wild environment. Similar traits may be part of biofilm formation to support colonisation.

1.5 Mat formation in response to nutrient availability

Most mat formation studies of *S. cerevisiae* have been conducted in rich media. However, regulation of the key gene in mat formation, *FLO11*, involves pathways that are dependent on nutritional signals including glucose and nitrogen (Fig. 1.3). The impact of glucose on mat formation has been reported. For instance, formation of the 'hub and spokes' structure on mats was delayed if glucose concentration was increased (Reynolds et al., 2008). In contrast, *S. cerevisiae* formed a filamentous mat, a mat that has filamentous periphery, on a glucose-limiting medium (Fig. 1.6; Karunanithi et al., 2012). It appeared that both 'hub and spokes' structure on mats and filamentous growth are impacted by glucose availability. It is unclear if filamentous growth contributed to the 'hub and spokes' formation.

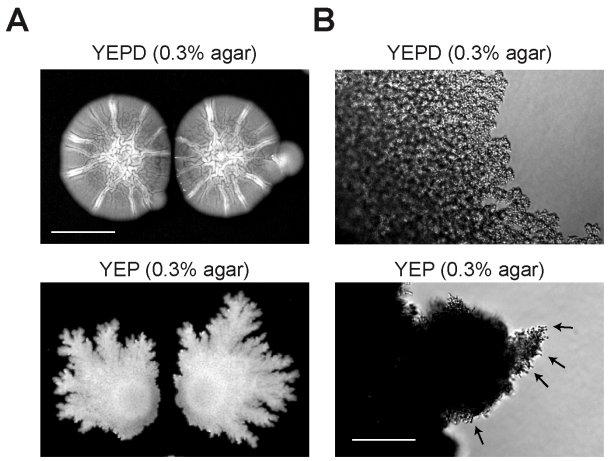

Figure 1.6: (A) Mats formed by Σ1278b on 0.3% agar YEPD media (top panel; containing glucose) and 0.3% agar YEP media (bottom panel; lacking glucose). Photographs were taken after 4 days (YEPD) and 15 days (YEP) of incubation. Scare bar, 1 cm. (B) Microscopic examination of mat perimeters in (A). Scale bar, 100 μm. Figure adapted from Karunanithi et al. (2012).

Nitrogen is well known to be essential for yeast growth, and therefore required for wine yeast to function efficiently for alcoholic fermentation (Bell and Henschke, 2005). Inadequate nitrogen in the second half of oenological fermentations is common and often results in stuck or sluggish fermentation. Yeast readily utilise all available nitrogen in a must fermentation, and thus they would be commonly exposed to a nitrogen-depleted environment. Since a mat is formed by expansion through the continuous cell division from the mat edge, nitrogen, or lack thereof may be an important factor for this expansion. This nutrient has not been thoroughly investigated for its influence on mat formation, although a few studies demonstrated that nitrogen limitation induced filamentous and invasive growth (Gimeno et al., 1992; Casalone et al., 2005; Chen and Fink, 2006). Filamentous and invasive growth can be affected by other metabolites or environmental factors. For example, fusel

alcohols, by-products of amino acid catabolism via the Ehrlich pathway, have been shown to stimulate hyphal-like elongated cells, which could lead to multicellular filamentation (Dickinson, 1994, 1996). Other environmental factors that have been reported to affect invasive growth included salt, preservatives, pH, temperature, and modified atmosphere (Zupan and Raspor, 2010). This wide variety of stimulators suggest that there are many factors and biological pathways affecting this mode of growth and these may be synergetic or antagonistic in the presence of multiple stimulators.

1.6 Regulation of mat formation, filamentous growth and invasive growth

Although mat formation, filamentous growth and invasive growth require Flo11p and some shared core signalling pathways, large-scale studies have found specific genes regulating each phenotype (Jin et al., 2008; Ryan et al., 2012; Shively et al., 2013). To identify genes necessary for filamentous growth induced by butanol in *S. cerevisiae*, Jin and colleagues (2008) screened a library of $3,627$ transposon insertion gene disruption constructs and $2,043$ overexpression constructs in a haploid version of filamentous strain Σ1278b. Of 487 genes identified as being necessary for filamentous growth, 243 were also necessary for haploid invasive growth. To study genes required for mat formation, filamentous growth as well as invasive growth, Ryan and colleagues (2012) screened both haploid and homozygous diploid Σ1278b gene deletion libraries. The group identified 688, 600 and 577 genes required for mat formation in rich nutrient low-density agar medium, diploid pseudohyphal growth in nitrogen-limited medium, and haploid invasive growth in rich medium, respectively. Haploid invasive growth and mat formation were found to be significantly correlated, with 300 genes common to both phenotypes. Sixty-one core genes required for all three phenotypes, included *FLO11* and a number of genes encoding proteins involving in the regulation of *FLO11* gene expression. These were components of the Rpd3L histone deacetylase complex, members of the Rim101 signalling pathway, and transcription factors for *FLO11*, Mit1p, Tec1p, Flo8p, and Mss11p. In contrast, Shively and colleagues (2013) found 551 genes that when overexpressed exaggerated diploid invasive growth in sufficient nitrogen and highlighted the potential role of nuclear Hog1p in repressing invasive growth. The findings from these studies suggest that each of these growth transitions have unique regulatory networks and these may be different for haploid and diploid cells.

1.7 Cell-cell communication in morphological transitions

Cell-cell communication via signals could lead to morphological changes and contribute to yeast community organisation (Honigberg, 2011). Intercellular communication such as quorum sensing (QS) is responsible for group motility, biofilm formation and maintenance, and production of virulence factors in bacteria (Miller and Bassler, 2001; Sperandio et al., 2002). This is similar to the communication system that controls physiological functions in multicellular organisms.

Cell-cell communication involves a chemical signalling molecule, secreted by one cell and sensed by another to trigger diverse behaviours (Youk and Lim, 2014). A well-studied example is the yeast mating system (Cottier and Mühlschlegel, 2011). Pheromones are peptides, namely a-factor produced by *MAT*a cells and α-factor produced by α cells. Haploid cells of each mating type sense and respond to the opposite factor, triggering a morphological response, forming a structure called a 'shmoo', resulting in directional growth towards the other cell. When shmoos touch, mating occurs and diploid cells are formed.

A QS system, on the other hand, relies on a particular cell density to be reached before a function is triggered. The concentration of a signalling molecule increases as cell numbers increase. When the 'quorum' threshold is reached, the molecule induces intracellular signalling pathway(s), altering gene expression, and resulting in a population response. This is widely used and well researched in bacterial populations, and to some extent in yeast populations (Henke and Bassler, 2004; Albuquerque and Casadevall, 2012).

1.8 Quorum sensing in yeast

The QS phenomenon was not described in eukaryotes until the 21^{st} century when farnesol was identified as a cell-density-dependent signalling molecule in *Candida albicans* (Hornby et al., 2001). Farnesol inhibits, while tyrosol initiates, the switch from yeast-form cells to hyphae formation at a threshold concentration (Hornby et al., 2001; Chen et al., 2004). However, there are conflicting reports on the molecular pathway acted on by farnesol to prevent this morphological switch. Davis-Hanna and colleagues (2008) and Hall and colleagues (2011) showed that farnesol inhibited genes involved in the Ras-cAMP pathway that leads to hyphal formation but Sato and colleagues (2004) showed no effect from farnesol on this pathway.

Quorum sensing in *S. cerevisiae* has more recently been proposed. Tryptophol and 2-phenylethanol have been described as QS molecules as their production and action is cell-density-dependent (Chen and Fink, 2006). These aromatic alcohols are generated

from their corresponding amino acids, tryptophan and phenylalanine, via the Ehrlich pathway (Hazelwood et al., 2008). Similar to other fusel alcohols, they were shown to induce *S. cerevisiae* pseudohyphal formation (Dickinson, 1996; Chen and Fink, 2006). The effect was enhanced when nitrogen was scarce. For example, pseudohyphal formation was present on Synthetic Low Ammonium Dextrose agar which contained 50 μM ammonium sulfate, but not on Synthetic Minimal Dextrose agar which contained 37 mM ammonium sulfate (Chen and Fink, 2006). The production of these aromatic alcohols was also greatly reduced when cells were grown in a medium containing greater than 500 μM ammonium sulfate. Therefore, the production of tryptophol and 2-phenylethanol is regulated by both population density and the nutritional state of the environment independently.

Aromatic alcohols are important in wine production as they contribute to the complexity of wine aroma profiles (Francis and Newton, 2005). They are produced by yeast during fermentation in three enzymatic reactions comprising transamination, decarboxylation and dehydrogenation (Hazelwood et al., 2008). Two of the enzymes used in the transamination and decarboxylation steps, encoded by *ARO9* and *ARO10*, are regulated by the transcription factor Aro80p (Iraqui et al., 1999). Tryptophol can upregulate *ARO9* and *ARO10* expression via Aro80p, resulting in a positive feedback loop to further stimulate aromatic alcohol synthesis (Chen and Fink, 2006). Likewise, high cell density also induces production via the same feedback regulation. On the contrary, *ARO9* and *ARO10* expression is repressed in high nitrogen conditions, consistent with the observation of low aromatic alcohol production when large amounts of ammonium sulfate are available (Chen and Fink, 2006).

Although the biosynthesis of tryptophol and 2-phenylethanol is understood, how these putative QS molecules induce the morphological transition from yeast-form to filamentous form is unclear. There are four signalling pathways known to regulate filamentous transition: the cAMP-PKA, MAPK, SNF and TOR pathways, which all target *FLO11*, the same genes required for mat formation, adhesion between cells, cell-to-surface adhesion, pseudohyphae formation and agar invasion (Sengupta et al., 2007; Cullen and Sprague, 2012). Both cAMP-PKA and MAPK pathways activate *FLO11* while the SNF pathway regulates repressors of the *FLO11* promoter (Kuchin et al., 2002; Braus et al., 2003). The *FLO11* transcription factor regulated by the TOR pathway requires further investigation. Chen and Fink (2006) showed that tryptophol and 2-phenylethanol induced *FLO11* expression and filamentation through Tpk2p, and its downstream Flo8p. Tpk2p is a subunit of PKA whereas Flo8p is the transcription factor of *FLO11*. The upstream elements of Tpk2p in the cAMP-PKA pathway were not required, neither were the elements of the MAPK pathway. Besides that, two transcription factors, Cat8p and Mig1p, were predicted to be responsible for regulating genes that were differentially expressed in response to the proposed QS aromatic alcohols (Wuster and Babu, 2010).

1.9 Hydrogen sulfide is a potential cell-cell signalling molecule in *S. cerevisiae*

Although work to fully describe a QS system is still underway for *S. cerevisiae*, there are molecules excreted by *S. cerevisiae* that result in a cell-cell signalling phenomenon and coordination, such as ammonia. Ammonia is produced by yeast colonies and is perceived as a signal by neighbouring colonies, resulting in growth inhibition towards the ammonium-producing neighbouring colonies (Palková et al., 1997). Another potential signalling molecule is hydrogen sulfide (H_2S). This molecule is released during fermentation when nitrogen is deficient (Jiranek et al., 1995; Gardner et al., 2002; Wang et al., 2003). Stuck fermentations caused by insufficient nitrogen are often difficult to restart, even when additional nitrogen is supplied thereafter. Reports suggested that this is due to inactivation of glucose transporters (Busturia and Lagunas, 1986). The presence of signalling compounds, such as H_2S, may prevent the re-activation of the glucose transport system but this requires further investigation.

The production of H_2S is part of the sulfate assimilation pathway that leads to the biosynthesis of sulfur-containing amino acids, cysteine, methionine and glutathione (Thomas and Surdin-Kerjan, 1997). Hydrogen sulfide is an undesirable product in wine due to its rotten egg aroma. However, intracellular H_2S is thought to be responsible for metabolic synchronisation in a yeast population (Murray et al., 2003). When pulses of Na_2S were added, the respiratory cycle of the whole population spontaneously reset, suggesting that H_2S may act as a microbial cell-cell signalling molecule (Murray et al., 2003; Lloyd, 2006). Hydrogen sulfide signalling is recognised in animal systems to maintain oxygen homeostasis and mediate the response to nutritional status (Iranon and Miller, 2012).

In mammals, nitrogen restriction, particularly cysteine and methionine, delivers health benefits and longevity (Miller et al., 2005; Plaisance et al., 2011; Elshorbagy et al., 2013; Lees et al., 2014). Exposure of mice to H_2S resulted in the same health benefits as nitrogen restriction and offered protection against oxygen deprivation (Blackstone and Roth, 2007; Hine and Mitchell, 2015). Hydrogen sulfide also increased thermotolerance and lifespan in the nematode *Caenorhabditis elegans* (Miller and Roth, 2007). Similarly, H_2S-mediated biological benefits have also been reported in yeast. The deletion of *MET17* leads to H_2S accumulation and increased H_2S production on both BiGGY agar (containing bismuth salt and sulfite to be reduced to bismuth and sulfide forming brown to black precipitate) and synthetic grape juice medium (Linderholm et al., 2008). This mutant has an extended chronological lifespan when grown in minimal medium (Johnson and Johnson, 2014). Other benefits include increased resistance to heat shock, oxidative and heavy metal stresses, and metal chelate toxicity (Singh and Sherman, 1974; Brown et al., 2006; Hwang et al., 2007; Johnson et al., 2014). A microarray experiment has shown that there is significant overlap of gene expression in the presence of H_2S and a stress

response (Jia et al., 2011). Since the formation of H_2S integrates with a number of stress responses, including nitrogen restriction, H_2S could potentially be a signalling molecule that influences other nitrogen-deficient responses such as filamentous and invasive growth. Further work is required for this to be confirmed.

1.10 Research questions and objectives

S. cerevisiae is the common commercial wine yeast used in inoculated fermentations. The persistence of this species in the vineyard and winery is an important question, especially as this would affect winemaking that pursuits geographical characteristics from the native microflora. *S. cerevisiae* has been shown to be capable of forming biofilms in both environmental (wine and medical) and laboratory strains. These properties have however not been fully evaluated in commercial wine yeast strains. It is not clear whether the biofilm-related phenotypes such as filamentous and invasive growth co-existed with wine yeast biofilms. The relatedness of biofilm assays to the winemaking context is also lacking. The first part of this study is to investigate biofilm traits of commercial wine yeast on the standard assays – mat formation on a rich medium and plastic adhesion in a low glucose medium. The investigation is extended to mat formation on grape pulp and adhesion to winery hose plastic. This knowledge will contribute to determining if and how the yeast colonise and survive in a winery/vineyard environment.

Yeast are frequently exposed to nutrient fluctuation including nitrogen depletion. Filamentous colonies are formed on nitrogen-limited solid agar and can be enhanced by the putative *S. cerevisiae* quorum sensing molecules, tryptophol and 2-phenylethanol (Chen and Fink, 2006). However, mat formation response (on semisolid agar) to low nitrogen conditions has not been investigated. The second part of this study will contribute to this knowledge and determine if quorum sensing and signalling molecules have a synergetic or antagonistic effect on mat formation in a low nitrogen environment.

Biofilm formation by laboratory *S. cerevisiae* requires Flo11p (Reynolds and Fink, 2001). There are several signalling pathways leading to the expression of *FLO11*. It is unknown if biofilms formed by commercial wine yeast also require Flo11p and whether it is regulated in a similar way. The final part of this study aims to understand the biological processes of commercial wine yeast biofilms or associated phenotypes using RNA-sequencing.

Chapter 2

Wine yeast biofilms

Contextual statement

The manuscript in this chapter addresses the first aim; to investigate the biofilm-forming ability of commercial wine yeasts. The study was conducted based on methods described by Reynolds and colleagues (2001) in the first *S. cerevisiae* biofilm publication. During attempts to reproduce mat and adhesion assays as per published methods, it became evident that further optimisation of these methods was required. Therefore, preliminary studies were conducted to finalise the methodology used in this manuscript and are outlined in Appendix A.

Statement of Authorship

Title of Paper	Evaluation of the ability of commercial wine yeasts to form biofilms (mats) and adhere to plastic: impact on microbiota in the winery environment
Publication Status	☐ Published ☐ Accepted for Publication ☐ Submitted for Publication ☑ Unpublished and Unsubmitted work written in manuscript style
Publication Details	Written in manuscript style for FEMS Microbiology Ecology

Principal Author

Name of Principal Author (Candidate)	Ee Lin Tek
Contribution to the Paper	Performed all experiments and data analysis, interpreted data, and wrote manuscript.
Overall percentage (%)	70%
Certification:	This paper reports on original research I conducted during the period of my Higher Degree by Research candidature and is not subject to any obligations or contractual agreements with a third party that would constrain its inclusion in this thesis. I am the primary author of this paper.
Signature	Date 04/09/17

Co-Author Contributions

By signing the Statement of Authorship, each author certifies that:

i. the candidate's stated contribution to the publication is accurate (as detailed above);

ii. permission is granted for the candidate in include the publication in the thesis; and

iii. the sum of all co-author contributions is equal to 100% less the candidate's stated contribution.

Name of Co-Author	Joanna F. Sundstrom
Contribution to the Paper	Construction of *FLO11* deletion in prototrophic Σ1278b, L2056 and AWRI796, supervised development of work, helped in data interpretation and editing of the manuscript.
Signature	Date 4/09/2017

Name of Co-Author	Jennie M. Gardner
Contribution to the Paper	Supervised development of work, helped in data interpretation and editing of the manuscript.
Signature	Date 6/09/17

Name of Co-Author	Stephen G. Oliver

Contribution to the Paper	Supervised development of work, helped in data interpretation and editing of the manuscript.
Signature	Date 30.08.17

Name of Co-Author	Vladimir Jiranek
Contribution to the Paper	Supervised development of work, helped in data interpretation and editing of the manuscript.
Signature	Date 4.9.17

Please cut and paste additional co-author panels here as required.

Evaluation of the ability of commercial wine yeasts to form biofilms (mats) and adhere to plastic: implications for the microbiota of the winery environment

Ee Lin Tek[1], Joanna F. Sundstrom[1], Jennie M. Gardner[1], Stephen G. Oliver[2], Vladimir Jiranek[1,3*]

[1]Department of Wine and Food Science, University of Adelaide, Waite Campus, South Australia 5064, Australia.
[2]Department of Biochemistry & Cambridge System Biology Centre, University of Cambridge, United Kingdom.
[3]Australian Research Council Training Centre for Innovative Wine Production.

*Corresponding author: PMB 1, Glen Osmond, South Australia 5064, Australia. Tel: 618-8313-6651; E-mail: vladimir.jiranek@adelaide.edu.au

2.1 Abstract

Commercially available active dried wine yeasts are regularly used by winemakers worldwide to achieve reliable fermentations and obtain quality wine. This practice has led to increased evidence of traces of commercial wine yeast in the vineyard, winery and uninoculated musts. The mechanism(s) that enables commercial wine yeast to persist in the winery environment and the impact on native microbial communities by this persistence is poorly understood. This study has investigated the ability of commercial wine yeasts to form biofilms and adhere to plastic. The results indicate that the biofilms formed by commercial yeasts consist of cells with a combination of different lifestyles (replicative and non-replicative) and growth modes including invasive growth, bud elongation, sporulation and a mat sectoring-like phenotype. Invasive growth was greatly enhanced on grape pulp regardless of strain, while adhesion on plastic varied between strains. The findings suggest a possible mechanism that allows commercial yeast to colonise and survive in the winery environment, which may have implications for the indigenous microbiota profile as well as the population profile in uninoculated fermentations if their dissemination is not controlled.

2.2 Keywords

Saccharomyces cerevisiae; wine yeast; biofilms; mats; plastic adhesion; invasive growth

2.3 Introduction

The fermentation of must with deliberately inoculated commercial strains of *Saccharomyces cerevisiae* is a common practice in winemaking throughout the world. This practice ensures consistent and reliable fermentations that achieve specific sensory outcomes. The alternative, the use of uninoculated musts in which 'wild' yeast species from the grapes and winery undertake the fermentation, is believed to bring out the regional character of wines since the indigenous yeast population will vary in different geographical locations (Gayevskiy and Goddard, 2012; Bokulich et al., 2014; Knight et al., 2015; Pinto et al., 2015). There is increased interest in using both methods in individual wineries, as well as using mixed starter cultures, to impart a regional character to the product of fermentations predominantly carried out by commercial yeast strains (Ciani et al., 2010). However, the frequent use of commercial strains without containment, prompts the question as to whether such practices could have an important impact on shaping the microbial ecology of the vineyard or the winery.

The country of New Zealand represents an island group that has only been inhabited by humans in comparatively recent time (800–1000 BP; Hurles et al., 2003).

Nevertheless, some *S. cerevisiae* isolates from uninoculated fermentation were found to be genotypically similar to isolates from a French oak barrel, suggesting that human activity has a role in affecting the endogenous yeast population and the resulting fermentations (Goddard et al., 2010). Reports show the prevalence and survival of commercial yeast strains in the winery, and in the vineyard at up to 700 m from the winery. While this suggests that the dissemination of such commercial strains to the environment has already occurred, their incidence was inconsistent from vintage to vintage (Valero et al., 2005, 2007; Cordero-Bueso et al., 2011; Martiniuk et al., 2016). Within a single vintage, the microbial communities residing winery surfaces at the University of California, Davis fluctuated during harvest (Bokulich et al., 2013). However, *S. cerevisiae*, one of the common inoculum in that winery, appeared to colonise the winery surfaces. A seven-year study of uninoculated fermentations in a winery that had routinely used commercial strains prior to this to inoculate fermentations, found that eight out of ten of the dominant yeasts isolated were commercial strains that had previously been used in the winery (Blanco et al., 2011). Whilst there is increasing evidence from different parts of the world to suggest commercial yeast remain in the winemaking environment, there is limited information on how such residual commercial yeasts behave and survive in this environment, and the properties that permit these yeasts to become members of the vineyard and/or winery microbiota remain unclear.

It is known that surface attachment and different modes of growth, such as biofilms, enable the long-term survival of fungi and bacteria in diverse ecological niches. The yeast *S. cerevisiae* is able to form biofilms as evidenced by two tests: mat formation on low density agar and adhesion to plastic (Reynolds and Fink, 2001). Both mat formation and plastic adhesion require the cell surface protein Flo11p. *S. cerevisiae* can also undergo nutrient-regulated filamentous and invasive growth, which are believed to be mechanisms used to forage for nutrients (Cullen and Sprague, 2000, 2012). These properties are not found in the universal laboratory reference strain S288C, due to a mutation in the *FLO8* gene, whose product is required for *FLO11* transcription (Liu et al., 1996; Rupp et al., 1999). In contrast, the laboratory strain Σ1278b, like many wild yeasts, displays biofilm-forming ability, filamentation and invasive growth (Hope and Dunham, 2014). It has been suggested that the loss of biofilm-like characteristics was due to domestication in the laboratory where yeast are grown routinely in rich media (Kuthan et al., 2003). This suggests that biofilms, surface adhesion and filamentous/invasive growth may confer on wild *S. cerevisiae* strains the ability to invade and thrive in unfavourable nutrient environments.

Many wild *S. cerevisiae* isolates, from a variety of geographical niches including those from wine grapes and must, have been shown to form mats exhibiting a range of shapes and sizes (Hope and Dunham, 2014; Sidari et al., 2014). This is different to the commonly studied laboratory strain Σ1278b that forms a large mat consisting of a central hub and spokes. This result challenges our understanding of the genetic basis and phenotypic roles of yeast biofilms in ecological contexts, since most studies that characterise

yeast mats have been based on Σ1278b (Reynolds, 2006; Martineau et al., 2007, 2010; Sarode et al., 2011, 2014; Chen et al., 2014).

Currently, limited information exists for the biofilm-forming ability of commercial wine yeast strains, which could be the mechanism enabling them to persist in the vineyard and winery (Zara et al., 2005; Rodriguez et al., 2014). To date, no research has addressed the details of mat formation for commercial wine yeast strains (such as cell and mat morphology, filamentation and invasive growth). Additionally, most biofilm studies on *S. cerevisiae* have been focused on mat formation of cells grown on the rich Yeast Extract Peptone Dextrose (YPD) medium and on adhesion to hard plastics. Little is known about how these yeast biofilm test results translate to survival in winery conditions. Sidari and colleagues (2014) investigated the biofilm formation of wild *S. cerevisiae* strains using deficient media for carbon and nitrogen such as SLAD and low glucose YPD to simulate fermentation conditions. The present study was undertaken to assess the mat-forming ability of commercial wine yeast strains as well as to investigate features of their mats, including structure, cellular morphology and any incidence of filamentous and invasive growth. Mats were grown on low-density (0.3%) agar to approximate the density of grape pulp. This study demonstrated how mat features change in response to grape pulp and the ability of commercial wine yeasts to adhere to the soft plastics of which hoses in the winery are made. We believe the results of this study provide a functional perspective on the role of commercial wine yeast biofilms in the wine ecosystem.

2.4 Materials and Methods

2.4.1 Yeast strains and media

Yeast strains used in this study are listed in Table 2.1. Five wine yeasts and a derivative were selected from preliminary experiments in this laboratory suggesting diverse mat phenotypes. Yeast Peptone Dextrose broth (YPD, 1% yeast extract, 2% bacto peptone, 2% glucose) or YPD-agar (YPD with 0.3 or 2% agar) was used to grow yeast strains. Deletion of *FLO11* in prototrophic Σ1278b, L2056 and AWRI796 strains was achieved by transformation (Gietz and Schiestl, 2007) with a *Kan*MX gene replacement cassette (Wach et al., 1994) generated by PCR using FLO11_A and FLO11_D primers (Table 2.2) and genomic DNA of the BY4741 Δ*flo11* strain (Winzeler et al., 1999). Positive transformants were selected using YPD-agar (2%) + 0.02% G418-sulfate (Astral, NSW, Australia). Homozygous diploid deletants were then isolated by sporulation using the PRE5 and SPO2 media (Codon et al., 1995), dissection and re-diploidisation, and verified by PCR amplification and sequencing using the primers FLO11_783bpup_F and FLO11_506bpdown_R (Table 2.2). Strain I1 was generated by transformation of the *Kan*MX cassette (generated with PCR using primers SUL1_A and SUL1_D, Table 2.2, and genomic DNA of the BY4741 Δ*sul1* strain; Winzeler et al., 1999) into the commercial wine yeast 'Distinction', followed

by sporulation, dissection and isolation of the re-diploidised wild type progeny.

Table 2.1: Yeast strains used in this study.

Yeast strain	**Genotype and comments**	**Reference**
L2056	Commercial wine yeast strain; diploid	Lallemand Australia
EC1118	Commercial wine yeast strain; diploid	Lallemand Australia
AWRI796	Commercial wine yeast strain; diploid	Mauri Yeast Australia
PDM	Commercial wine yeast strain; diploid	Mauri Yeast Australia
Distinction	Commercial wine yeast strain; diploid	Mauri Yeast Australia
I1	Diploid derivative of Distinction	This study
Prototrophic Σ1278b	Wild type laboratory strain; diploid	Ryan et al. (2012)
Auxotrophic Σ1278b	Y12958; *MAT*a/α *can1*Δ*:STE2pr-Sp-his5/CAN1 lyp1*Δ*::STE3pr-LEU2/LYP1 his3::his3G/his3::his3G leu2*Δ*/leu2*Δ *ura3*Δ*/ura3*Δ	Dowell et al. (2010)
P Σ1278b Δ*flo11*/Δ*flo11*	*flo11*Δ*::Kan*MX/*flo11*Δ*::Kan*MX	This study
A Σ1278b Δ*flo11*/Δ*flo11*	Y12958; *flo11*Δ*::Kan*MX/*flo11*Δ*::Kan*MX	Ryan et al. (2012)
L2056 Δ*flo11*/Δ*flo11*	*flo11*Δ*::Kan*MX/*flo11*Δ*::Kan*MX	This study
AWRI796 Δ*flo11*/Δ*flo11*	*flo11*Δ*::Kan*MX/*flo11*Δ*::Kan*MX	This study
BY4741 Δ*flo11*	*MAT*a *his3*Δ*1 leu2*Δ*0 met15*Δ*0 ura3*Δ*0 flo11*Δ*::Kan*MX	Thermo Fisher Scientific Australia
BY4741 Δ*sul1*	*MAT*a *his3*Δ*1 leu2*Δ*0 met15*Δ*0 ura3*Δ*0 sul1*Δ*::Kan*MX	Thermo Fisher Scientific Australia

P = prototrophic; A = auxotrophic

Table 2.2: Primers for amplification and expected product sizes.

Primer name	**Sequence (5′ to 3′)**	**Product size of BY4741 (bp)**
FLO11_A	AATGTCCGTGTTCGAATTAAATAAA	4666 (WT[1]);
FLO11_D	CCAATACTACCGGTACTTGTTCTTG	2146 (del[2])
FLO11_783bpup_F	TGTTGTCTTTTTAACGGTCGTACTG	5394 (WT);
FLO11_506bpdown_R	CCTGGTCGAAGATTATTAGTTGTGC	2876 (del)
SUL_A	TCGAACACTGTCATTTGAAATTATG	3104 (WT);
SUL_D	GGACATTTGTAGAAAATAGGCTCAA	2108 (del)

[1]wild type

[2]deletion

2.4.2 Mat formation assays

YPD-agar (0.3%) was prepared by mixing an equal volume of autoclaved 0.6% w/v bacteriological agar (Amyl Media; Cat No. RM250) and filter sterilised 2× YPD. 25 mL of medium was aliquoted per 90 mm plate, and then used within 24 h.

Exponential-phase cultures were prepared by inoculation of YPD broth with an overnight culture at 1.25×10^6 cells mL^{-1} and incubating for 5–7 h. The culture was diluted in Phosphate Buffered Saline (PBS; 137 mM NaCl, 2.7 mM KCl, 10 mM Na_2HPO_4, 1.8 mM KH_2PO_4, pH 7.4) to 1×10^6 cells mL^{-1} and an aliquot of 5 μL was spotted at the centre of a 90 mm YPD-agar (0.3%) plate. At least six replicate mats of each strain were prepared. The plates were wrapped in cling film and incubated with yeast inoculum side up at 25 °C for 13 days, unless otherwise indicated. To determine whether auxotrophy reduced spoke formation merely by reducing growth, 0.029% histidine, 0.117% leucine and 0.029% uracil were supplemented into YPD-agar (0.3%).

L2056 mats with a sectoring-like phenotype were subcultured to determine if each sector formed the same distinct mat structure. For direct subculturing, cells were picked up with a 1 μL inoculation loop and transferred to a fresh YPD-agar (0.3%) plate. To remove any temporary stress-induced phenotypes, cells were subcultured after re-growing in YPD. For this method, cells were grown in YPD broth to stationary phase before being used to prepare exponential-phase cultures and plating as described above.

Where indicated, mats were washed off the plate with a gentle stream of water to reveal invasive growth specific to mat formation on 0.3% agar. Plates were first incubated at 4 °C for 30 min before washing as this prevented the agar from being removed during washing. Where indicated, to confirm adherence to agar, cells were also subjected to rubbing with a gloved finger. Invasive growth was confirmed by needing to break the agar to reach those cells.

Mats were photographed using either a Samsung Galaxy S3 camera, S5 camera or ProtoCOL 3 (Synbiosis). Mat areas were measured from ProtoCOL 3 images using Fiji software (Schindelin et al., 2012). Detailed steps for processing and measuring are in the Supplementary Data.

The morphology of cells obtained from mats mounted in PBS were observed and imaged at 400× and 1000× magnification using a Nikon Eclipse 50i microscope and an attached Digital Sight DS-2MBWc camera with NIS-Elements F3.0 imaging software (Nikon).

For the grape-pulp assay, organic table grapes were surface sterilised with 70% v/v ethanol before skinning. Pulp was homogenised with a stick blender. Grape pulp agar (0.3% w/v agar) was prepared by mixing homogenised pulp and autoclaved agar in a 3:1 ratio. 25 mL of medium was aliquoted per 90 mm plate, and then used within 24 h. Yeast

were inoculated at the centre of the agar using a toothpickwith cells cultured on YPD-agar (2%). Plates were wrapped and incubated at 25 °C as described above. Negative controls with no inoculum resulted in no contamination. Mat images were taken using a Nikon SMZ1270 stereomicroscope and an attached DS-Fi3 camera with the NIS-Elements F4.60 software. Mats were washed off as described above. Cross-section samples were prepared by slicing the agar with a scalpel blade and placed on a glass slide with the cut side facing up.

High-sugar YPD-agar (5% glucose, 5% fructose, 1% yeast extract, 2% bacto peptone, 0.3% agar) was prepared as described for YPD-agar (0.3%). Yeast were inoculated using a toothpick for this assay. Images were taken on Day 3 using the ProtoCOL 3.

2.4.3 Vitality and nuclear staining

Cells with elongated buds were stained for vitality and nuclear DNA to visualise the physiological state. For vitality staining, yeast cells were resuspended in 20 μL of 1× PBS containing 6.5 μg mL^{-1} propidium iodide (PI; Life Technologies, formerly Invitrogen; Cat No. P3566) and 4.75 μg mL^{-1} bis-(1,3-dibarbituric acid)-trimethine oxonol (DiBAC4(3); Sigma-Aldrich; Cat No. D8189) on a glass slide. The slide was incubated for 5 min in a black humid chamber. DAPI (Sigma-Aldrich; Cat No. D9542) staining was performed according to Meluh's Protocol (John Hopkins School of Medicine, 1999) for staining of the nucleus. Stained cells were observed using a Nikon Eclipse 50i microscope with an attached Nikon Intensilight C-HGFI illuminator and a suitable filter set. Filter sets used included G2-A (excitation 510–560, barrier 590) for PI, GFP-B (excitation 460–500, barrier 510–560) for DiBAC4(3) and UV-2A (excitation 330–380, barrier 420) for DAPI. Black and white fluorescence images were obtained. Fluorescence colours were then applied using the Fiji software (Schindelin et al., 2012).

2.4.4 DNA preparation and PCR conditions

Genomic DNA was extracted as described in Adams et al. (1998). Other DNA preparations for PCR amplification were carried out according to the Chelex-based procedure described by Antonangelo et al. (2013) with the heating step substituted with boiling for 10 min. 25 μL PCR reactions consisted of 1× Hi-Fi Buffer, 1 mM dNTP Mix (Bioline; Cat No. BIO-39028), 0.2 μM primer, 0.5 units polymerase (Bioline Velocity DNA Polymerase; Cat No. BIO-21098) and 2 μL of the Chelex-extracted DNA. The thermocycling program was 98 °C for 2 min, followed by 30 cycles of 30 s at 98 °C, 30 s at 58 °C and 1.5 min at 72 °C, followed by 5 min at 72 °C. Primers used and the expected product sizes are listed in Table 2.2. PCR products were separated on a 0.8–1% w/v TAE-agarose gel containing GelRed nucleic acid stain (Biotin; Cat No. 41003). DNA fragments of deletion products were excised from the gel and purified using the *Wizard SV* Gel and PCR Clean-Up System

(Promega, Madison, WI; Cat No. A9282).

2.4.5 Mat culture harvest and total RNA extraction

Spoked and non-spoked mats of L2056 were harvested by using a cover slip with forceps to pick up cells across all regions from rim to centre. An inoculation loop was used to transfer and resuspend cells in 1 mL Trizol reagent (Life Technologies; Cat No. 15596-018). The sample was snap frozen in liquid nitrogen for 20 s. RNA extraction was performed using a combination of Trizol reagent and a Qiagen RNeasy Mini kit (Cat No. 74104). Samples were thawed on ice. Glass beads were added up to the halfway mark of the meniscus. Six cycles of 45 s of vortexing and 45 s of rest on ice were used to disrupt cells. Tubes were incubated at 65 °C for 3 min and 200 μL of chloroform was added, followed by vortexing for 15 s before leaving at room temperature for 5 min. Tubes were centrifuged at $20,817 \times g$ for 10 min at 4 °C. Supernatant was recovered to a fresh tube and an equal volume of 70% v/v ethanol was added, mixed by pipetting, before continuing according to the Qiagen RNeasy Mini kit manufacturer's instructions. RNA quality and quantity were checked using a NanoDrop ND-1000 UV-visible light spectrophotometer (Thermo Fisher Scientific) and on 1% TAE-agarose gel. The absence of genomic DNA contamination in RNA preparations was confirmed using RNA as a template in real-time PCR assays.

2.4.6 Quantitative real-time PCR

Quantitative real-time PCR was performed to compare the two L2056 mat structures that resulted from subculturing and determine whether this was associated with differential gene expression of *FLO11*. Primers for reference genes and the gene of interest (Table 2.3) used in real-time PCR were as published in Teste et al. (2009) and Van Mulders et al. (2009). Two micrograms of total RNA was reverse-transcribed into cDNA using an iScript cDNA synthesis kit (Bio-Rad; Cat No. 1708891) in a 40 μL reaction mixture. The RT-PCR reaction mix (10 μL total volume) consisted of 5 μL SsoFast EvaGreen Supermix (Bio-Rad; Cat No. 1725203), 0.2 μM of each primer, 2 μL water and 2 μL of a 1:10 dilution of the cDNA preparation. Each reaction was done in triplicate. Triplicates of no template control were included for each primer pair run. The thermocycling program was 95 °C for 30 s, followed by 40 cycles of 5 s at 95 °C and 5 s at 60 °C, followed by a hold at 65 °C for 5 s before an end at 95 °C. The melt curve data was checked to confirm primer specificity and contamination.

Table 2.3: Primer sequences for qRT-PCR.

Target	Sequence
Reference gene	
ALG9	F: CACGGATAGTGGCTTTGGTGAACAATTAC
	R: TATGATTATCTGGCAGCAGGAAAGAACTTGGG
TAF10	F: ATATTCCAGGATCAGGTCTTCCGTAGC
	R: GTAGTCTTCTCATTCTGTTGATGTTGTTGTTG
UBC6	F: GATACTTGGAATCCTGGCTGGTCTGTCTC
	R: AAAGGGTCTTCTGTTTCATCACCTGTATTTGC
Gene of interest	
FLO11	F: GTTCAACCAGTCCAAGCGAAA
	R: GTAGTTACAGGTGTGGTAGGTGAAGTG
gDNA contamination verification	
ACT1	F: ATTATATGTTTAGAGGTTGCTGCTTTGG
	R: CAATTCGTTGTAGAAGGTATGATGCC

A standard curve was used to determine the PCR reaction efficiency for each primer pair. Quantitative PCR was performed on a ten-fold serial dilution of cDNA samples over six points. Each concentration was done in triplicate. The standard curve for all primer pairs used in the study had 90–110% reaction efficiency and an r^2 value > 0.980.

Three reference genes, *ALG9*, *TAF10* and *UBC6*, were used for normalisation as suggested by Teste et al. (2009). Analysis of qRT-PCR reactions with qBase^{PLUS} (Biogazelle) using all reference genes returned an M value below 1, an acceptable range of stable expression for heterogeneous sample according to Taylor et al. (2015) and Vandesompele et al. (2002). Results were imported to GraphPad Prism version 7.02 software for a two-way analysis of variance (ANOVA) with a Sidak multiple comparisons test.

2.4.7 Plastic adhesion assays

Plastic adhesion was performed for auxotrophic Σ1278b, prototrophic Σ1278b, L2056, AWRI796 and prototrophic Σ1278b Δ*flo11*/Δ*flo11* as described by Reynolds and Fink (2001) with slight modifications. Cells were grown in Synthetic Complete medium (SC; 0.17% Yeast Nitrogen Base without amino acids and ammonium sulfate, 0.079% Complete Supplement Mixture, 0.5% ammonium sulfate) with 2% glucose overnight, washed with sterile ultrapure water, resuspended in 10 mL sterile ultrapure water and split into two 50 mL tubes. The cells were harvested and resuspended in SC with either 0.1% or 2% glucose to an OD_{600} of 1.0. Six replicates of 100 μL aliquots were transferred to 96-well non-treated polystyrene plates (Corning; Manufacturing No. 3370). The plates were incubated for 0, 1, 3 or 6 h at 28 °C. An equal volume of 1% v/v Crystal Violet solution

(Sigma-Aldrich; Cat No. HT90132) was added to each well and removed after 15 min. This step was repeated before washing with 100 μL once and 200 μL twice with Reverse Osmosis water. 100 μL of 10% sodium dodecyl sulfate (SDS) was added to each well to solubilise Crystal Violet for 30 min. Absorbance at 590 nm was measured after mixing with 100 μL sterile ultrapure water. Σ1278b Δ*flo11*/Δ*flo11* was excluded in 2% glucose due to poor growth and therefore insufficient overnight culture for both conditions.

2.4.8 Winery hose adhesion assays

This assay is a modified version of the plastic adhesion assay. A new winery hose (Red Heliflex composed of polyvinyl chloride, the most commonly used hose for wine transfer) was cut into half-circle strips and sterilised by dipping into 70% v/v ethanol. Four sterile hose strips were placed in a 90 mm plate. 10 mL Synthetic Low Ammonium Dextrose (SLAD; 0.17% Yeast Nitrogen Base without amino acids and ammonium sulfate, 2% glucose, 50 μM ammonium sulfate) cultures of two overnights were harvested and resuspended in 25 mL of fresh SLAD before being added to the plate. Plate were incubated at 30 °C for seven days. Sterile forceps were used to pick up strips and dip them in water to rinse off unattached cells. The strips were then observed with a light microscope for attached cells. Negative control with a blank medium showed no cells attached.

For the assay incorporating shaking, winery hose was cut into quarter strips and sterilised with 70% v/v ethanol. A strip was added to a 50 mL tube containing 10 mL SLAD after inoculation of yeast. Cultures were incubated at 30 °C with shaking at 130 rpm for four days. Cell attachment on strips was observed as above. Cells were imaged at 400× magnification using the Nikon Eclipse 50i microscope with the attached camera and NIS-Elements F4.60 software.

2.5 Results

2.5.1 Prototrophic diploid Σ1278b as a laboratory reference

Σ1278b is the most commonly used strain in mat studies since, unlike S288C, it has a functional *FLO8* gene and is considered to have wild type adhesion and filamentation phenotypes. Since the wine yeast strains in this study were diploid, diploid Σ1278b was selected as the reference strain. Furthermore, auxotrophic and prototrophic diploid strains produced different mats. Auxotrophic Σ1278b formed a smaller mat (Fig. 2.1A and B; YPD) with fewer spokes, defined as raised cables radiating from the hub (Fig. 2.1C), compared to the prototrophic Σ1278b mat. Deletion of *FLO11* in either background abolished spokes (Fig. 2.1A). Since auxotrophic Σ1278b has been reported to form a spoked mat, the incubation time was extended to check for spoke formation. More spokes arose as

the mats aged. Ten percent of the mats developed spokes by Day 16 compared to none on Day 11 (Fig. 2.1C), thus confirming the ability of auxotrophic Σ1278b to form mats with spokes. However, the average number of spokes per mat was markedly less for auxotrophic than for prototrophic Σ1278b (ca. 0.16 vs 5.74 after 16 days). Supplementation with histidine, leucine and uracil improved growth, as evidenced by increased mat areas (Fig. 2.1B) and indeed restored spoked mat features (Fig. 2.1D). Accordingly, in order to avoid the potential complication of exogenous amino acid supplementation on mat formation and given the similarity of its mat formation to that previously published, prototrophic Σ1278b was selected as the laboratory strain reference in this study of wine yeast mat morphology.

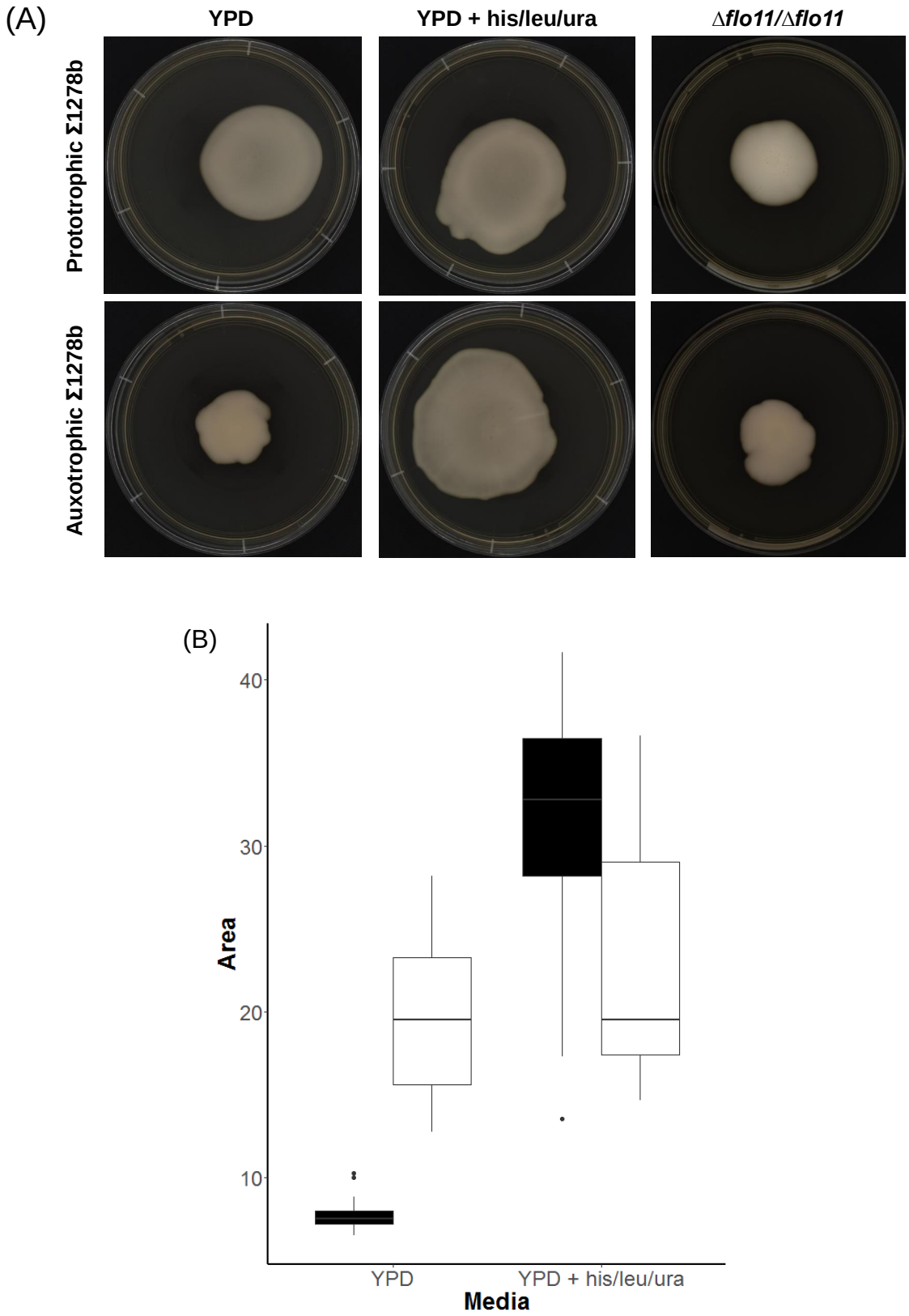

Figure 2.1: Mat features of Σ1278b. (A) Mats formed by prototrophic and auxotrophic Σ1278b on YPD-agar (0.3%) and YPD-agar (0.3%) supplemented with 0.029% histidine, 0.117% leucine and 0.029% uracil. Last column shows mats of prototrophic and auxotrophic Σ1278b Δ*flo11*/Δ*flo11* on YPD-agar (0.3%). Images were taken on Day 9. (B) Boxplot showing mat areas (cm^2) of auxotrophic (black) and prototrophic (white) Σ1278b growing on YPD-agar (0.3%) and supplemented YPD-agar (0.3%). Please refer to next page for (C) and (D).

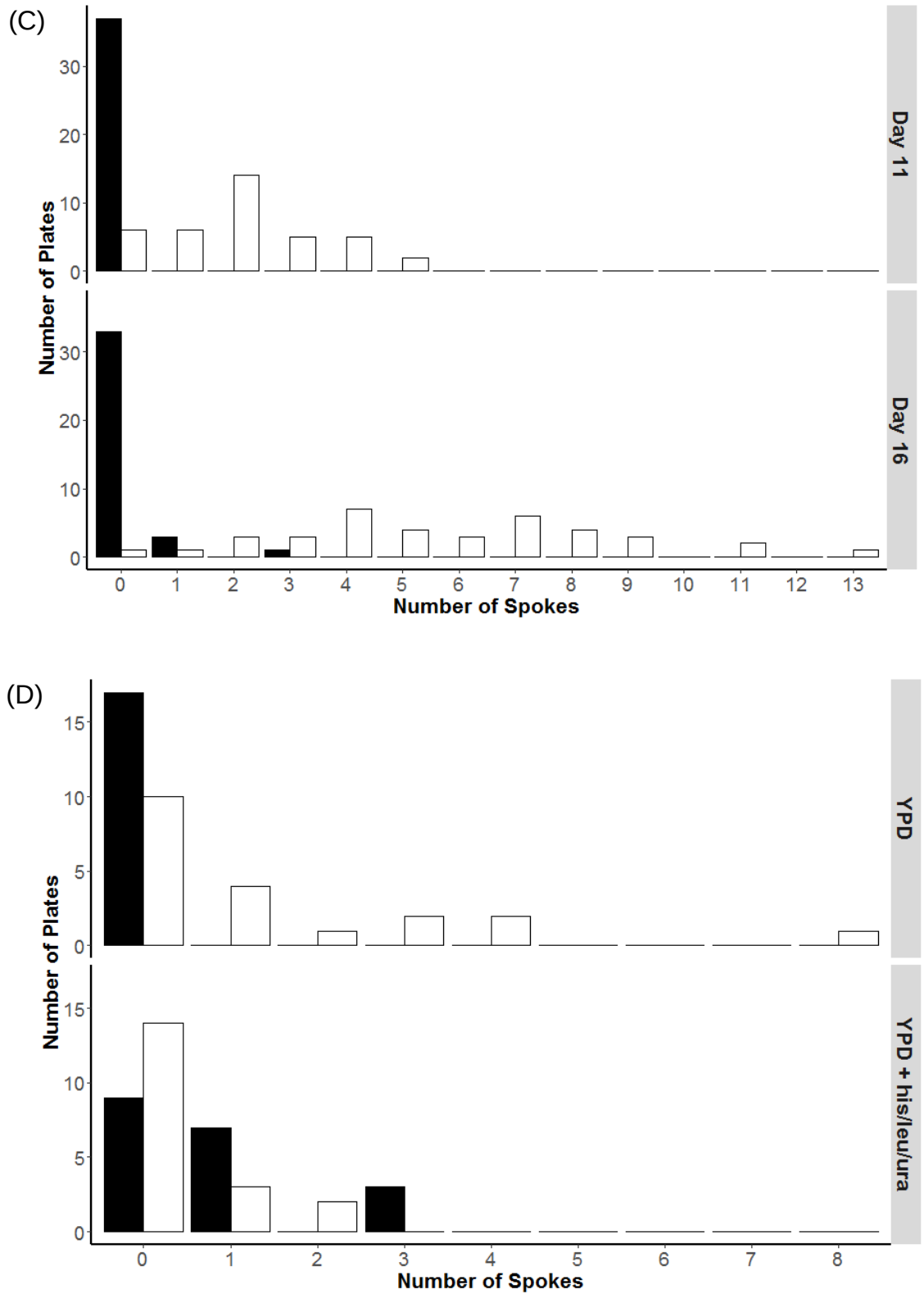

Figure 2.1: (C) Number of spokes formed by 37 auxotrophic (black) and 38 prototrophic (white) Σ1278b mats on YPD-agar (0.3%) on Day 11 and 16. (D) Number of spokes formed by auxotrophic (black) and prototrophic (white) Σ1278b mats grown on YPD-agar (0.3%) (Day 12 for prototrophic and Day 21 for auxotrophic to normalise mat size) and supplemented YPD-agar (0.3%) (Day 12).

2.5.2 Wine yeasts display diverse mat architectures

Commercial wine yeast strains L2056, AWRI796, EC1118 and PDM formed similar sized mats to those of prototrophic Σ1278b when they matured (Fig. 2.2A). Both L2056 and AWRI796 grew into circular mats and relatively smooth surfaces but those of L2056 had crinkled edges. In contrast, the mats formed by EC1118 and PDM had a petal-like shape, with curved spokes. 'Distinction', a commercial strain derived from PDM via ethyl methanesulfonate (EMS) mutagenesis (strain 22.1 in Cordente et al., 2009), formed a smaller petal-like mat, but without distinct spokes. I1, the product of a re-diploidised spore of 'Distinction', formed a round, smooth-surfaced mat similar to that of AWRI796 but smaller in size.

2.5.3 Cell morphologies in the mat rim and mat body reveal distinct lifestyles

The morphology of cells from different regions of each yeast mat, including the rim, centre, body and spokes (if present) was examined. In most cases, cells from the mat rim had a uniform, actively-dividing population (Fig. 2.2B, Fig. S1A). The cells from the mat body, centre or spokes each formed a non-uniform population made up of cells of various sizes and morphology; for example, cells with enlarged vacuoles, elongated buds and cells undergoing sporulation. The wine strains L2056 (arrows in Fig. 2.2B), EC1118 and Distinction had more sporulation events compared to other strains tested. In addition, cell-cell adhesion observed in PBS mount slides was more prevalent in the mat body compared to the mat rim (data not shown). Elongated buds of cells taken from mats were most likely non-viable as both vitality stains (DiBAC4(3) and PI) were readily taken up, DAPI staining also revealed that these contained no nuclear DNA (Fig. 2.2C).

2.5.4 Some wine strains grow invasively at the start of mat formation

Mats of Σ1278b and the commercial wine strains tested were washed off with water to observe agar invasion events. All strains (as represented by Σ1278b and 'Distinction' in Fig. 2.2D), except the strain I1, were able to grow invasively from 2 days after inoculation, indicating that agar invasion occurred at or soon after inoculation in the early stage of mat formation. Invasive growth was confirmed by needing to break the agar to reach those cells. Invasive growth only developed at the centre of the mat where the inoculum had been applied (boxes in Fig. 2.2D; plate). No correlation between mat size and agar invasion was observed. The invasive growth structures were similar between strains (Fig. 2.2D; micrograph). No filamentous cells were observed on the edge of the invasive structures.

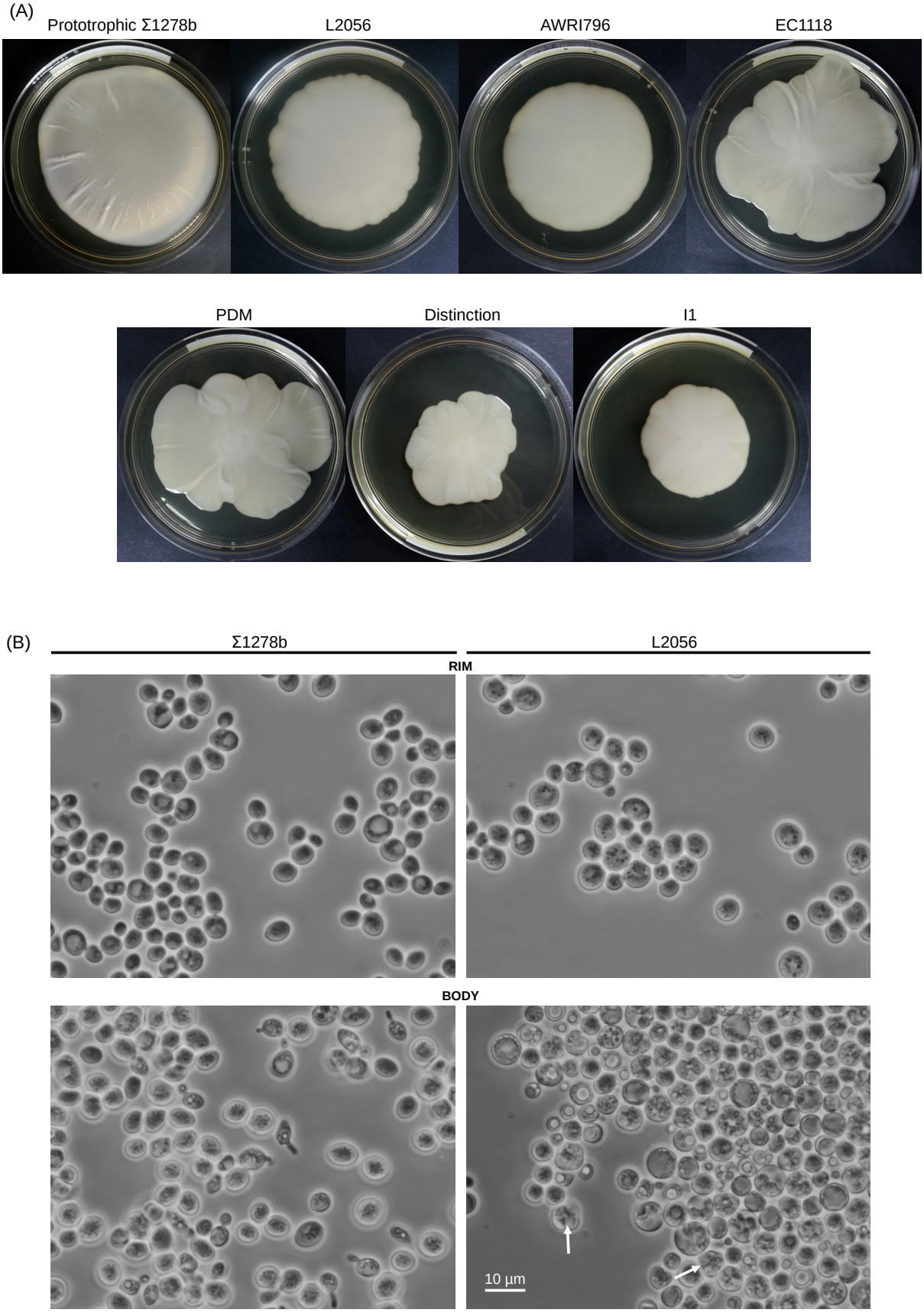

Figure 2.2: Features of yeast mats on YPD-agar (0.3%), prototrophic Σ1278b at Day 8, wine yeast at Day 13. Representative images were chosen to display the range of morphological features observed. (A) Images of mats typical of prototrophic Σ1278b and each wine yeast strain. (B) Morphologies of cells from mat rim and mat body of Σ1278b and L2056. Arrows indicate sporulation. Please refer to next two pages for (C), (D) and (E).

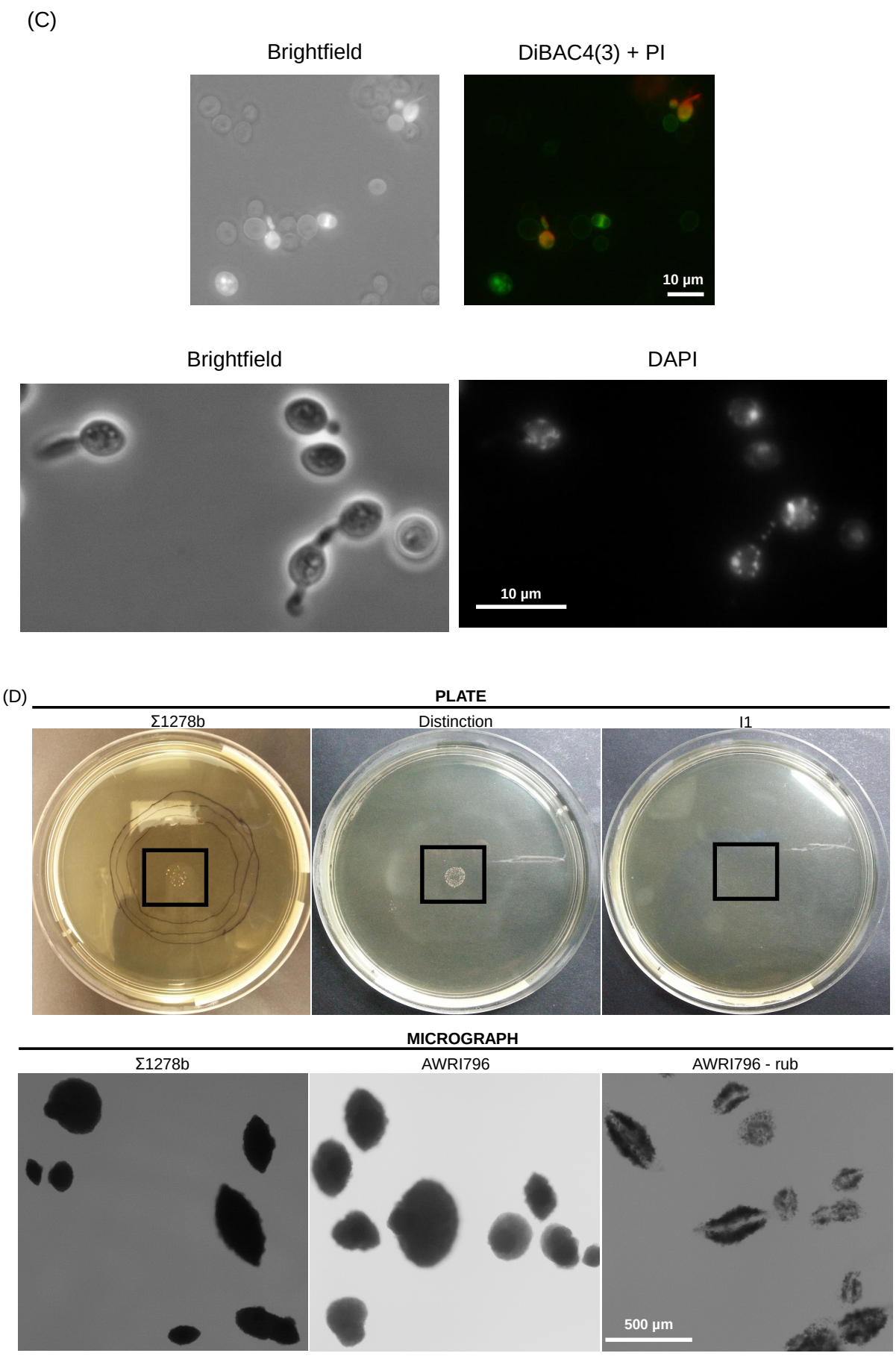

Figure 2.2: (C) Fluorescence micrographs of prototrophic Σ1278b cells with elongated buds stained with a combination of DiBAC4(3) (green) and PI (red) or L2056 cells with DAPI. Co-staining with both DiBAC4(3) and PI is visualised by an orange fluorescence. (D) Plate and micrograph images of invasively growing cells from washed yeast mats, with and without rubbing. Please refer to next page for (E).

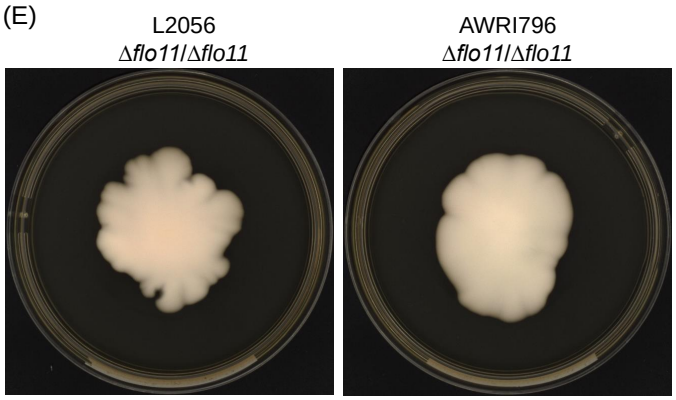

Figure 2.2: (E) Mats formed by L2056 Δ*flo11*/Δ*flo11* and AWRI796 Δ*flo11*/Δ*flo11* (Day 13).

Compared to the mats formed by wine yeasts, the Δ*flo11*/Δ*flo11* strains had reduced mat size (compare images in Fig. 2.2E with those in Fig. 2.2A; the plate size and incubation time (13 days) were the same in both cases). The L2056 mutant had more petal structures than the AWRI796 mutant.

2.5.5 Wine strain L2056 forms mats with a more rapidly expanding sector

Some L2056 mats developed a sector that expanded across the agar more quickly than the rest of the mat. Of 38 biological replicates, 55% developed a sector with such growth (Fig. 2.3A). Cells were subcultured from the typical part of the mat and the expanding sector to fresh plates (primary direct subculturing) to compare mat morphologies. Cells from the expanding sector formed a Σ1278b-like spoked mat, whilst cells from the standard part of the mat produced a smooth mat similar to the original L2056 mat (Fig. 2.3A). The spoked and smooth mat phenotypes, respectively, persisted when cells were subcultured from the primary direct subculture to fresh plates (secondary direct subculturing; Fig. 2.3A). This was independent of whether the inoculum came from the rim, body, spokes or centre (data not shown). After overnight growth of cells from the original L2056 mat in YPD broth, aimed to remove any temporary stress-induced phenotypes, the differences were still evident. However, when the inoculum came from the secondary direct subculture, the difference was minimal: here the expanding sector had more structured surfaces compared to the standard sector, which formed smooth surfaces. No distinct differences on cellular morphology between the two types of mats were observed (Fig. S1B).

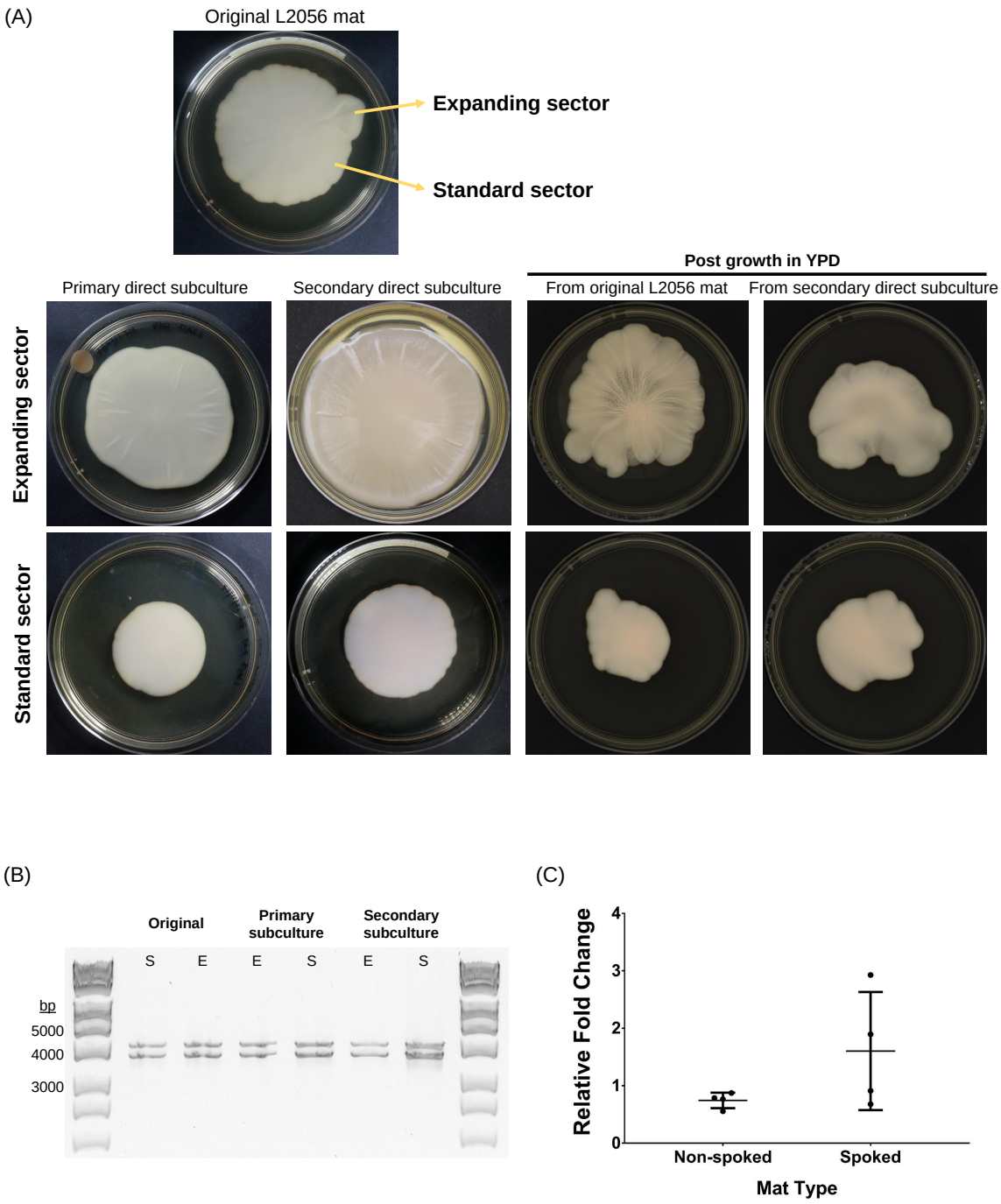

Figure 2.3: Mat morphology of an L2056 'sectoring' mat and its subcultures on YPD-agar (0.3%). (A) An example of an original L2056 mat with a more rapidly expanding sector. Expanding and standard sectors from the original L2056 mat were subcultured directly onto YPD-agar (0.3%; primary direct subculture; n = 2). Cells from the rim, body, spokes (if any) and centre of the primary subculture mats were subcultured (secondary direct subculture, n = 4 for each mat section). Expanding and standard sectors from the original mat were also grown in YPD broth prior to plating on a fresh YPD-agar (0.3%; n = 5), as were cells from the mat body of the secondary subcultures (n = 4). (B) *FLO11* PCR products from genomic DNA isolated from L2056 mats, amplified with FLO11_A and FLO11_D primers. E = expanding sector; S = standard sector. (C) Relative fold change in *FLO11* gene expression between non-spoked and spoked mats produced by cells in the expanding and standard sector of an L2056 mat (n = 4). Each replicate is indicated by an enclosed circle. The long horizontal lines represent the mean and the error bars represent standard deviation. The difference is not statistically significant.

FLO11 is well known to affect cell adhesion and filamentation, and various gene sizes have been reported to affect biofilm-forming ability (Zara et al., 2009). Previous work in this laboratory had shown that PCR amplification of *FLO11* from L2056 yields two amplicons. *FLO11* was PCR amplified from cells within expanding and standard sectors of the original, primary and secondary subcultured mats to determine if these two amplicons were lost due to a meiotic event. Two products of expected sizes were amplified in each case (Fig. 2.3B), suggesting this had not occurred. *FLO11* gene expression level was then compared between spoked and non-spoked mats produced by cells in the expanding sector and standard sector, respectively. Two out of four spoked mats showed increased *FLO11* gene expression by two- and three-fold compared to non-spoked mats (Fig. 2.3C).

2.5.6 Plastic adhesion

Auxotrophic Σ1278b showed the most adhesion to plastic in both low and sufficient glucose conditions (Fig. 2.4). Prototrophic Σ1278b and L2056 displayed a modest increase in plastic adhesion ability in 0.1% glucose compared to that in 2% glucose, while AWRI796 was not affected by this nutrient change and showed less adhesion compared to Σ1278b Δ*flo11*/Δ*flo11* after 3 and 6 h in 0.1% glucose.

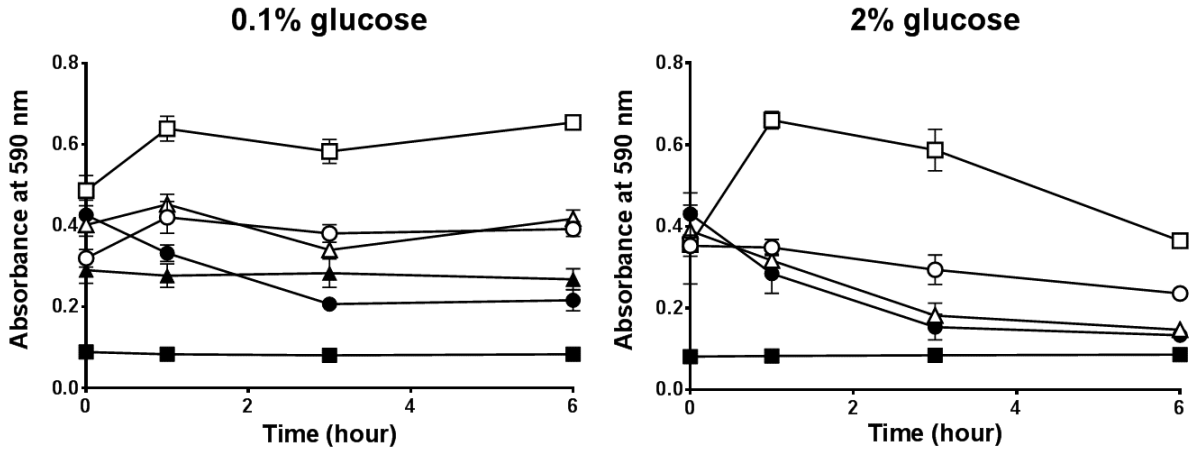

Figure 2.4: Plastic adhesion of laboratory and wine strains grown in SC medium with either 0.1 or 2% glucose. Absorbance at 590 nm was measured after 0, 1, 3 and 6 h of incubation. Each data point represents the mean of six samples: (□) auxotrophic Σ1278b, (○) prototrophic Σ1278b, (△) L2056, (●) AWRI796, (▲) prototrophic Σ1278b Δ*flo11*/Δ*flo11*, (■) no cells (control). The error bars represent standard deviation and are included for all time points.

2.5.7 Wine yeast grow invasively and conduct fermentation on grape pulp soft agar

Σ1278b and several commercial wine yeast strains were plated onto grape pulp agar for mat assays. Instead of forming a large mat, grape pulp induced fermentation. Bubble-forming mats were observed on Day 3. There was no structured morphology observed on the culture surfaces (Fig. 2.5A). On Day 9, gas was observed trapped underneath the agar (Fig. 2.5B) which raised the agar, resulting in some surface culture (e.g. Σ1278b) coming into contact with the plate lid (Fig. 2.5A). Occurrence of cell adhesion and invasive growth can be seen after gently washing with water. Compared to the YPD mat assay, where the invasive growth only occurred in a few patches (Fig. 2.2D), the invasive growth in grape pulp agar was extensive (Fig. 2.5B; post-wash, cross-section).

The Brix of grape pulp was 17°, which means 75% pulp agar would have approximately 12.75° (12.7% sugar). To investigate whether the fermentation phenotype was solely induced by the high sugar concentration in grape pulp, YPD containing 10% total sugar (equimolar glucose and fructose) was prepared for mat assays. The high-sugar YPD-agar, however, did not induce the fermentation phenotype observed on grape pulp (Fig. 2.5C). Flat mats instead of bubble-forming mats were observed.

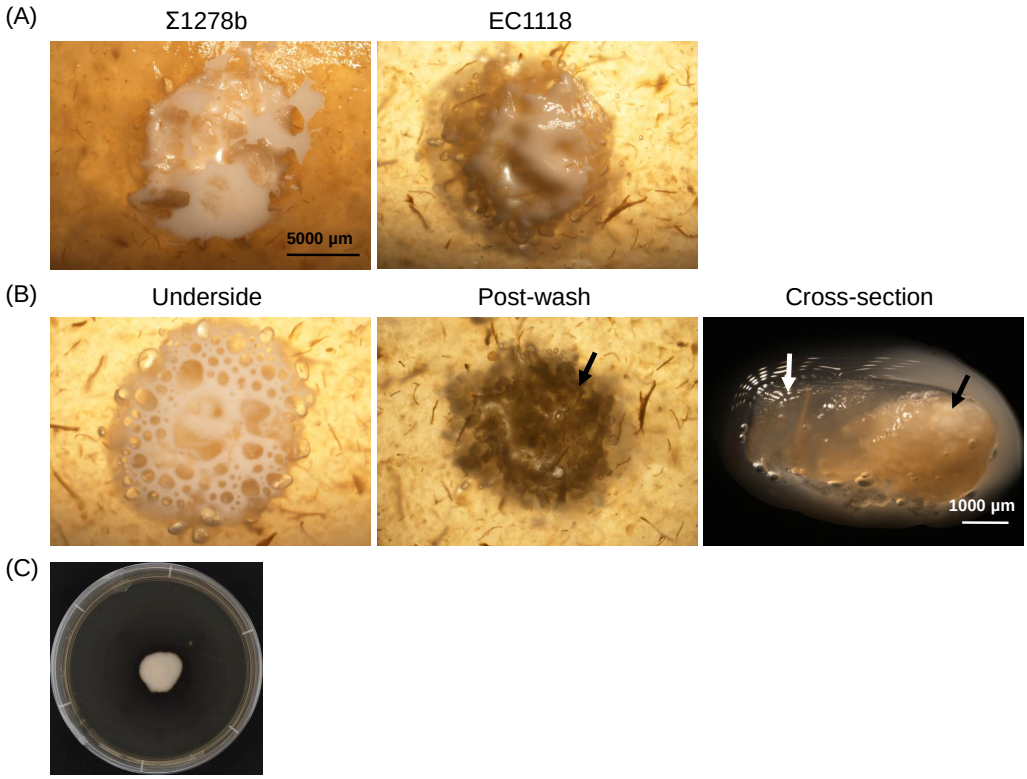

Figure 2.5: Grape-pulp mat assay. (A) Mat images of Σ1278b and a representative wine strain, EC1118, on grape pulp agar (0.3%) at Day 9. (B) Images of EC1118 from the underside of the agar, post-wash and cross-section. Black arrows indicate invasively growing cells; white arrow indicates the grape pulp agar. (C) Day 3 image of EC1118 on high-sugar (10%) YPD-agar (0.3%).

2.5.8 Wine strain L2056 forms initial attachment on winery hose soft plastic

To begin to provide some insight into the potential significance of adhesion in a winemaking context, two assays were performed to investigate whether wine yeast are able to adhere to the soft plastics of commonly used winery hose. The first assay was modified from that used above to monitor plastic adhesion. All four strains tested, Σ1278b, L2056, AWRI796 and prototrophic Σ1278b Δ*flo11*/Δ*flo11* showed no adhesion. The second assay was performed in a 50 mL tube with shaking to imitate juice flowing through a winery hose. Σ1278b and L2056 were observed to have initial attachment to the hose plastic, but this was not true for AWRI796 and prototrophic Σ1278b Δ*flo11*/Δ*flo11* (Fig. 2.6). This matches the plastic adhesion result in plates, that AWRI796 did not adhere well, Σ1278b had the most adhesion followed by L2056 (Fig. 2.4).

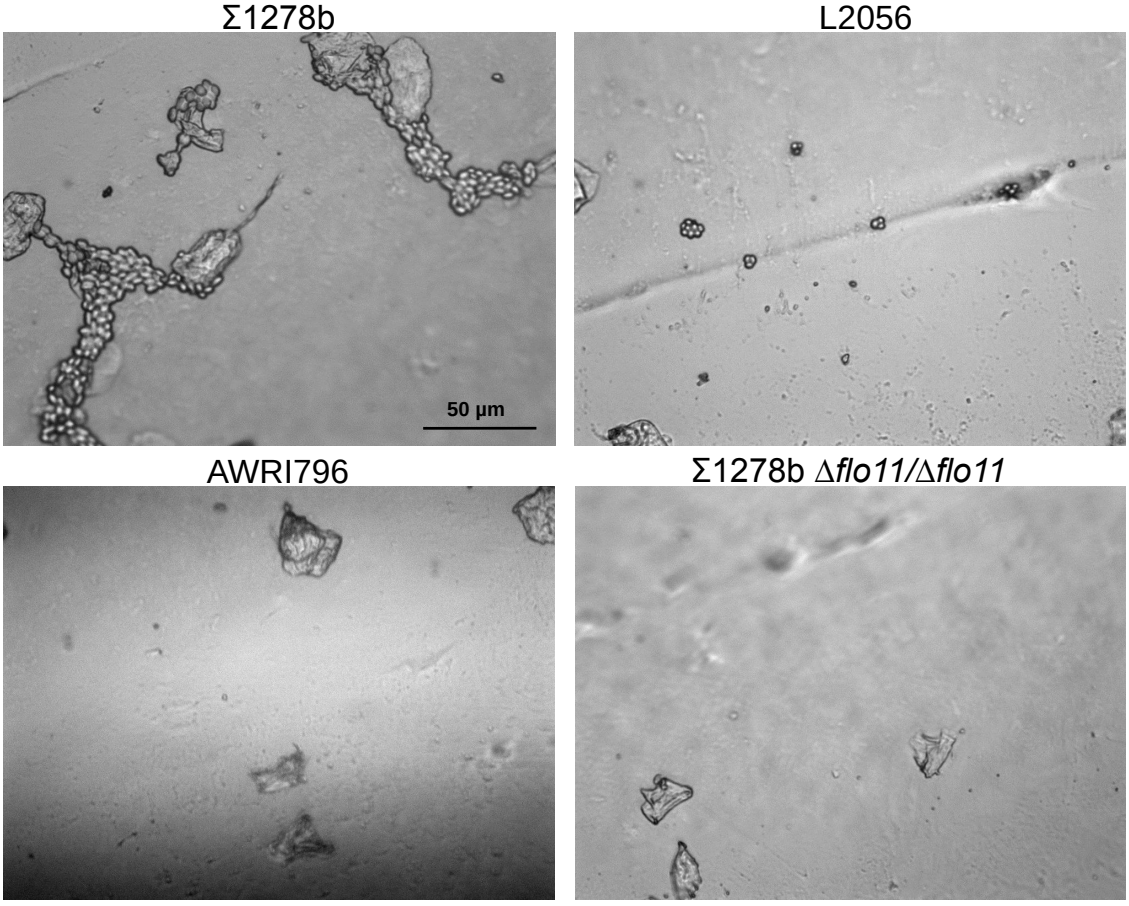

Figure 2.6: Cell adhesion on plastic of a common winery hose, Red Heliflex. Images of plastic after four days of incubation in SLAD culture with shaking and after rinsing with water to remove unbound cells.

2.6 Discussion

Similar to the wild *S. cerevisiae* strains isolated from wine grapes and must (Sidari et al., 2014), commercial wine yeast strains were found to form varied mat sizes with structured architecture that differed from those formed by the laboratory yeast, Σ1278b. This may be explained by the genome differences between wine strains (Borneman et al., 2008, 2011, 2016). In this study, EC1118, PDM, Distinction and I1 are closely related whereas L2056 and AWRI796 are different from each other and from the others. Other wild yeasts have also been shown to produce mats with morphologies that did not conform with the standard 'hub and spokes' structure. For example, the mats formed by wild flor strains, V80, V23 and M23 (Zara et al., 2009), did not fully cover the agar plate and had no spoke formation, similar to 'Distinction' and I1 in this study, but differing in rim shape. The baking yeast YS2 (Hope and Dunham, 2014) formed a relatively larger, smooth surface mat, like AWRI796. Highly complex mats, which were formed by soil yeast YPS128 and bee yeast UWOPS05-227.2 (Hope and Dunham, 2014) were distinct from each other as well as from any of the strains in this study. Deletion of the *FLO11* gene in two wine strains, L2056 and AWRI796, resulted in smaller sized mats, confirming that *FLO11* is also required for a full-sized wine yeast mat formation.

The ability to form mats by a panel of commercial wine yeast strains suggests the ability to adhere to surfaces in the wine environment, which could include equipment, grapevine and grape berries. It could also help these yeast to form associations with other microbes. The results in grape-pulp mat assay suggest that commercial wine yeast could adhere and even invade grapes for colonisation. The winery hose adhesion trial also provides an indication of an initial attachment to soft plastic by wine yeast. In addition to the ability to co-flocculate with other wine-associated yeast strains (Rossouw et al., 2015), the adhesion and invasion properties shown in this study could drive the microbial population resident in the vineyard and winery, and subsequently affecting the population in fermentations. This may explain the previous reports that commercial strains contribute to the yeast population in uninoculated fermentations (Hall et al., 2011; Martiniuk et al., 2016; Scholl et al., 2016).

Mat formation can be considered as an expansion of colony formation. Analysis of the cellular morphologies between the mat rim and body reveals distinct lifestyles between these populations. The replicative phase is characterised by many actively dividing cells and these were present in the mat rim of all yeast mats examined. The non-replicative phase as observed in mat body is when cells are no longer proliferating, similar to colonies growing on rich medium. Yeast biofilm colonies described by Váchová et al. (2011) also have distinct cell types on different parts of the structure: non-dividing cells on the surface of the aerial region and dividing cells inside the colonies. However, unlike biofilm colonies, mats are thin and have no aerial regions. The cell type differences were more distinct between mat body and rim. Cells of the mat body were heterogenous. They included

cells that were sporulating, had elongated buds or enlarged vacuoles. This heterogeneous population has been described in aging yeast colonies, which consist of upper and lower regions with different stress resistances (Palková et al., 2014). The diversity of stress tolerance within a community arises from metabolic specialisation and cooperation between cells (Campbell et al., 2016). This mixture of differentiated cells within the mat body may contribute to supporting the survival of cells in the expanding edge *i.e.* mat rim.

An interesting cell type was found through microscopic observation in the mat body. Cells with an elongated bud were visualised with nuclear staining, the results suggesting the cell cycle arrested before nuclear migration (no nuclear DNA in elongated buds shown in Fig. 2.2C). Gladfelter and colleagues (2005) have shown that elongated bud morphology occurs due to Swe1p-mediated G_2 arrest. Whilst other studies (Gladfelter et al., 2004; Homoto and Izawa, 2016) have shown this morphology is often associated with septin mislocalisation, Gladfelter and colleagues (2005) also showed G_2 arrest could aggravate the effect of septin disorganisation. Ethanol has been shown to increase Swe1p expression, which inhibits Cdc28p kinase activity and subsequently causes G_2 arrest cell cycle delay (Booher et al., 1993; Kubota et al., 2004). There may be environmental signals other than ethanol causing either G_2 arrest or septin mislocalisation during mat formation, which requires further investigation.

Similar to the report by Rodriguez et al. (2014), L2056 formed crinkled-edge mats. In addition, this study also reports, for the first time, that mats formed by L2056 can be sectored (Fig. 2.3A). When the original L2056 mat was subcultured, cells from the expanding growth sector formed a typical Σ1278b 'hub and spokes' mat whereas the standard growth sector formed a non-spoked mat, similar to the original L2056 mat. Sectoring colonies have been observed in other fungi. For example, it is an indication of phenotypic switching in haploid *Candida tropicalis* (Porman et al., 2011), where the opaque sector shows more mating-competence. The fungus *Metarhizium anisopliae* forms a sector that has lost sporulation capacity, activity of certain enzymes, and changes in secondary metabolite profiles (Ryan et al., 2002). Sectoring can also occur when a fungus mutates and adapts to become drug resistance (He et al., 2014). In this study, two types of mats were formed persistently after two cycles of direct subculturing as well as subculturing after re-growing in rich medium. Since Flo11p is known to be important for forming 'hub and spokes' in Σ1278b mats and the gene length is related to the biofilm-forming ability in flor strains (Zara et al., 2009), the length of *FLO11* genes in cells of the two types of mats was studied. No difference in *FLO11* allele sizes of either sectors in the original L2056 mat, primary or secondary subcultures was seen (Fig. 2.3B), suggesting no meiotic events had occurred. *FLO11* expression levels were then compared between the two types of mats. Two out of four spoked mats showed an increase in expression compared to non-spoked mats (Fig. 2.3C), which suggests *FLO11* may be involved in mat expansion and/or spoke formation through differential expression, similar to the model suggested by Regenberg et al. (2016). Differential expression of *FLO11* in Σ1278b was shown to generate Flo11^+ and Flo11^- cells, containing adhesive and non-adhesive cells, in

mat formation (Regenberg et al., 2016). The differentiated mat had a spoked structure and was larger than the undifferentiated Flo11$^-$ mat. This may explain the formation of the rapidly expanding sector in the original L2056 mat, being due to the differentiated state. This differentiated state was carried on to the subcultures and resulted in spoked mats (Fig. 2.3A). Since L2056 has two unequal sized *FLO11* alleles, it is also possible that the differential expression involves switching of the expression of either allele.

While most mat studies use auxotrophic Σ1278b strains, in this study auxotrophic Σ1278b did not form mat structures as widely reported. However, the 'hub and spokes' structure was formed with extended incubation or nutrient supplementation (Fig. 2.1C and D). There have been cases when supplementation did not compensate for auxotrophies (Corbacho et al., 2011). The particular amino acids used for supplementation may also influence physiological regulation because some amino acid biosynthesis pathways are connected (Niederberger et al., 1981). In the plastic adhesion experiment, adhesion ability was affected by auxotrophies – the auxotrophic Σ1278b was shown to be more adhesive than prototrophic Σ1278b (Fig. 2.4). Changes in metabolic flux induced by auxotrophic vs prototrophic states, may interfere with system-wide regulatory processes (Grüning et al., 2010). Therefore, it is suggested that prototrophic strains are more representative of the natural state and should be used in future studies.

It is noticeable that the number of spokes formed by Σ1278b in this study was less than those reported previously (Reynolds and Fink, 2001). This was probably due to the size of the inoculum. Toothpick inoculation (widely used in other mat publications) generated > 10 spokes while inoculation of 800 and 50 cells yielded almost none (Fig. S2). In order to control initial cell numbers, an inoculum size of $5,000$ cells was chosen, which produced representative spokes.

Despite showing a variety of mat structures by commercial wine yeast, this study also demonstrated broad responses accompanied with mat features by visualising cell morphologies and growth modes. The findings contribute to a better understanding of commercial yeast lifestyle on biofilms and adhesion with respect to wine environments. The observations may provide an explanation for the survival of commercial strains which might influence the natural microflora in the vineyard and winery in the long-term.

2.7 Funding

This work was supported by Wine Australia [GWR Ph1305] awarded to ELT and Australian Research Council [DP 20111529] awarded to VJ and SGO, which also supported JFS and JMG. ELT was supported by a University of Adelaide Graduate Research Scholarship.

Conflict of interest: None declared.

2.8 Acknowledgements

Prototrophic Σ1278b, auxotrophic Σ1278b and A Σ1278b Δ*flo11*/Δ*flo11* were kindly donated by Dr Charles Boone (University of Toronto). The authors thank the Australian Wine Research Institute for providing the Red Heliflex hose and access to ProtoCOL 3, and Dr Michelle Walker (University of Adelaide) for generating strain I1.

2.9 Supplementary Data

2.9.1 Methods

Mat area measurement from ProtoCOL 3 images

1. Capture images as described in ProtoCOL 3 manual. Exposure was set at 60 ms.
2. Download and install Fiji from http://imagej.net/Fiji/Downloads.
3. Open the application.
4. Open an image that needs to be measured.
5. Click **Analyze** from the menu, select **Set Scale**. Enter 583 pixels = 9 cm, check **Global** and press **OK**. Now the image and the following images opened within this session have been calibrated.
6. To convert into a black and white image, click **Image** from the menu, choose **Adjust** and select **Threshold**. Change the **Threshold colour** to **B&W**, press **Close**.
7. Click **Wand (tracing) tools** from the icon menu, move cursor to anywhere in the mat (black area), click on the mat. This will select the thresholded object – mat.
8. Click **Analyze** from the menu, select **Set Measurement**. Check **Area** and press **OK**.
9. To measure, click **Analyze** from the menu, select **Measure**. A result table with the area measurement will pop up. Save the results for future use and close all the boxes.
10. To measure subsequent images in the same session, open a new image, **Image** > **Adjust** > **Threshold** > **Close**, click on the mat, **Analyze** > **Measure**.

2.9.2 Figures

Figure S1: Cellular morphology from yeast mats grown on YPD-agar (0.3%). (A) Prototrophic Σ1278b and wine strains (B) L2056 subcultures. Scale bars, 50 μm. N/A = not applicable.

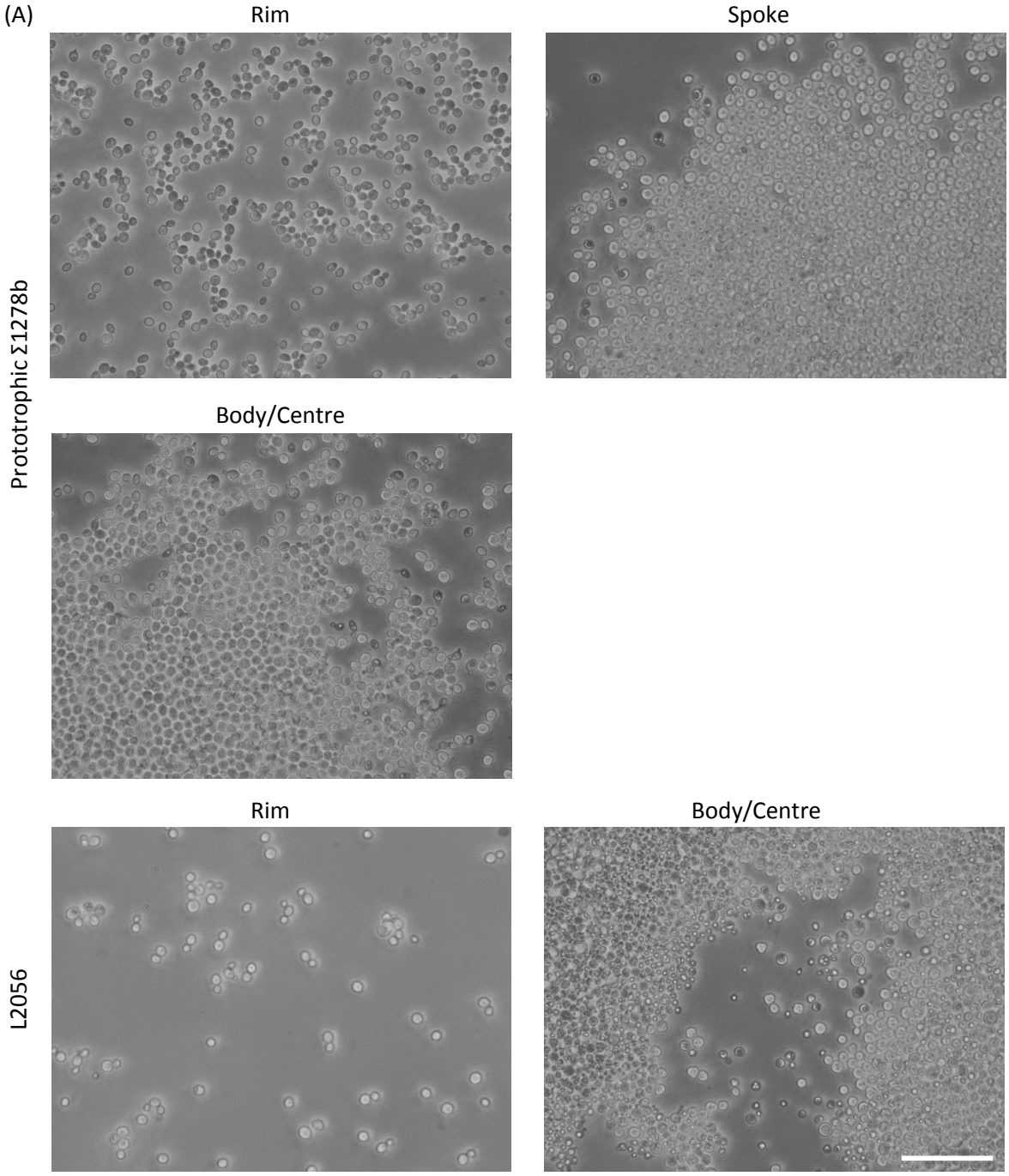

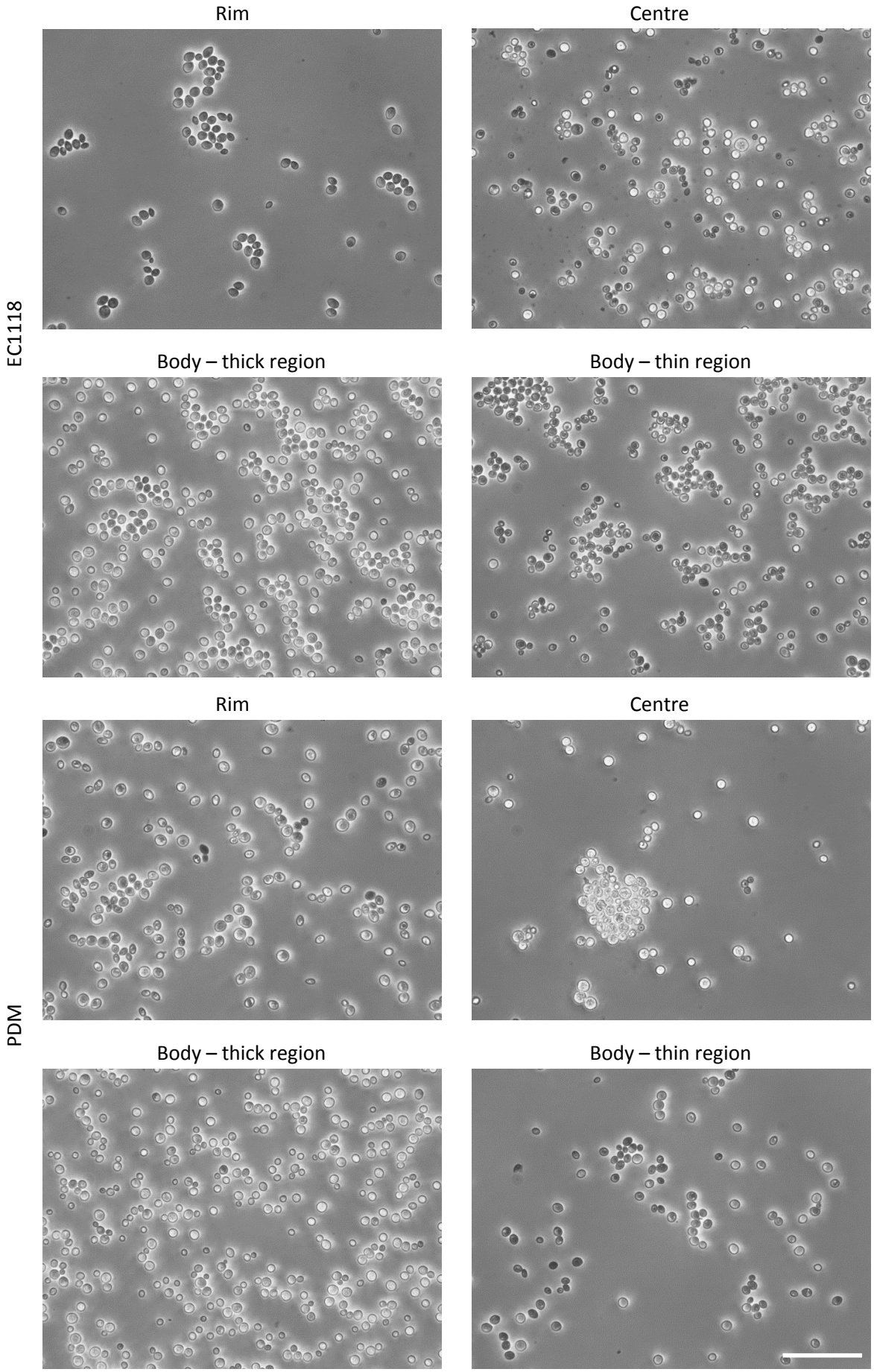
Rim
Centre
EC1118
Body – thick region
Body – thin region
Rim
Centre
PDM
Body – thick region
Body – thin region

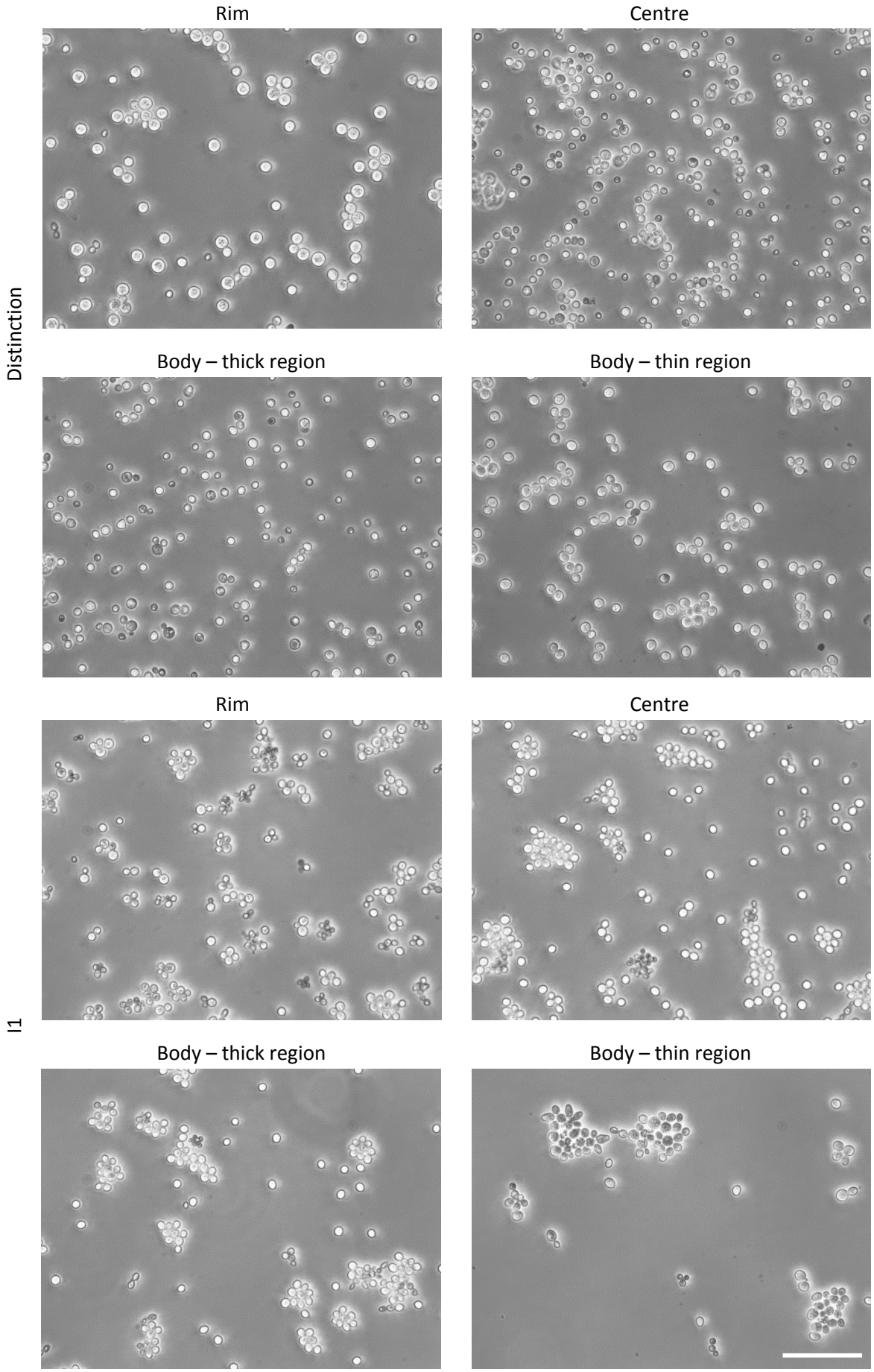
Rim
Centre
Distinction
Body – thick region
Body – thin region
Rim
Centre
I1
Body – thick region
Body – thin region

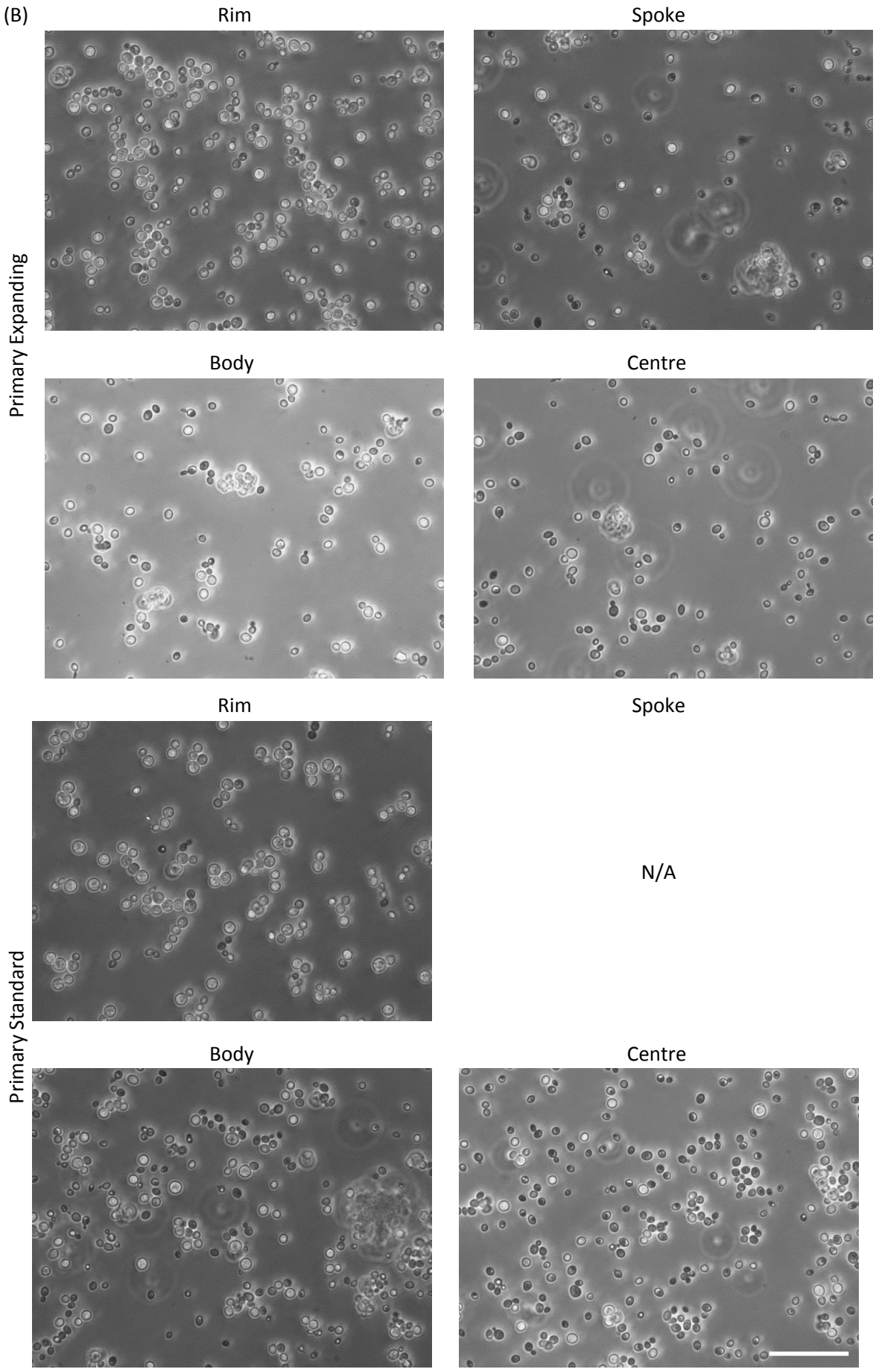
(B)
Rim
Spoke
Primary Expanding
Body
Centre
Rim
Spoke
N/A
Primary Standard
Body
Centre

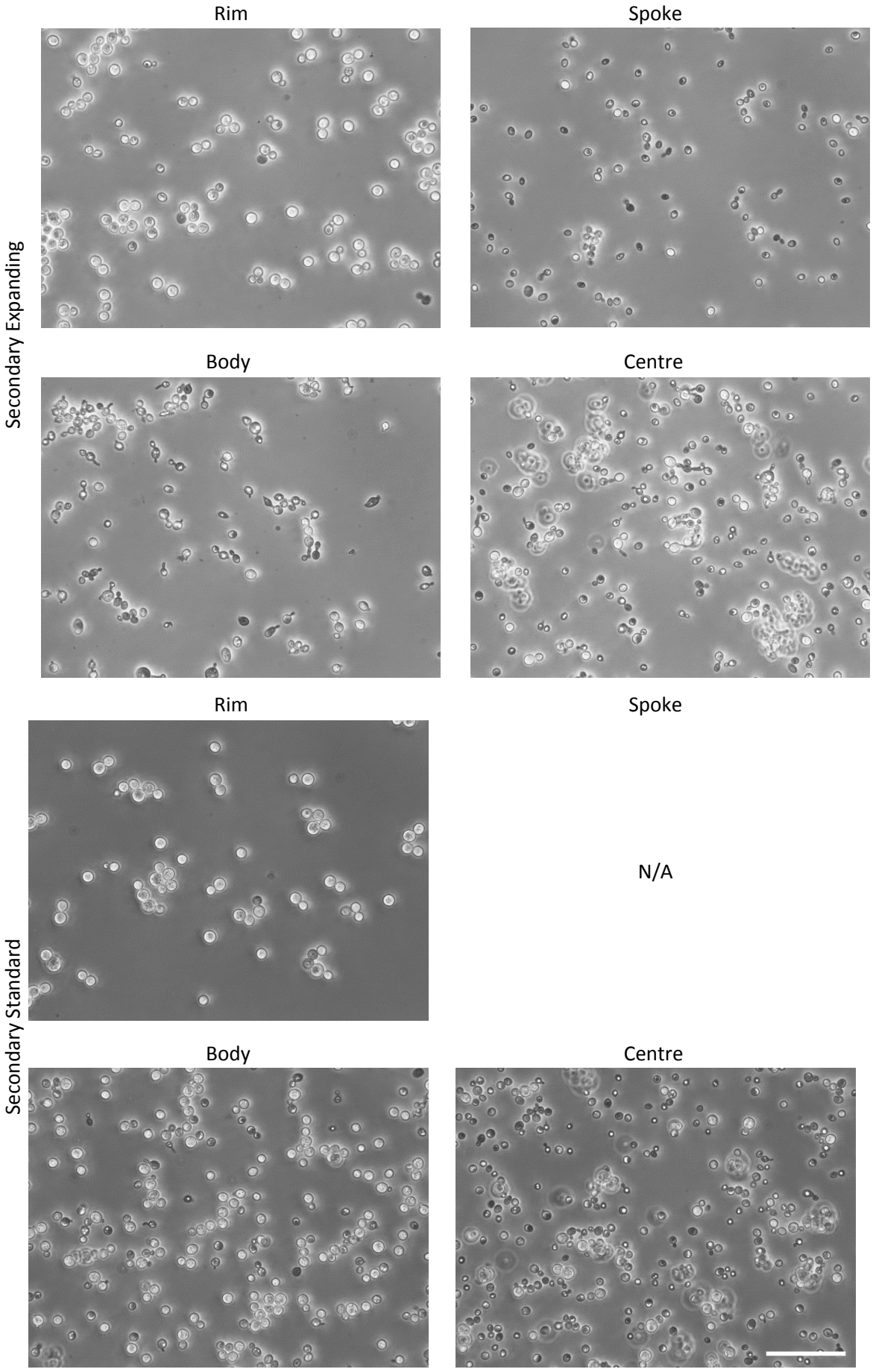
Rim
Spoke
Secondary Expanding
Body
Centre
Rim
Spoke
N/A
Secondary Standard
Body
Centre

Figure S2: Mat formation of prototrophic Σ1278b on YPD-agar (0.3%) with inocula from either a toothpick with cells or cell suspensions (800 or 50 cells per 5 μL).

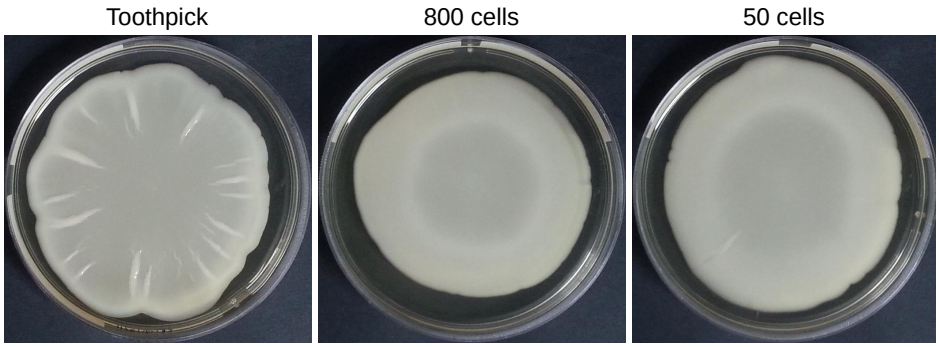

Chapter 3

Mat formation in a low nitrogen medium

Contextual statement

Chapter 2 illustrated a variety of mat features for several commercial wine yeast strains. The manuscript in this chapter evaluated the response of wine yeast during mat formation under limiting nitrogen conditions and several factors that could affect the response, which corresponds to the second aim (p. xiii) of this project. Wine yeast assimilate nitrogen since it is an essential nutrient enabling growth. Fermenting wine musts commonly utilise all available nitrogen, often before all sugars are catabolised, the depletion of nitrogen from rotting grapes on the vine is expected to be similar. Thus, whether it be a fermenting must in a winery or grapes in the vineyard, exposure of yeast to an environment with significantly depleted nitrogen is common. Previous studies with a filamentation focus have used solid medium (2% agar) with very low nitrogen as it stimulates diploid cells to undergo pseudohyphal growth. The availability of nitrogen could also be an important factor in mat formation on less dense media (0.3% agar). Preliminary studies were performed to refine methodology used in this section of work, including optimal inoculation rate and the effect of a putative cell signalling compound (Appendix B), in order to establish the scope of work undertaken.

Statement of Authorship

Title of Paper	Factors influencing filamentous and invasive growth of yeast cells in mat formation in a low nitrogen environment
Publication Status	☐ Published ☐ Accepted for Publication ☐ Submitted for Publication ☑ Unpublished and Unsubmitted work written in manuscript style
Publication Details	Written in manuscript style for FEMS Yeast Research

Principal Author

Name of Principal Author (Candidate)	Ee Lin Tek
Contribution to the Paper	Performed all experiments and data analysis, interpreted data, and wrote manuscript.
Overall percentage (%)	80%
Certification:	This paper reports on original research I conducted during the period of my Higher Degree by Research candidature and is not subject to any obligations or contractual agreements with a third party that would constrain its inclusion in this thesis. I am the primary author of this paper.
Signature	Date 04/09/17

Co-Author Contributions

By signing the Statement of Authorship, each author certifies that:

i. the candidate's stated contribution to the publication is accurate (as detailed above);

ii. permission is granted for the candidate in include the publication in the thesis; and

iii. the sum of all co-author contributions is equal to 100% less the candidate's stated contribution.

Name of Co-Author	Jennie M. Gardner
Contribution to the Paper	Supervised development of work, helped in data interpretation and editing of the manuscript.
Signature	Date 6/09/17

Name of Co-Author	Joanna F. Sundstrom
Contribution to the Paper	Supervised development of work, helped in data interpretation and editing of the manuscript.
Signature	Date 4/09/2017

Name of Co-Author	Stephen G. Oliver

Contribution to the Paper	Supervised development of work and helped in data interpretation.
Signature	Date: 30.08.17

Name of Co-Author	Vladimir Jiranek
Contribution to the Paper	Supervised development of work, helped in data interpretation and editing of the manuscript.
Signature	Date: 4.9.17

Please cut and paste additional co-author panels here as required.

Factors influencing filamentous and invasive growth of yeast cells in mat formation in a low nitrogen environment

Ee Lin Tek[1], Jennie M. Gardner[1], Joanna F. Sundstrom[1], Stephen G. Oliver[2], Vladimir Jiranek[1,3*]

[1]Department of Wine and Food Science, University of Adelaide, Waite Campus, South Australia 5064, Australia.
[2]Department of Biochemistry & Cambridge System Biology Centre, University of Cambridge, United Kingdom.
[3]Australian Research Council Training Centre for Innovative Wine Production.

*Corresponding author: PMB 1, Glen Osmond, South Australia 5064, Australia. Tel: 618-8313-6651; E-mail: vladimir.jiranek@adelaide.edu.au

3.1 Abstract

Saccharomyces cerevisiae forms complex mat structures on low agar YPD. In response to nutrient limitation, budding yeast can become adherent, switch to a filamentous form and grow invasively. Accordingly, mat structure is affected *i.e.* a filamentous mat is formed on a glucose-limited medium. In this study, a proportion of yeast in a mat switched to filamentous and invasive growth on a nitrogen-limited medium. Also, increasing nitrogen content increased cellular growth and mat size. The formation of filamentous and invasive foci within a mat was enhanced by ethanol and hydrogen sulfide but was inhibited by aromatic alcohols and sulfite. As previously reported, filamentous growth was also affected by neighbouring mats. This growth transition to filamentation and invasion, in low nitrogen low-density agar, may be a response adapted to the environmental niche typical of yeast, rotting fruit, which has low density and decreasing nutrients.

3.2 Keywords

Filamentous growth; invasive growth; low nitrogen; mats; aromatic alcohols; sulfide and sulfite

3.3 Introduction

Saccharomyces cerevisiae forms mats on a low-density agar (0.3%) medium (Reynolds and Fink, 2001). Mat structures are complex and diverse and depend on the strain background (Hope and Dunham, 2014). The laboratory yeast strain Σ1278b generates a mat with characteristics of a central hub and radiating spokes. Hub and spoke formation can be delayed if glucose concentration is increased (Reynolds et al., 2008). Conversely, a filamentous mat is formed if glucose is removed (Karunanithi et al., 2012). The direction of filamentous growth has also been shown to be affected by the presence of a neighbouring mat (Karunanithi et al., 2012).

Yeast also undergo filamentous and invasive growth on medium-density agar (2%) when nitrogen is limited (Gimeno et al., 1992). Hyphal-like elongated cells can be stimulated by a number of fusel alcohols, which are by-products from catabolism of some amino acids (Dickinson, 1994, 1996). Conditioned medium from a Σ1278b stationary-phase culture was reported to stimulate filamentous and invasive growth (Chen and Fink, 2006). The group demonstrated that tryptophol and 2-phenylethanol were acting as quorum sensing molecules that enhanced the filamentous and invasive phenotype on low nitrogen agar.

Hydrogen sulfide (H_2S) is associated with nitrogen deficiency during fermentation

(Jiranek et al., 1995). Nitrogen deficiency can cause a stuck fermentation. This is often difficult to restart even when additional nitrogen is supplied. Many reports have suggested that this is largely based on delayed nitrogen ameliorations being ineffective due to reduced hexose transporter activity. However, there is evidence that H_2S may also act as a cell-cell signalling molecule (Lloyd, 2006). Its presence has been postulated to alter the metabolic clock of the yeast population (Sohn et al., 2000). Microarrays have shown significant overlap of gene expression in the presence of H_2S and a stress response (Jia et al., 2011). It is possible that the presence of by-products such as H_2S could inhibit yeast cell metabolism resulting in reduced fermentation of residual sugars. Like tryptophol and 2-phenylethanol, H_2S could potentially be a signalling molecule that affects other nitrogen-deficient responses such as filamentous and invasive growth. Interestingly, within the sulfate assimilation pathway, the precursor of sulfide is sulfite, which has been shown to block invasive growth (Zupan and Raspor, 2010). Several mechanisms have been proposed how sulfite inhibits growth (see review in Divol et al., 2012). Briefly, these include the reduction of intracellular ATP by activating ATPase, inhibition of key metabolic enzymes such as GAPDH, binding to co-enzymes, co-factors and to a number of metabolites including acetaldehyde (Schimz and Holzer, 1979; Schimz, 1980; Hinze and Holzer, 1986; Carmack et al., 1950; Rankine and Pocock, 1969). These could lead to cell death as energy metabolism is negatively impacted.

Since yeast cells are able to produce filamentous and invasive mats on glucose-limited low-density (0.3%) agar and limited nitrogen can induce this form of growth on medium-density (2%) agar, a hypothesis is made that filamentous and invasive mats would form when nitrogen is scarce on low-density agar. Agar of a lower density has similar consistency to the material where yeast are commonly found in nature; fruit, e.g. grape pulp, and thus is relevant when considering this microorganism's environmental niche. Yeast growing on grapes would deplete nutrients in their immediate vicinity and may switch to filamentous and invasive growth modes to enhance survival. With this in mind, this study investigated mat formation in a low nitrogen environment by *S. cerevisiae* including Σ1278b and several wine yeast strains to see if the response is widespread for different genetic backgrounds. The addition of compounds or factors known or hypothesised to influence filamentous and invasive growth such as the presence of a neighbouring mat, tryptophol, 2-phenylethanol, H_2S and sulfite was also evaluated.

3.4 Materials and Methods

3.4.1 Yeast strains and media

Yeast strains used in this study are listed in Table 3.1. Strain I1 was generated by transformation (Gietz and Schiestl, 2007) of a *Kan*MX cassette (generated with PCR using primers 5′-TCGAACACTGTCATTTGAAATTATG-3′ and 5′-GGACATTTGTAGAAAA

TAGGCTCAA-3′, and genomic DNA of the BY4741 Δ*sul1* strain; Wach et al., 1994; Winzeler et al., 1999) into the commercial wine yeast 'Distinction', followed by sporulation, dissection and isolation of the re-diploidised wild type progeny.

Table 3.1: Yeast strains used in this study.

Yeast strain	**Genotype and comments**	**Reference**
Prototrophic Σ1278b	Wild type laboratory strain; diploid	Ryan et al. (2012)
L2056	Commercial wine yeast strain; diploid	Lallemand Australia
EC1118	Commercial wine yeast strain; diploid	Lallemand Australia
AWRI796	Commercial wine yeast strain; diploid	Mauri Yeast Australia
PDM	Commercial wine yeast strain; diploid	Mauri Yeast Australia
Distinction	Commercial wine yeast strain; diploid	Mauri Yeast Australia
I1	Diploid derivative of Distinction	This study
BY4741 Δ*sul1*	*MAT*a *his3*Δ*1 leu2*Δ*0 met15*Δ*0 ura3*Δ*0 sul1*Δ*::Kan*MX	Thermo Fisher Scientific Australia

Synthetic Low Ammonium Dextrose (SLAD; 0.17% Yeast Nitrogen Base without amino acids and ammonium sulfate (Beckton Dickinson; Cat No. 233520), 2% glucose and 50 μM ammonium sulfate) was filter sterilised as a 10× stock and diluted as required with sterile ultrapure water. Bacto agar (BD; Cat No. 260001) was washed twice in 800 mL ultrapure water in a 1 L Schott bottle, swirled to mix and rested for 15 min before decanting, followed by autoclaving. SLAD low-density agar (0.3%) used in mat assays was prepared by mixing equal volumes of 2× SLAD and 0.6% molten Bacto agar, and where indicated, the addition of one or more of the following chemicals: 0.05% v/v ethanol, 50 μM tryptophol, 50 μM 2-phenylethanol, 0.4 mg L^{-1} sodium sulfide ($Na_2S.9H_2O$) and/or 0.01% w/v sodium metabisulfite ($Na_2S_2O_5$). Tryptophol and 2-phenylethanol stock solutions (50 mM) were prepared in 50 mL of 25% v/v ethanol making the final concentration of ethanol in SLAD agar containing aromatic alcohols 0.05%. All chemicals were sourced in ultrapure form from Sigma Aldrich. Aliquots of 10 mL were poured onto 60 mm polystyrene Petri dishes (Techno Plas; Cat No. S6014S10). Media were only made and poured one day prior to plating.

Conditioned medium (CM) was prepared as follows. Yeast were inoculated from glycerol stocks and cultured in 25 mL SLAD in two separate Erlenmeyer flasks for 48 h at 28 °C with agitation. Cultures were mixed and centrifuged at $20,817 \times g$ for 10 min to collect the supernatant. Supernatant was tested for nitrogen (ammonia) and glucose content using enzymatic assays (see below). The supernatant was supplemented up to the original nitrogen (50 μM ammonium sulfate) and glucose (2%) content in SLAD and filter sterilised.

3.4.2 SLAD mat assays

Yeast were inoculated from glycerol stocks into 10 mL SLAD and incubated for 48 h at 28 °C with agitation. Cells were subsequently inoculated into 25 mL of fresh SLAD at 1×10^4 cells mL^{-1} and incubated for 16–18 h to obtain an exponential-phase culture.

The exponential-phase culture was diluted in Phosphate Buffered Saline (PBS; 137 mM NaCl, 2.7 mM KCl, 10 mM Na_2HPO_4, 1.8 mM KH_2PO_4, pH 7.4) to 2×10^5 cells mL^{-1}. An aliquot of 5 μL diluted culture was spotted at the centre of each plate (four to nine replicates per strain, per medium). Plates were incubated at 25 °C, yeast inoculum side up. Images of each mat were taken after 3, 6 and 9 days of incubation. To observe invasive growth structures, mats were washed with a gentle stream of water from a laboratory squeeze bottle after being kept at 4 °C for half an hour.

For paired SLAD mat assays, two diluted cultures were inoculated approximately 1 mm apart on SLAD agar.

3.4.3 Microscopy imaging and image processing

Mats were observed and imaged at 40× magnification from the underside of the plates (with lid on) using a Nikon Eclipse 50i microscope and an attached Digital Sight DS-2MBWc camera with NIS-Elements F3.0 imaging software (Nikon). Four to six images were taken for each mat to capture all sectors. The sector images were stitched (Preibisch et al., 2009; Thévenaz and Unser, 2007) using Fiji software (Schindelin et al., 2012) to reconstruct a complete single mat image. The stitched image size of each mat was standardised using the stacking function in the same software. Detailed steps for image stitching and stacking are in the Supplementary Data.

3.4.4 Conditioned medium mat assays

Yeast were cultured in 50 mL SLAD for 48 h. Cultures were washed twice with PBS before being inoculated into 20 mL of fresh SLAD or CM at 1×10^4 cells mL^{-1} and incubated for 16 h. Following incubation, cell images were taken at 400× magnification using the microscope and camera described above. Images were processed and cell elongation ratio (ratio of major to minor axis) was measured using Fiji software (Schindelin et al., 2012). Steps are described in the Supplementary Data. Cultures were also plated as described in SLAD mat assays.

Statistical analysis was performed with a Welch's T-test using GraphPad Prism version 7.02 software for Windows.

3.4.5 Nitrogen and glucose measurement

Residual nitrogen and glucose were analysed spectrophotometrically with enzymatic methods. Nitrogen was analysed with a Megazyme Ammonia Assay Kit (Rapid; Cat No. K-AMIAR), according to the manufacturer's instructions. Glucose was measured according to the method of Mannheim (1989). For both assays, 1× SLAD was used to generate a calibration curve.

3.5 Results

3.5.1 Nitrogen limitation induces filamentous and invasive growth in mats

Several commercial wine yeast strains and laboratory strain prototrophic Σ1278b were tested for mat formation in SLAD to stimulate nitrogen limitation. Maximum mat size was approximately 4–5 mm in diameter, and this was often observed at the first time point analysed (3 days). In comparison, the maximum size of a colony grown from the same strains on SLAD with 2% agar reaches 1 mm (Joanna Sundstrom, *pers. comm.*). As the maximum mat size is at least 4-fold wider than colonies formed on SLAD with 2% agar, and cell growth occurs as a thin layer across the surface, these have been defined as mats rather than colonies. Mat expansion also extends beyond the boundary of the inoculum drop. This can be visualised in Appendix B, Figure B.1A, where growth of the mat inoculated with a single cell doubles in size between 3 and 9 days. The mats had no complex structures, but a subset of yeast cells grew filamentously and invaded the agar in all strains except I1 (Fig. 3.1A). The number of invasive foci varied between strains. Wine yeast had large, round invasive growth structures in comparison to Σ1278b which were more filamentous (Fig. 3.1B). These structures can only be reached by breaking the agar, and thus were classified as invasive. The progression of filamentous, invasive mat formation for Σ1278b, AWRI796 and EC1118 after 3, 6 and 9 days can be seen in Figure 3.1C. Interestingly, the size of the mat has limited changes, cells on the mat rim did not grow along the surface, yet the invasively growing cells continued to grow over time. Invasively growing cells at the mat rim grew much quicker than those inside the mat as shown by the different sizes of the structure.

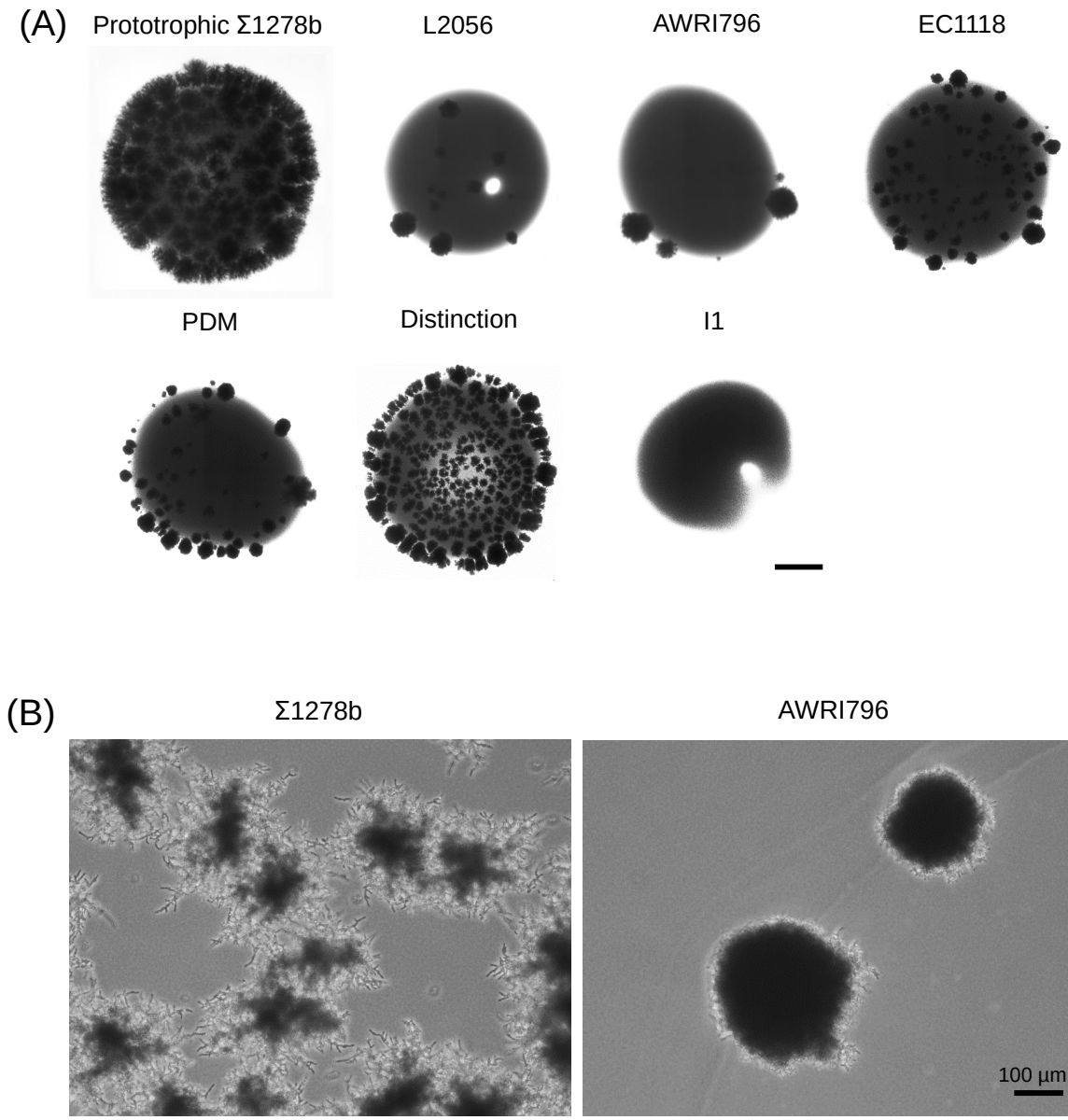

Figure 3.1: SLAD mat assays on SLAD low-density agar (0.3%). (A) SLAD mat morphologies of Σ1278b and selected wine yeast strains. Approximately 1000 cells were spotted on the plate. Four to six images were taken for each mat after 9 days and stitched to generate a single mat image. A typical representative image of each strain is shown. Scale bar, 1 mm. (B) Micrographs of mats post-wash showing invasive growth structures of Σ1278b and the wine strain AWRI796. Please refer to next page for (C).

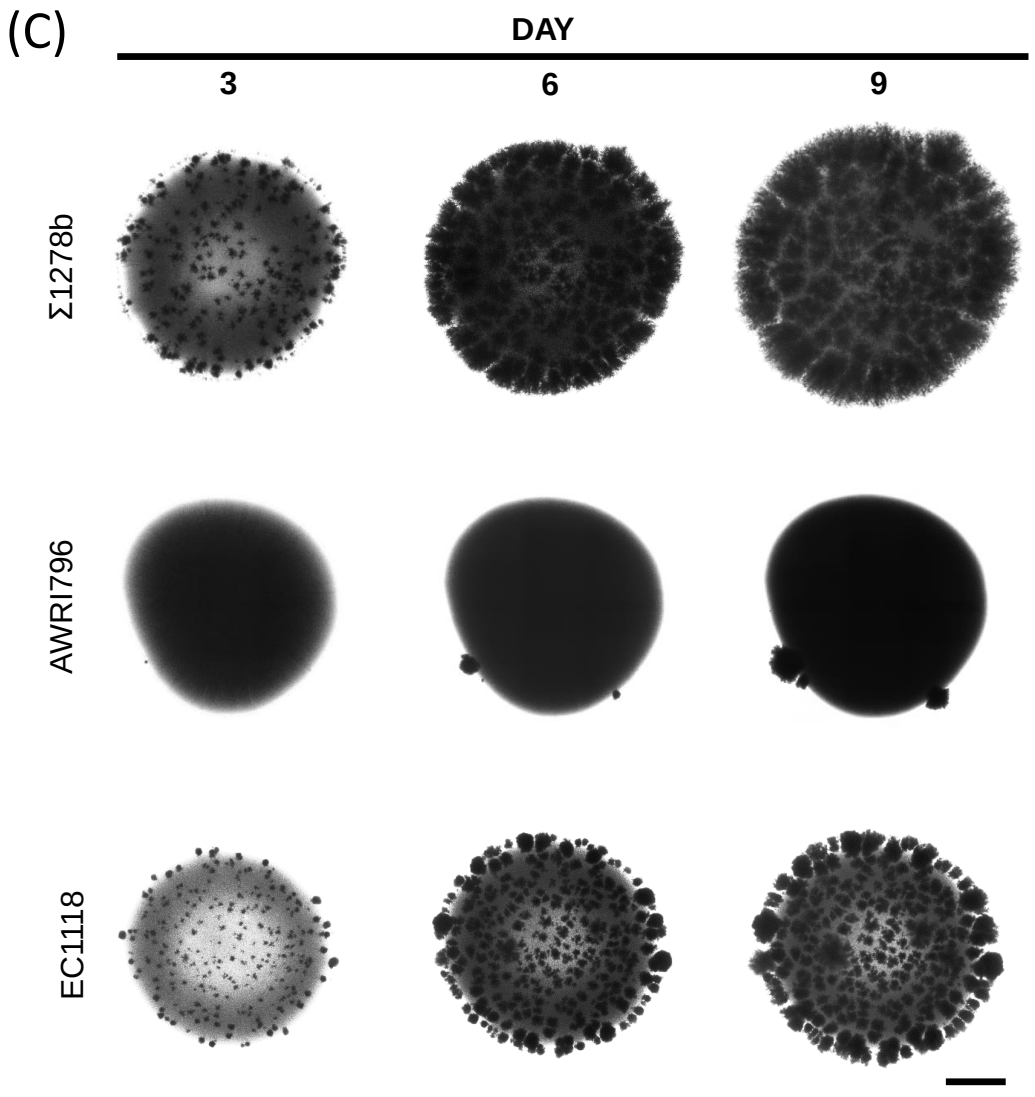

Figure 3.1: (C) Stitched mat images of Σ1278b and the wine strains, AWRI796 and EC1118, after 3, 6 and 9 days. Note the same mat for each strain is imaged over the time series. Scale bar, 1 mm.

3.5.2 Mat size and biomass increases with increasing ammonium sulfate

Since nitrogen is a limiting growth factor and mat size on SLAD is reduced significantly compared to mats reported in rich medium, this section investigated whether there were any structural or size changes to mats as the amount of nitrogen increased. The filamentous invasive structures of Σ1278b changed to a more rounded invasive structure when ten times more ammonium sulfate (500 μM) was included in the medium (Fig. 3.2). The structures were still observed underneath the agar surface. The overall mat biomass and size increased with increasing ammonium sulfate for both Σ1278b and AWRI796. With 100 times more ammonium sulfate (5 mM), the invasive structures of both strains were similar.

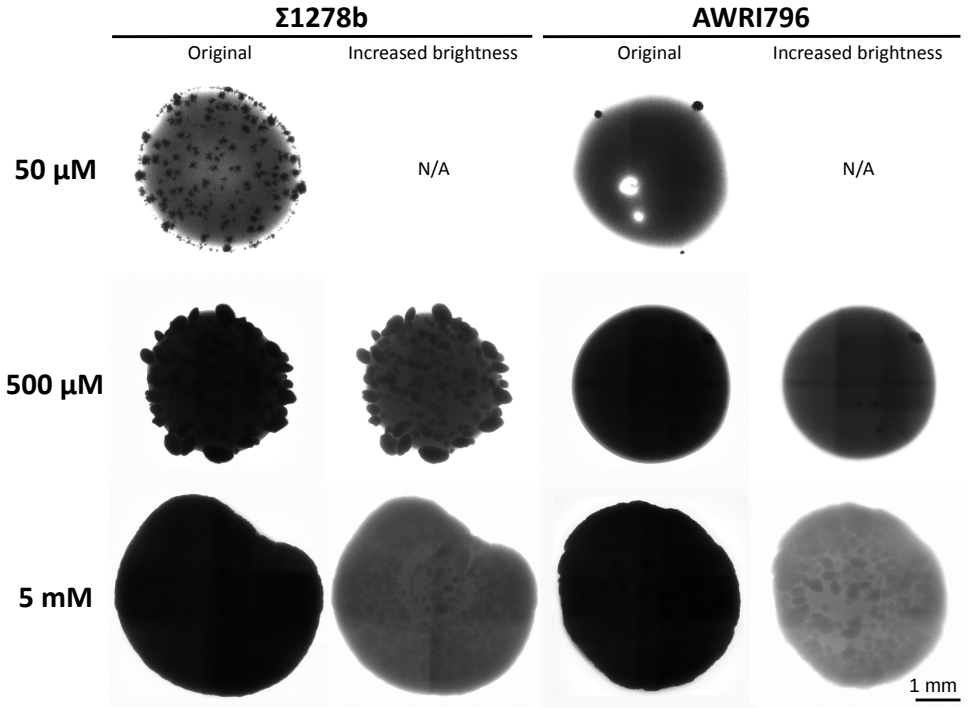

Figure 3.2: SLAD mat morphologies of Σ1278b and AWRI796 after 3 days on SLAD low-density agar (0.3%) with 50 μM, 500 μM and 5 mM ammonium sulfate. The invasive structures of cells grown on 500 μM and 5 mM ammonium sulfate could not be shown in the original brightness due to increased biomass. Therefore, brightness was increased to reveal the invasive structures.

3.5.3 Filamentous growth is inhibited by a neighbouring mat

In order to test whether filamentous growth can be enhanced or inhibited by a neighbouring filamentous mat, paired SLAD mat assays were performed with cells inoculated at a distance of approximately 1 mm on the same plate. Filamentous growth was inhibited by

a neighbouring mat, regardless of whether it was the same or a different strain (Fig. 3.3). Cells at the rim away from a neighbouring inoculum continued to grow and were highly filamentous. When two inocula were close enough, filamentous growth was completely inhibited. In the case of a larger distance between inocula, filamentous growth was initiated but stopped when the gap reached approximately 3 μm.

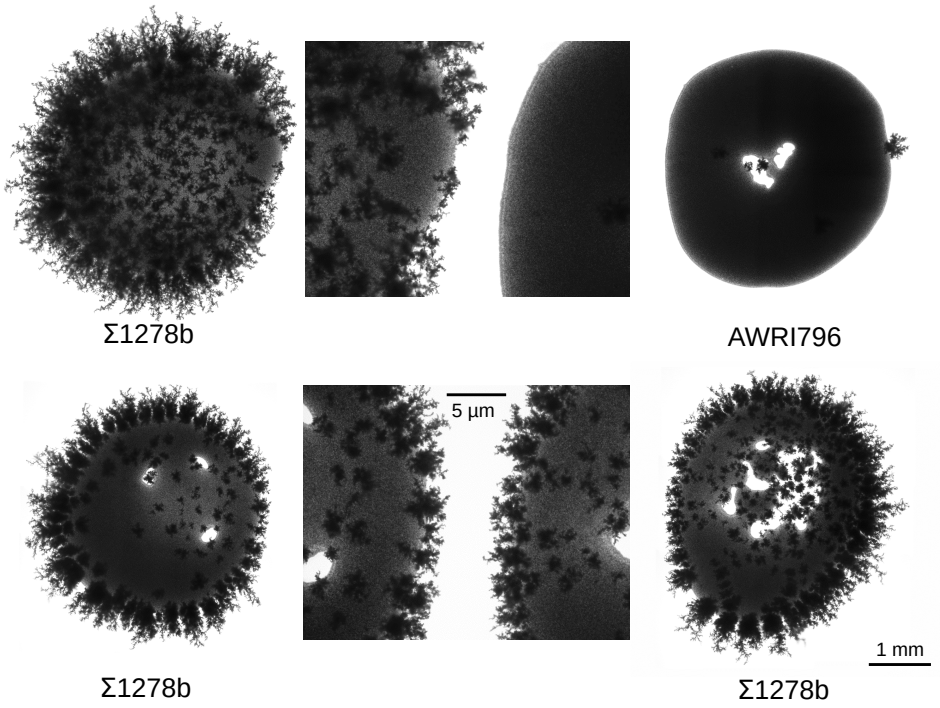

Figure 3.3: Paired SLAD mats at a close distance between Σ1278b and AWRI796 (top panel) and Σ1278b and Σ1278b (bottom panel) on SLAD low-density agar (0.3%). Each whole mat is shown (left and right panels) while the middle panel shows a magnified view of the gap between the paired mats. Images were taken 18 days after inoculation. Each of the whole mat images has a scale of 1 mm and the middle images have a scale of 5 μm.

3.5.4 Conditioned medium affects cell elongation in liquid culture but not invasive growth

Conditioned medium from a Σ1278b stationary-phase culture has been previously shown to stimulate filamentous and invasive growth when it was used as the assay medium (Chen and Fink, 2006). This study tested if pre-exposure to conditioned medium would enhance the filamentous and invasive growth phenotype on SLAD agar. Stationary-phase cultures of Σ1278b and AWRI796 were collected to prepare CM as described. These were then used to culture (in liquid) the same two strains overnight before analysis in a SLAD mat assay. After growing overnight in either CM, cell elongation ratio of both strains increased compared to an overnight culture in fresh SLAD (Fig. 3.4). The CM derived from AWRI796 resulted in a more enhanced response with longer cells formed by both

strains (p-value < 0.0001). However, pre-culturing in CM from either strain did not result in enhanced filamentous invasive growth on SLAD agar for either strain (data not shown).

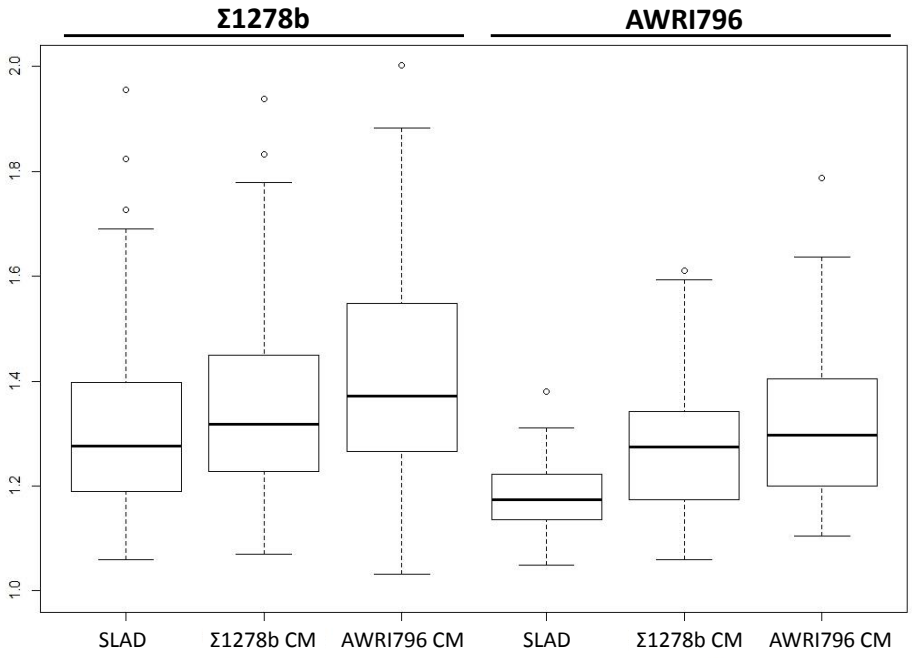

Figure 3.4: A boxplot showing cell elongation ratio (y-axis) of Σ1278b and AWRI796 cultured in either SLAD, Σ1278b CM or AWRI796 CM for 16 h. Cell elongation ratio is the ratio of major to minor axis of an ellipse (cell). For Σ1278b cells, the mean cell elongation ratios were not significantly greater in Σ1278b CM but significant in AWRI796 CM compared to in SLAD (p-values = 0.145 and 0.00984; df = 111.49 and 122.60). Mean cell elongation ratios of AWRI796 cells in Σ1278b CM and AWRI796 CM were significantly greater than in SLAD (p-values = 1.291e-7 and 4.873e-10; df = 117.33 and 107.39).

3.5.5 Effect of aromatic alcohols, ethanol, hydrogen sulfide and sulfite on yeast growing on SLAD mat assays

Aromatic alcohols (tryptophol and 2-phenylethanol in combination) and sulfur compounds (H_2S and sulfite) were examined for any effects on yeast mats growing on SLAD. Stock solutions of aromatic alcohols needed to be first dissolved in ethanol which has been reported to stimulate hyperfilamentation in diploid Σ1278b (Lorenz et al., 2000). Therefore, the impact of ethanol alone was evaluated, in addition to aromatic alcohols, H_2S (supplied as sodium sulfide) and sulfite. Without any additions to the medium, Σ1278b had a larger proportion of cells that initiated agar invasion and filamentation compared to AWRI796 (Fig. 3.5A). Σ1278b is commonly observed to rapidly undergo filamentation and invasive growth, and subsequently results in difficulty in deciphering differences in filamentous/invasive growth between conditions, except for the addition of sodium

metabisulfite (SMS) (Fig. 3.5A–E and F–J). SMS addition (0.01%) resulted in delays in both agar surface and invasive growth (Fig. 3.5F–J).

For AWRI796, the addition of 0.05% ethanol in SLAD increased the number of invasive foci and triggered early development of agar invasion (Fig. 3.5A and B). The presence of a total 100 μM aromatic alcohols, however, suppressed this effect (Fig. 3.5C compared to B). The addition of 0.4 mg L^{-1} sodium sulfide produced large numbers of invasive foci and reduced biomass on the agar surface (Fig. 3.5D). The effect remained with the combination of both aromatic alcohols and sulfide (Fig. 3.5E). All media containing SMS (Fig. 3.5F–J) resulted in reduced biomass (both surface and invasive). When ethanol, sodium sulfide and SMS were added, the majority of AWRI796 cells grew invasively (Fig. 3.5I). However, inclusion of aromatic alcohols returned cells to almost exclusively surface growth (Fig. 3.5J). Thus, it seems that the suppressive effect on invasive growth of aromatic alcohols is alleviated when sulfide is present and is supported in the presence of SMS, indicating an interplay between sulfide and sulfite.

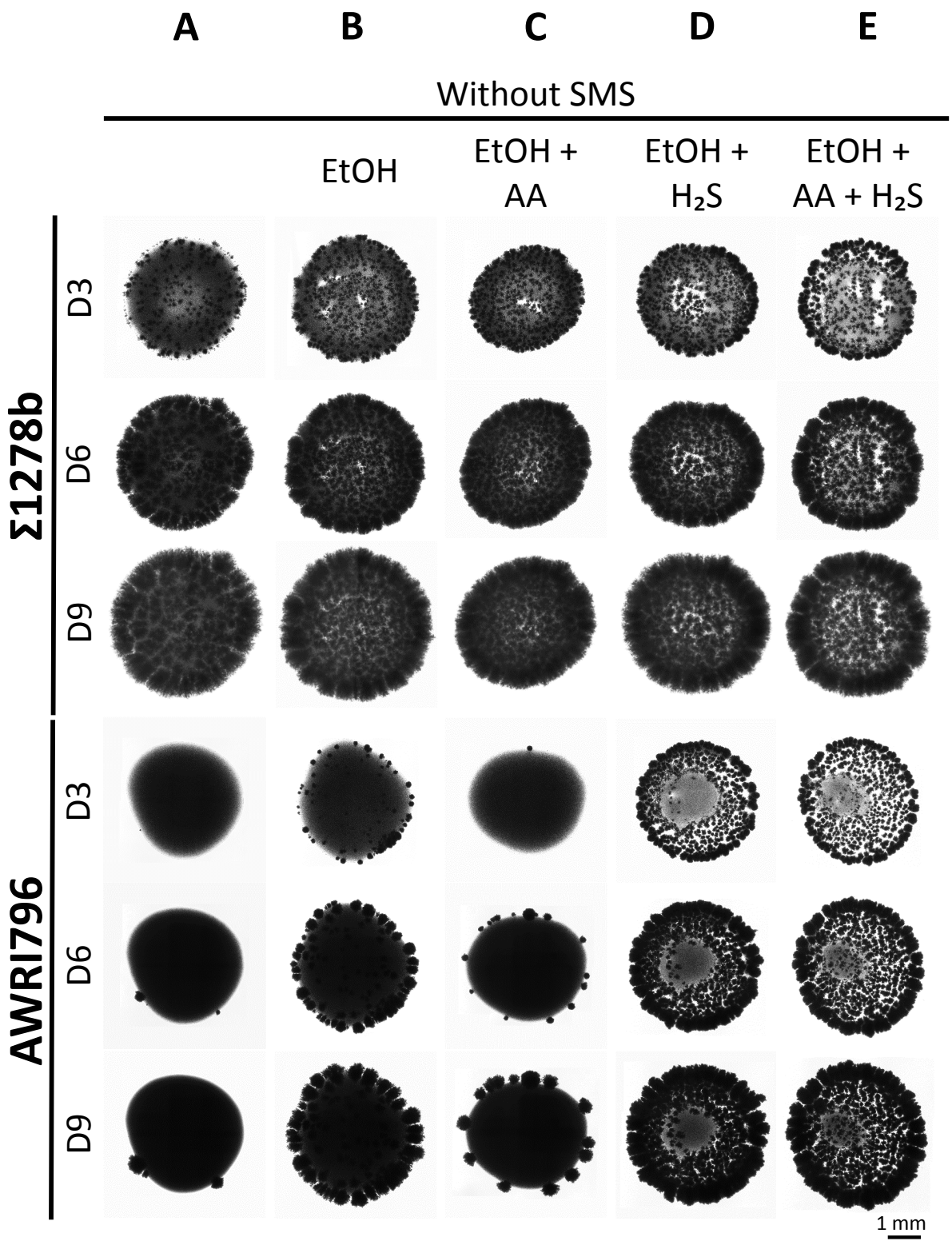

Figure 3.5: SLAD mat morphologies of Σ1278b and AWRI796 on Day 3 (D3), 6 (D6) and 9 (D9) on SLAD low-density agar (0.3%) (A) without any additions, with the addition of (B) ethanol (EtOH), (C) combination of ethanol and aromatic alcohols (AA), (D) combination of ethanol and sulfide (H_2S), (E) combination of ethanol, aromatic alcohols and sulfide. Please refer to next page for (F–J).

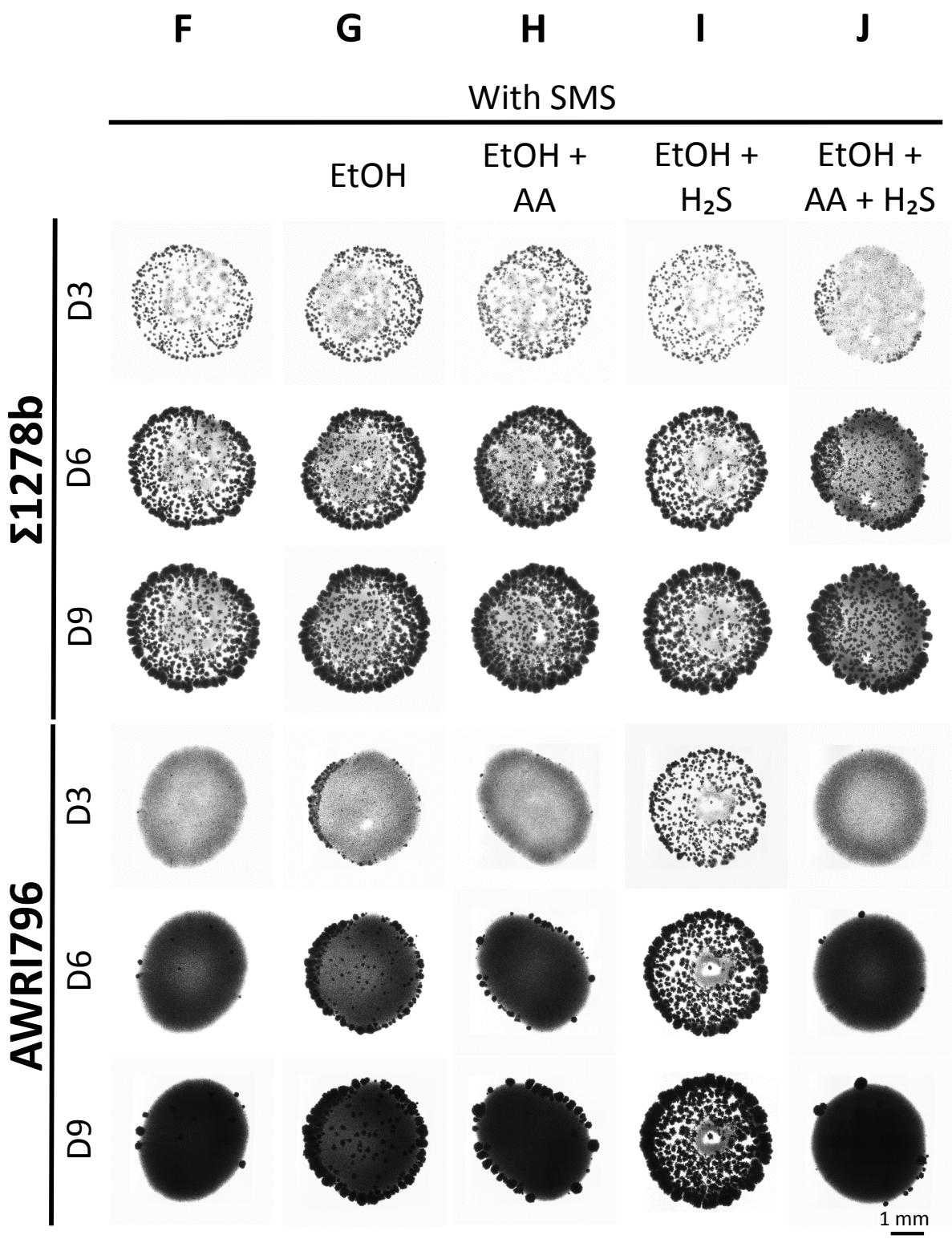

Figure 3.5: (F–J) the same combinations as in A–E with the addition of sulfite (SMS).

3.6 Discussion

Yeast grow into a large mat of a thin layer of cells across the surface of low-density YPD agar with some strains forming complex architecture (Reynolds and Fink, 2001; Hope and Dunham, 2014). Karunanithi and colleagues (2012) showed that filamentous mats can also be formed by Σ1278b on YP medium in which glucose is limited. This study reports a different mat morphology formed by Σ1278b and wine yeast strains on SLAD, where nitrogen is limited. Mat size was reduced, no complex architecture was formed and a proportion of cells switched to filamentous and invasive growth. This study further show that addition of some key yeast metabolic compounds affects invasive growth of these mats.

The low nitrogen conditions of SLAD agar limited cell spreading across the agar and instead, a subset of cells underwent pseudohyphal growth and invaded the agar. This response is consistent with the findings reported in other studies investigating nitrogen limitation on medium-density agar (Gimeno et al., 1992; Zupan and Raspor, 2010). Whilst there were no obvious morphology variations in the surface growing cells between strains, the number of invasive foci did vary between strains. The invasive foci of wine yeasts were more rounded in structure compared to those of Σ1278b (Fig. 3.1B). This may simply represent more rapidly growing or less pseudohyphal cells. One reason may be that wine yeast have developed the ability to utilise nitrogen more efficiently, and thus be able to grow rapidly in the presence of limited nutrients compared to laboratory yeast, since they have evolved to survive multiple stresses in the winemaking environment. This is supported by the observations of increased nitrogen content in SLAD, Σ1278b also grew into rounded invasive structures similar to wine yeasts (Fig. 3.2). This indicates that nutrient sufficiency may be reflected by rounded invasive structures. The increase in overall mat size also suggests that nitrogen is important for mat expansion, primarily for cellular growth.

Within each mat, (filamentous) invasive growth continued over time and was most rapid at the mat rim compared to the centre. This may be a result of less competition for nutrients at the rim due to lower cell density, and therefore cell division is supported and more likely to expand. In order to determine if filamentous growth can be induced by another filamentous mat in close proximity, cells of AWRI796 (less filamentous) and Σ1278b (highly filamentous) were inoculated close to each other. In this experiment, filamentous growth was inhibited on the side closest to the neighbouring mat. The same occurred when two inocula of Σ1278b were spotted next to each other, suggesting that the inhibition is neither strain dependent nor unidirectional. This observation is consistent with the repulsion between two neighbouring filamentous colonies of bacteria (Matsushita and Fujikawa, 1990). The inhibition was not evident in yeast surface filamentation colonies in other study in medium-density agar, but it may be due to the shorter incubation time *i.e.* three days (Liu et al., 1993). Non-filamentous yeast colony growth has been shown to be

affected by the presence of a neighbouring colony. This was due to the release of ammonia via the amino acid permease Shr3p as a signalling molecule from colonies to prevent growth towards a neighbouring colony (Palková et al., 1997). The ammonia signalling may be involved in the filamentous growth inhibition between the two neighbouring mats.

In this study, several compounds were found to affect filamentous and invasive growth of mats on SLAD agar. However, the effect was not obvious for Σ1278b. This strain readily forms filamentous and invasive cells, even in the control condition (SLAD). Σ1278b is well known for its expeditious ability to invasively grow and is chosen for filamentous studies since it seems to be extremely sensitive to ammonia repression of nitrogen assimilation pathways (Rytka, 1975; Wiame et al., 1985; Gimeno et al., 1992).

For AWRI796, the transition to invasive growth in response to low nitrogen was enahnced by the addition of ethanol (Fig. 3.5A and B). *FLO11* is required for filamentous and invasive growth during nitrogen starvation (Braus et al., 2003; Lo and Dranginis, 1998; Robertson and Fink, 1998). This gene can be regulated epigenetically by the binding of Sfl1p which requires histone deacetylase Hda1p (Halme et al., 2004; Octavio et al., 2009). Immunofluorescence analysis has shown that Flo11p was present on the cell surfaces of pseudohyphal or filament-forming cells and was silenced in the yeast form cells derived from the same clone (Guo et al., 2000; Halme et al., 2004). This may explain observations in this study that only a subset of cells transitioned to grow invasively. Ethanol has been previously shown to abolish Sfl1p-mediated silencing (Octavio et al., 2009), which is consistent with the observation that ethanol addition to SLAD increased and induced an early development of agar invasion and filamentous growth. Interestingly, no enhancement of invasive growth by aromatic alcohols was observed, as was reported by Chen and Fink (2006) on 2% agar, but instead their addition suppressed the enhancement effect of ethanol (Fig. 3.5B and C). This may be due to variation in experimental preparation as Chen and Fink (2006) did not report the method for preparation of the aromatic alcohols.

The effect of addition of H_2S was also analysed, since evidence suggests that H_2S is a signalling mediator for stress resistance and longevity. H_2S offers protection against nutrient and oxygen deprivation in mammals (Blackstone and Roth, 2007; Hine and Mitchell, 2015). Similar H_2S-mediated biological benefits are also found in yeast. For example, the mutant Δ*met17* has increased H_2S production and an extended chronological lifespan (Johnson and Johnson, 2014; Linderholm et al., 2008). The mutant also had increased resistance to heat shock, oxidative and heavy metal stresses, and metal chelate toxicity, suggesting that H_2S could lead to an adaptive response to environmental stresses (Singh and Sherman, 1974; Brown et al., 2006; Hwang et al., 2007; Johnson et al., 2014). This study reports a novel response to H_2S, which is to enhance invasive growth. Historically, invasive growth has been hypothesised to be a survival strategy adopted by yeast during nitrogen starvation that is believed to be a mode of action to forage for nutrients. H_2S is well known to be released by yeast upon nitrogen limitation, perhaps this extruded sulfide is sensed by nearby cells as a cue to switch to invasive growth. The mechanism that may

allow cells to respond to this putative H_2S cue is not yet known, however evidence supports involvement of the Retrograde-MAPK pathway. *RTG3* that activates the mitochondrial retrograde (RTG) signalling was shown to be required by a Δ*met17* mutant to confer longevity and stress tolerance (Johnson and Johnson, 2014). The RTG pathway is usually activated when mitochondrial function is compromised, but the signalling pathway is unclear (Liu and Butow, 2006). Several eukaryotic models have demonstrated a tight inverse relationship between oxygen availability and H_2S production in mitochondria, leading to the proposal of sulfide metabolism as an oxygen sensor (Doeller et al., 2005; Furne et al., 2008; Olson and Whitfield, 2010; Olson et al., 2010; Olson, 2012). Fission yeast, *Schizosaccharomyces pombe*, exposed to H_2S results in downregulation of many mitochondrial genes and reduced mitochondrial oxygen consumption, which may result in RTG pathway activation (Jia et al., 2011). Many genes involved in the RTG pathway have been identified as positive regulators of filamentous MAPK cascade, thus supporting the enhancement of filamentous and invasive growth by H_2S via the RTG-MAPK pathway (Chavel et al., 2014).

Exposure to sulfite delayed cellular and invasive growth in both Σ1278b and AWRI796 (Fig. 3.5F–J). Less filamentous growth was also observed in Σ1278b in the presence of sulfite. Cells undergoing filamentous growth display prolonged apical growth leading to highly polarised growth at the bud tip, and this is tightly regulated with cell cycle (Pruyne and Bretscher, 2000). A transcriptomics study of *S. cerevisiae* strain 3090-1d showed that sulfite exposure downregulated cell cycle and polarity-related genes including *MYO1*, *BNR1* and *PCL1* (Park and Hwang, 2008). This may reduce the hyperpolarisation event and in turn filamentous growth upon sulfite exposure. Growth, although delayed, did occur upon sulfite exposure suggesting adaption and tolerance to sulfite. Sulfite is produced as part of the sulfate assimilation pathway. The effect of sulfite is of interest to this study because sulfite is usually converted to sulfide and eventually metabolised into methionine, cysteine and glutathione. However, sulfite can be produced and excreted in the form of sulfur dioxide (SO_2). Excess sulfite has antioxidant and antimicrobial activity and has previously been shown to reduce invasive growth (Zupan and Raspor, 2010). In comparison, this study used a lower concentration of sulfite (1.05 vs 9.61 mM) and hence did not completely block invasive growth.

Pre-exposure of CM was found to have no impact on invasive growth despite having triggered cell elongation in liquid culture (Fig. 3.4). This result suggests that cells decide their phenotypic fate based on an environmental trigger after inoculation onto agar plates. This supports the claim that yeast have developed mechanisms to quickly adapt to environmental changes. Several studies have investigated short and long term responses to the fluctuations in environmental factors. A transient transcriptional change was found immediately after temperature shifts before an adaptation to a new steady state of transcript levels (Gasch et al., 2000). Another transcriptomics study also showed that yeast re-programmed a number of metabolic networks rapidly towards nutritional perturbation (Dikicioglu et al., 2011). The findings from integrated data from both transcriptomics

and metabolomics studies showed that glucose impulse in glucose-starved conditions provoked changes in carbon metabolism, purine and pyrimidine biosynthetic pathways, folate metabolism, superpathway of serine and glycine and the methionine biosynthetic pathways, and aspartate and glutamate biosynthetic pathways (Dikicioglu et al., 2012). Ammonium impulse in nitrogen-starved conditions also affected these metabolic pathways with different profiles. These reports suggest that in the present study, it could be possible that the yeast cells were re-programmed to elongate when cultured in CM, and quickly re-programmed again when transferred to SLAD agar.

The findings of this study build upon the current understanding of the effect of nitrogen limitation on mat formation and the influence of yeast metabolites, ethanol, aromatic alcohols, H_2S and sulfite. Further study should involve genetic analysis of the induction or inhibition of invasive growth by these compounds. These observations provide a further opportunity to study the physiological role of each of the metabolites and the pathways leading to the effect upon cellular differentiation.

3.7 Funding

This work was supported by Wine Australia [GWR Ph1305] and Australian Research Council [DP 20111529]. ELT was supported by an Adelaide Graduate Research Scholarship.

Conflict of interest: None declared.

3.8 Acknowledgements

Prototrophic Σ1278b was kindly donated by Dr Charles Boone (University of Toronto). The authors thank Dr Michelle Walker (University of Adelaide) for generating strain I1.

3.9 Supplementary Data

3.9.1 Methods

Mat image stitching and stacking

1. Create a folder for stitching process, only import the group of images needing to be stitched one at one time.

2. Download and install Fiji from http://imagej.net/Fiji/Downloads.

3. Open the application.
4. Click **Plugins** from the menu, select **Stitching**, and select **Grid/Collection stitching**.
5. Choose **Sequential Images** from the drop-down menu for Type, click **OK**.
6. In the Directory, choose the path to the folder created for stitching containing images to be stitched, click **OK**.
7. Click **OK** to confirm image files to be stitched.
8. A stitched image will be generated. Save the image as a TIFF file.
9. For images that cannot be stitched using the method above, use MosaicJ to manually assemble the images.
10. Click **Plugins** from the menu, select **Stitching**, and select **MosaicJ**.
11. A new window will open.
12. Click **File**, select **Open Image Sequence**.
13. Select the first image in the stitching folder, click **Open**.
14. All images in the folder will be loaded.
15. Click an image, the image will be in the working space. Drag images to assemble at the correct position.
16. Click **File** from the menu, select **Create Mosaic**.
17. A stitched image will be generated. Save the image as a JPEG file as the TIFF image created using this method is very large.
18. For stacking, open the largest image which all other images will be normalised to.
19. Open other images to be normalised.
20. Click **Image** from the menu, select **Stacks**, and select **Images to Stack**.
21. Click **OK**. Images are now stacked.
22. Click **Image** from the menu, select **Stacks**, and select **Stack to Images**.
23. Individual images are shown with the normalised size.
24. To fill black area with background colour of the original image, click **Colour Picker** icon, and then click on the background to pick up colour. Click **Blood Fill Tool** icon, and click on the black area to fill with background colour.
25. Save the image.

Cell elongation ratio measurement

1. Open the image that needs to be measured (in this example, images were taken at 400× magnification).

2. Click **Analyze** from the menu, select **Set Scale**. Enter 64 pixels = 10 μm (Note: this needs to be checked for each individual microscope), check **Global** and click **OK**. Now the image and the following images opened within this session have been calibrated.

3. Click **Process** from the menu, select **Subtract Background**. Input **40** pixels for Rolling ball radius, check **Light background**, click **OK**.

4. To convert into a black and white image, click **Image** from the menu, choose **Adjust** and select **Threshold**. Select **Default** and **B&W** from the drop-down menu, click **Apply** and **Close**.

5. Click **Process** from the menu, select **Binary**, and select **Fill Holes**.

6. Click **Process** from the menu, select **Binary**, and select **Watershed**.

7. To remove non-cell particles, click **Colour Picker** icon, and then click on the white area in the image. Click **Paintbrush Tool** icon, double right-click the icon to set brush width, and click **OK**.

8. Click (and drag) on the non-cell particles to be removed. Save the processed image if necessary.

9. To set measurements that need to be performed (only need to do this once), click **Analyze** from the menu, select **Set Measurements**. Check Area, Shape descriptors, Fit ellipse, Feret's diameter and Display label. Choose **None** for Redirect to and **3** for Decimal places. Click **OK**.

10. To measure, click **Analyze**, select **Analyze particles**. Size (μm^2): 5–infinity; Circularity: 0–1; Show: Overlay Outlines; check Display results, Summarize, Exclude on edges, click **OK**.

11. Save Results table for later use. Save the outline image if necessary.

12. Use AR (aspect ratio) in the Results table as the cell elongation ratio for statistical analysis.

Chapter 4

Understanding wine yeast invasive growth through transcriptional analysis

Contextual statement

Chapter 3 highlighted that nitrogen limitation leads to yeast invasive growth in low-density agar medium. This response was consistent across all strains except for one which had poor overall growth. Several environmental factors could manipulate this invasive growth. Chapter 4 addresses the final aim of the project: to investigate the triggers and regulation of wine yeast biofilms and invasive growth. The manuscript in this chapter presents genes and biological processes associated with invasive growth in low-nitrogen mat conditions.

Statement of Authorship

Title of Paper	Transcriptional analysis of invasively growing wine strains of *Saccharomyces cerevisiae*
Publication Status	☐ Published ☐ Accepted for Publication ☐ Submitted for Publication ☑ Unpublished and Unsubmitted work written in manuscript style
Publication Details	Written in manuscript style for Molecular Microbiology

Principal Author

Name of Principal Author (Candidate)	Ee Lin Tek
Contribution to the Paper	Performed all experiments and data analysis, interpreted data, and wrote manuscript.
Overall percentage (%)	80%
Certification:	This paper reports on original research I conducted during the period of my Higher Degree by Research candidature and is not subject to any obligations or contractual agreements with a third party that would constrain its inclusion in this thesis. I am the primary author of this paper.
Signature	Date 04/09/17

Co-Author Contributions

By signing the Statement of Authorship, each author certifies that:

i. the candidate's stated contribution to the publication is accurate (as detailed above);

ii. permission is granted for the candidate in include the publication in the thesis; and

iii. the sum of all co-author contributions is equal to 100% less the candidate's stated contribution.

Name of Co-Author	Andrew R. Hesketh
Contribution to the Paper	Supervised RNA-sequencing data processing and analysis, editing of the manuscript.
Signature	Date 30th Aug.2017

Name of Co-Author	Joanna F. Sundstrom
Contribution to the Paper	Supervised development of work, helped in data interpretation and editing of the manuscript.
Signature	Date 4/09/2017

Name of Co-Author	Jennie M. Gardner

Contribution to the Paper	Supervised development of work, helped in data interpretation and editing of the manuscript.
Signature	Date 6/09/17

Name of Co-Author	Stephen G. Oliver
Contribution to the Paper	Supervised development of work and helped in data interpretation.
Signature	Date 30.08.17

Name of Co-Author	Vladimir Jiranek
Contribution to the Paper	Supervised development of work, helped in data interpretation and editing of the manuscript.
Signature	Date 4.9.17

Please cut and paste additional co-author panels here as required.

Transcriptional analysis of invasively growing wine strains of *Saccharomyces cerevisiae*

Ee Lin Tek[1], Andrew R. Hesketh[2], Joanna F. Sundstrom[1], Jennie M. Gardner[1], Stephen G. Oliver[2], Vladimir Jiranek[1,3*]

[1]Department of Wine and Food Science, University of Adelaide, Waite Campus, South Australia 5064, Australia.
[2]Department of Biochemistry & Cambridge System Biology Centre, University of Cambridge, United Kingdom.
[3]Australian Research Council Training Centre for Innovative Wine Production.

*Corresponding author: PMB 1, Glen Osmond, South Australia 5064, Australia. Tel: 618-8313-6651; E-mail: vladimir.jiranek@adelaide.edu.au

4.1 Keywords

Invasive growth; diploid wine yeast; *FPS1*; low nitrogen; hexose transporter

4.2 Summary

In response to unfavourable conditions such as nutritional and environmental stress, the yeast *Saccharomyces cerevisiae* can switch to filamentous growth and/or invasive growth by re-programing cellular systems. A number of signal transduction pathways have been identified that regulate these processes, some of which are common to both filamentous and invasive growth. Previous genome-wide studies have identified biological pathways specific to invasive growth, however, the regulation of these is yet to be completely understood. Using differential transcriptome analysis of surface and invasively growing cells of a diploid wine yeast strain, this study found genes and biological processes that have not previously been associated with invasive growth. The analysis identified 272 genes that were upregulated and 84 genes downregulated in invasively growing cells. Enriched Gene Ontology categories of upregulated genes included medium-chain fatty acid biosynthetic process, carbohydrate metabolic process, cellular water homeostasis, fungal-type cell wall organisation, and glucose import. Further analysis of deletion mutants confirmed that *FPS1*, encoding for the glycerol export protein, is required for invasive growth. This work also identified a hypothetical gene, that has a portion of translated gene sequence homologous to an amidase domain, may have a role in invasive growth.

4.3 Introduction

The budding yeast *S. cerevisiae* is able to adapt in response to various nutritional stresses (e.g. glucose and nitrogen limitation) to aid survival. This yeast is dimorphic, in that it can undergo a developmental switch from round, single cells to an elongated (pseudohyphal) multicellular filamentous form (Gimeno et al., 1992; Kron et al., 1994). This results in both haploid and diploid cell types capable of invasion into agar (Gimeno et al., 1992; Cullen and Sprague, 2000). Since yeast cells are non-motile, it is believed that this change in morphology allows them to forage for nutrients. These modes of growth have also been shown to be influenced by strain genetic backgrounds and other physiochemical factors rather than simply nutrient depletion, for example the presence of fusel alcohols, pH, temperature, salt and atmosphere (Zupan and Raspor, 2010; Dickinson, 1996). Yeast can also switch from fluffy and smooth colonies in response to environmental conditions and is accompanied with change in gene expression (Kuthan et al., 2003).

Four signalling pathways shown to regulate pseudohyphal growth have been

well documented and reviewed by Cullen and Sprague (2012). These include the cyclic AMP-dependent protein kinase A (cAMP-PKA) pathway, the Snf1 pathway, the target of rapamycin (TOR) pathway and the mitogen-activated protein kinase (MAPK) pathway. Some proteins in these pathways are also required for invasive growth. For example, components of the MAPK pathway, required for pseudohyphal formation, Ste20p, Ste11p, Ste7p, Kss1p, and Ste12p, are also required for invasive growth (Roberts and Fink, 1994; Cook et al., 1997). Likewise, Tpk2p of the cAMP-PKA pathway is essential for both pseudohyphal and invasive growth (Robertson and Fink, 1998). In relation to the Snf1 pathway, yeast with a deletion of *SNF1* were unable to invasively grow or undergo cell elongation (Vyas et al., 2003; Cullen and Sprague, 2000). Rapamycin inhibits invasive growth, which can be restored by overexpression of *TAP42*, showing that the TOR pathway is involved (Cutler et al., 2001). The cell surface flocculin, Flo11p, is widely regarded as the primary mechanism for cell-cell and cell-surface adhesion, important for pseudohyphal and invasive growth. Regulation of Flo11p is shared by the cAMP-PKA, Snf1 and MAPK pathways, *i.e.* Tpk2p, Snf1p, and Ste12p are all involved (Lo and Dranginis, 1998; Rupp et al., 1999; Kuchin et al., 2002; Pan and Heitman, 2002).

In diploid cells, pseudohyphal and invasive growth can occur simultaneously or independently, suggesting that apart from the shared core signalling pathways, it is likely there are invasive growth specific pathways. A number of studies have identified genes and biological pathways necessary for invasive growth, and these have involved screening of loss-of-function and overexpression mutants in a range of media (Jin et al., 2008; Ryan et al., 2012; Shively et al., 2013). Jin and colleagues (2008) screened a transposon insertion gene disruption and overexpression library in a haploid version of the filamentous strain of *S. cerevisiae*, Σ1278b, to identify genes necessary for filamentous growth induced by butanol. They found 243 out of 487 genes were also necessary for haploid invasive growth. Ryan and colleagues (2012) screened both haploid and diploid Σ1278b gene deletion libraries and identified 577 genes required for haploid invasive growth in rich medium, of these 132 were also required for diploid pseudohyphal growth. However, this group measured relative filamentous outgrowth to determine extent of pseudohyphal growth, which does not take into account agar invasion. In contrast, Shively and colleagues (2013) found 551 genes that when overexpressed exaggerated diploid invasive growth in sufficient nitrogen. The loss-of-function and overexpression studies were comprehensive, yet they are limited by the resources (*i.e.* number of mutants in the libraries versus number of verified ORFs) and they were studied in different media. Studying gene expression profiles offers an additional layer of information to understand active physiological processes that are associated with the condition of interest and potentially predict novel functions of genes.

In this study, RNA-sequencing technology was used to compare transcriptomes of diploid wine yeast cells collected from the agar surface to cells growing invasively which also included the filamentous phenotype. In the invasively growing population, 272 genes were upregulated and 84 genes were downregulated. Surprisingly, no transcripts from the mentioned four signalling pathways were differentially expressed. Enriched Gene Ontology

(GO) terms of the upregulated gene sets showed that medium-chain fatty acid biosynthetic process, carbohydrate metabolic process, cellular water homeostasis, fungal-type cell wall organisation, and glucose import may be important processes for invasive growth. A number of the upregulated genes identified in this study are common to previous mutant screening studies. The association of cellular water homeostasis to invasive growth is novel, and thus further deletion analysis of genes within this group identified *FPS1* as being necessary for invasive growth. Results from this work also uncovered a potential role for a hypothetical gene.

4.4 Results and Discussion

4.4.1 Global change in gene expression between surface and invasively growing cells

Total RNA was extracted from cells of the diploid wine yeast, AWRI796, collected from the surface and invasively growing into a low percentage (0.3%), low nitrogen agar medium. Three replicates for each growth type were used with an RNA-sequencing approach to profile global changes in gene expression between surface and invasively growing cells. Sequencing yielded between 35 and 37 million reads from each RNA sample. Differentially expressed genes were defined as those deemed to be statistically significant based on a t-test relative to a 1.3-fold-change threshold using the *limma* TREAT method of McCarthy and Smyth (2009). In the invasively growing population, 272 genes were upregulated and 84 genes downregulated, compared to surface growing cells (Table S1). Four of the ten genes having the largest change in expression were hexose transporter genes (*HXT3*, *HXT4*, *HXT6* and *HXT7*; Table 4.1). Among these genes, *HXT4* has been reported to affect filamentous growth and is required for invasive growth under butanol induction (Jin et al., 2008).

Table 4.1: Top 10 genes with the largest change in gene expression in invasively growing cells.

Gene Symbol	**Name**	**$\log_2$ Fold Change**	**Adj. p-value**
HXT7	HeXose Transporter	+3.78	1.39E-8
HXT4	HeXose Transporter	+3.04	1.58E-8
AWRI796_5153	Amidase	+2.69	3.30E-7
SSA2	Stress-Seventy subfamily A	+2.26	1.34E-7
HXT6	HeXose Transporter	+2.25	5.40E-8
RGI1	Respiratory Growth Induced	+1.92	5.77E-8
AWRI796_2017	*NA*	+1.79	3.30E-7
HXT3	HeXose Transporter	+1.74	3.72E-7
CAR1	Catabolism of ARginine	+1.73	3.30E-7
NCE103	NonClassical Export	-1.72	6.93E-8

To investigate the biological processes that are associated with invasive growth, GO enrichment analysis was performed. This analysis revealed 37 enriched GO terms for upregulated genes, while none were identified for downregulated genes (Table S2). The enriched GO terms were summarised into five main groups by clustering similar GO terms using REVIGO (Supek et al., 2011), these were medium-chain fatty acid biosynthetic process, carbohydrate metabolic process, cellular water homeostasis, fungal-type cell wall organisation, and glucose import (Fig. 4.1). KEGG pathway analysis of the upregulated and downregulated genes did not identify any overrepresented pathways, including signal transduction pathways required for invasive growth. This may be due to strain differences *i.e.* wine yeast versus laboratory yeast. Wine yeast may have conserved signalling pathways involving genes that have not yet been characterised, and thus not represented in this transcriptomics analysis.

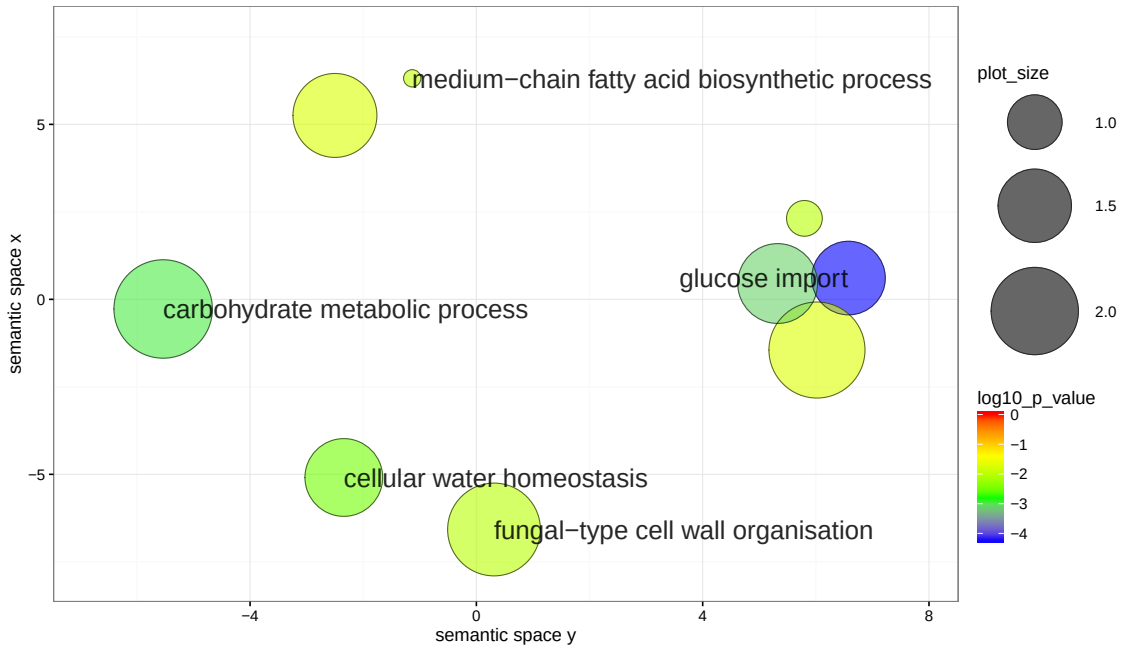

Figure 4.1: Enriched GO terms (37) of upregulated genes of the invasively growing cells submitted to the REVIGO program. Representative GO categories are shown by circles and visualised by clusters of semantically similar GO terms. Circle colour indicates $\log_{10}$ adjusted p-value from the GO enrichment analysis whereas size represents the frequency of the GO term in the underlying GOA database (circles of more general terms are larger).

A number of interesting findings were obtained from differential expression analysis. Approximately 25% (67 genes) of upregulated genes have been reported in other studies as important for invasive growth or associated phenotypes (*i.e.* diploid pseudohyphal growth, haploid and diploid invasive growth, and differential expression between fluffy and smooth colonies; Table S3). Ten genes were found in more than one other data set, these being *ARG8*, *ERG6*, *FLO11*, *IKI3*, *PMT2*, *SIN3*, *SLA1*, *MGA1*, *PUT4* and *HXT4*. However, this is not an exact comparison since: (1) each study used a different conditioned medium (e.g. rich YPD, low nitrogen SLAD, butanol treatment or alternative carbon source GMA); (2) strain ploidy and phenotypes assayed were different.

The present study focuses on the differences between surface and invasive growth, regardless of elongated or ovoid cells, expecting to identify genes and/or biological processes that are important but not easily detected in single gene deletion or overexpression screen studies. Interestingly, a handful of upregulated genes identified in invasively growing cells are common to previously reported upregulated genes of fluffy and downregulated genes of smooth colonies (19 of 165 and 14 of 147, respectively; Kuthan et al., 2003). Yeast colonies with fluffy structure were suggested as a metabolic strategy in unfavourable conditions (Kuthan et al., 2003). This structure changed to smooth when culturing in laboratory conditions and accompanied with a change in gene expression. The presence of common genes expressed in fluffy colonies as well as in invasive growth may indicate a similar strategy used for hostile conditions.

4.4.2 Glucose import

Four hexose transporter genes (*HXT3*, *HXT4*, *HXT6* and *HXT7*) with increased in gene expression ranging from 3.34- to 13.7-fold in the invasively growing cells may be related to the availability of nutrients in the medium. Previous studies have shown that these genes are important to recover glucose uptake after ammonium supplementation following a nitrogen-limited sluggish fermentation (Palma et al., 2012). Luyten and colleagues (2002) showed that *HXT6* and *HXT7* are essential at the end of alcoholic fermentation where the uptake of sugar is often perturbed by the stressful environment of low nutrient and high ethanol. It seems that these genes encoding high-affinity glucose transporters are equally important in the SLADS (containing limited nitrogen supplied solely by ammonium sulfate) conditions of this study. Furthermore, the expression of these four genes was also associated with structured morphologies (Table S3), suggesting a strategy to cope with unfavourable conditions (Kuthan et al., 2003).

4.4.3 Carbohydrate metabolism / fungal-type cell wall organisation

Transcriptomics analysis showed genes of carbohydrate metabolic processes were significantly upregulated in invasively growing cells (Fig. 4.1, Table S2). These included glucose phosphorylation (*GLK1*, *HXK1*, *HXK2*), phosphoglucomutase (*PGM2*), galactokinase (*GAL1*), and maltose permease (*MAL31*). Some genes present in both carbohydrate metabolic process and fungal-type cell wall organisation GO categories were also upregulated in invasively growing cells. For example, *YEA4*, *EXG2*, *GAS1* and *GAS5* are involved in chitin and β-glucan maintenance. Other genes encoding cell wall components, especially fungal-type cell wall components (GO:0009277; $p <$ 2.07E-5) were also upregulated in invasively growing cells (Table S2).

Since yeast cells are non-motile, access to nutrients is largely dependent on a cell's access to proximal space. For cells growing on a surface, the expansion of a colony is limited by the agar concentration and nutrients (Chen et al., 2014). If cells were pushed upward, access to nutrients from solid medium becomes limited. Eventually, these cells undergo chronological aging differentiation (Palková et al., 2014). The action of invasion into a medium results in three dimensional access to nutrients, allowing cellular growth and division to continue. Many genes encoding cell wall components were upregulated in the invasively growing cells compared to surface growing cells (Fig. 4.1; Table S2). This suggests cell wall construction is strongly coordinated with cell cycle progress and cell growth activity in the invasively growing population (Klis et al., 2006). Together with the upregulation of genes involved in glucose import and carbohydrate metabolic processes (Fig. 4.1; Table S2), and the time series images of limited surface cell expansion whilst continual invasive population growth occurred (Fig. 4.6B and S2), data in this study supports the hypothesis that invading cells have greater access to nutrients, which aids growth.

AWRI796_5153 is a hypothetical gene with the third largest change in expression (increased expression by 6.45-fold; Table 4.1). Interestingly, a portion of the gene sequence, when translated, is homologous to an amidase domain. Amidases (KEGG identifier EC 3.5.1.4) function by catalysing the hydrolysis of short-chain amides to organic acids, thereby releasing ammonia. Ammonia is known to be a yeast colony signalling molecule produced during starvation (Palková et al., 1997). To date, amidase is poorly characterised in yeast. However, in bacteria, this protein is normally used to breakdown peptidoglycan for cell wall recycling (Litzinger et al., 2010; Johnson et al., 2013). Other studies have also reported that amidase is involved in the regulation of quorum sensing, biofilms and virulence in bacteria (Ochiai et al., 2014; Clamens et al., 2017).

4.4.4 Medium-chain fatty acid biosynthesis pathway

All three genes, *EEB1*, *EHT1* and *MGL2*, categorised under the medium-chain fatty acid biosynthetic process (GO:0051792; $p < 0.015$) were upregulated in invasively growing cells. *EEB1* is required for invasive growth upon butanol induction whereas *EHT1* is required for pseudohyphal growth (Jin et al., 2008; Ryan et al., 2012). Eeb1p and Eht1p are part of medium-chain fatty acid ethyl ester production (Saerens et al., 2006). Ethyl ester is known to contribute to aroma and flavour in alcoholic beverages, but its role in yeast is unclear (Swiegers and Pretorius, 2005; Swiegers et al., 2005). Several reasons have been given for ethyl ester production: (1) to reduce the toxicity of medium-chain fatty acids, (2) to regenerate free co-enzyme A, and (3) to attract *Drosophila* for dispersal in nature (Thurston et al., 1982; Bardi et al., 1998; Lilly et al., 2006; Saerens et al., 2010; Christiaens et al., 2014).

Overexpression of *MGL2* reduced triacylglycerol and sterol ester but increased

phosphatidylcholine and phosphatidylethanolamine in the cell, indicating a change in lipid profile (Selvaraju et al., 2016). An increase in phospholipids as a result of increased *MGL2* expression may suggest a demand for plasma membrane synthesis, which may be due to an increase in cell size or cellular growth in the invasively growing population.

4.4.5 Genetic interaction network analysis predicts genes modulating invasive growth

Genetic interaction network analysis was used (see Experimental Procedures) to determine if any of the differentially expressed genes exhibited extensive connectivity. Network-based approaches are particularly useful in characterising complex biological systems (Barabási and Oltvai, 2004). By establishing a network graph using both differentially expressed genes in this study and interaction data from the Data Repository of Yeast Genetic Interactions, sum of interactions between genes in invasively growing cells can be shown at system-scale and this allowed determination of significant genes from their centrality and connectivity (Zotenko et al., 2008; Koh et al., 2010). In the hub of the largest connected network, three genes were shown to have high connectivity: *MSC1*, *SIN3* and *ARO1*, with each having at least 30 edges (degree) connected to the node (Fig. S1). Of the three genes, *SIN3*, which encodes a component of Rpd3 histone deacetylase complexes, has also been identified as being required for pseudohyphal and invasive growth (Carrozza et al., 2005; Ryan et al., 2012). After analysing the network, the connectivity (Betweenness Centrality) value of each gene was examined with the change in expression level. This allowed the discovery of genes that have a larger role in modulating or association with invasive growth. Several genes have been highlighted to have a relatively large value in both Betweenness Centrality and change in expression (Fig. 4.2).

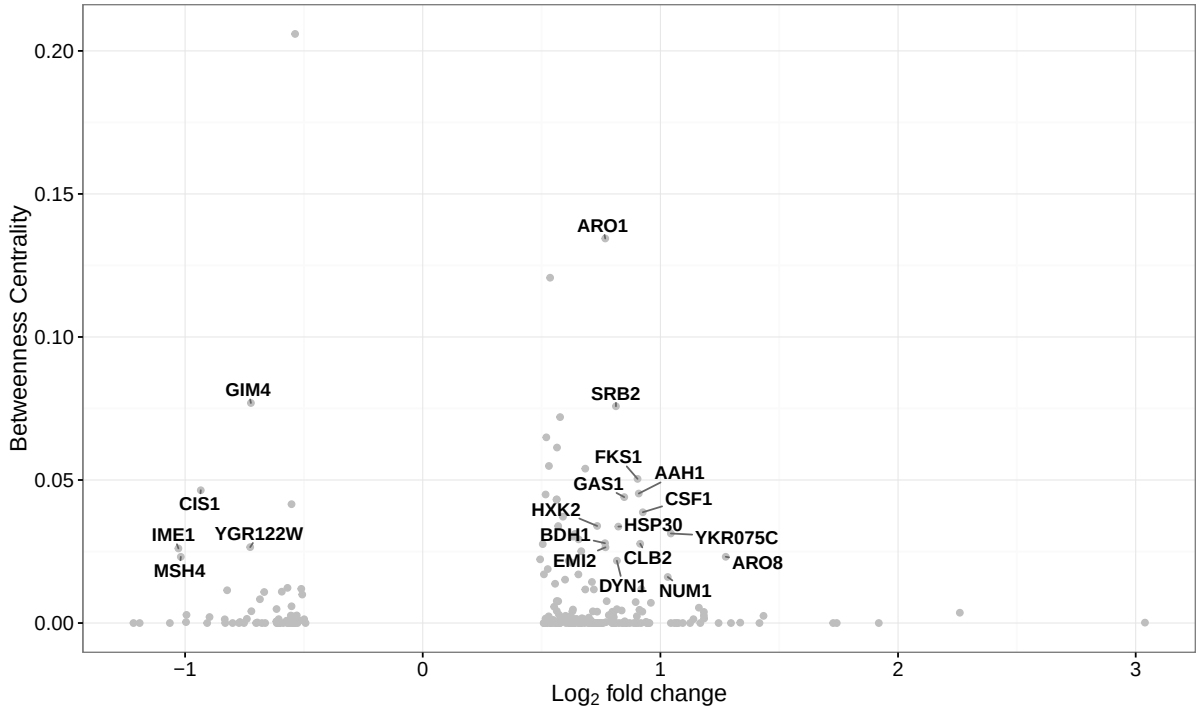

Figure 4.2: Relationship between Betweenness Centrality within the genetic interaction network of differentially expressed genes and changes in gene expression. Each circle represents a gene. Gene names are shown only for those meeting both criteria of absolute $\log_2$ fold change greater than 0.7 and Betweenness Centrality greater than 0.015.

Some of these are related to previously identified enriched GO categories: (fungal-type) cell wall organisation and carbohydrate metabolic process such as *HXK2*, *GAS1* and *FKS1*. Notably, *ARO1* and *ARO8* both upregulated in invasively growing cells, encode proteins that are involved in phenylalanine and tyrosine biosynthesis, which are precursors of suggested quorum sensing aromatic alcohols in *S. cerevisiae* (Chen and Fink, 2006). *ARO1* is downregulated in smooth colonies compared to fluffy colonies (Kuthan et al., 2003). Genes *IME1*, *MSH4* and *EMI2* are involved in meiotic events. *IME1* and *MSH4* were downregulated in invasively growing cells, while *EMI2* was upregulated. *EMI2* has a paralog, *GLK1*, which encodes for glucokinase. In this case, the upregulation of *EMI2* may not be due to meiotic function, but could be linked to glucose metabolism. The plot also identified genes related to mitochondria such as *CIS1*, *NUM1* and *CSF1*, and genes related to cell cycle: *DYN1*, encodes for protein involved in spindle assembly and orientation and *CLB2*, encodes for cyclin involved in cell cycle progression. *CLB2* overexpression delays G_2/M transition, which means apical growth is prolonged to induce invasive growth (Simpson-Lavy et al., 2009; Shively et al., 2013). Prolonged apical growth that is required for surface filamentation may also be involved in the induction of invasive growth.

RGI1, whose expression increased by 3.78-fold in the invasively growing cells (Table 4.1), has been reported to be involved in aerobic sugar metabolism (Rep et al., 2000; Domitrovic et al., 2010). Anaerobiosis within a nitrogen atmosphere inhibits invasive growth (Zupan and Raspor, 2010). Previous work in this laboratory has also shown that invasive growth is inhibited in the absence of oxygen as well as in 'petite' strains (Joanna

Sundstrom and Vladimir Jiranek, *pers. comm.*). Together with the upregulation of several genes related to or found in mitochondria, as identified from the plot in Figure 4.2 and *AIM17* (Table S1; Hess et al., 2009), this suggests that respiration may be required for invasive growth.

4.4.6 Protein interaction network analysis suggests Ssa2p as the major determinant of invasive growth

Protein-protein interactions were visualised (see Experimental Procedures) between the differentially expressed genes in a network graph using the *mentha* database (Calderone et al., 2013). Similar to the genetic network analysis, this enabled the discovery of high connectivity proteins, thereby reflecting their biological importance in invasive growth. In comparison to genetic interactions that provide information on how genes control cellular processes, protein interactions present functional connections. In the latter, Ssa2p was identified as the key node of the largest connected network, having the most number of edges (degree = 14) and the largest Betweenness Centrality value (0.77; Fig. 4.3). In addition, *SSA2* had the fourth largest change in gene expression with nearly a five-fold increase in invasively growing cells (Table 4.1).

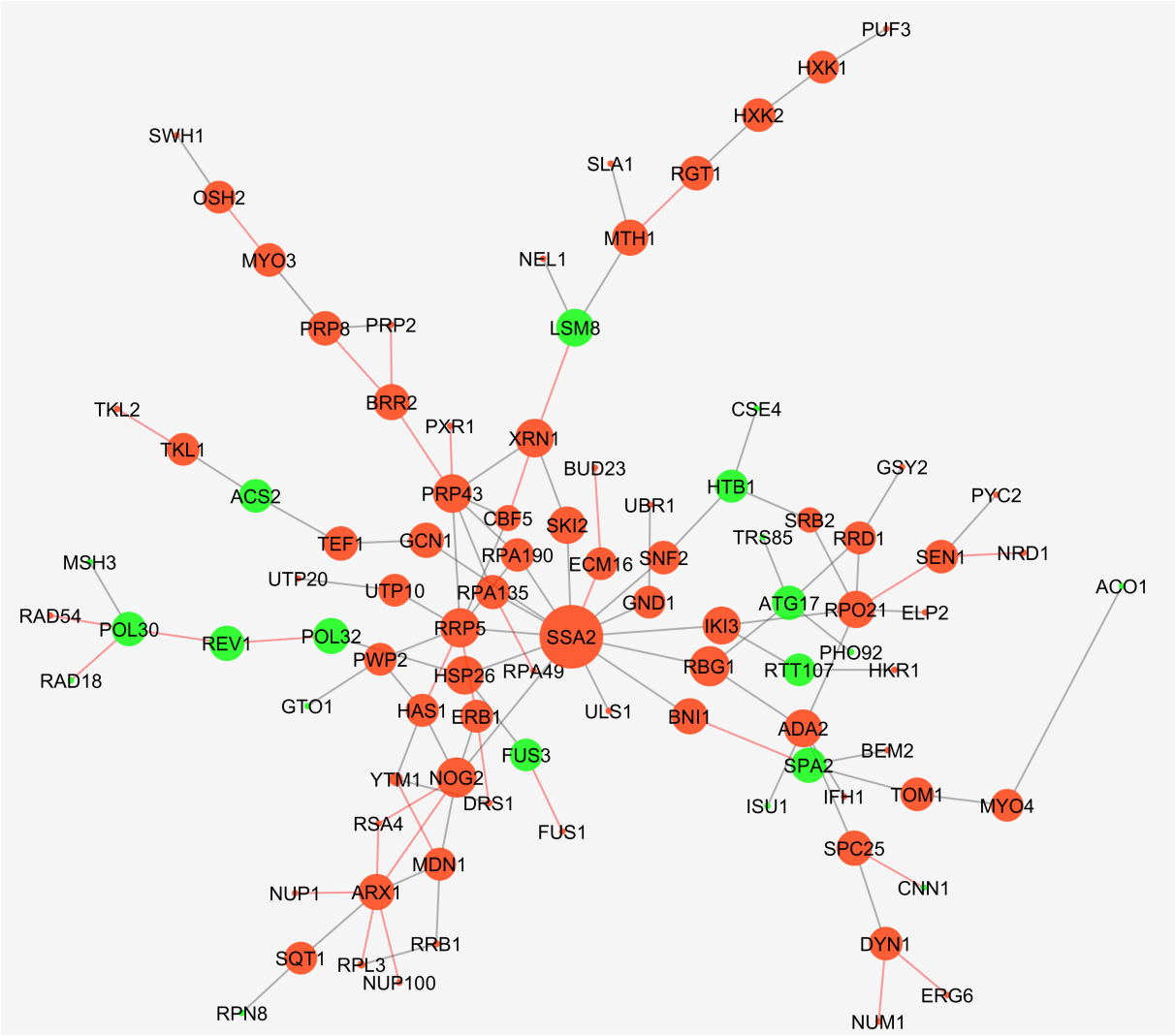

Figure 4.3: Protein-protein interaction network of differentially expressed genes between surface and invasively growing cells. A 25% fold-change threshold was applied for the differential expression analysis. The largest connected network with an interaction confidence score of at least 0.3 is shown. Red and green node colours represent upregulation and downregulation in invasively growing cells respectively; larger node size represents higher values of Betweenness Centrality, and vice versa.

SSA2 is required for pseudohyphal growth but not haploid invasive growth (Ryan et al., 2012). However, Shively and colleagues (2013) reported that it enhanced invasive growth (agar invasion score 0.96) when overexpressed in diploids. This protein is involved in protein folding and transport, suggesting that it may act as a checkpoint protein to ensure functionality of other proteins involving in invasive growth. The importance of this gene, along with *NOG2* and *HSP26*, is also shown in the relationship plot between their protein connectivity and change in expression (Fig. 4.4). Nog2p is a putative GTPase involved in exporting the large ribosomal subunit while Hsp26p is a chaperone which binds and prevents unfolded proteins forming large aggregates (Saveanu et al., 2001; White et al., 2006).

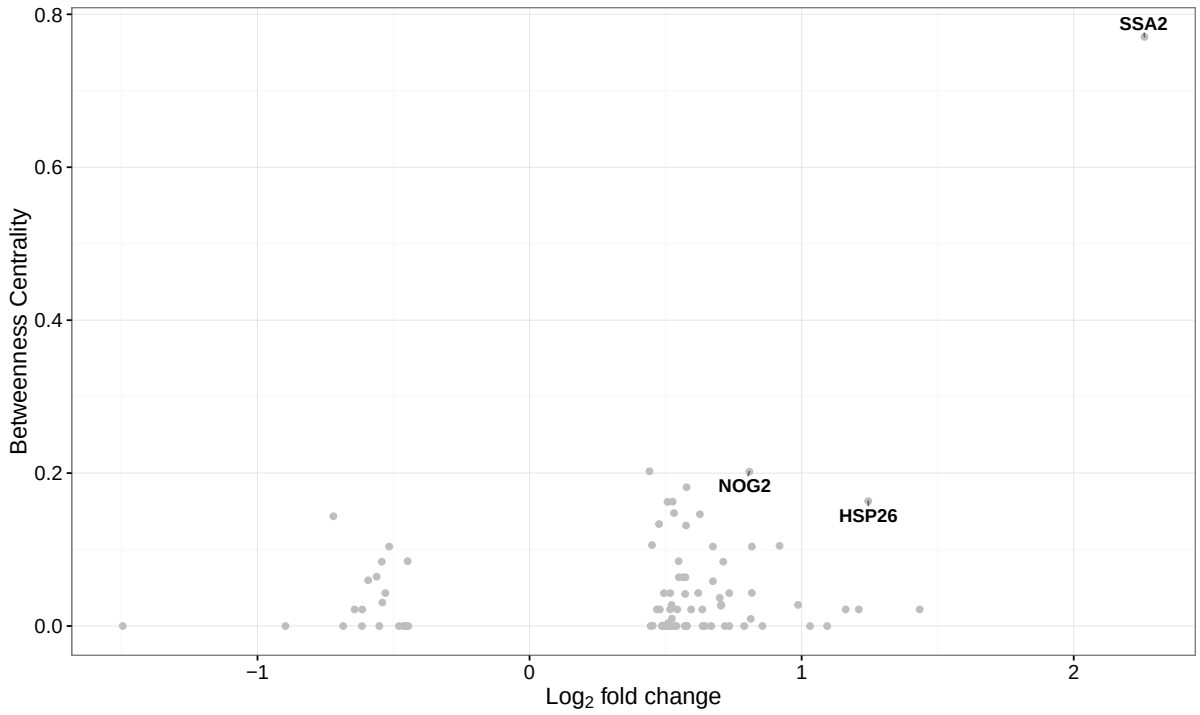

Figure 4.4: Relationship between the Betweenness Centrality of each gene in the protein interaction network and their corresponding change in gene expression. Each circle represents a single gene. Gene names are shown only for those meeting both criteria of absolute $\log_2$ fold change greater than 0.8 and Betweenness Centrality greater than 0.125.

4.4.7 Expression levels of transcription factor genes do not correlate with their previously reported involvement in invasive growth

Interestingly, in this study the differentially expressed genes encoding transcription factors did not correlate with previous studies that highlighted their involvement in invasive growth (Jin et al., 2008; Van Mulders et al., 2009; Shively et al., 2013). Fifteen genes encoding known transcription factors increased expression and 12 decreased gene expression in invasively growing cells (Fig. 4.5).

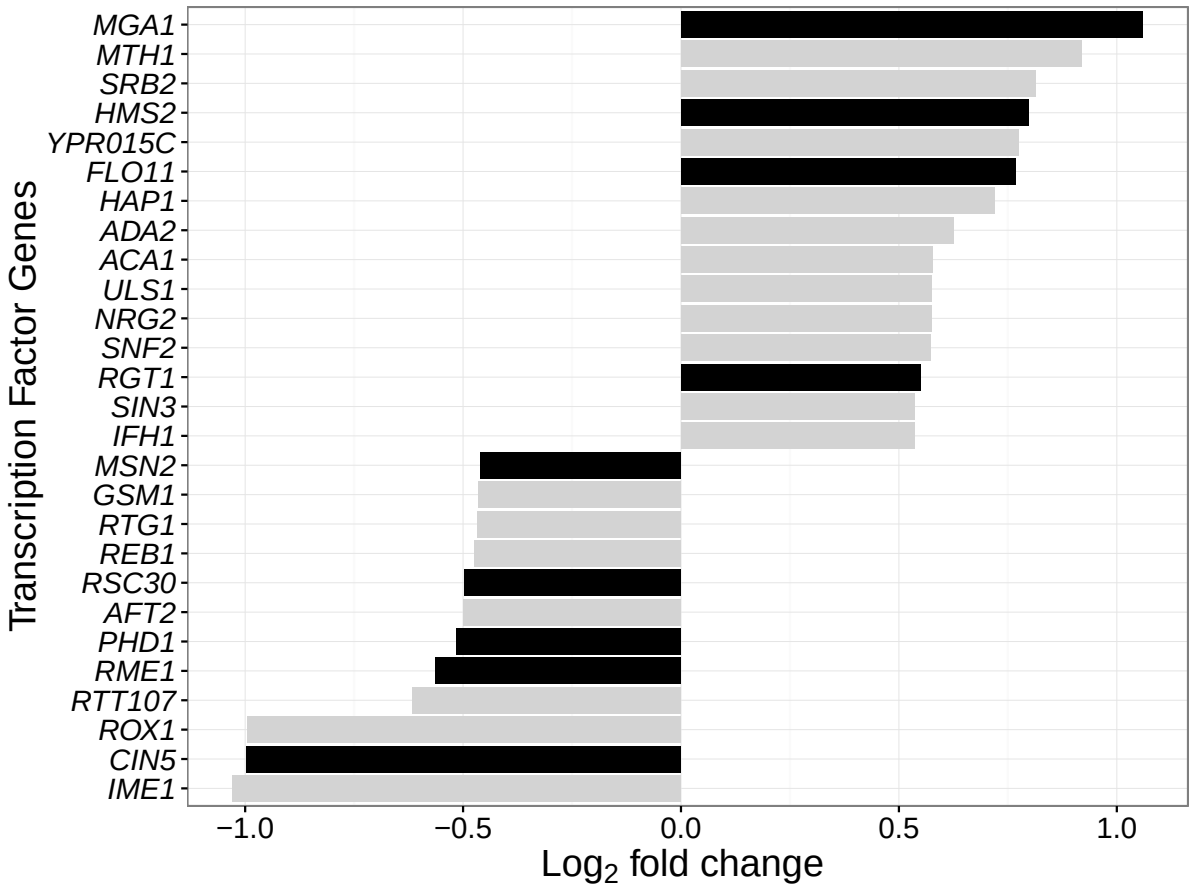

Figure 4.5: Change in gene expression of genes encoding transcription factors in invasively growing cells compared to surface growing cells. Genes with black bars were shown to be involved in invasive growth in other studies (overexpression results in increased invasive growth or deletion results in no invasive growth).

Of these, *MGA1*, whose encoded protein restores filamentation defects by multicopy expression (Lorenz and Heitman, 1998), had the largest increase in expression. This was followed by *MTH1*, which encodes for a negative regulator of the glucose-sensing signal transduction pathway for *HXT* gene expression (Lafuente et al., 2000). The upregulation of many glucose transporter genes in the invasively growing cells suggests that *MTH1* had released its repression on these genes. Similarly, *NRG2*, encoding a negative glucose regulator that interacts with Snf1p (Kuchin et al., 2002), was also upregulated in invasively growing cells. *SNF2*, encoding for a transcriptional activator of *FLO11* under glucose limitation (Barrales et al., 2008), had increased expression. Conversely, *ROX1*, *CIN5* and *IME1* had the largest decrease in gene expression (approx. two-fold). When comparing to previously reported genes encoding transcription factor required for or to enhance invasive growth when overexpressed, four were upregulated in this study: *MGA1*, *HMS2*, *FLO11* and *RGT1* (Harashima and Heitman, 2002; Shively et al., 2013). Several genes reported to be involved in invasive or pseudohyphal growth had decreased in expression in invasively growing cells, these being *MSN2*, *RSC30*, *PHD1*, *RME1* and *CIN5*.

4.4.8 Cellular water homeostasis: aquaglyceroporin gene *FPS1* is required for invasive growth

Cellular water homeostasis (GO:0009992; $p < 0.0032$) was one of the enriched GO categories identified in the upregulated gene set (Fig. 4.1). All five genes classified within this biological process showed an increase in gene expression (four were significant) in invasively growing cells compared to surface growing cells (*AQY1*, *AQY2*, *YLL053C*, *FPS1* and *AQY3*; increased by 1.43–2.25 fold; Fig. 4.6A). None of these genes have previously been identified as being required for invasive growth, although *AQY1* was reported to have increased gene expression in fluffy colonies compared to smooth colonies (Kuthan et al., 2003). To confirm if these genes are important for invasive growth, yeast deletants were constructed for each gene of interest and the deletants were screened for reduced invasive growth. Yeast deletants Δ*fps1* and Δ*aqy3* had a reduced number of invasive growth foci whereas Δ*aqy2* and Δ*yll053c* had a similar number of invasive growth foci compared to the wild type AWRI796 on Day 4 (Fig. 4.6B). By Day 10, the invasive foci that had formed developed to a comparable size in all strains. Therefore, the decreased invasive growth observed for Δ*fps1* and Δ*aqy3* was more related to fewer foci rather than due to reduced or delayed growth. The reduced number of invasive growth foci was still observed on Day 10. These deletants and other progeny from the same spore were further evaluated to ensure the differences were due to the gene deletion and not spore variability. In this assay, the Δ*fps1* progeny had less invasive growth than the wild type progeny whilst Δ*aqy3* progeny gave mixed results (Fig. S2). Δ*aqy1* was not evaluated in this analysis due to difficulties in generating the strain (Appendix C).

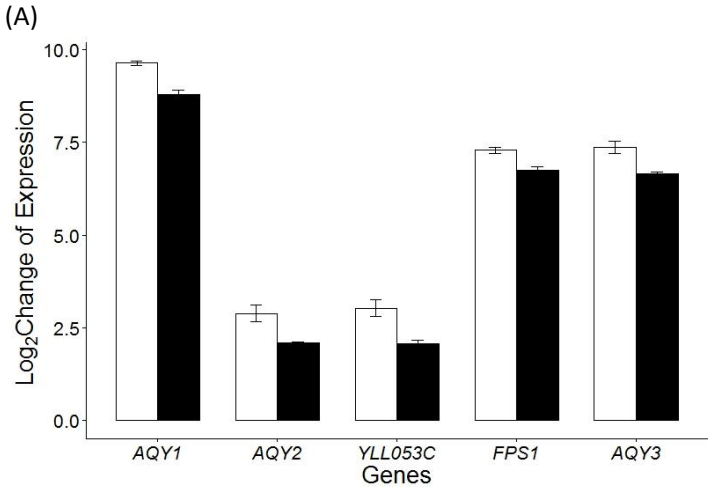

Figure 4.6: Evaluation of genes encoding proteins involved in cellular water homeostasis and their importance for invasive growth. (A) Comparison of aquaporin and aquaglyceroporin gene expression between invasively (white) and surface (black) growing cells SLADS-agar (0.3%). Please refer to next page for (B).

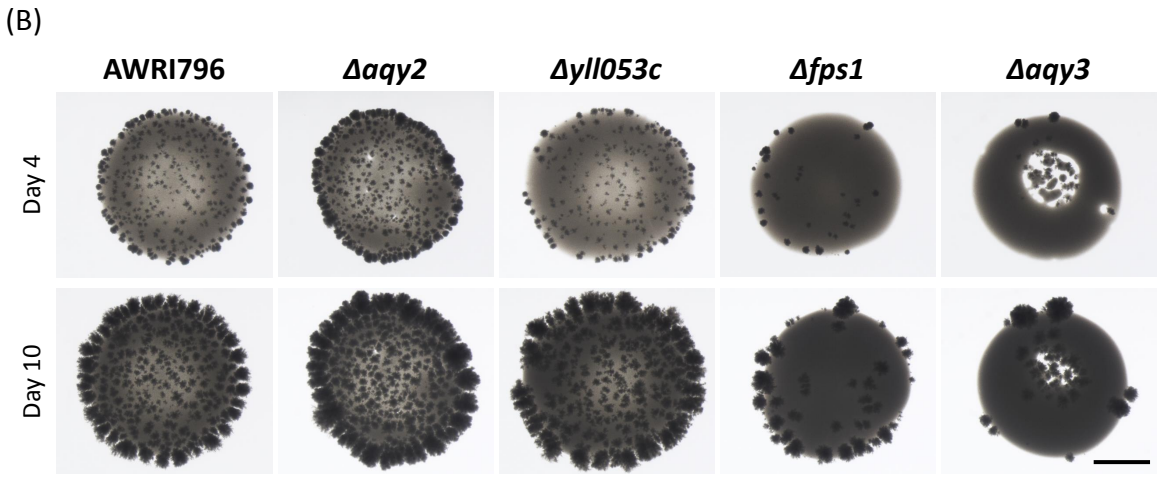

Figure 4.6: (B) Invasive growth evaluation of AWRI796 and homozygous deletants of indicated genes on SLADS-agar (0.3%). Images were photographed from the underside of the agar plates. Surface growing cells were in a large round mat. Multiple small spots on top of that were invasively growing cells. Scale bar, 1 mm.

The deletion analysis confirmed that *FPS1* is important for invasive growth. *FPS1* encodes a channel protein that regulates glycerol export (Oliveira et al., 2003). Lack of Fps1p results in cell wall stress due to high turgor pressure from accumulation of glycerol (Tamas et al., 1999). Cells then fortify their cell wall by displaying less sensitivity to the cell wall degrading enzyme, zymolyase (Beese et al., 2009). As the transcriptomics profile indicates that cell wall remodelling and organisation is actively performed in invasive growth, this fortified cell wall may have prevented the wall from being flexibly modified for growing invasively. This suggests that high turgor pressure or fortified cell wall may not be beneficial when growing invasively. Alternatively, invasive growth may also require the export of glycerol.

4.5 Conclusions

In summary, this study has identified that genes of glucose import and carbohydrate metabolic process are upregulated in invasively growing cells compared to those growing on the agar surface, indicating improved access to nutrients. Fungal-type cell wall organisation is involved in invasive growth, potentially to enhance cell wall stability and adhesion. The protein of a hypothetical gene that has an amidase domain may have a role in invasive growth through the involvement of cell wall recycling process or cell-cell signalling. Ssa2p, which is involved in protein folding and transport, was identified as being significant in association with invasive growth from the protein interaction network analysis. Cellular water homeostasis is also important, especially the glycerol export channel protein Fps1p. Genes involved in medium-chain fatty acid biosynthetic process and ethyl ester production were upregulated in invasive growth but their roles in invasive growth remain elusive.

4.6 Experimental Procedures

4.6.1 Yeast strains

Yeast strains used in this study are listed in Table 4.2. To generate deletants of genes of interest (GOI) in AWRI796, the corresponding gene deletant in a BY4741 background was used. The GOI *Kan*MX gene replacement cassettes were generated by PCR using GOI specific primer pairs (GOI_A and GOI_D, Table S4) and genomic DNA of the corresponding BY4741 deletant (Wach et al., 1994; Winzeler et al., 1999). Deletion in AWRI796 was generated by transformation of the GOI *Kan*MX gene replacement cassette, followed by selection on YPD agar (1% yeast extract, 2% bacto peptone, 2% glucose, 2% bacteriological agar) + 200 mg L^{-1} G418-sulfate (Gietz and Schiestl, 2007). Homozygous deletants were isolated by sporulation, dissection and re-diploidisation, followed by verification with PCR amplification and sequencing using GOI specific primer pairs GOI_A2 and GOI_D2 (Table S4) located outside the original gene replacement cassette. *AQY1* deletion in AWRI796 was omitted in this study due to difficulties in generating the correct strain (Appendix C).

Table 4.2: Yeast strains used in this study.

Yeast strain	**Genotype**	**Reference**
AWRI796	Commercial wine yeast strain; diploid	Mauri Yeast Australia
AWRI796 Δ*aqy2*	*aqy2*Δ*::Kan*MX/*aqy2*Δ*::Kan*MX	This study
AWRI796 Δ*aqy3*	*aqy3*Δ*::Kan*MX/*aqy3*Δ*::Kan*MX	This study
AWRI796 Δ*fps1*	*fps1*Δ*::Kan*MX/*fps1*Δ*::Kan*MX	This study
AWRI796 Δ*yll053c*	*yll053c*Δ*::Kan*MX/*yll053c*Δ*::Kan*MX	This study
BY4741 Δ*aqy2*	*MAT*a *his3*Δ*1 leu2*Δ*0 met15*Δ*0 ura3*Δ*0 aqy2*Δ*::Kan*MX	Thermo Fisher Scientific Australia
BY4741 Δ*aqy3*	*MAT*a *his3*Δ*1 leu2*Δ*0 met15*Δ*0 ura3*Δ*0 aqy3*Δ*::Kan*MX	Thermo Fisher Scientific Australia
BY4741 Δ*fps1*	*MAT*a *his3*Δ*1 leu2*Δ*0 met15*Δ*0 ura3*Δ*0 fps1*Δ*::Kan*MX	Thermo Fisher Scientific Australia
BY4741 Δ*yll053c*	*MAT*a *his3*Δ*1 leu2*Δ*0 met15*Δ*0 ura3*Δ*0 yll053c*Δ*::Kan*MX	Thermo Fisher Scientific Australia

4.6.2 Genomic DNA preparation and PCR conditions

Genomic DNA was extracted according to Lõoke et al. (2011). TE buffer (10 mM Tris-HCl pH 8.0, 1 mM EDTA) was used to solubilise DNA, and 2 μL was used as the template in a 50 μL PCR reaction. PCR reactions were performed with Bioline Velocity DNA Polymerase (Cat No. BIO-21098), according to the manufacturer's instructions. PCR products were separated on a 0.8–1% TAE-agarose gel containing GelRed nucleic acid stain (Biotin; Cat No. 41003). DNA fragments of GOI *Kan*MX gene replacement cassettes

were purified using the *Wizard SV* Gel and PCR Clean-Up System (Promega, Madison, WI; Cat No. A9282).

4.6.3 Low nitrogen invasive growth assays

AWRI796 was grown in 10 mL SLAD (0.17% Yeast Nitrogen Base without amino acids and ammonium sulfate, 2% glucose, 50 μM ammonium sulfate, prepared according to Binder et al., 2015) for 48 h at 30 °C before re-inoculation into 25 mL SLAD at 1×10^4 cells mL^{-1} in an Erlenmeyer flask and grown for a further 24 h. Prior to plating, the exponential-phase culture was diluted in Phosphate Buffered Saline (PBS; 137 mM NaCl, 2.7 mM KCl, 10 mM Na_2HPO_4, 1.8 mM KH_2PO_4, pH 7.4) to 2×10^5 cells mL^{-1}. An aliquot of 5 μL was spotted at the centre of SLADS-agar (10 mL SLAD, 0.4 mg L^{-1} sodium sulfide ($Na_2S.9H_2O$), 0.3% agar) in a 60 mm Petri dish (Techno Plas; Cat No. S6014S10). For RNA-sequencing, cells were harvested after 8 days of incubation at 25 °C. Three independent assays were conducted; the number of agar plates from which cells were harvested for each independent assay were 188, 190 and 192 respectively. For invasive growth screening of AWRI796 GOI deletants, invasive growth mats were imaged from the underside of the plate on Day 4 and 10 at 0.5×0.63 magnification using a Nikon SMZ1270 stereomicroscope and an attached DS-Fi3 camera with NIS-Elements F4.60 software.

4.6.4 Sample harvest and RNA extraction

Cells growing on the agar surface were harvested with a disposable plastic inoculation loop and resuspended in 1 mL Trizol (Life Technologies; Cat No. 15596-018). Any remaining surface cells were rinsed off with ultrapure water. A scalpel blade was used to slice out the piece of agar containing invasively growing cells and transferred to a separate 1 mL Trizol. The cells from all agar plates making up each replicate were pooled for each of the three assays for both surface and invasively growing cells (*i.e.* six samples in total). Harvested cells in Trizol were heated at 60 °C for 3 min and then centrifuged at $3,824 \times g$ for 30 s. Supernatant was removed and 1 mL fresh Trizol was added before being snap frozen in liquid nitrogen.

RNA extraction was performed using a combination of Trizol reagent and a Qiagen RNeasy Mini kit (Cat No. 74104). Samples were thawed on ice. Glass beads were added up to the halfway mark of the meniscus. Six cycles of 45 s of vortexing and 45 s of rest on ice were used to disrupt cells. Tubes were incubated at 65 °C for 3 min and 200 μL of chloroform was added, followed by vortexing for 15 s before leaving at room temperature for 5 min. Tubes were centrifuged at $20,817 \times g$ for 10 min at 4 °C. Supernatant was recovered to a fresh tube and an equal volume of 70% v/v ethanol was added, mixed by pipetting, before continuing according to the Qiagen RNeasy Mini kit manufacturer's instructions. RNA quality and quantity were checked using a Nanodrop

ND-1000 UV-visible light spectrophotometer (Thermo Fisher Scientific), separation on 1% TAE-agarose gel and an Experion Automated Electrophoresis System (Bio-Rad).

4.6.5 RNA sequencing and analysis

RNA-sequencing was performed with an Illumina Hiseq instrument in one lane (Australian Genome Research Facility, Melbourne, Australia). Reads were mapped to the *S. cerevisiae* AWRI796 genome sequence located at the NCBI (GenBank assembly accession: GCA_000190195.1) with TopHat (Trapnell et al., 2009). Reads were counted for each gene using *featureCounts* in the Rsubread software package (Liao et al., 2013). The translation sequence of genes annotated as "hypothetical protein" was used to search for any domain hits in the Pfam database (Finn et al., 2016). Gene Ontology IDs for the matched protein domains were extracted from InterPro database (Mitchell et al., 2015). These GO IDs were added to the latest gene association file downloaded from the *Saccharomyces* Genome Database (Date: 04/02/2016). This was used for downstream GO analysis. Counts and gene lengths were merged for genes that had sequences located next to each other in the genome and have matched part of the same domain. Genes with counts less than 50 were not considered in the downstream analysis. Differential expression analysis was performed using the *limma* package (Ritchie et al., 2015) in R with voom (Law et al., 2014) and TREAT (McCarthy and Smyth, 2009) functions, incorporating a 30% fold-change threshold in the hypothesis test. GOseq was used to perform GO enrichment and KEGG analysis (Young et al., 2010). The significantly enriched GO list was summarised and visualised using REVIGO (Supek et al., 2011).

4.6.6 Network analysis

The interactions between significant differentially expressed genes were visualised using a network graph in Cytoscape (Shannon et al., 2003). The protein-protein interaction database of *S. cerevisiae* was downloaded from *mentha* (Calderone et al., 2013, Date: 24/04/2016) while genetic interaction data was obtained from the DRYGIN database (Costanzo et al., 2010; Koh et al., 2010). For protein-protein network graphs, interactions with a confidence score of at least 0.3 were used with the resulting differentially expressed genes from the hypothesis test with a 25% fold-change threshold. Basic network analysis was performed in Cytoscape. Some parameters were visualised in graphs: node color was mapped to up- or down-regulation whereas node size was mapped to Betweenness Centrality value which represents connectivity of each node in the graph. The Betweenness Centrality of each node was plotted with the change in gene expression value. The betweenness of a node v is obtained by counting the number of all shortest paths, connecting any pair of nodes within the network, which are going through that particular node v. The value is divided by the number of all shortest paths connecting two nodes.

The *S. cerevisiae* transcription factor database was downloaded from YEASTRACT and was used to determine the differentially expressed transcription factor genes (Teixeira et al., 2014). A graph was plotted to show change in gene expression levels of differentially expressed transcription factor genes.

4.7 Acknowledgements

This work was supported by Wine Australia [GWR Ph1305] and the Australian Research Council [DP 20111529]. ELT was supported by an Adelaide Graduate Research Scholarship, a DR Stranks Postgraduate Travelling Fellowship and a Research Abroad Scholarship provided by the University of Adelaide. The authors thank Dr Valarie Wood for providing suggestions on annotations for hypothetical proteins.

The authors have no conflict of interest to declare.

4.8 Supporting Information

4.8.1 Tables

Table S1: Due to the size of the table, this can be found in Appendix D.

Table S2: List of enriched Gene Ontology terms from the upregulated gene set in invasively growing cells.

Category	Number of DE Genes in Category	Number of Genes in Category	GO Term	Ontology	Adj. *p*-value	Genes
GO:0005886	60	398	plasma membrane	CC	5.67E-06	*AQR1, AQY1, AQY2, ATO2, ATO3, BEM2, BNI1, BUL1, CCH1, CIS3, CWH43, CYR1, DIP5, DNF1, DNF2, DUR3, ENA1, EXG2, FET3, FKS1, FLO11, FUI1, GAP1, GAS1, GLK1, HKR1, HSP30, HXT1, HXT2, HXT3, HXT4, HXT6, HXT7, INA1, KRE6, MCH5, MEP1, MMP1, PDR10, PDR11, PDR15, PDR5, PHM7, PHO90, PUN1, PUT4, RGI1, SLA1, SRO77, SSA2, SSU1, STT4, TCB3, TDH1, THI7, TOR1, TOR2, TPO1, TPO4, YLR194C*
GO:0009277	17	75	fungal-type cell wall	CC	2.06E-05	*CIS3, CWP1, DSE2, EXG2, FIT1, FIT3, FLO5, GAS1, GAS5, PIR1, PRY3, SIM1, SSA2, SUN4, TDH1, ZPS1, YLR194C*
GO:0005618	14	54	cell wall	CC	2.06E-05	*CIS3, CWP1, DSE2, FIT1, FIT3, FLO11, FLO5, GAS1, GAS5, PIR1, PRY3, SIM1, SSA2, SUN4*
GO:0005887	22	95	integral component of plasma membrane	CC	3.91E-05	*AGP2, AQY1, AQY2, CWH43, DIP5, ENA1, FUS1, GAP1, HXT1, HXT2, HXT3, HXT4, HXT6, HXT7, MAL31, MEP1, MMP1, PMC1, PUT4, YPK9, YFL054C, YLL053C*
GO:0046323	10	22	glucose import	BP	6.14E-05	*GLK1, HXK1, HXK2, HXT1, HXT2, HXT3, HXT4, HXT6, HXT7, MAL31*
GO:0005353	6	7	fructose transmembrane transporter activity	MF	9.28E-05	*HXT1, HXT2, HXT3, HXT4, HXT6, HXT7*
GO:0015578	6	7	mannose transmembrane transporter activity	MF	9.28E-05	*HXT1, HXT2, HXT3, HXT4, HXT6, HXT7*
GO:0005215	16	69	transporter activity	MF	9.28E-05	*AQR1, AQY1, AQY2, DUR3, FUI1, HXT1, HXT2, HXT3, HXT4, HXT6, HXT7, MAL31, THI7, TPO4, YFL054C, YLL053C*
GO:0055085	34	205	transmembrane transport	BP	9.65E-05	*AGP2, AQR1, AQY1, AQY2, ATO3, AVT6, CCH1, DIP5, DUR3, ECM3, ENA1, FUI1, GAP1, HXT1, HXT2, HXT3, HXT4, HXT6,*
GO:0005576	15	81	extracellular region	CC	0.00064	*CIS3, CWP1, DSE2, FIT1, FIT3, FLO11, FLO5, GAS1, GAS5, PIR1, PRY3, SIM1, SSA2, SUN4, ZPS1*
GO:0008643	8	19	carbohydrate transport	BP	0.000789	*HXT1, HXT2, HXT3, HXT4, HXT6, HXT7, MAL31, YEA4*
GO:0005975	17	91	carbohydrate metabolic process	BP	0.001161	*EMI2, EXG2, GAL1, GAS1, GAS5, GDB1, GLC3, GLK1, GPH1,*
GO:0031225	11	49	anchored component of membrane	CC	0.00136	*CWP1, DSE2, EXG2, FIT1, FIT3, FLO11, FLO5, GAS1, GAS5, PRY3, YLR194C*
GO:0015146	4	4	pentose transmembrane transporter activity	MF	0.003212	*HXT1, HXT2, HXT4, HXT7*
GO:0009992	4	5	cellular water homeostasis	BP	0.003212	*AQY1, AQY2, YFL054C, YLL053C*
GO:0015250	4	5	water channel activity	MF	0.003212	*AQY1, AQY2, YFL054C, YLL053C*
GO:0015254	4	5	glycerol channel activity	MF	0.003212	*AQY1, AQY2, YFL054C, YLL053C*
GO:0005355	7	18	glucose transmembrane transporter activity	MF	0.006459	*HXT1, HXT2, HXT3, HXT4, HXT6, HXT7, MAL31*
GO:0001678	4	5	cellular glucose homeostasis	BP	0.006772	*EMI2, GLK1, HXK1, HXK2*
GO:0004340	4	5	glucokinase activity	MF	0.006772	*EMI2, GLK1, HXK1, HXK2*
GO:0004396	4	5	hexokinase activity	MF	0.006772	*EMI2, GLK1, HXK1, HXK2*
GO:0008865	4	5	fructokinase activity	MF	0.006772	*EMI2, GLK1, HXK1, HXK2*
GO:0019158	4	5	mannokinase activity	MF	0.006772	*EMI2, GLK1, HXK1, HXK2*
GO:0008645	4	5	hexose transport	BP	0.006826	*HXT3, HXT4, HXT6, HXT7*
GO:0005351	7	19	sugar:proton symporter activity	MF	0.007095	*HXT1, HXT2, HXT3, HXT4, HXT6, HXT7, MAL31*
GO:0035428	7	19	hexose transmembrane transport	BP	0.007095	*HXT1, HXT2, HXT3, HXT4, HXT6, HXT7, MAL31*
GO:0031505	17	95	fungal-type cell wall organization	BP	0.009746	*CIS3, CWH43, CWP1, EXG2, GAS1, HKR1, KRE6, MHP1, MYO3,*
GO:0006833	3	3	water transport	BP	0.009746	*AQY1, AQY2, YFL054C*
GO:0051792	3	3	medium-chain fatty acid biosynthetic process	BP	0.011764	*EEB1, EHT1, MGL2*
GO:0071555	15	79	cell wall organization	BP	0.014346	*CIS3, DSE1, DSE2, ECM3, EXG2, FKS1, GAS1, GAS5, GSC2, KRE6, PIR1, SIM1, SUN4, YPK2, YLR194C*
GO:0006006	7	21	glucose metabolic process	BP	0.01791	*DOG2, GLK1, HXK1, HXK2, PGM2, RGT1, TDH1*
GO:0034220	6	13	ion transmembrane transport	BP	0.018779	*AQY1, AQY2, CCH1, MCH5, YFL054C, YLL053C*
GO:0022891	7	23	substrate-specific transmembrane transporter activity	MF	0.022168	*HXT1, HXT2, HXT3, HXT4, HXT6, HXT7, MAL31*
GO:0005536	4	7	glucose binding	MF	0.048257	*EMI2, GLK1, HXK1, HXK2*
GO:0005199	4	13	structural constituent of cell wall	MF	0.048257	*CIS3, CWP1, PIR1, YLR194C*
GO:0022857	7	26	transmembrane transporter activity	MF	0.048257	*HXT1, HXT2, HXT3, HXT4, HXT6, HXT7, MAL31*
GO:0046835	5	14	carbohydrate phosphorylation	BP	0.048257	*EMI2, GAL1, GLK1, HXK1, HXK2*

Table S3: Genes upregulated in invasively growing cells in this study and common to other related studies. Genes in bold are those that are reported in more than one of these studies.

Study	**Phenotype**	**Medium**	**Common genes**
Ryan et al. (2012)	Haploid null mutant with reduced invasive growth	YPD agar	***ARG8***, ***ERG6***, ***FLO11***, ***IKI3***, *MEF2*, ***PMT2***, ***PUT4***, ***SIN3***, ***SLA1***, *YFL054C*, *ZPS1*
Ryan et al. (2012)	Diploid null mutant with reduced pseudohyphal growth	SLAD + 2% agar	***ARG8***, *BNI1*, *EHT1*, ***ERG6***, ***FLO11***, *GCN1*, ***IKI3***, *MMP1*, *NUM1*, *PEX25*, ***PMT2***, ***SIN3***, ***SLA1***, *SSA2*, *TPO1*, *YBL029W*, *YPK9*
Shively et al. (2013)	Overexpression in a diploid with increased invasive growth (score > 0.99)	Nitrogen-sufficient minimal medium with galactose induction	*HMS2*, ***MGA1***, *MTO3*, *NUP1*, *NRD1*, *RGT1*, *TMA108*
Jin et al. (2008)	Haploid null mutant with no invasive growth	Low nitrogen agar + 1% butanol	*EEB1*, ***HXT4***, *MEF2*, *MGR1*, *NOG2*, *PDR5*, *PDR11*, *PWP2*, *RPO21*, *UBR1*
Kuthan et al. (2003)	Upregulated genes in fluffy colonies	GMA	*AAH1*, *ALD4*, *AQY1*, *ATO3*, *CAR1*, *DUR3*, *FAA3*, *FIT3*, *GAP1*, *GDH1*, *INO1*, *KRS1*, *MAL31*, ***MGA1***, ***PUT4***, *RRD1*, *SAH1*, *SSU1*, *THI7*
Kuthan et al. (2003)	Downregulated genes in smooth colonies	GMA	*ARG5,6*, *ARO1*, *FET3*, *HSP30*, *HXT3*, ***HXT4***, *HXT6*, *HXT7*, *SPS100*, *SPS4*, *TOR1*, *YLR194C*, *YNL144C*

Table S4: Primers used in this study for amplification of gene of interest *Kan*MX gene replacement cassettes and sequencing.

Primer	**Sequence (5′ to 3′)**
AQY2_A[1]	AATAATGACTTACCTCCTCCAATCC
AQY2_D[1]	TTTCGGCATTAACGTATGTAGTGTA
AQY3_A[1]	CTCCCTATTTGGTACTACGATACGA
AQY3_D[1]	GCACAATTAGTTTATTTGGCAACTT
FPS1_A[1]	TATATGTCGTGTAATACCGTCCCTT
FPS1_D[1]	ATGTATAGTAGGTGACCAGGCTGAG
YLL053C_A[1]	ATGTCTAACGAATCTAACGACCTTG
YLL053C_D[1]	TACTTCACATCATCTTTGTTTCCAA
AQY2_A2	GCACCGTAACTACTACAGT
AQY2_D2	TACGATGGGAGCGTTATG
AQY3_A2	TTATCCAACTATGGTGACG
AQY3_D2	TGGTCAATCATACAGAACG
FPS1_A2	GGACGGAGAGAGTTACGGC
FPS1_D2	CGAATCGCTGCTTGATGTT
YLL053C_A2	TATCGTGAATCATATCTGCC
YLL053C_D2	GTCCTGGTTCCACTTCGTAG

[1]GOI_A and GOI_D primers are from Yeast Deletion Project (www-sequence.stanford.edu/group/yeast_deletion_project/deletions3.html).

4.8.2 Figures

Figure S1: Genetic interaction network between differentially expressed genes (only the largest connected network is shown). Red and green node colours represent upregulated and downregulated genes in invasively growing cells; larger node size represents high value of Betweenness Centrality, and vice versa.

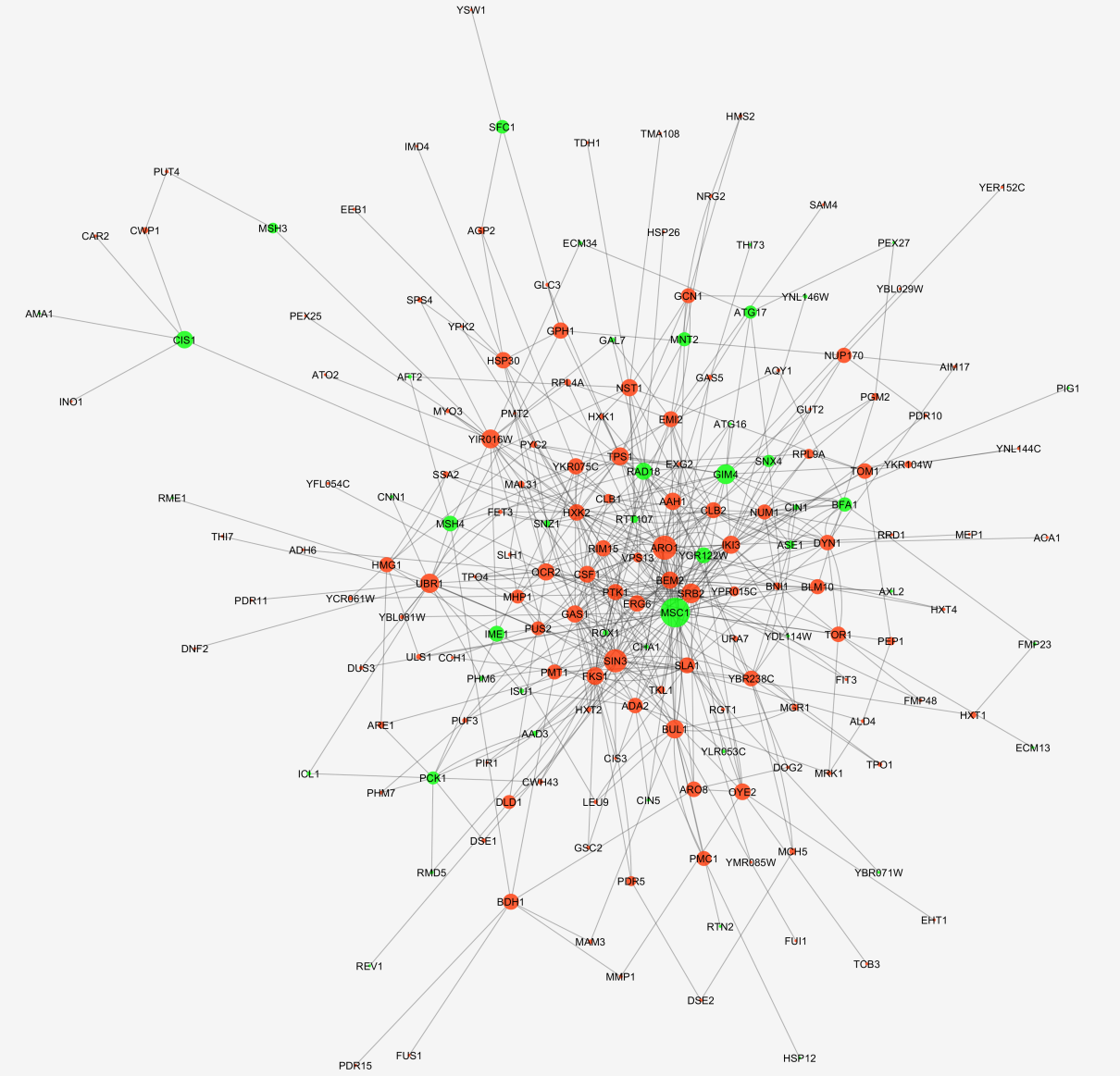

Figure S2: Invasive growth evaluation of strains from a tetrad set produced by sporulation and spontaneous re-diploidisation of a heterozygous deletion AWRI796 on SLADS-agar. Scale bar, 1 mm.

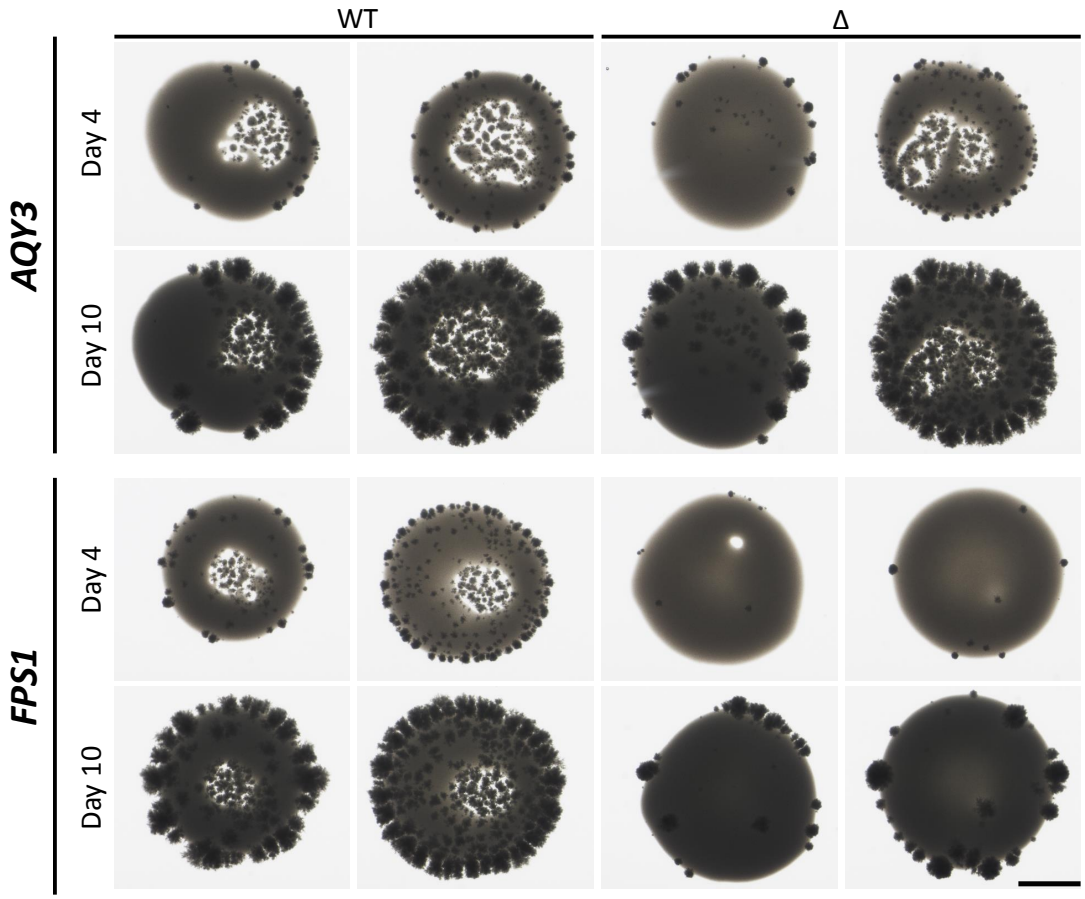

Chapter 5

Conclusions

5.1 Summary of findings

The studies reported in this dissertation led to the following main conclusions:

1. Commercial wine yeast strains are able to form biofilms as determined by mat formation on a rich medium with low density (0.3%) agar. These mats consisted of replicative and non-replicative cells and featured invasive growth, bud elongation, sporulation, and in one case, a sector that was morphologically distinct. The use of a medium containing grape pulp resulted in enhanced invasive growth of yeast mats, while the ability to adhere to plastic was variable between strains.

2. Nitrogen limitation resulted in reduced mat sizes (maximum size was approximately 5 mm in diameter in comparison to up to a full 90 mm plate on rich medium) and induced filamentous and invasive growth. The mat regions where invasive growth occurred were in distinct foci, which did not increase in number markedly over the course of the experiment, indicating that invasively growing cells were triggered soon after inoculation. The number of invasive foci in each mat was strain dependent. Many factors were shown to influence the formation of filamentous invasive foci, these being nitrogen content, the presence of a neighbouring mat and the presence of exogenous yeast metabolites. For instance, ethanol and hydrogen sulfide enhanced filamentous invasive growth, while aromatic alcohols and sulfite inhibited their formation.

3. Differential expression analysis by RNA-sequencing of surface and invasively growing cells on low nitrogen, low density agar medium revealed genes associated with glucose import, carbohydrate metabolic processes, fungal-type cell wall organisation, medium-chain fatty acid biosynthesis and cellular water homeostasis were upregulated in invasively growing cells. Evaluation of deletants of genes involved in cellular water homeostasis confirmed that the aquaglyceroporin gene, *FPS1*, is important for

invasive growth of yeast mats in a low nitrogen medium.

5.2 Contribution to knowledge

The characterisation of mat architecture and visualisation of cell morphologies formed by commercial wine yeast strains broaden the current knowledge beyond the typical and simple 'hub and spokes' description of mat structures. The complexity of cell morphologies within a mat suggests that cells may differentiate for different roles. This may be advantageous for the mat community since they are likely to adapt quicker to changing conditions as opposed to an individual cell morphology. This interesting feature challenges the current knowledge and calls for investigation of how each differentiated cell interacts with others and contributes to mat survival. The simple macro features (petal-like formation) of these mat structures have recently been described mathematically with a collaborating group determining algorithms that result in strikingly similar computer-generated patterns (Alexander Tam, *pers. comm.* 2017). It is important to understand the formation of these structures as this will aid knowledge of how non-laboratory yeast biofilms occur in nature. The findings of grape-pulp mat assays and winery hose plastic adhesion contribute to the knowledge of biofilm formation in relation to a winery/vineyard environment. The capability of commercial wine yeasts to form invasive biofilms on grape pulp agar supports this as a method for residency and persistence in and on damaged wine grapes, which might lead to a change in the profiles of indigenous microflora in vineyards and wineries in the long-term. The surprising ability of wine yeasts to adhere to commonly used winery hose suggests that in the absence of rigorous sanitation, yeast could remain in these hoses, and potentially be transferred between fermentations and wines. Other plastics or rubbers also commonly found in wineries have not been examined here. Plastic tanks, valve caps or internal components of pumps, presses and crushers warrant attention as these surfaces may also serve as areas for yeast residence.

This work is the first to report mat morphologies under low nitrogen conditions. Nitrogen limitation was chosen since this is a common environment that yeast in the vineyard and winery are exposed to. Previous studies as well as in this laboratory on non-mat (2% agar) conditions reported morphological changes when cells were limited for nitrogen, which lead to a hypothesis for this study that these conditions may also trigger similar responses to yeast mats (low density agar) enabling survival. Consistent with previous reports on 2% agar, yeast cells switched to filamentous and invasive growth in a low nitrogen environment on 0.3% agar. This morphological switch is believed to extend access to nutrients since limited proliferation prevents non-motile cells moving towards fresh nutrients. In order to develop filamentous and invasive growth, yeast cells undergo polarised growth, resulting in extension of the growth periphery and existence at a less crowded position, and thus having reduced competition for nutrients. In the vineyard, wine yeast that colonise damaged grapes may consume available nitrogen rapidly. As

nitrogen is depleted, these cells may differentiate into filamentous growth, accompanied with their ability to invade grape pulp, to access fresh nutrients, enhance residency and survival. In the winery, nitrogen is usually exhausted within the first 48 hours of must fermentation. Filamentous growth that will increase surface area to mass ratios of a cell may aid nutrient exposure and facilitate uptake during fermentation.

The invasive growth response can also be influenced by the presence of several yeast metabolites, such as ethanol (previously shown to induce elongation), aromatic alcohols (previously reported to enhance filamentous and invasive growth), hydrogen sulfide (novel), and sulfite (previously shown to inhibit growth). These were chosen since they are common metabolites produced by wine yeast in fermentation and have an effect on filamentous and/or invasive growth on 2% agar. The involvement of metabolites of the yeast sulfur metabolic pathway infers their involvement in the nutrient stress response. Particularly, hydrogen sulfide enhanced the morphological switch that occurs in response to nutrient starvation; the release of this compound is also linked to nutrient starvation, suggesting that this metabolite may be an intermediate signalling molecule enabling the response. This is important since hydrogen sulfide has so far been only linked to resistance to other stresses such as heat shock, heavy metal and oxidative stresses in yeast. The connection between nutrient starvation response and sulfur metabolism could help to understand hydrogen sulfide-related fermentation problems or biofilm formation occurring in a sulfur-rich environment.

The transcriptomics analysis revealed that many genes are upregulated in invasively growing cells and the processes involved were glucose import and carbohydrate metabolism, reflecting better access to fresh nutrients and potentially breakdown and utilisation of agar to allow invasive growth. Upregulation of genes involved in fungal-type cell wall organisation suggests biogenesis, assembly, re-arrangement and disassembly of cell wall components are associated with invasive growth, which infers certain composition or arrangement of the cell wall may be required for growing invasively. Upregulation of *FLO11* also suggests the encoded protein is not just required for initial attachment to agar where invasive growth began, but is also required during growth inside the agar. The attachment facilitated by Flo11p may hold invaded cells in place to push daughter cells further into the agar instead of being replaced by the buds and moving away from the agar. A hypothetical gene (AWRI796_5153) having part of its translation sequence homologous to an amidase, was one of the few genes with a large increase in transcript abundance (6.45-fold) in invasively growing cells, suggesting an important role in invasive growth. Amidases have not been linked to invasive growth or biofilm formation but have been shown to be involved in cell wall recycling processes in bacteria. The identification of several biological processes, previously not associated with invasive growth significantly expands the current knowledge of this field. In particular, gene deletant analysis revealed that *FPS1*, encoding the glycerol exporter, is important for invasive growth in low nitrogen agar. These are novel findings in nitrogen-limited conditions as opposed to glucose limitation in other genome-wide studies. As part of the transcriptomics studies, an RNA extraction

method has also been developed for yeast cells growing into agar.

5.3 Limitations and future directions

The study of mat formation is challenging due to a variety of factors, including genetic variation between strains, occurrence of multiple events such as cell differentiation, cell-cell communication, adhesion and invasive growth. Future work could involve a deeper understanding of how a mat is formed, which factors influence their structure, and how cells choose their fate. Incorporation of mathematical modelling will help identify parameters resulting in the structures or formation of interest and make hypotheses for subsequent experimental design. The experimental approach could also include onsite experiments in a winery setting, followed by confirmation with laboratory experiments. The ultimate output would aid decision making in winemaking management regarding microbial impact.

For the first time, hydrogen sulfide is reported to enhance invasive growth in this study. Nitrogen limitation induces invasive growth and the liberation of hydrogen sulfide by yeast often occurs when nitrogen is insufficient. It has been suggested that hydrogen sulfide, alike to ammonia, may be involved in cell-cell signalling. Future work should investigate how hydrogen sulfide is detected by cells and the mechanism to stimulate invasive growth. The work could also be extended to confirm if hydrogen sulfide is a yeast cell-cell signalling molecule.

While assessing the impact of gene deletions involved in cellular water homeostasis on invasive growth, one deletant, Δ*aqy1*, could not be generated, and hence was not evaluated. It appears that the gene replacement cassette was mis-targeted, and thus although transformants were obtained, unexpected amplified allele sizes were observed from spore progeny (Appendix C). Further work needs to be done to investigate why deletion of *AQY1* was unsuccessful, for instance, study the AWRI796 genome sequence and investigate PCR conditions to optimise cassette generation and transformation.

Although the transcriptomics analysis has provided new information on invasive growth, there were limitations. For instance, transcriptomics analysis only examined gene expression, while post-translational modifications and protein activity were not examined. Assumptions have been made that an increase in gene expression results in an increase in protein levels. However, the regulation of many genes and their products can occur at many stages post transcription. Furthermore, gene expression may not directly support the phenotype observed. For example, *ARO1* and *ARO8*, encoding for enzymes that are responsible for aromatic amino acid production, were upregulated in invasively growing cells. These amino acids are precursors to aromatic alcohols which were shown to inhibit invasive growth in this work. This result is contradictory to the findings that aromatic alcohols enhanced invasive growth as reported by Chen and Fink (2006), which could be due to different medium preparation such as 2% versus 0.3% agar or ethanol concentration

in preparation of aromatic alcohols. Metabolite analysis could be undertaken to identify if the amino acids were in fact produced. Future work could include both proteomics and metabolomics studies to gain a holistic view on the process.

Differential transcriptome analysis requires a well-annotated genome of a strain to be analysed. AWRI796 was chosen for this analysis since this strain has its genome annotated close to completion. The genome sequence is also very similar to the reference sequence of S288C. All currently annotated genes in AWRI796 are also present in the S288C genome. In addition, the AWRI796 genome has several hypothetical genes predicted. The translation sequence of these genes was blasted for homology to protein families. Most translated sequences were matched to a protein family, suggesting they are protein coding genes. GO information was obtained and used in the analysis. A number of the hypothetical genes, previously predicted to be individual genes, were merged based on the evidence of their location in the genome and the matching protein domain region. Further annotation of this reference sequence has contributed to an understanding of these hypothetical genes. Future work could evaluate the functions of these, including whether they appear in the commonly used S288C reference genome. This will continue to improve the annotation for the AWRI796 genome.

Deletion of *FPS1*, encoding the glycerol exporter led to reduced invasive growth. Previous work reports accumulation of glycerol inside the cell of *FPS1* deletants which could therefore alter turgor pressure and cause cell wall fortification that may disable invasive growth. Further analysis of deletants that similarly result in glycerol accumulation ($\Delta adk1$, $\Delta sch9$) would contribute to this understanding. Cells could also be stained with Calcofluor White to determine the intensity of chitin and β-glucan, and consequently examine if an increased glycerol accumulation results in fortification of the cell wall. Enzyme digestibility of cell walls could also be tested and compared between both wild type and mutant. Alternatively, the presence of glycerol in extracellular fluid may be important for invasive growth. Filamentous invasive growth was induced when glycerol was used to replace glucose in a medium (Palecek et al., 2002). Addition of glucose was shown to repress invasive growth in a dose-dependent manner. Future experiments could use glycerol in SLAD in the presence and absence of glucose to test if this would rescue invasive growth in the $\Delta fps1$ deletant. This would also confirm the role of extracellular glycerol in invasive growth.

This study is significant since *S. cerevisiae* is a well-studied model organism, but processes such as mat formation are still not fully understood, especially for non-laboratory strains. Mat formation forms the basic understanding of biofilm formation, which has implications such as persistence and survival of clinical yeasts in medical devices, invasiveness into human and plant tissues, interactions between microorganisms and the use of metabolites in wastewater, and in this study, survival of commercial wine yeasts in the wine environment. Many tantalising questions and possibilities have been revealed by this work.

Appendix A

Method development for mat formation and plastic adhesion assays

A.1 Mat formation assays

A.1.1 Reproduction of results by Reynolds and Fink (2001) and test mat formation ability of commercial wine yeast strains

Background and methods

Mat formation methods described by Reynolds and Fink (2001) were reviewed in order to test if common commercial wine yeast strains also have the ability to form mats. Unfortunately, some steps were not detailed in this short form publication. For example, how the medium was prepared and whether the plates were incubated yeast inoculum side up or down since the agar concentration was very low. In this first preliminary study, the method reported was repeated with some modifications and additional details. Laboratory yeast strain prototrophic diploid Σ1278b and two wine yeast strains, L2056 and AWRI796, were used. Yeast Peptone Dextrose (YPD; 1% yeast extract, 2% bacto peptone, 2% glucose) with 0.3% agar was made by dissolving all components in RO water and autoclaved to sterilise. Instead of inoculation with a toothpick as reported, to standardise initial cell number, this experiment used inoculation of 5 μL of a diluted overnight YPD culture (1×10^4 cells mL^{-1}). Plates were incubated yeast inoculum side down. Plate images were photographed after 16 days of incubation using a Samsung Galaxy S3 camera. Mats were washed with a stream of ultrapure water from a laboratory squeeze bottle for approximately 30 s to check for adhesive cells.

Results

Mats were small (< 40 mm; Fig. A.1) and Σ1278b had a different mat structure (no spokes) compared to those reported by Reynolds and Fink (2001) where mats were described to have a 'hub and spokes' structure. Post-wash observations showed cells adhered to the agar near the mat rim.

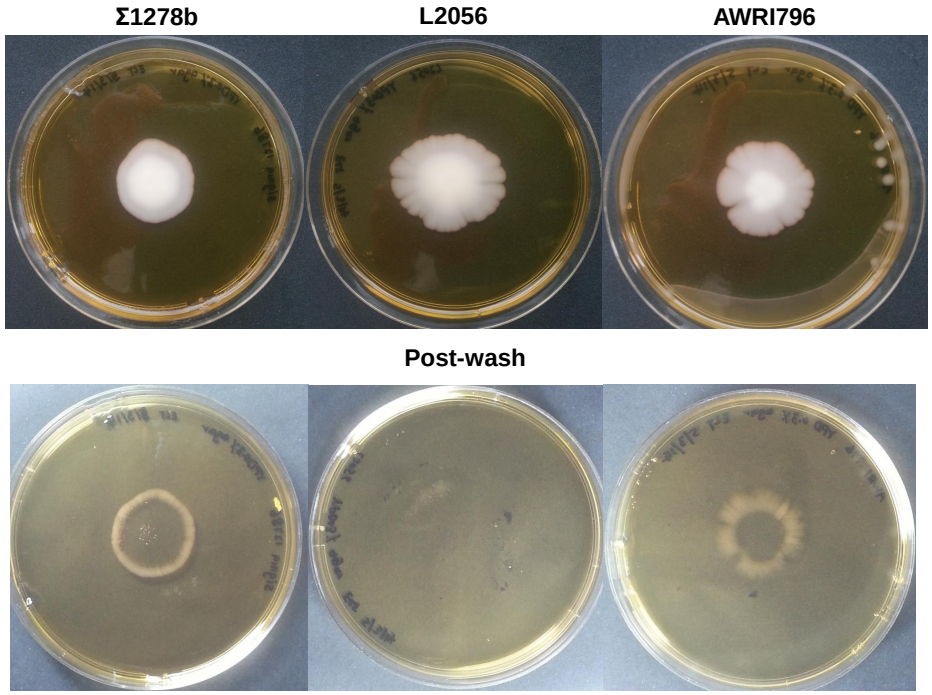

Figure A.1: Mat formation pre- and post-wash by Σ1278b, L2056 and AWRI796 on YPD with 0.3% agar on 90 mm Petri dishes on Day 16.

Liquid YPD discharged from agar during incubation, and the medium agar concentration may have increased, which may explain the differences in mat size and structure compared to those described by Reynolds and Fink (2001).

A.1.2 Evaluation of medium preparation methods for mat assays

Background and methods

In this experiment, three approaches were tested to find the best solution to prepare dry low-density agar YPD:

1. YPD with 0.5% Bacto agar, autoclaved (increased agar concentration)
2. YPD with 0.5% agarose, autoclaved (alternative gelling agent)

3. Filtered 2× YPD and autoclaved 2× Bacto agar (0.6 %) (washed twice with 800 mL ultrapure water in a 1 L Schott bottle, swirled to mix and rested for 15 min before decanting), then mixed equal volumes before pouring into Petri dishes

4. Filtered 2× YPD and autoclaved 2× Bacto agar (0.6 %), then mixed equal volumes before pouring into Petri dishes

Results

Agar medium made using all approaches was dry even after two-week incubation. However, the Σ1278b mat was smaller on YPD with 0.5% agar than 0.3% agar whereas the mat structure on YPD with 0.3% agar resembled those commonly reported (Fig. A.2).

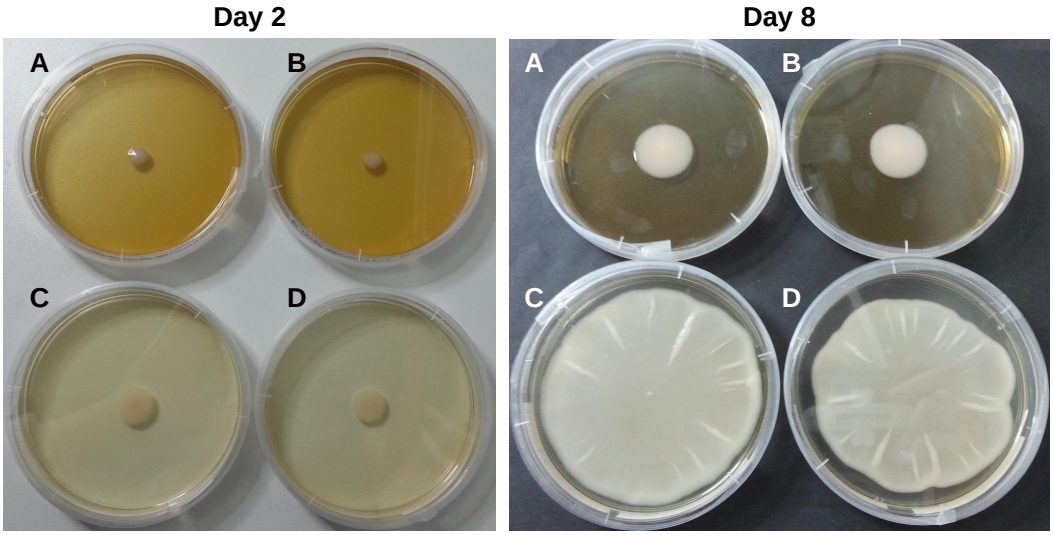

Figure A.2: Mat formation by Σ1278b on medium prepared using four different approaches: (A) autoclaved YPD with 0.5% Bacto agar; (B) autoclaved YPD with 0.5% agarose; (C) filtered YPD with 0.3% washed and autoclaved Bacto agar; (D) filtered YPD with 0.3% autoclaved Bacto agar. 90 mm Petri dishes were used.

Conclusions

The mat shape and size between washed and non-washed agar were similar. Therefore, approach '4' was used for the preparation of medium.

A.1.3 Evaluation of mat inoculation with cells at exponential growth phase

Background and methods

Biological variability of mat size and structure had been observed across replications. In order to decrease this, mats were inoculated with cells standardised for initial cellular metabolic state. Following the initial overnight YPD culture, a fresh YPD culture was inoculated and incubated for a set amount of time to achieve exponential-phase cultures (instead of stationary phase). The following experiment was set up to identify the incubation time required after the re-inoculation. Overnight YPD cultures of prototrophic Σ1278b, auxotrophic Σ1278b and auxotrophic Σ1278b Δ*flo11*/Δ*flo11* were re-inoculated into 25 mL fresh YPD at 1.25×10^6 cells mL^{-1}. Cells were counted using a haemocytometer at several time points to determine the time required for cells to produce approximately three generations.

Results

All strains achieved three generations ($\sim 1 \times 10^7$ cells mL^{-1}) within 4.5 h and approximately four generations within 7 h, indicating rapid growth (Fig. A.3).

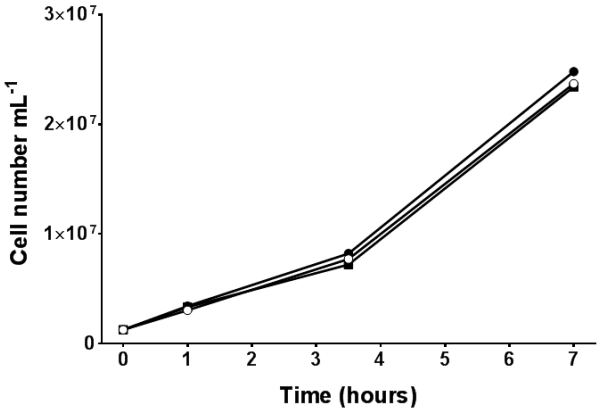

Figure A.3: Growth curve after re-inoculation of an overnight YPD culture into fresh YPD. Inoculation rate was 1.25×10^6 cells mL^{-1}. (●) Prototrophic Σ1278b, (■) auxotrophic Σ1278b, (○) auxotrophic Σ1278b Δ*flo11*/Δ*flo11*.

Conclusions

The mat assay method was modified to include a re-inoculation step using an overnight culture, inoculated into fresh YPD at a rate of 1.25×10^6 cells mL^{-1} and incubated for 6

h prior to inoculation of YPD agar (0.3%).

A.2 Plastic adhesion assays

A.2.1 Refinement of staining and washing methods

Background and methods

This experiment followed plastic adhesion methods described by Reynolds and Fink (2001) with modifications and additional details described below. Three strains used were kindly donated by J. Gardner (Uni. of Adelaide): (a) ISO C9 C (L2056 *MAT*α Δho); (b) ISO C9 D (L2056 *MAT*a Δho); and (c) ISO C9 C/D (L2056 $\Delta ho/\Delta ho$). In brief, these strains are derivatives of the commercial wine yeast strain L2056, considered to be very close to isogenic. They were created by three rounds of meiosis and re-diploidisation of the haploid wine yeast C9 (originally derived from L2056, as described in Walker et al., 2003). Homothallism was enabled by introduction of a functional *HO* gene carried on a plasmid also enabling G418-sulfate resistance. Loss of resistance and inability to sporulate were used to confirm plasmid loss. Mitochondrial RFLP analysis was used to check genetic similarity.

Media used were Synthetic Complete (SC; 0.17% Yeast Nitrogen Base without amino acids and ammonium sulfate, 0.079% Complete Supplement Mixture, 0.5% ammonium sulfate, 0.1% glucose) and Synthetic Low Ammonium Dextrose (SLAD; 0.17% Yeast Nitrogen Base without amino acids and ammonium sulfate, 50 μM ammonium sulfate, 0.1% glucose). Following a one-hour incubation, cells were stained with 1% Crystal Violet solution for 15 min as described by Reynolds and Fink (2001). To remove unbound Crystal Violet, cells were washed with ultrapure water using a pipette to load water and a tipping and tapping motion to remove water. Cells adhered to the plastic were observed not to have been stained by the Crystal Violet. Therefore, cells were stained again for 20 min. For subsequent experiments, cells were stained twice for 20 min each time.

Results

The number of adhered cells was reflected by differences in absorbance values at 570 nm (Fig. A.4).

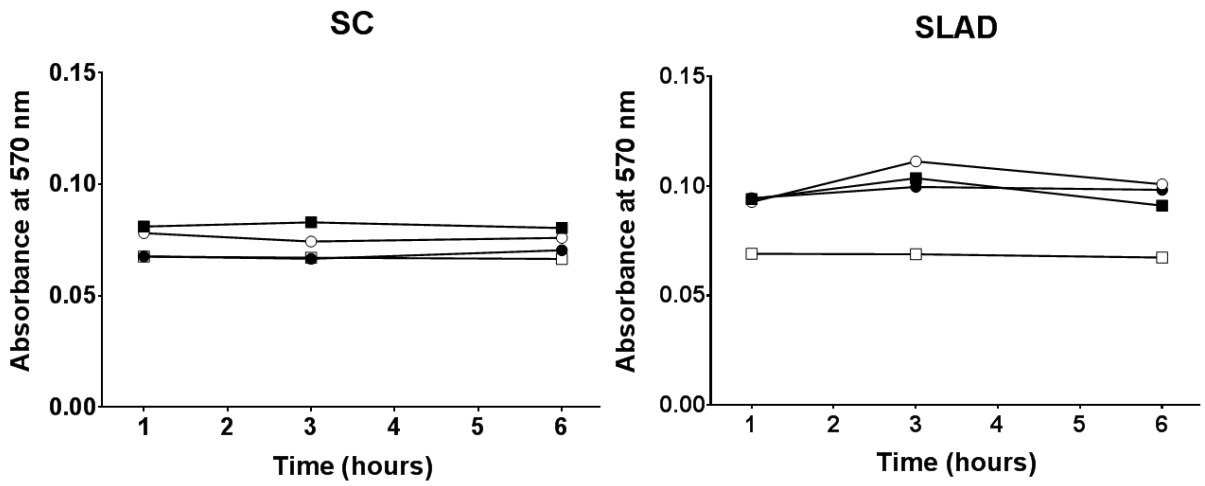

Figure A.4: Plastic adhesion of yeast strains, as measured by absorbance of Crystal Violet-stained residual cells post-washing at 570 nm. (●) ISO C9 C, (○) ISO C9 D, (■) ISO C9 C/D, and (□) no cell control in SC and SLAD.

Conclusions

The plastic adhesion assay was modified with cells stained twice after incubation. Washing steps would include adding ultrapure water by pipetting, followed by inverting the microplate to tap the water out.

A.2.2 Determination of the maximum absorption of Crystal Violet

Background and methods

Several publications have used either 570 or 590 nm to quantify absorbance of Crystal Violet (Reynolds and Fink, 2001; Zara et al., 2009; Gori et al., 2011; Granek et al., 2013). This experiment determined the best wavelength to use by performing an absorbance scan on three samples after one-hour incubation in specified medium: (a) no cell control in SLAD; (b) AWRI796 in SLAD; (c) L2056 in SC. The scan was performed using a Tecan Infinite M200 PRO microplate reader from 230 nm to 1000 nm in 10 nm increments.

Results

Maximum absorption of Crystal Violet was observed at 590 nm (Fig. A.5).

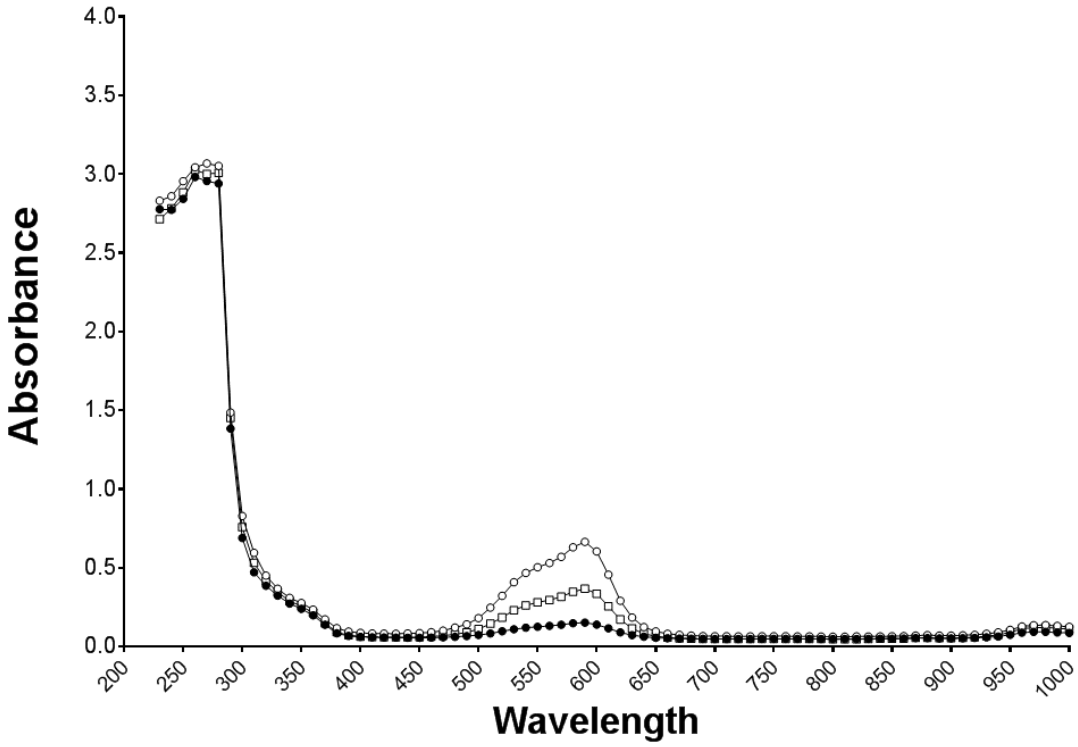

Figure A.5: Wavelength scan for Crystal Violet-stained cultures adhered to plastic. (○) AWRI796 incubated in SLAD, (□)L2056 incubated in SC, (●) no cell control.

Conclusions

For all future assays, absorbance at 590 nm was chosen to quantify cell adhesion on plastic.

Appendix B

Method development for mat formation assays in a low nitrogen medium (SLAD)

B.0.1 Determination of inoculation rate

Background and methods

Mat formation was performed as described by Reynolds and Fink (2001) with the substitution of SLAD for YPD and several defined inoculation rates instead of the undefined toothpick inoculation. Σ1278b and two commercial wine strains, L2056 and AWRI796, were tested in this experiment. Inoculation rates were 5 μL of 2×10^2, 2×10^3, 2×10^4 and 2×10^5 cells mL^{-1} of an overnight Synthetic Low Ammonium Dextrose (SLAD; 0.17% Yeast Nitrogen Base without amino acids and ammonium sulfate, 2% glucose, 50 μM ammonium sulfate) culture, equating to approximately 1, 10, 100 and 1000 cells. Four to six images were photographed for each mat to capture all sectors on Day 3, 5, 7 and 9 using a Nikon Eclipse 50i microscope at 40× magnification and an attached Digital Sight DS-2MBWc camera with NIS-Elements F3.0 imaging software. The image of a whole mat was generated by stitching the sector images using Fiji software (Thévenaz and Unser, 2007; Preibisch et al., 2009; Schindelin et al., 2012).

Results

In general, a higher inoculation rate led to a greater number of invasive growth foci initiated at an early stage (Fig. B.1). Replications from higher inoculation rates produced more consistent results than lower inoculation rates (data not shown). Independent of the initial inoculum used, all mats reached a very similar maximum mat size, suggesting that growth is limited by a factor independent of initial cell numbers. This may be nitrogen

availability. Maximum mat size was approximately 4–5 mm in diameter, and this was often observed at the first time point analysed (Day 3), except when only 1 cell was used as the inoculum. In comparison, the maximum size of a colony grown from the same strains on SLAD with 2% agar reaches approximately 1 mm (Joanna Sundstrom, *pers. comm.*). As the maximum mat size is at least 4-fold wider than colonies formed on SLAD with 2% agar, and cell growth occurs as a thin layer across the surface, these were defined as mats rather than colonies. Mat expansion also extends beyond the boundary of the inoculum drop. This can also be visualised in Figure B.1A, where growth of the mat inoculated with a single cell doubles in size between 3 and 9 days.

Conclusions

An inoculation rate of 5 μL of 2×10^5 cells mL^{-1} (1000 cells) was selected for all future SLAD mat assays. Use of rapidly growing cells (exponential phase) as the inoculum was also introduced as in the YPD mat assays to standardise the growth phase of cells. When capturing microscopic images, phase contrast was changed from dark field to the phase corresponding to the objective lens to obtain a white background image.

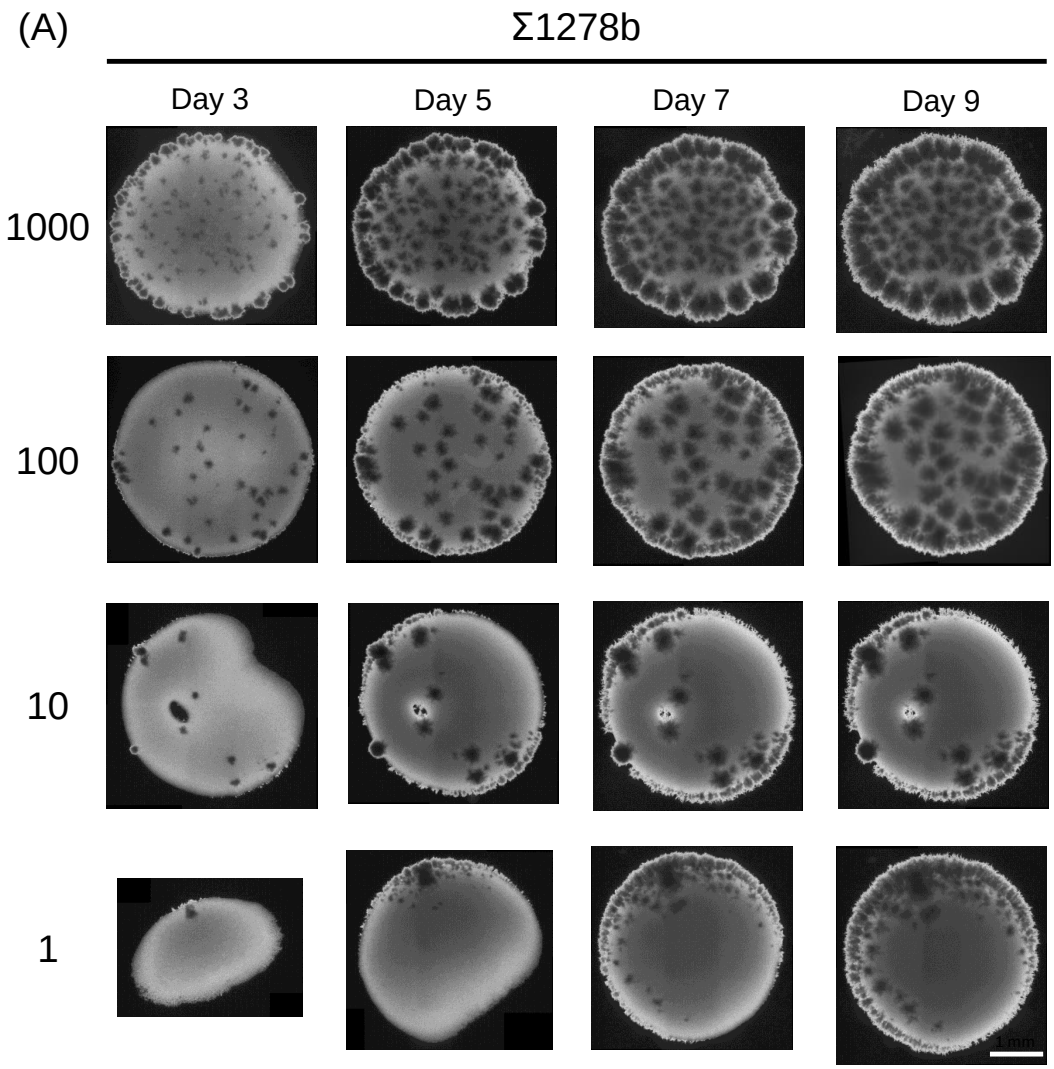

Figure B.1: Mat formation in a low nitrogen medium (SLAD with 0.3% agar) for a range of initial inoculum over time. (A) Prototrophic Σ1278b inoculated with either 1, 10, 100 or 1000 cells. Scale bar, 1 mm. Please refer to next two pages for (B) and (C).

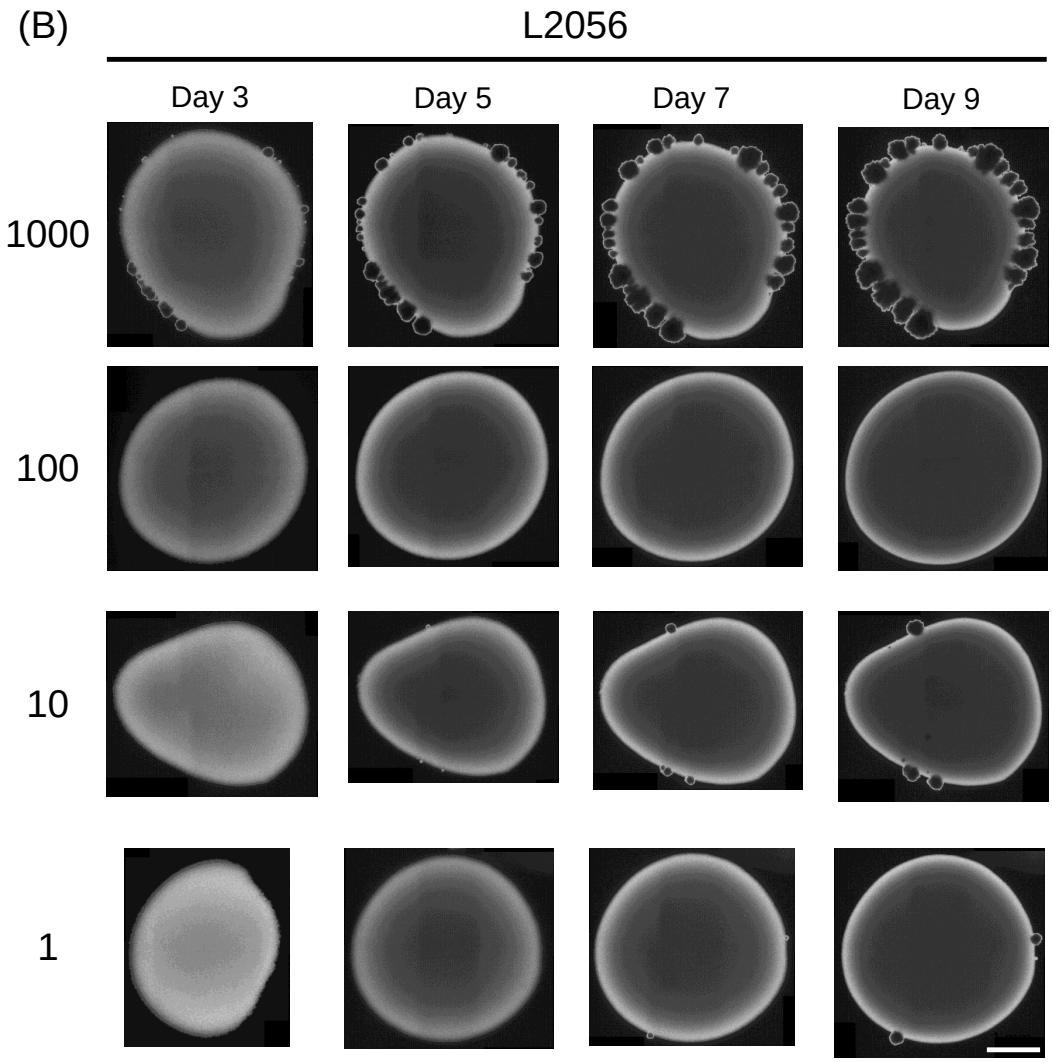

Figure B.1: (B) L2056 inoculated with either 1, 10, 100 or 1000 cells. Scale bar, 1 mm. Please refer to next page for (C).

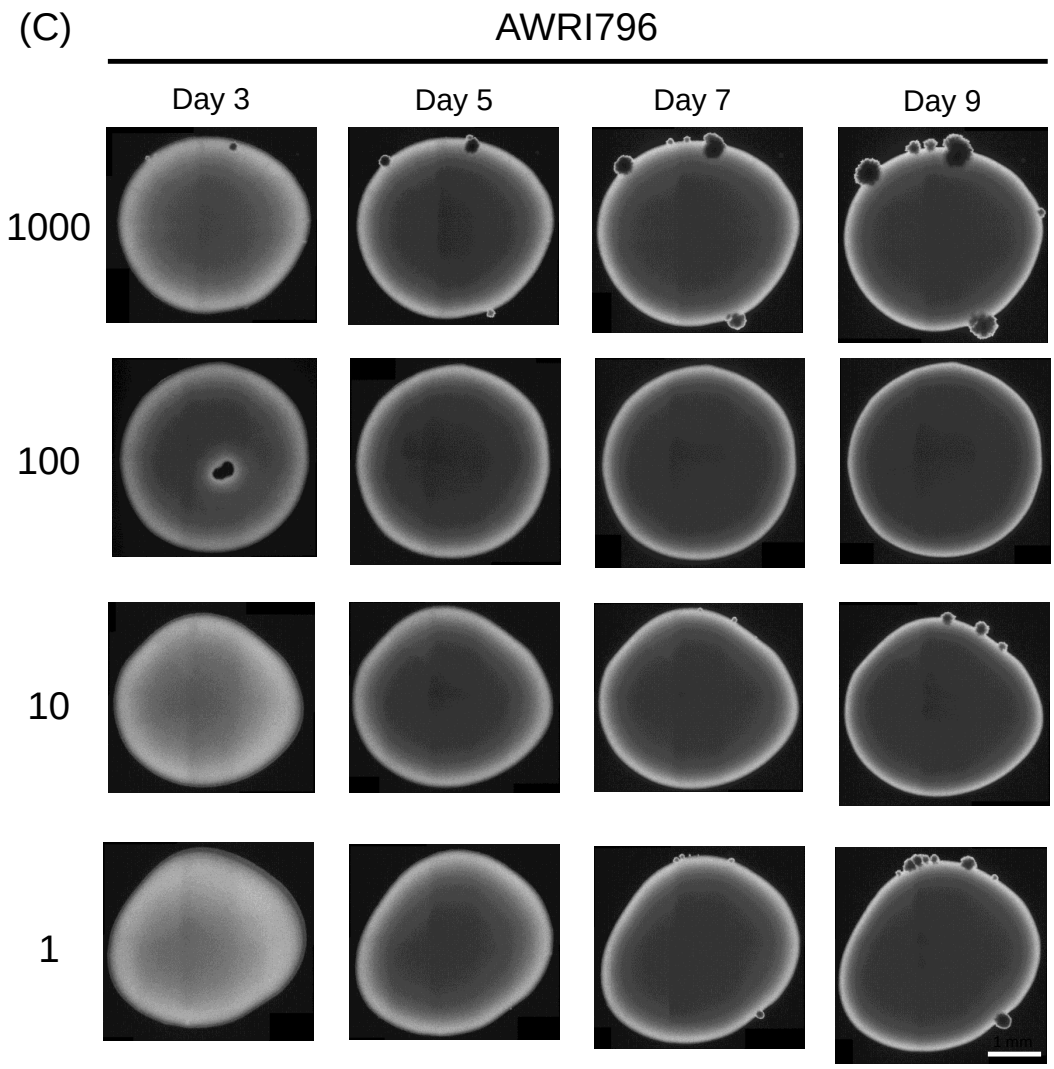

Figure B.1: (C) AWRI796 inoculated with either 1, 10, 100 or 1000 cells. Scale bar, 1 mm.

B.0.2 Preliminary study on the effect of sulfide on mat formation in SLAD

Background and methods

Sulfide is of interest to this project since it is a yeast metabolite that preliminary evidence from this laboratory suggests a possible role in cell signalling and it has a significant impact on wine quality. This experiment compared mats from a low nitrogen medium (SLAD) formed by prototrophic Σ1278b, L2056, AWRI796, EC1118, PDM and Distinction with and without the influence of sulfide. Yeast cultures were grown in either SLAD or SLADS (SLAD with 0.4 mg L^{-1} sodium sulfide) for two overnights before being re-inoculated into a fresh SLAD or SLADS at 1×10^4 cells mL^{-1} and incubated for 16 h. The cell concentration of cultures was adjusted to 2×10^5 cells mL^{-1} with PBS. A 5 μL aliquot was spotted to Petri dishes containing SLAD or SLADS with 0.3% agar (*i.e.* 1000 cells were inoculated). EC1118, PDM and Distinction were evaluated in a separate experiment, and therefore there was a slight variation in the days where images were captured. Imaging and stitching methods were as described in Study B.0.1.

Results

All strains consistently showed an enhancement of invasive growth in the presence of exogenous sulfide (Fig. B.2A and B). Σ1278b, EC1118, PDM and Distinction also had reduced surface growth.

Conclusions

Cell counts of liquid cultures confirmed that the re-inoculation rate and incubation period described achieved more than three generations and cultures had not reached saturation. Sulfide enhanced invasive growth and the addition would be tested in combinations with other compounds.

Figure B.2: Mat formation of yeast strains in a low nitrogen medium over time. (A) Σ1278b, L2056, AWRI796, (B) EC1118, PDM and Distinction on SLAD and SLADS (containing 0.4 mg L^{-1} sodium sulfide).

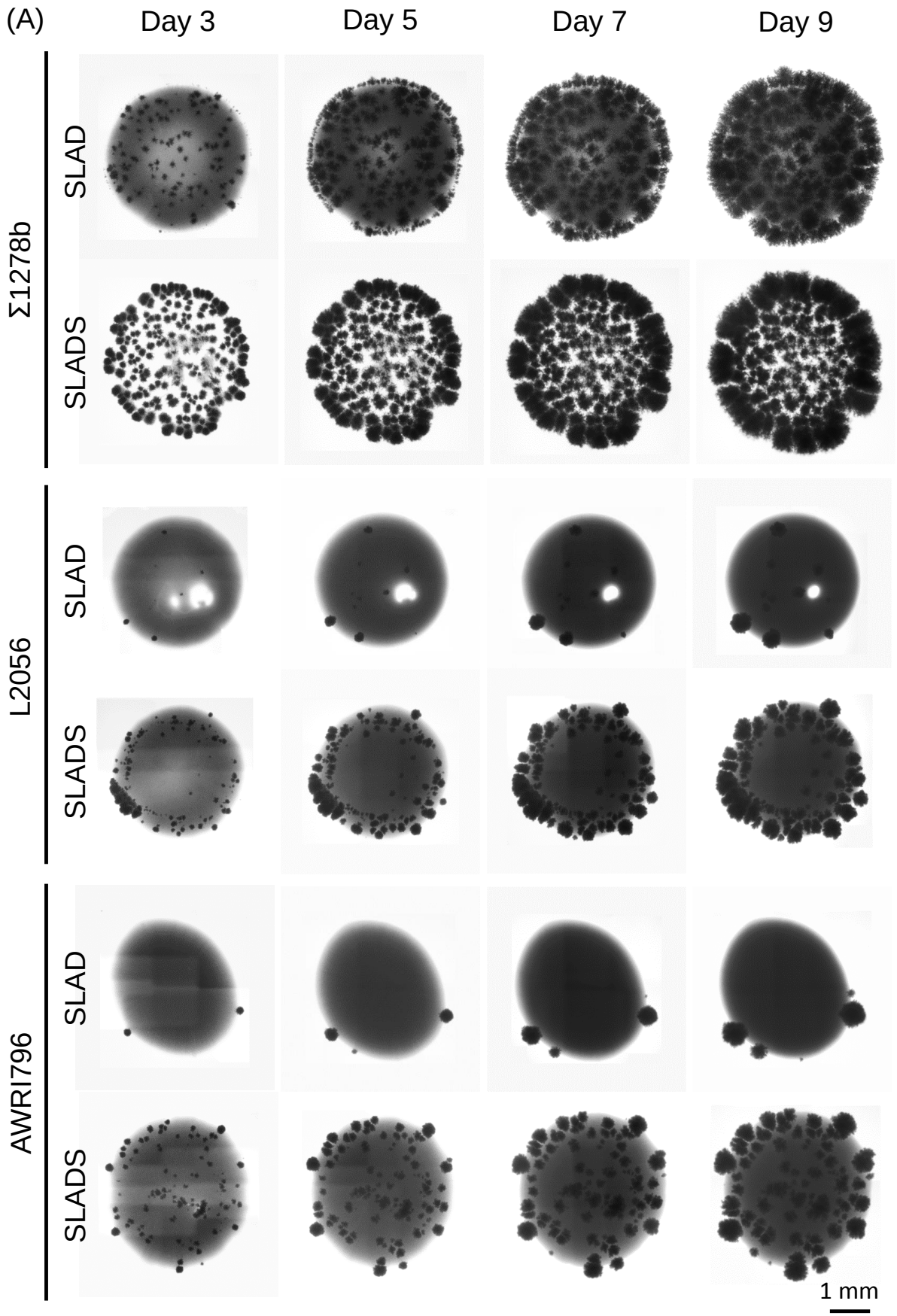

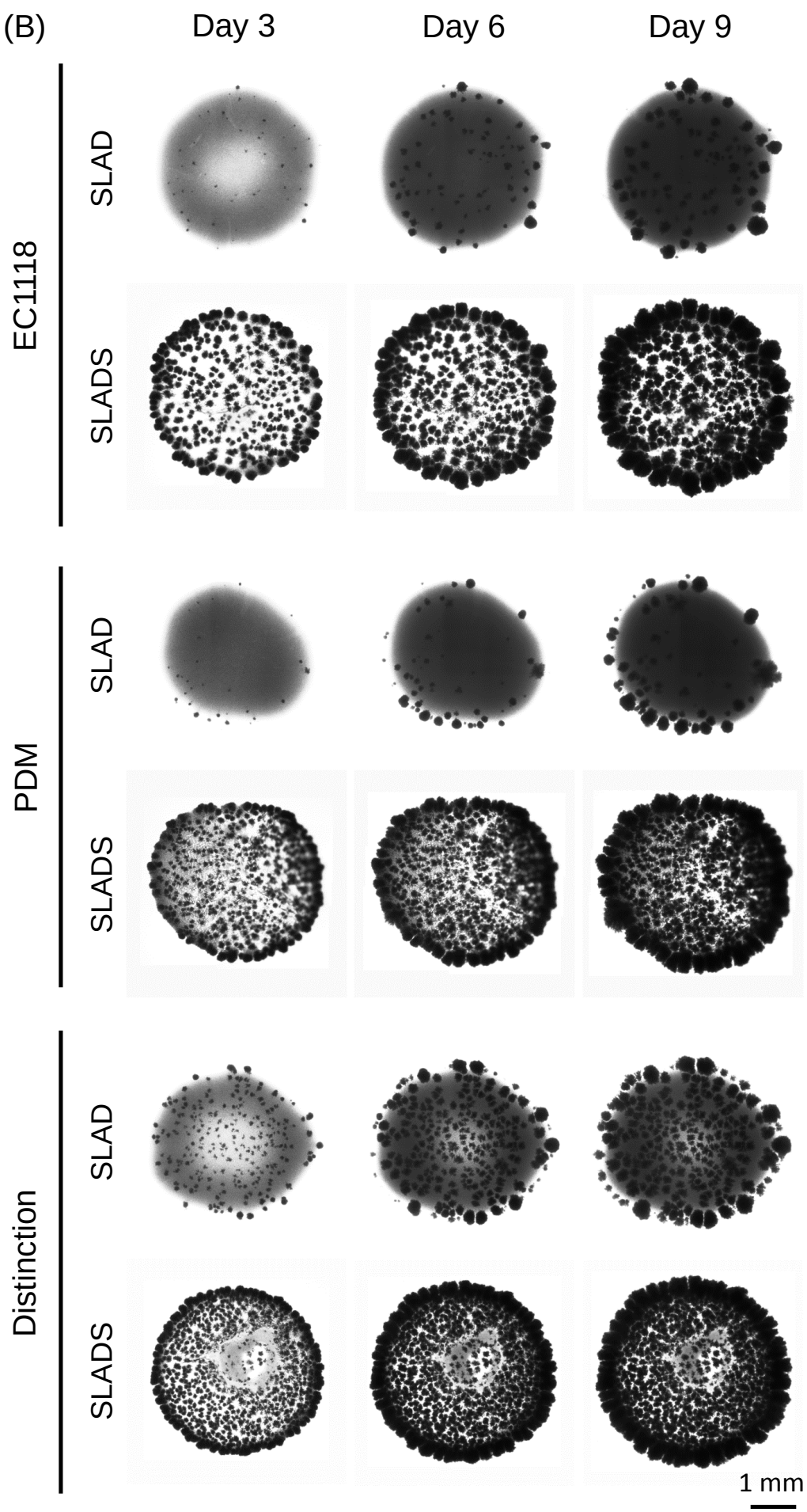
(B)
Day 3
Day 6
Day 9
EC1118
SLAD
SLADS
PDM
SLAD
SLADS
Distinction
SLAD
SLADS
1 mm

Appendix C

Attempt to construct Δ*aqy1* in AWRI796

C.0.1 Transformation with homologous recombination

Methods

A *Kan*MX gene replacement cassette was generated by PCR from the genomic DNA of BY4741 Δ*aqy1* using the primers AQY1_A (5′-TAGAAGTGGTAAATTGCAGGATAGC-3′) and AQY1_D (5′-TCAACCATATGACTACTTGGGATTT-3′) (Winzeler et al., 1999; Wach et al., 1994). *AQY1* deletion in AWRI796 was attempted by transformation of the cassette, followed by selection on YPD + 200 mg L^{-1} G418-sulfate (Gietz and Schiestl, 2007). Homozygous deletants were isolated by sporulation, dissection and re-diploidisation, followed by verification with PCR amplification.

Results

The resulting progeny showed 2:2 segregation of the alleles with two corresponding to the wild type allele size and the other two corresponding to both wild type and deletion allele sizes (Fig. D.1A). When the alleles were amplified with the primer pairs located outside the gene replacement cassette, AQY1_A2 (5′-TTCCAAGTGAATATCTGC-3′) and AQY1_D2 (5′-GATTCCTAGATCCTAACAT-3′), all four progenies showed wild type allele sizes (Fig. D.1B).

Conclusion

The results suggest that the *Kan*MX cassette has a preferential recombination locus other than *AQY1* in AWRI796.

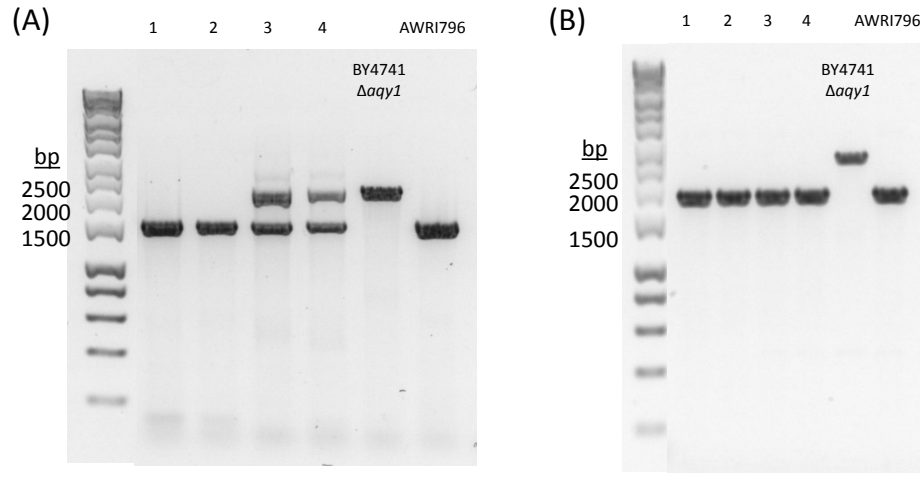

Figure D.1: *AQY1* PCR products from genomic DNA of four spore progenies (1–4), BY4741 Δ*aqy1* and AWRI796 using primers (A) AQY1_A and AQY1_D, (B) AQY1_A2 and AQY1_D2.

C.0.2 Construction of *Kan*MX gene replacement cassette from a plasmid

Methods

To increase specificity to AWRI796, a *Kan*MX gene replacement construct was PCR amplified from a plasmid (pBS418; kindly donated by M. Walker, Uni. of Adelaide) using a long primer pair with 40 bp specific to the AWRI796 sequence and 20 bp homologous to either the TEF promoter or terminator on the plasmid. These primers were AQY1_TEFp_fwd (5′-CCTTACACAGTAGGATTAGTCTAGAAGTGGTAAATTGAAGC CTTGACAGTCTTGACGTGC-3′) and AQY1_TEFt_rev (5′-CGCACTTAACTTCGC ATCTGGACTACTTGGGATTTCAAGGACAAGATATACATCAACGAT-3′).

Results

The PCR product quantity was low. When the product was used as a template in a new PCR reaction, no products were obtained.

Appendix D

Supporting information for Chapter 4

Table S1: Results of differential gene expression analysis comparing transcriptomes of cells growing invasively and on the surface of SLADS-agar (0.3%). Genes with low read counts (< 50) were excluded. Differentially expressed genes were selected on the basis of satisfying testing significance (FDR < 0.05) relative to a 1.3-fold-change threshold. Adjusted p-value is shown zero for less than 1×10^{-6}. Significantly upregulated, no change and downregulated genes in invasively growing cells are indicated by 1, 0 and -1 in the column Score.

AWRI796 Gene ID	Gene Name	log_2 Fold Change	Adj. *p* -value	Score	AWRI796 Gene ID	Gene Name	log_2 Fold Change	Adj. *p* -value	Score
AWRI796_1051	HXT7	3.781	0	1	AWRI796_2590	TDH1	0.731	0.002984	1
AWRI796_2159	HXT4	3.039	0	1	AWRI796_0070	PAU5	0.729	0.007187	1
AWRI796_5153	AWRI796_5153	2.686	1.00E-06	1	AWRI796_1561	IRC7	0.729	0.003954	1
AWRI796_3083	SSA2	2.26	0	1	AWRI796_4656	YPK9	0.726	0.001067	1
AWRI796_5256	HXT6	2.251	0	1	AWRI796_0144	YBL029W	0.724	4.40E-05	1
AWRI796_1349	RGI1	1.919	0	1	AWRI796_0617	DLD1	0.72	0.000194	1
AWRI796_2017	AWRI796_2017	1.789	1.00E-06	1	AWRI796_3327	HAP1	0.72	4.10E-05	1
AWRI796_5255	HXT3	1.742	1.00E-06	1	AWRI796_1703	SRM1	0.719	0.001178	1
AWRI796_4889	CAR1	1.727	1.00E-06	1	AWRI796_3329	GSY2	0.718	0.000191	1
AWRI796_1052	HXT3	1.524	0	1	AWRI796_4406	CSI2	0.718	0.149065	0
AWRI796_1560	HXK1	1.434	0	1	AWRI796_0449	MGR1	0.716	0.003327	1
AWRI796_0081	SRO77	1.417	1.00E-06	1	AWRI796_4902	EEB1	0.713	0.022128	1
AWRI796_4257_58	AWRI796_4257_58	1.35	2.00E-06	1	AWRI796_1619	GCN1	0.712	7.00E-05	1
AWRI796_2502	CIS3	1.336	0.003327	1	AWRI796_4905	SSU1	0.712	0.002694	1
AWRI796_2813	PIR1	1.297	0.000181	1	AWRI796_4187	ATO2	0.71	0.000402	1
AWRI796_1614	ARO8	1.275	1.00E-06	1	AWRI796_1273	GLC3	0.708	0.000167	1
AWRI796_0236	HSP26	1.245	2.90E-05	1	AWRI796_4077	KRE33	0.707	0.000697	1
AWRI796_2240	GND1	1.21	1.00E-06	1	AWRI796_2284	RRD1	0.705	0.000133	1
AWRI796_3653	FET3	1.184	1.80E-05	1	AWRI796_3222	DIP2	0.705	0.000825	1
AWRI796_2160	HXT1	1.183	0	1	AWRI796_3647	ERB1	0.703	3.20E-05	1
AWRI796_3611	HXT2	1.183	1.00E-06	1	AWRI796_4752	DIP5	0.703	0.000359	1
AWRI796_3060	YLL053C	1.168	0.00017	1	AWRI796_1809	GSC2	0.701	0.000204	1
AWRI796_5047	TKL1	1.162	0	1	AWRI796_1530	FAB1	0.699	0.002214	1
AWRI796_0102	YBL081W	1.139	0.000225	1	AWRI796_3079	TPO1	0.699	0.000908	1
AWRI796_2568	PRY3	1.125	0.000608	1	AWRI796_4700	RPA190	0.699	0.000289	1
AWRI796_1119B	HKR1	1.094	3.20E-05	1	AWRI796_3468	CAR2	0.696	0.001067	1
AWRI796_2201	SPS100	1.076	2.70E-05	1	AWRI796_0875	DOP1	0.695	0.00034	1
AWRI796_1107	PDR15	1.068	1.30E-05	1	AWRI796_4135	GCD10	0.687	0.000268	1
AWRI796_1988	MGA1	1.059	0.000144	1	AWRI796_0280	TPS1	0.684	0.000194	1
AWRI796_3020	YKR075C	1.044	0	1	AWRI796_2600	MHP1	0.684	0.000484	1
AWRI796_3274	YLR194C	1.044	4.10E-05	1	AWRI796_1964	CCH1	0.681	0.000408	1
AWRI796_4782	FAS2	1.038	0	1	AWRI796_3438	DUS3	0.678	0.000351	1
AWRI796_0883B	NUM1	1.031	1.00E-06	1	AWRI796_1446	BRR2	0.674	0.000728	1
AWRI796_3414	ELO3	1.009	1.00E-06	1	AWRI796_4995	RPA135	0.674	0.001538	1
AWRI796_4912	SEC16	0.996	1.00E-06	1	AWRI796_4837	OYE3	0.673	0.08583	0
AWRI796_3204	MDN1	0.987	1.00E-06	1	AWRI796_5151	ERR2	0.672	0.000955	1
AWRI796_1873	CLB1	0.96	0.000841	1	AWRI796_1402	DSE1	0.67	0.001535	1
AWRI796_3553	IMD4	0.954	0.000268	1	AWRI796_1771	ERG4	0.67	0.000631	1
AWRI796_3677	YMR085W	0.951	8.00E-06	1	AWRI796_2893	NUP100	0.668	0.00031	1
AWRI796_2041	GUT1	0.944	1.00E-06	1	AWRI796_0378	YBR238C	0.667	0.005337	1
AWRI796_5135	GDB1	0.944	5.00E-06	1	AWRI796_3695	YPK2	0.666	0.003246	1
AWRI796_1463	YJL225C	0.94	4.00E-06	1	AWRI796_0983	EXG2	0.664	0.027963	1
AWRI796_2282	GUT2	0.94	2.00E-06	1	AWRI796_4003	POP1	0.66	0.000217	1
AWRI796_3447	INA1	0.927	0.001756	1	AWRI796_3309	THI7	0.657	0.001704	1
AWRI796_3186	CSF1	0.926	2.30E-05	1	AWRI796_0041	PMT2	0.656	0.000508	1
AWRI796_4670	MCH5	0.924	0.000387	1	AWRI796_2782	PTK1	0.656	0.000337	1
AWRI796_1730	PUS2	0.92	0.00037	1	AWRI796_1505	BLM10	0.655	0.001481	1
AWRI796_0995	MTH1	0.919	0	1	AWRI796_4614	SSP2	0.655	0.143366	0
AWRI796_4272	ZPS1	0.919	0.000214	1	AWRI796_1323	SAH1	0.654	0.00406	1
AWRI796_5083	CLB2	0.915	0.01243	1	AWRI796_4455	RSB1	0.651	0.084879	0
AWRI796_3696	PGM2	0.912	2.00E-06	1	AWRI796_0527	YCR061W	0.647	0.001089	1
AWRI796_4069	AAH1	0.909	7.00E-05	1	AWRI796_4705	PUT4	0.647	0.001156	1
AWRI796_1525	GSY1	0.907	3.60E-05	1	AWRI796_3978	NRD1	0.646	0.006427	1
AWRI796_3391	FKS1	0.904	1.10E-05	1	AWRI796_3679	YMR087W	0.641	0.001037	1
AWRI796_4676	SPS4	0.901	0.018242	1	AWRI796_5114	GPH1	0.641	0.001116	1
AWRI796_0432	MAL31	0.899	0.000421	1	AWRI796_0534	RSA4	0.638	0.003246	1
AWRI796_3061	AQY2	0.897	0.001162	1	AWRI796_5243	FLO5	0.638	0.005408	1
AWRI796_3070	VPS13	0.896	4.00E-06	1	AWRI796_2311	SIM1	0.637	0.00837	1
AWRI796_0293	IRA1	0.892	1.00E-06	1	AWRI796_4495	NUP1	0.636	0.000773	1
AWRI796_4731	GDH1	0.888	1.70E-05	1	AWRI796_4503	LEU9	0.636	0.0013	1
AWRI796_2472	PHO90	0.871	1.00E-05	1	AWRI796_0524	PWP2	0.635	0.006427	1
AWRI796_3443	UTP21	0.87	0.000157	1	AWRI796_1883	MEP1	0.635	0.00084	1
AWRI796_4491	ECM3	0.858	3.60E-05	1	AWRI796_3801	GUA1	0.635	0.000101	1
AWRI796_0464	FUS1	0.856	0.005336	1	AWRI796_1482	RIM15	0.634	0.000156	1
AWRI796_2204	DSE2	0.85	0.00219	1	AWRI796_4641	TPO4	0.633	0.004081	1
AWRI796_3893	GAS1	0.848	1.30E-05	1	AWRI796_0592	HEM3	0.632	0.006036	1
AWRI796_3482	FMP27	0.845	8.00E-06	1	AWRI796_3048	YKR104W	0.632	0.010288	1
AWRI796_0835	DNF2	0.839	5.00E-05	1	AWRI796_0197	RPL4A	0.63	0.000523	1
AWRI796_0286	AGP2	0.837	0.000168	1	AWRI796_0187	GAL1	0.629	0.016585	1
AWRI796_2458	ZNF1	0.832	0.00017	1	AWRI796_1527	IGD1	0.629	0.225841	0
AWRI796_4285	ARG8	0.827	0.000126	1	AWRI796_1141	ADA2	0.626	0.017211	1
AWRI796_1087	ATO3	0.826	0.000901	1	AWRI796_1461	YRF1-7	0.625	0.036767	1
AWRI796_2780	TOR2	0.824	0.000131	1	AWRI796_0878	MKC7	0.624	0.140556	0
AWRI796_0496	HSP30	0.823	0.013751	1	AWRI796_2501	HSP150	0.623	0.574468	0
AWRI796_2626	CYR1	0.819	1.70E-05	1	AWRI796_4383	GAS5	0.622	0.002543	1
AWRI796_3001	DYN1	0.817	0.000283	1	AWRI796_3461	SEN1	0.62	0.000211	1
AWRI796_3961	BNI1	0.817	0.00014	1	AWRI796_3845	AWRI796_3845	0.62	0.090731	0
AWRI796_2111	SRB2	0.813	0.034664	1	AWRI796_4356	MAM3	0.619	0.000937	1
AWRI796_4737	FIT3	0.813	0.001375	1	AWRI796_0130	FUI1	0.618	0.000327	1
AWRI796_4234	NOG2	0.808	2.60E-05	1	AWRI796_4132	SUN4	0.618	0.007419	1
AWRI796_1211	FIT1	0.807	0.002506	1	AWRI796_2119	FSH1	0.616	0.03499	1
AWRI796_0698	MRK1	0.804	2.90E-05	1	AWRI796_4334	PHM7	0.616	0.001008	1
AWRI796_2868	CWP1	0.802	0.000162	1	AWRI796_2682	TOR1	0.614	0.000803	1
AWRI796_5142	AQY1	0.802	7.00E-05	1	AWRI796_3365	STT4	0.614	0.002408	1
AWRI796_3149	YLR046C	0.799	0.000265	1	AWRI796_4688	PDR10	0.614	0.00301	1
AWRI796_2026	MAL31	0.798	0.037474	1	AWRI796_0552	CDC39	0.612	0.001107	1
AWRI796_0451	GLK1	0.797	3.10E-05	1	AWRI796_2008	SLH1	0.61	0.006695	1
AWRI796_2750	HMS2	0.797	0.003833	1	AWRI796_4255_56	AWRI796_4255_56	0.608	0.006771	1
AWRI796_2407	FAA3	0.793	4.10E-05	1	AWRI796_0024	CLN3	0.606	0.300806	0
AWRI796_0166	UTP20	0.789	0.000156	1	AWRI796_2988	GAP1	0.603	0.003409	1
AWRI796_0133	URA7	0.783	2.70E-05	1	AWRI796_0493	CWH43	0.601	0.003833	1
AWRI796_0789	ENA1	0.779	0.003133	1	AWRI796_0685	PMT1	0.599	0.005214	1
AWRI796_4998	YPR015C	0.774	0.001538	1	AWRI796_1368	AWRI796_1368	0.596	0.037497	1
AWRI796_4067	YNL144C	0.771	0.000204	1	AWRI796_0546	YCR087C-A	0.595	0.013038	1
AWRI796_1197	EMI2	0.769	6.10E-05	1	AWRI796_1761	STT3	0.594	0.00837	1
AWRI796_0864	ARO1	0.768	0.000131	1	AWRI796_3718	ECM16	0.594	0.002275	1
AWRI796_0007	BDH1	0.767	5.40E-05	1	AWRI796_4729	ALD4	0.594	0.006771	1
AWRI796_2431	FLO11	0.767	0.006992	1	AWRI796_3448	PUN1	0.593	0.011501	1
AWRI796_5193	YRF1-6	0.763	0.00011	1	AWRI796_4511	RPO31	0.591	0.005763	1
AWRI796_1278	YEA4	0.759	0.020327	1	AWRI796_2238	OYE2	0.59	0.003327	1
AWRI796_4745	SAM4	0.759	0.006878	1	AWRI796_1351	ARG5,6	0.587	0.007087	1
AWRI796_3904	ADH6	0.75	0.000582	1	AWRI796_2798	FAS1	0.583	0.003833	1
AWRI796_3986	ATG2	0.748	0.000268	1	AWRI796_4287	RTC1	0.583	0.005287	1
AWRI796_2279	AIM20	0.747	0.017069	1	AWRI796_1935	UBR1	0.578	0.002163	1
AWRI796_2456	YFL054C	0.741	0.000139	1	AWRI796_3098	DRS1	0.578	0.016281	1
AWRI796_0362	PYC2	0.734	9.20E-05	1	AWRI796_3855	YMR265C	0.578	0.018991	1
AWRI796_1571	HXK2	0.734	3.80E-05	1	AWRI796_3812	RRP5	0.577	0.021872	1

AWRI796 Gene ID	Gene Name	$\log_2$ Fold Change	Adj. p-value	Score	AWRI796 Gene ID	Gene Name	$\log_2$ Fold Change	Adj. p-value	Score
AWRI796_1325	ACA1	0.576	0.002414	1	AWRI796_4592	SPR2	0.494	1	0
AWRI796_0645	RPO21	0.575	0.027963	1	AWRI796_0694	NDE2	0.493	0.081069	0
AWRI796_0229	NRG2	0.574	0.010703	1	AWRI796_2222	MPC2	0.492	0.049849	1
AWRI796_0300	YSW1	0.574	0.032219	1	AWRI796_0068	KIN3	0.49	0.499814	0
AWRI796_4574	ULS1	0.574	0.010703	1	AWRI796_1373	TSC11	0.489	0.077414	0
AWRI796_4746	PBI1	0.574	0.055349	0	AWRI796_0822	SED1	0.488	1	0
AWRI796_0934	EBS1	0.573	0.003126	1	AWRI796_1929	ATF2	0.488	0.998045	0
AWRI796_2225	PRP8	0.573	0.025081	1	AWRI796_3557	SUR7	0.488	0.419134	0
AWRI796_3891	SCW10	0.573	0.331383	0	AWRI796_4465	RPL3	0.488	0.085525	0
AWRI796_4655	SNF2	0.572	0.00618	1	AWRI796_1949	ELP2	0.487	0.161312	0
AWRI796_0788	KRS1	0.57	0.001442	1	AWRI796_2016	PXR1	0.487	0.339458	0
AWRI796_3594	ERG6	0.57	0.001099	1	AWRI796_3047	NFT1	0.487	1	0
AWRI796_4543	PDR5	0.57	0.011218	1	AWRI796_4636	HRK1	0.487	0.312734	0
AWRI796_3864	BUL1	0.565	0.007286	1	AWRI796_0375	VHC1	0.484	0.124417	0
AWRI796_0519	ARE1	0.564	0.01127	1	AWRI796_2306	TAO3	0.483	0.171666	0
AWRI796_1657	RPL9A	0.564	0.006771	1	AWRI796_0167	HTA2	0.482	0.384813	0
AWRI796_2546	MEF2	0.564	0.03499	1	AWRI796_5224	ENA1	0.482	0.081818	0
AWRI796_4111	NST1	0.564	0.000841	1	AWRI796_1885	PPT1	0.479	0.360763	0
AWRI796_5051	TEF1	0.564	0.058011	0	AWRI796_2440	DAL2	0.479	0.198057	0
AWRI796_0327	EHT1	0.563	0.005577	1	AWRI796_2540	UTP10	0.479	0.136223	0
AWRI796_5141	QCR2	0.563	0.014402	1	AWRI796_4826	RTT10	0.477	0.707279	0
AWRI796_0513	TAF2	0.562	0.026974	1	AWRI796_5029	SMK1	0.477	0.728989	0
AWRI796_1685	YGL117W	0.561	0.080163	0	AWRI796_1355	ALD5	0.476	0.18698	0
AWRI796_2716	LIH1	0.561	0.019518	1	AWRI796_3046	FLO10	0.476	0.485835	0
AWRI796_2404	PDR11	0.56	0.006771	1	AWRI796_3436	SKI2	0.476	0.152831	0
AWRI796_1440	DNF1	0.559	0.002568	1	AWRI796_4203	ARE2	0.476	0.135731	0
AWRI796_1776	PMC1	0.557	0.020233	1	AWRI796_5078	YPR114W	0.476	0.690813	0
AWRI796_3388	VRP1	0.555	0.071279	0	AWRI796_2088	ARG4	0.475	0.464202	0
AWRI796_0154	PEP1	0.553	0.011871	1	AWRI796_4792	FLC1	0.475	0.337584	0
AWRI796_4200	ACC1	0.553	0.005028	1	AWRI796_5011	CSR2	0.475	0.17496	0
AWRI796_2925	MAE1	0.551	0.112574	0	AWRI796_4602	HER1	0.471	0.214497	0
AWRI796_3528	YML082W	0.551	0.023854	1	AWRI796_2166	KIC1	0.47	0.238884	0
AWRI796_0215	REG2	0.55	0.097384	0	AWRI796_0424	SNF5	0.469	0.700881	0
AWRI796_2919	RGT1	0.549	0.005596	1	AWRI796_0428	SUL1	0.468	1	0
AWRI796_1299	SPC25	0.548	0.039632	1	AWRI796_0745	OSH2	0.468	0.38368	0
AWRI796_2113	DOG2	0.548	0.041796	1	AWRI796_2264	SET5	0.468	0.652644	0
AWRI796_4133	AQR1	0.547	0.035965	1	AWRI796_3454	DCK1	0.468	0.219935	0
AWRI796_5201	YRF1-7	0.547	0.378139	0	AWRI796_5096	RRP9	0.468	0.487406	0
AWRI796_1758	TRP5	0.545	0.025594	1	AWRI796_5181	CRH1	0.468	1	0
AWRI796_1953	TDA10	0.544	0.011501	1	AWRI796_2993	YKR045C	0.467	1	0
AWRI796_2425	SQT1	0.543	0.014463	1	AWRI796_3360	ECM38	0.465	0.112574	0
AWRI796_1565	YPS5	0.542	0.437484	0	AWRI796_3463	IMD3	0.465	0.16451	0
AWRI796_2105	NEL1	0.54	0.136688	0	AWRI796_0619	GLT1	0.464	0.366947	0
AWRI796_5158	AWRI796_5158	0.539	0.23021	0	AWRI796_1577	GUS1	0.464	0.159048	0
AWRI796_1831	SPR3	0.538	0.627803	0	AWRI796_2018	YOR1	0.463	0.560707	0
AWRI796_2298	TMA108	0.538	0.026549	1	AWRI796_0916	ATC1	0.462	0.965612	0
AWRI796_2507	INO1	0.538	0.013751	1	AWRI796_3064	YBT1	0.46	0.174723	0
AWRI796_3180	GAL2	0.538	1	0	AWRI796_1137	APT2	0.459	1	0
AWRI796_3162	FRS1	0.537	0.003954	1	AWRI796_0247	MIS1	0.458	0.455464	0
AWRI796_5113	KRE6	0.537	0.034567	1	AWRI796_1192	GNP1	0.458	1	0
AWRI796_0465	HBN1	0.536	0.252784	0	AWRI796_0263	VID24	0.457	0.464202	0
AWRI796_1824	FMP48	0.536	0.014843	1	AWRI796_0355	DUR1,2	0.457	0.438589	0
AWRI796_3053	MMP1	0.536	0.015807	1	AWRI796_0082	PKC1	0.456	0.373255	0
AWRI796_3299	IFH1	0.536	0.009361	1	AWRI796_3869	CAT8	0.456	0.540032	0
AWRI796_4409	SIN3	0.536	0.017069	1	AWRI796_4701	YOR342C	0.455	0.442478	0
AWRI796_2567	PRY1	0.535	0.813497	0	AWRI796_4915	MOT1	0.455	0.281108	0
AWRI796_0203	CHS2	0.532	0.08767	0	AWRI796_2525	URA2	0.454	0.437481	0
AWRI796_2054	AIM17	0.531	0.010209	1	AWRI796_3291	CRR1	0.454	0.668226	0
AWRI796_3424	IKI3	0.531	0.022776	1	AWRI796_1231	PRB1	0.453	0.690813	0
AWRI796_0548B	FIG2	0.53	0.194484	0	AWRI796_2616	BBC1	0.453	0.566396	0
AWRI796_3094	PUF3	0.53	0.038635	1	AWRI796_3721	RRB1	0.453	0.205346	0
AWRI796_4733	AMF1	0.53	0.158011	0	AWRI796_1259	SNU13	0.451	1	0
AWRI796_0078	FLO1	0.528	0.526974	0	AWRI796_0841	ARX1	0.45	0.473642	0
AWRI796_5097	MEP3	0.528	0.424087	0	AWRI796_2447	IRC24	0.448	0.280158	0
AWRI796_0104	NUP170	0.526	0.040223	1	AWRI796_2291	PAN6	0.447	1	0
AWRI796_1635	XRN1	0.526	0.021872	1	AWRI796_0732	PUS9	0.446	0.751808	0
AWRI796_4888	PEX25	0.525	0.037714	1	AWRI796_2920	UGP1	0.446	0.278208	0
AWRI796_3257	CBF5	0.523	0.021297	1	AWRI796_0076	SWH1	0.445	0.538055	0
AWRI796_3878	HAS1	0.522	0.032219	1	AWRI796_0748	NOP1	0.444	1	0
AWRI796_2428	YIR016W	0.52	0.021872	1	AWRI796_0172	GPI18	0.443	1	0
AWRI796_3067	FPS1	0.52	0.050173	0	AWRI796_0028	RBG1	0.441	0.52669	0
AWRI796_5191	YML133C	0.52	0.148872	0	AWRI796_3783	CLN1	0.44	1	0
AWRI796_0272	LYS2	0.519	0.035114	1	AWRI796_1112	DFM1	0.439	0.373255	0
AWRI796_0455	GFD2	0.519	0.461205	0	AWRI796_1586	MTO1	0.439	0.814725	0
AWRI796_2059	DUR3	0.519	0.032219	1	AWRI796_5251	PAU3	0.438	1	0
AWRI796_2117	AAP1	0.519	0.15397	0	AWRI796_0182	MNN2	0.437	0.52669	0
AWRI796_1342	FCY22	0.518	0.781044	0	AWRI796_1466	ALR2	0.437	1	0
AWRI796_0035	MYO4	0.517	0.03341	1	AWRI796_3645	NUP116	0.437	1	0
AWRI796_1430	BEM2	0.517	0.011502	1	AWRI796_0600	SEC31	0.436	0.584003	0
AWRI796_2840	MYO3	0.517	0.022802	1	AWRI796_1650	AMS1	0.436	1	0
AWRI796_4028	CHS1	0.517	0.419134	0	AWRI796_1915	NSR1	0.436	0.701509	0
AWRI796_0188	FUR4	0.516	0.678758	0	AWRI796_1419	UBP5	0.435	1	0
AWRI796_1839	ART5	0.515	0.135431	0	AWRI796_3606	PLB2	0.434	0.690813	0
AWRI796_1528	YFR018C	0.514	0.045177	1	AWRI796_4832	TRE1	0.434	0.686491	0
AWRI796_2642	ILV3	0.514	0.050633	0	AWRI796_4919	GCR1	0.434	0.788578	0
AWRI796_3095	YEH1	0.514	0.08767	0	AWRI796_2029	ARN2	0.433	1	0
AWRI796_3608	PLB1	0.514	0.091116	0	AWRI796_3034	TGL4	0.433	0.642353	0
AWRI796_1427	YER152C	0.513	0.020552	1	AWRI796_3255	YLR173W	0.432	0.743273	0
AWRI796_3535	HMG1	0.51	0.038446	1	AWRI796_4236	HOL1	0.432	1	0
AWRI796_3537	TCB3	0.51	0.034998	1	AWRI796_2101	ERC1	0.431	0.891607	0
AWRI796_3780	YMR196W	0.51	0.161658	0	AWRI796_4192	LRO1	0.431	1	0
AWRI796_3981	RPA49	0.51	0.022479	1	AWRI796_3950	WSC2	0.43	1	0
AWRI796_1397	AVT6	0.509	0.017018	1	AWRI796_5230	YOR389W	0.43	0.95918	0
AWRI796_1643	RAD54	0.508	0.122635	0	AWRI796_0570	SSB1	0.429	0.988704	0
AWRI796_4640	YTM1	0.508	0.027963	1	AWRI796_2190	FUR1	0.429	1	0
AWRI796_1683	PRP43	0.507	0.046019	1	AWRI796_3952	HCH1	0.429	1	0
AWRI796_4735	FRE3	0.507	0.770615	0	AWRI796_1243	GLY1	0.428	1	0
AWRI796_0163	SLA1	0.505	0.049586	1	AWRI796_3988	NAR1	0.427	1	0
AWRI796_3516	TSL1	0.505	0.474875	0	AWRI796_1450	ECM32	0.426	1	0
AWRI796_1708	NUP145	0.504	0.050633	0	AWRI796_1827	MUP1	0.425	1	0
AWRI796_1369	DOT6	0.502	0.327954	0	AWRI796_4652	RRP36	0.425	1	0
AWRI796_3791	HFA1	0.5	0.106623	0	AWRI796_0711	SYO1	0.424	1	0
AWRI796_3794	MGL2	0.5	0.045177	1	AWRI796_3564	RRN11	0.424	1	0
AWRI796_0273	TKL2	0.499	0.300067	0	AWRI796_2944	UFD4	0.423	1	0
AWRI796_4195	PRP2	0.499	0.083998	0	AWRI796_3569	AMD1	0.421	1	0
AWRI796_0518	BUD23	0.498	0.223283	0	AWRI796_0766	GAL3	0.419	1	0
AWRI796_1148	TOM1	0.494	0.022507	1	AWRI796_1352	RNR1	0.419	1	0

AWRI796 Gene ID	Gene Name	log_2 Fold Change	Adj. *p* -value	Score	AWRI796 Gene ID	Gene Name	log_2 Fold Change	Adj. *p* -value	Score
AWRI796_0242	RPG1	0.418	1	0	AWRI796_1098	SXM1	0.368	1	0
AWRI796_2153	RTC3	0.418	1	0	AWRI796_3521	UTP14	0.368	1	0
AWRI796_4787	NEW1	0.418	1	0	AWRI796_4747	MDL2	0.368	1	0
AWRI796_2138	ERG7	0.417	1	0	AWRI796_0359	SDS24	0.367	1	0
AWRI796_4673	NOP58	0.415	1	0	AWRI796_2265	BAT1	0.367	1	0
AWRI796_1438	CHD1	0.414	1	0	AWRI796_3823	YHM2	0.367	1	0
AWRI796_0216	RFS1	0.413	1	0	AWRI796_4075	YNL134C	0.367	1	0
AWRI796_1492	FRS2	0.413	1	0	AWRI796_4796	BMS1	0.367	1	0
AWRI796_1036	UTP4	0.412	1	0	AWRI796_3503	DAT1	0.366	1	0
AWRI796_1295	HEM14	0.412	1	0	AWRI796_1806	ERV1	0.365	1	0
AWRI796_0468	AGP1	0.411	1	0	AWRI796_2031	YHL044W	0.365	1	0
AWRI796_1384	NUP157	0.411	1	0	AWRI796_4186	CIT1	0.365	1	0
AWRI796_0266	AIM3	0.409	1	0	AWRI796_2278	BNR1	0.364	1	0
AWRI796_1375	RAD51	0.409	1	0	AWRI796_2346	KTR7	0.364	1	0
AWRI796_2091	YHR022C	0.408	1	0	AWRI796_3122	MEU1	0.364	1	0
AWRI796_1994	COQ6	0.407	1	0	AWRI796_3223	ZRT2	0.364	1	0
AWRI796_4342	YOL075C	0.406	1	0	AWRI796_4201	TIM23	0.364	1	0
AWRI796_2442	DAL7	0.405	1	0	AWRI796_2368	YIL055C	0.363	1	0
AWRI796_2768	OXP1	0.405	1	0	AWRI796_3676	ADH3	0.363	1	0
AWRI796_0483	CIT2	0.404	1	0	AWRI796_4052	RIA1	0.363	1	0
AWRI796_0942	ADR1	0.404	1	0	AWRI796_4223	COQ2	0.363	1	0
AWRI796_1363	UTP7	0.404	1	0	AWRI796_3052	MHT1	0.362	1	0
AWRI796_1495	PAU5	0.404	1	0	AWRI796_4768	YPL247C	0.362	1	0
AWRI796_0381	YBR241C	0.403	1	0	AWRI796_2015	SCW4	0.361	1	0
AWRI796_0901	SEC7	0.403	1	0	AWRI796_0561	ADY3	0.36	1	0
AWRI796_2881	TEF4	0.403	1	0	AWRI796_2799	PRS1	0.36	1	0
AWRI796_4858	PPT2	0.403	1	0	AWRI796_2736	NMD5	0.359	1	0
AWRI796_2829	LTV1	0.402	1	0	AWRI796_2981	SPO14	0.359	1	0
AWRI796_3719	POM152	0.402	1	0	AWRI796_3968	POL2	0.359	1	0
AWRI796_4337	IRA2	0.402	1	0	AWRI796_5102	ASN1	0.358	1	0
AWRI796_1808	IMO32	0.4	1	0	AWRI796_2253	UTP9	0.357	1	0
AWRI796_1833	ADE6	0.399	1	0	AWRI796_2405	TIR3	0.357	1	0
AWRI796_4237	BIO5	0.399	1	0	AWRI796_2862	APE1	0.357	1	0
AWRI796_4357	GPD2	0.399	1	0	AWRI796_2258	PPX1	0.356	1	0
AWRI796_2471	ACO2	0.398	1	0	AWRI796_4642	MOD5	0.356	1	0
AWRI796_3929	KRI1	0.397	1	0	AWRI796_4844	SVS1	0.356	1	0
AWRI796_1000	GCN2	0.396	1	0	AWRI796_0069	CDC15	0.354	1	0
AWRI796_1502	WWM1	0.396	1	0	AWRI796_1503	CDC4	0.354	1	0
AWRI796_0031	FUN19	0.395	1	0	AWRI796_3106	YLR001C	0.354	1	0
AWRI796_1664	YGL140C	0.395	1	0	AWRI796_3232	SLS1	0.354	1	0
AWRI796_3707	ASC1	0.395	1	0	AWRI796_4996	YPR011C	0.354	1	0
AWRI796_4821	GUP2	0.395	1	0	AWRI796_0730	PRM7	0.353	1	0
AWRI796_2289	SLN1	0.394	1	0	AWRI796_1119A	HKR1	0.353	1	0
AWRI796_1930	PBP1	0.393	1	0	AWRI796_1691	NSA1	0.353	1	0
AWRI796_2090	YHR020W	0.393	1	0	AWRI796_2789	DPH2	0.353	1	0
AWRI796_3233	RRN5	0.393	1	0	AWRI796_3195	KIN2	0.353	1	0
AWRI796_3254	DPH5	0.393	1	0	AWRI796_3369	CDC25	0.353	1	0
AWRI796_0743	GPM2	0.392	1	0	AWRI796_4384	YOL029C	0.353	1	0
AWRI796_0958	LYS4	0.392	1	0	AWRI796_0668	TRM3	0.352	1	0
AWRI796_1344	GPP2	0.392	1	0	AWRI796_3514	CAC2	0.352	1	0
AWRI796_3525	ALO1	0.392	1	0	AWRI796_2137	TRM5	0.351	1	0
AWRI796_4653	MPD1	0.392	1	0	AWRI796_4753	YPL264C	0.35	1	0
AWRI796_4754	KEL3	0.392	1	0	AWRI796_1246	GDA1	0.348	1	0
AWRI796_4806	TYW1	0.392	1	0	AWRI796_1886	ASN2	0.348	1	0
AWRI796_3158	ERG3	0.391	1	0	AWRI796_3349	CTS1	0.348	1	0
AWRI796_4527	BAG7	0.391	1	0	AWRI796_1198	GRH1	0.347	1	0
AWRI796_1403	RSP5	0.39	1	0	AWRI796_3258	RFX1	0.347	1	0
AWRI796_1900	BTN2	0.39	1	0	AWRI796_3345	YLR278C	0.347	1	0
AWRI796_3800	SKY1	0.39	1	0	AWRI796_3888	YME2	0.346	1	0
AWRI796_0583	PRR2	0.389	1	0	AWRI796_1602	KIP3	0.345	1	0
AWRI796_1420	FTR1	0.389	1	0	AWRI796_1904	ECL1	0.345	1	0
AWRI796_2140	QNS1	0.389	1	0	AWRI796_2945	MRT4	0.345	1	0
AWRI796_5076	MRD1	0.389	1	0	AWRI796_0970	VHS1	0.343	1	0
AWRI796_0536	SOL2	0.388	1	0	AWRI796_3774	GCV2	0.343	1	0
AWRI796_0121	YBL055C	0.387	1	0	AWRI796_0421	APE3	0.342	1	0
AWRI796_0941	AHA1	0.387	1	0	AWRI796_4484	LPX1	0.342	1	0
AWRI796_1491	BUD27	0.386	1	0	AWRI796_4526	EFT2	0.342	1	0
AWRI796_3123	POM34	0.385	1	0	AWRI796_4980	NCR1	0.342	1	0
AWRI796_4504	INP53	0.385	1	0	AWRI796_4033	SWT21	0.341	1	0
AWRI796_3652	AAC1	0.384	1	0	AWRI796_4353	CRT10	0.341	1	0
AWRI796_4293	ALR1	0.384	1	0	AWRI796_0025	CYC3	0.34	1	0
AWRI796_1484	AGX1	0.383	1	0	AWRI796_2398	HIS6	0.34	1	0
AWRI796_3330	HSP60	0.383	1	0	AWRI796_3141	PAU23	0.34	1	0
AWRI796_3519	YML096W	0.383	1	0	AWRI796_5154_55	AWRI796_5154_55	0.34	1	0
AWRI796_4442	AKR2	0.383	1	0	AWRI796_2148	KSP1	0.339	1	0
AWRI796_0756	MCD1	0.382	1	0	AWRI796_4063	RPC31	0.339	1	0
AWRI796_1569	ZRT1	0.382	1	0	AWRI796_4333	ADH1	0.339	1	0
AWRI796_2254	RIX1	0.382	1	0	AWRI796_0865	MTC5	0.338	1	0
AWRI796_3285	HRD3	0.382	1	0	AWRI796_2746	PMT4	0.338	1	0
AWRI796_5008	ATH1	0.382	1	0	AWRI796_2177	BZZ1	0.337	1	0
AWRI796_0871	YCF1	0.38	1	0	AWRI796_3761	ECM5	0.337	1	0
AWRI796_1655	INO80	0.379	1	0	AWRI796_1341	FCY21	0.336	1	0
AWRI796_2043	ECM29	0.379	1	0	AWRI796_3000	YSR3	0.336	1	0
AWRI796_3879	TDA1	0.379	1	0	AWRI796_0006	BDH2	0.335	1	0
AWRI796_1677	SCS3	0.377	1	0	AWRI796_0159	SCT1	0.335	1	0
AWRI796_3018	SIS2	0.377	1	0	AWRI796_2124	CPR2	0.335	1	0
AWRI796_3218	YLR125W	0.377	1	0	AWRI796_4321	WRS1	0.335	1	0
AWRI796_0733	GPR1	0.376	1	0	AWRI796_3963	LYP1	0.334	1	0
AWRI796_3790	YMR206W	0.376	1	0	AWRI796_1155	RMT2	0.333	1	0
AWRI796_4070	THO2	0.376	1	0	AWRI796_1287	NUG1	0.333	1	0
AWRI796_2003	YGR266W	0.374	1	0	AWRI796_2161	HXT5	0.333	1	0
AWRI796_2102	YHR033W	0.374	1	0	AWRI796_4567	LAS17	0.333	1	0
AWRI796_2396	TIM44	0.374	1	0	AWRI796_4364	SPE2	0.332	1	0
AWRI796_2628	AVT1	0.374	1	0	AWRI796_5209	YML133C	0.332	1	0
AWRI796_0461	HIS4	0.373	1	0	AWRI796_1210	HSP31	0.331	1	0
AWRI796_0488	ADP1	0.373	1	0	AWRI796_3851	TPS3	0.331	1	0
AWRI796_0640	COP1	0.373	1	0	AWRI796_0223	AKL1	0.33	1	0
AWRI796_2331	DPH1	0.373	1	0	AWRI796_1370	PTC2	0.33	1	0
AWRI796_1233	SDD1	0.372	1	0	AWRI796_2321	SDP1	0.33	1	0
AWRI796_2995	NAP1	0.371	1	0	AWRI796_2341	UTP25	0.329	1	0
AWRI796_1846	PAC10	0.37	1	0	AWRI796_4713	CIR2	0.329	1	0
AWRI796_3496	NDI1	0.37	1	0	AWRI796_0168	HTB2	0.328	1	0
AWRI796_4358	ARG1	0.37	1	0	AWRI796_2112	NCP1	0.328	1	0
AWRI796_4963	MET12	0.37	1	0	AWRI796_2688	OPI3	0.328	1	0
AWRI796_3945	PCL1	0.369	1	0	AWRI796_2884	DHR2	0.328	1	0
AWRI796_4839	MEX67	0.369	1	0	AWRI796_3413	ROM2	0.328	1	0
AWRI796_0474	GBP2	0.368	1	0	AWRI796_4210	BUD17	0.328	1	0

AWRI796 Gene ID	Gene Name	$\log_2$ Fold Change	Adj. p-value	Score	AWRI796 Gene ID	Gene Name	$\log_2$ Fold Change	Adj. p-value	Score
AWRI796_0608	VMA1	0.327	1	0	AWRI796_4778	RVB2	0.296	1	0
AWRI796_0723	STP4	0.327	1	0	AWRI796_2974	DBP7	0.295	1	0
AWRI796_1862	VAS1	0.327	1	0	AWRI796_5101	NOC4	0.295	1	0
AWRI796_0346	TAF5	0.326	1	0	AWRI796_0022	ERV46	0.294	1	0
AWRI796_0577	CDC13	0.326	1	0	AWRI796_3908	SAM3	0.294	1	0
AWRI796_2326	YIL108W	0.326	1	0	AWRI796_4402	PLB3	0.294	1	0
AWRI796_0231	TIP1	0.325	1	0	AWRI796_1984	SDA1	0.293	1	0
AWRI796_1889	YGR127W	0.325	1	0	AWRI796_4598	ODC2	0.293	1	0
AWRI796_2597	YJL045W	0.325	1	0	AWRI796_4849	TGS1	0.293	1	0
AWRI796_3259	YLR177W	0.325	1	0	AWRI796_2116	INM1	0.292	1	0
AWRI796_4486	TCB1	0.325	1	0	AWRI796_2575	UTP18	0.292	1	0
AWRI796_1195	YDR514C	0.324	1	0	AWRI796_2735	MNS1	0.292	1	0
AWRI796_3499	NAB6	0.324	1	0	AWRI796_4084	ESBP6	0.292	1	0
AWRI796_0116	SKT5	0.323	1	0	AWRI796_0452	GID7	0.291	1	0
AWRI796_1143	YHP1	0.323	1	0	AWRI796_1428	PET122	0.291	1	0
AWRI796_4586	RET1	0.323	1	0	AWRI796_1950	YGR201C	0.291	1	0
AWRI796_3133	ADE16	0.322	1	0	AWRI796_2796	SPE1	0.291	1	0
AWRI796_3767	RGM1	0.322	1	0	AWRI796_3444	VIP1	0.291	1	0
AWRI796_4743	FDH1	0.322	1	0	AWRI796_3513	NUP188	0.291	1	0
AWRI796_4847	CDC60	0.322	1	0	AWRI796_0580	TIM22	0.29	1	0
AWRI796_1254	MCM3	0.321	1	0	AWRI796_1958	YGR210C	0.29	1	0
AWRI796_2604	IRC18	0.321	1	0	AWRI796_3078	FRA1	0.29	1	0
AWRI796_2652	RAV1	0.321	1	0	AWRI796_3803	ESC1	0.29	1	0
AWRI796_4407	TOP1	0.321	1	0	AWRI796_1479	RPO41	0.289	1	0
AWRI796_0601	SNF3	0.32	1	0	AWRI796_3583	YML020W	0.289	1	0
AWRI796_0796	HEM12	0.32	1	0	AWRI796_4583	DED1	0.289	1	0
AWRI796_4425	AWRI796_4425	0.32	1	0	AWRI796_4726	GPB1	0.289	1	0
AWRI796_5156	AWRI796_5156	0.32	1	0	AWRI796_4945	NOP4	0.289	1	0
AWRI796_0257	VPS15	0.319	1	0	AWRI796_3138	SMF3	0.288	1	0
AWRI796_1014	BFR2	0.319	1	0	AWRI796_3276	PWP1	0.288	1	0
AWRI796_3467	DIF1	0.319	1	0	AWRI796_4214	SSK2	0.288	1	0
AWRI796_3470	SEC39	0.319	1	0	AWRI796_5089	YPR127W	0.288	1	0
AWRI796_3992	SIN4	0.318	1	0	AWRI796_1759	PGD1	0.287	1	0
AWRI796_1410	PMD1	0.317	1	0	AWRI796_2395	YKE4	0.287	1	0
AWRI796_2058	YHL017W	0.317	1	0	AWRI796_3793	YMR209C	0.287	1	0
AWRI796_4302	MCH4	0.317	1	0	AWRI796_4441	EXO1	0.287	1	0
AWRI796_2233	ENO2	0.316	1	0	AWRI796_0096	TEL1	0.286	1	0
AWRI796_4575	THI72	0.316	1	0	AWRI796_2443	DAL3	0.286	1	0
AWRI796_0306	RPB5	0.315	1	0	AWRI796_3422	NAM2	0.286	1	0
AWRI796_0504	SNT1	0.315	1	0	AWRI796_3565	CAT2	0.286	1	0
AWRI796_2451	AWRI796_2451	0.315	1	0	AWRI796_3806	FSH2	0.286	1	0
AWRI796_4094	DBP2	0.315	1	0	AWRI796_4696	TEA1	0.286	1	0
AWRI796_4699	RPA43	0.315	1	0	AWRI796_0812	RTR2	0.285	1	0
AWRI796_0712	TSR1	0.314	1	0	AWRI796_2449	YPS6	0.285	1	0
AWRI796_1238	AFG1	0.314	1	0	AWRI796_2526	TRK1	0.285	1	0
AWRI796_2808	NNK1	0.314	1	0	AWRI796_0540	PTC6	0.284	1	0
AWRI796_1940	HIP1	0.313	1	0	AWRI796_1887	YGR125W	0.284	1	0
AWRI796_3987	ZWF1	0.312	1	0	AWRI796_2277	POT1	0.284	1	0
AWRI796_0274	TEF1	0.311	1	0	AWRI796_3025	MTD1	0.284	1	0
AWRI796_2283	IMP2'	0.311	1	0	AWRI796_3633	HOF1	0.284	1	0
AWRI796_2766	JEN1	0.311	1	0	AWRI796_4415	YSP3	0.284	1	0
AWRI796_3830	GAD1	0.311	1	0	AWRI796_4893	SSE1	0.284	1	0
AWRI796_3831	GTO3	0.311	1	0	AWRI796_4997	CMR3	0.284	1	0
AWRI796_0045	FUN30	0.31	1	0	AWRI796_0043	CCR4	0.283	1	0
AWRI796_2445	LYS1	0.31	1	0	AWRI796_3555	CYB2	0.283	1	0
AWRI796_2559	ARG3	0.31	1	0	AWRI796_2438	DAL1	0.282	1	0
AWRI796_4350	RIB2	0.31	1	0	AWRI796_2664	ANB1	0.282	1	0
AWRI796_0351	COS111	0.309	1	0	AWRI796_3074	RIX7	0.282	1	0
AWRI796_1678	MET13	0.309	1	0	AWRI796_0634	SAS10	0.281	1	0
AWRI796_2564	IML2	0.309	1	0	AWRI796_3092	BPT1	0.281	1	0
AWRI796_2592	MTR4	0.309	1	0	AWRI796_0219	PRP6	0.28	1	0
AWRI796_0140	RIB1	0.308	1	0	AWRI796_1926	RBG2	0.28	1	0
AWRI796_2608	HCA4	0.308	1	0	AWRI796_3894	PSE1	0.28	1	0
AWRI796_2732	RSF2	0.308	1	0	AWRI796_0195	CDS1	0.279	1	0
AWRI796_3657	ARG7	0.308	1	0	AWRI796_1162	JIP4	0.279	1	0
AWRI796_4403	RCL1	0.308	1	0	AWRI796_1312	YPT31	0.279	1	0
AWRI796_2490	CPS1	0.307	1	0	AWRI796_1371	TRP2	0.279	1	0
AWRI796_3183	RAX2	0.307	1	0	AWRI796_2164	TRA1	0.279	1	0
AWRI796_3433	CST9	0.307	1	0	AWRI796_2904	TMA19	0.279	1	0
AWRI796_0598	GGC1	0.306	1	0	AWRI796_1282	MNN1	0.278	1	0
AWRI796_3007	KTR2	0.306	1	0	AWRI796_4021	YNL200C	0.278	1	0
AWRI796_3308	TOP3	0.306	1	0	AWRI796_1110	SIZ1	0.277	1	0
AWRI796_4281	NOP8	0.306	1	0	AWRI796_2940	URB1	0.277	1	0
AWRI796_0184	KAP104	0.305	1	0	AWRI796_4974	RRP12	0.277	1	0
AWRI796_2350	THS1	0.305	1	0	AWRI796_5022	THP3	0.277	1	0
AWRI796_4718	PRT1	0.305	1	0	AWRI796_2224	DNA2	0.276	1	0
AWRI796_2109	MSC7	0.304	1	0	AWRI796_1309	MIG3	0.275	1	0
AWRI796_3732	YMR144W	0.304	1	0	AWRI796_2548	LSB6	0.275	1	0
AWRI796_4564	GAC1	0.304	1	0	AWRI796_4343	DSC2	0.274	1	0
AWRI796_0616	AIR2	0.303	1	0	AWRI796_5203	COS3	0.274	1	0
AWRI796_1023	SUM1	0.303	1	0	AWRI796_4246	YNR065C	0.273	1	0
AWRI796_2342	ICE2	0.303	1	0	AWRI796_2095	PPA1	0.273	1	0
AWRI796_4224	MVD1	0.303	1	0	AWRI796_0781	REG1	0.272	1	0
AWRI796_4791	FMP40	0.303	1	0	AWRI796_1377	UBP9	0.272	1	0
AWRI796_0697	THI3	0.302	1	0	AWRI796_1982	YAP1802	0.272	1	0
AWRI796_3529	TDA9	0.302	1	0	AWRI796_2155	GAR1	0.272	1	0
AWRI796_4541	RPB2	0.302	1	0	AWRI796_2793	FAT3	0.272	1	0
AWRI796_4820	NAB3	0.302	1	0	AWRI796_3862	ZDS1	0.272	1	0
AWRI796_1769	PUF4	0.301	1	0	AWRI796_3230	RKM5	0.271	1	0
AWRI796_4016	RIO2	0.301	1	0	AWRI796_3261	YLR179C	0.271	1	0
AWRI796_4582	HIS3	0.301	1	0	AWRI796_2729	YJR124C	0.27	1	0
AWRI796_4235	ESF2	0.299	1	0	AWRI796_3802	TRS130	0.27	1	0
AWRI796_4986	CIT3	0.299	1	0	AWRI796_4150	LAP2	0.27	1	0
AWRI796_0567	MFG1	0.298	1	0	AWRI796_4852	PEP4	0.27	1	0
AWRI796_3172	LAM6	0.298	1	0	AWRI796_5058	SRP54	0.27	1	0
AWRI796_4060	YCK2	0.298	1	0	AWRI796_0052	CYS3	0.269	1	0
AWRI796_4166	EFM6	0.298	1	0	AWRI796_0434	HMLALPHA2	0.269	1	0
AWRI796_1606	NCS6	0.297	1	0	AWRI796_1903	ENP2	0.269	1	0
AWRI796_5133	SEC23	0.297	1	0	AWRI796_2086	YSC84	0.269	1	0
AWRI796_0200	PDX3	0.296	1	0	AWRI796_2961	TOF2	0.269	1	0
AWRI796_0389	ARO4	0.296	1	0	AWRI796_3895	NIP1	0.269	1	0
AWRI796_1613	KEX1	0.296	1	0	AWRI796_1270	EDC3	0.268	1	0
AWRI796_3043	BAS1	0.296	1	0	AWRI796_1699	YGL101W	0.268	1	0
AWRI796_3128	IZH3	0.296	1	0	AWRI796_1890	UTP8	0.268	1	0
AWRI796_3380	PEX30	0.296	1	0	AWRI796_4355	PRS5	0.268	1	0
AWRI796_4320	SDD3	0.296	1	0	AWRI796_1429	OXA1	0.267	1	0
AWRI796_4558	YRM1	0.296	1	0	AWRI796_1598	EDC1	0.267	1	0

AWRI796 Gene ID	Gene Name	log_2 Fold Change	Adj. *p* -value	Score	AWRI796 Gene ID	Gene Name	log_2 Fold Change	Adj. *p* -value	Score
AWRI796_1720	HNM1	0.267	1	0	AWRI796_3269	ATG26	0.241	1	0
AWRI796_1881	NUP57	0.267	1	0	AWRI796_3941	MSB3	0.241	1	0
AWRI796_4043	NOP13	0.267	1	0	AWRI796_4147	ALG11	0.241	1	0
AWRI796_1183	ITR1	0.266	1	0	AWRI796_5050	MRL1	0.241	1	0
AWRI796_1603	CLG1	0.266	1	0	AWRI796_0287	HSL7	0.24	1	0
AWRI796_2139	OSH3	0.266	1	0	AWRI796_0759	NTH1	0.24	1	0
AWRI796_2656	YJR039W	0.266	1	0	AWRI796_1611	CHC1	0.24	1	0
AWRI796_3884	PRC1	0.266	1	0	AWRI796_3460	CRN1	0.24	1	0
AWRI796_4228	FPK1	0.266	1	0	AWRI796_4269	HPF1	0.24	1	0
AWRI796_2841	PMU1	0.265	1	0	AWRI796_4732	ATF1	0.24	1	0
AWRI796_2873	YKL091C	0.265	1	0	AWRI796_0169	NTH2	0.239	1	0
AWRI796_5210	YHL049C	0.265	1	0	AWRI796_0988	HEL2	0.239	1	0
AWRI796_0550	KIN82	0.264	1	0	AWRI796_1116	SYF1	0.239	1	0
AWRI796_1275	MIT1	0.264	1	0	AWRI796_2743	HIR3	0.239	1	0
AWRI796_3362	HRI1	0.264	1	0	AWRI796_3938	MON2	0.239	1	0
AWRI796_2714	ADO1	0.263	1	0	AWRI796_0190	CHS3	0.238	1	0
AWRI796_0370	ROT2	0.262	1	0	AWRI796_0734	SLM3	0.238	1	0
AWRI796_2020	YGR283C	0.262	1	0	AWRI796_1177	PKH1	0.238	1	0
AWRI796_2167	SBE22	0.262	1	0	AWRI796_2228	MTG2	0.238	1	0
AWRI796_2822	YKL151C	0.262	1	0	AWRI796_3024	TRZ1	0.238	1	0
AWRI796_3990	KEX2	0.262	1	0	AWRI796_0262	YMC2	0.237	1	0
AWRI796_4456	ETT1	0.262	1	0	AWRI796_0767	SNQ2	0.237	1	0
AWRI796_0217	YBR053C	0.261	1	0	AWRI796_2202	YHR140W	0.237	1	0
AWRI796_0503	BPH1	0.261	1	0	AWRI796_2275	SUC2	0.237	1	0
AWRI796_2922	YKL033W-A	0.261	1	0	AWRI796_3900	PRE5	0.237	1	0
AWRI796_5111	TDA6	0.261	1	0	AWRI796_4101	POL1	0.237	1	0
AWRI796_0058	SSA1	0.26	1	0	AWRI796_4848	AIM44	0.237	1	0
AWRI796_0418	SSH1	0.26	1	0	AWRI796_0515	PER1	0.236	1	0
AWRI796_0623	NRP1	0.26	1	0	AWRI796_2073	TCD1	0.236	1	0
AWRI796_2889	STB6	0.26	1	0	AWRI796_2797	LOT5	0.236	1	0
AWRI796_4131	RPL9B	0.26	1	0	AWRI796_3027	NUP133	0.236	1	0
AWRI796_1391	TMN3	0.259	1	0	AWRI796_4378	YOL036W	0.236	1	0
AWRI796_0059	VPS8	0.258	1	0	AWRI796_0039	MAK16	0.235	1	0
AWRI796_1050	YDR341C	0.258	1	0	AWRI796_2495	HAL5	0.235	1	0
AWRI796_2602	NUP192	0.258	1	0	AWRI796_2583	YHC3	0.235	1	0
AWRI796_4298	TRM11	0.258	1	0	AWRI796_2680	CCT5	0.235	1	0
AWRI796_4605	WTM1	0.258	1	0	AWRI796_4872	RPL5	0.234	1	0
AWRI796_1096	SHE9	0.257	1	0	AWRI796_0817	IPT1	0.233	1	0
AWRI796_4559	DCS2	0.257	1	0	AWRI796_2120	SMF2	0.233	1	0
AWRI796_0400	SHM1	0.256	1	0	AWRI796_0768	RPL4B	0.232	1	0
AWRI796_0477	STP22	0.256	1	0	AWRI796_1936	TYS1	0.232	1	0
AWRI796_1587	ADE5,7	0.256	1	0	AWRI796_2045	WSC4	0.232	1	0
AWRI796_1719	DBP3	0.256	1	0	AWRI796_2437	YVH1	0.232	1	0
AWRI796_1858	UTP22	0.256	1	0	AWRI796_4624	SEC63	0.232	1	0
AWRI796_2128	GIC1	0.256	1	0	AWRI796_0005	GDH3	0.231	1	0
AWRI796_4089	DCP2	0.256	1	0	AWRI796_1680	RPS2	0.231	1	0
AWRI796_4110	YNL092W	0.256	1	0	AWRI796_2007	YTA7	0.231	1	0
AWRI796_4770	YPL245W	0.256	1	0	AWRI796_3628	YMR027W	0.231	1	0
AWRI796_0238	PFF1	0.255	1	0	AWRI796_3914	EGT2	0.231	1	0
AWRI796_1228	CAN1	0.255	1	0	AWRI796_4209	SEC12	0.231	1	0
AWRI796_2049	SNF6	0.255	1	0	AWRI796_0441	SPB1	0.23	1	0
AWRI796_2741	IML1	0.255	1	0	AWRI796_1300	ISC1	0.23	1	0
AWRI796_2965	YKR015C	0.255	1	0	AWRI796_2686	LIA1	0.23	1	0
AWRI796_4802	NIP7	0.255	1	0	AWRI796_4020	PSY2	0.23	1	0
AWRI796_0539	PAT1	0.254	1	0	AWRI796_1636	NUP49	0.229	1	0
AWRI796_2243	KOG1	0.254	1	0	AWRI796_3586	PSP2	0.229	1	0
AWRI796_2712	URA8	0.254	1	0	AWRI796_4825	MRN1	0.229	1	0
AWRI796_0774	GCV1	0.253	1	0	AWRI796_0647	RGT2	0.228	1	0
AWRI796_2349	AIR1	0.253	1	0	AWRI796_0896	TRM82	0.228	1	0
AWRI796_3260	TFS1	0.253	1	0	AWRI796_1121	SIP1	0.228	1	0
AWRI796_4046	PSD1	0.253	1	0	AWRI796_1800	MTL1	0.228	1	0
AWRI796_1265	PXP1	0.252	1	0	AWRI796_4174	HEF3	0.228	1	0
AWRI796_1531	ATG18	0.252	1	0	AWRI796_0548A	FIG2	0.227	1	0
AWRI796_2721	RSM7	0.252	1	0	AWRI796_2806	SNU114	0.227	1	0
AWRI796_2860	SEG2	0.252	1	0	AWRI796_4876	NAN1	0.227	1	0
AWRI796_3469	MRPL4	0.252	1	0	AWRI796_0020	GCV3	0.226	1	0
AWRI796_4170	KTR5	0.252	1	0	AWRI796_1688	YGL114W	0.226	1	0
AWRI796_4950	MET31	0.252	1	0	AWRI796_1792	SNU71	0.226	1	0
AWRI796_1128	CYM1	0.251	1	0	AWRI796_3209	HOG1	0.226	1	0
AWRI796_2034	ARN1	0.251	1	0	AWRI796_2488	KRE9	0.225	1	0
AWRI796_4695	KRE5	0.251	1	0	AWRI796_4173	PUB1	0.225	1	0
AWRI796_1496	LPD1	0.25	1	0	AWRI796_5036	FCY1	0.225	1	0
AWRI796_3951	POP3	0.25	1	0	AWRI796_0729	NAT1	0.224	1	0
AWRI796_4887	YPL113C	0.25	1	0	AWRI796_2752	YJR149W	0.224	1	0
AWRI796_1667	SEC27	0.249	1	0	AWRI796_4766	GYP5	0.224	1	0
AWRI796_2002	MES1	0.249	1	0	AWRI796_5134	DPM1	0.224	1	0
AWRI796_2330	SHQ1	0.249	1	0	AWRI796_1656	ARO2	0.223	1	0
AWRI796_2896	MNR2	0.249	1	0	AWRI796_2223	SOL3	0.223	1	0
AWRI796_3021	ECM4	0.249	1	0	AWRI796_3697	YKU80	0.223	1	0
AWRI796_3866	FCP1	0.249	1	0	AWRI796_4579	MCA1	0.223	1	0
AWRI796_0482	YCP4	0.248	1	0	AWRI796_1557	RET2	0.222	1	0
AWRI796_4697	YOR338W	0.248	1	0	AWRI796_4520	RGA1	0.222	1	0
AWRI796_4704	PYK2	0.248	1	0	AWRI796_4744	SAM3	0.222	1	0
AWRI796_0662	HEM25	0.247	1	0	AWRI796_0009	CNE1	0.221	1	0
AWRI796_4001	ATG4	0.247	1	0	AWRI796_1416	COX15	0.221	1	0
AWRI796_0720	SLC1	0.246	1	0	AWRI796_1946	SNG1	0.221	1	0
AWRI796_0833	YDR089W	0.246	1	0	AWRI796_0244	SPT7	0.22	1	0
AWRI796_0903	HSP42	0.246	1	0	AWRI796_0793	HEM13	0.22	1	0
AWRI796_0956	HEM1	0.246	1	0	AWRI796_1115	YDR415C	0.22	1	0
AWRI796_3173	RFU1	0.246	1	0	AWRI796_1658	RRT6	0.22	1	0
AWRI796_3306	BNA5	0.246	1	0	AWRI796_3277	NOP56	0.22	1	0
AWRI796_3714	EPO1	0.246	1	0	AWRI796_3560	RSE1	0.22	1	0
AWRI796_4025	YNL195C	0.246	1	0	AWRI796_3786	ERG2	0.22	1	0
AWRI796_2064	PRS3	0.245	1	0	AWRI796_4022	GCR2	0.22	1	0
AWRI796_3179	EMP46	0.245	1	0	AWRI796_4529	SIA1	0.22	1	0
AWRI796_5166	AAD4	0.245	1	0	AWRI796_0106	ILS1	0.219	1	0
AWRI796_1100	UTP5	0.244	1	0	AWRI796_0156	ACH1	0.218	1	0
AWRI796_1617	MDS3	0.244	1	0	AWRI796_0157	RRN6	0.218	1	0
AWRI796_1917	TIF4631	0.244	1	0	AWRI796_2763	FRE2	0.218	1	0
AWRI796_3089_90	AWRI796_3089_90	0.244	1	0	AWRI796_3835	ROY1	0.218	1	0
AWRI796_2663	TAH11	0.243	1	0	AWRI796_4155	BDP1	0.218	1	0
AWRI796_3320	RCK2	0.243	1	0	AWRI796_4450	WHI2	0.218	1	0
AWRI796_3550	NTE1	0.243	1	0	AWRI796_1139	YDR444W	0.217	1	0
AWRI796_3953	ERG24	0.243	1	0	AWRI796_2083	ARD1	0.217	1	0
AWRI796_0126	EDE1	0.241	1	0	AWRI796_2309	KGD1	0.217	1	0
AWRI796_1741	TIF4632	0.241	1	0	AWRI796_4202	RCF2	0.217	1	0
AWRI796_1912	PTI1	0.241	1	0	AWRI796_4638	VPH1	0.217	1	0

AWRI796 Gene ID	Gene Name	$\log_2$ Fold Change	Adj. p -value	Score	AWRI796 Gene ID	Gene Name	$\log_2$ Fold Change	Adj. p -value	Score
AWRI796_0502	SYP1	0.216	1	0	AWRI796_3188	ALT1	0.191	1	0
AWRI796_1748	HEM2	0.216	1	0	AWRI796_3663	NAT4	0.191	1	0
AWRI796_2367	VHR1	0.216	1	0	AWRI796_0295	MAK5	0.189	1	0
AWRI796_2907	ASK1	0.216	1	0	AWRI796_0411	RIF1	0.189	1	0
AWRI796_3171	RGR1	0.216	1	0	AWRI796_2908	YKL050C	0.189	1	0
AWRI796_3939	MRX6	0.216	1	0	AWRI796_1168	PHO8	0.188	1	0
AWRI796_0388	HIS7	0.215	1	0	AWRI796_2480	MNN5	0.188	1	0
AWRI796_1324	ERG28	0.215	1	0	AWRI796_2569	NET1	0.188	1	0
AWRI796_2773	UBA1	0.215	1	0	AWRI796_2861	GFA1	0.188	1	0
AWRI796_3081	HSP104	0.215	1	0	AWRI796_4517	UBP2	0.188	1	0
AWRI796_3685	UTP15	0.215	1	0	AWRI796_4615	PUS7	0.188	1	0
AWRI796_4325	TRM10	0.215	1	0	AWRI796_1364	AWRI796_1364	0.187	1	0
AWRI796_1458	PUG1	0.214	1	0	AWRI796_1952	ADE3	0.187	1	0
AWRI796_2107	PUT2	0.214	1	0	AWRI796_2118	YHK8	0.187	1	0
AWRI796_2193	ECM14	0.214	1	0	AWRI796_3267	SKG3	0.187	1	0
AWRI796_3042	UBP11	0.214	1	0	AWRI796_3700	MYO5	0.187	1	0
AWRI796_3573	NDC1	0.214	1	0	AWRI796_0499	NPP1	0.186	1	0
AWRI796_1701	LSG1	0.213	1	0	AWRI796_3175	RPL10	0.186	1	0
AWRI796_0170	RER2	0.212	1	0	AWRI796_0921	RVB1	0.185	1	0
AWRI796_2103	YHR033W	0.212	1	0	AWRI796_1863	TPC1	0.185	1	0
AWRI796_2990	UTH1	0.212	1	0	AWRI796_2094	THR1	0.185	1	0
AWRI796_3883	LCB1	0.212	1	0	AWRI796_3602	CDC5	0.185	1	0
AWRI796_1870	NOP7	0.211	1	0	AWRI796_3912	PEX6	0.185	1	0
AWRI796_2025	MAL33	0.211	1	0	AWRI796_1404	NSA2	0.184	1	0
AWRI796_2466	LAA1	0.211	1	0	AWRI796_1407	SAK1	0.184	1	0
AWRI796_3312	VPS34	0.211	1	0	AWRI796_1854	PIL1	0.184	1	0
AWRI796_3919	VNX1	0.211	1	0	AWRI796_2286	ESL1	0.184	1	0
AWRI796_3958	GOR1	0.21	1	0	AWRI796_2374	SYG1	0.184	1	0
AWRI796_4877	KAP120	0.21	1	0	AWRI796_4107	YNL095C	0.184	1	0
AWRI796_2978	SAP190	0.209	1	0	AWRI796_5015	ARP7	0.184	1	0
AWRI796_3212	MSL5	0.209	1	0	AWRI796_4689	SCD5	0.183	1	0
AWRI796_4085	NAF1	0.209	1	0	AWRI796_4725	MRS6	0.183	1	0
AWRI796_5160	AWRI796_5160	0.209	1	0	AWRI796_2097	DAP2	0.182	1	0
AWRI796_0819	TPS2	0.208	1	0	AWRI796_4890	GDE1	0.182	1	0
AWRI796_4193	NRM1	0.208	1	0	AWRI796_5013	SRO7	0.182	1	0
AWRI796_4934	PDR12	0.208	1	0	AWRI796_4521	ADE2	0.181	1	0
AWRI796_1046	MSN5	0.207	1	0	AWRI796_0639	LDB17	0.18	1	0
AWRI796_1692	CUE3	0.207	1	0	AWRI796_1164	SNF1	0.18	1	0
AWRI796_2370	MMF1	0.207	1	0	AWRI796_1891	SYF2	0.18	1	0
AWRI796_3013	GPT2	0.207	1	0	AWRI796_3396	DIC1	0.18	1	0
AWRI796_3231	NHA1	0.207	1	0	AWRI796_3925	EMW1	0.18	1	0
AWRI796_4618	ENV9	0.207	1	0	AWRI796_4948	ISM1	0.18	1	0
AWRI796_2182	SET1	0.206	1	0	AWRI796_3982	YNL247W	0.179	1	0
AWRI796_2934	SPT23	0.206	1	0	AWRI796_4612	ABP140	0.179	1	0
AWRI796_3738	IMP1	0.206	1	0	AWRI796_0626	CDC9	0.178	1	0
AWRI796_0568	BRE4	0.205	1	0	AWRI796_0955	COX20	0.178	1	0
AWRI796_0276	GRS1	0.204	1	0	AWRI796_1679	MON1	0.178	1	0
AWRI796_0395	RIB5	0.204	1	0	AWRI796_1997	RAD2	0.178	1	0
AWRI796_2299	OM45	0.204	1	0	AWRI796_2666	UTR1	0.178	1	0
AWRI796_2637	MET3	0.204	1	0	AWRI796_3674	NAM7	0.178	1	0
AWRI796_4595	STE13	0.204	1	0	AWRI796_5062	SYT1	0.178	1	0
AWRI796_1009	DPL1	0.203	1	0	AWRI796_0597	YDL199C	0.177	1	0
AWRI796_1967	PET54	0.203	1	0	AWRI796_2162	YHR097C	0.177	1	0
AWRI796_2504	SSY5	0.203	1	0	AWRI796_3119	PPR1	0.177	1	0
AWRI796_0128	COR1	0.202	1	0	AWRI796_1083	ARO10	0.176	1	0
AWRI796_0940	UPC2	0.202	1	0	AWRI796_1134	THI74	0.176	1	0
AWRI796_1337	FCY2	0.202	1	0	AWRI796_1271	VAC8	0.176	1	0
AWRI796_3012	CCP1	0.202	1	0	AWRI796_1766	ATE1	0.176	1	0
AWRI796_0387	ENP1	0.201	1	0	AWRI796_0491	CTO1	0.175	1	0
AWRI796_2256	AIM46	0.201	1	0	AWRI796_0918	YDR186C	0.175	1	0
AWRI796_2675	PTK2	0.201	1	0	AWRI796_2325	SEC24	0.175	1	0
AWRI796_2933	MAK11	0.201	1	0	AWRI796_3763	YMR178W	0.175	1	0
AWRI796_3354	GCD7	0.201	1	0	AWRI796_4061	GIM3	0.175	1	0
AWRI796_3593	SPT5	0.201	1	0	AWRI796_4983	ULA1	0.175	1	0
AWRI796_4536	PNO1	0.201	1	0	AWRI796_0406	BIT2	0.174	1	0
AWRI796_1612	POX1	0.2	1	0	AWRI796_3022	MSA2	0.174	1	0
AWRI796_2281	UBP7	0.2	1	0	AWRI796_3096	SOF1	0.174	1	0
AWRI796_3107	NOC3	0.2	1	0	AWRI796_3517	ARG81	0.174	1	0
AWRI796_4086	NMA111	0.2	1	0	AWRI796_1437	GCG1	0.173	1	0
AWRI796_4418	TSR3	0.2	1	0	AWRI796_2322	HOS4	0.173	1	0
AWRI796_3174	BUD20	0.199	1	0	AWRI796_2476	YJL193W	0.173	1	0
AWRI796_4339	AVO1	0.199	1	0	AWRI796_2758	AAD10	0.173	1	0
AWRI796_4446	HIR2	0.199	1	0	AWRI796_2093	MAS2	0.172	1	0
AWRI796_4952	PMA2	0.199	1	0	AWRI796_2491	TOH1	0.172	1	0
AWRI796_2332	XBP1	0.198	1	0	AWRI796_2963	PRY2	0.172	1	0
AWRI796_3829	RKR1	0.198	1	0	AWRI796_3157	SPT8	0.172	1	0
AWRI796_4739	YOR385W	0.198	1	0	AWRI796_3374	TAD3	0.172	1	0
AWRI796_1251	RAD23	0.197	1	0	AWRI796_4188	RPC34	0.172	1	0
AWRI796_1362	SER3	0.197	1	0	AWRI796_5080	RRG8	0.172	1	0
AWRI796_2411	CFD1	0.197	1	0	AWRI796_5110	TPO3	0.172	1	0
AWRI796_3272	HCR1	0.197	1	0	AWRI796_0516	RRT12	0.171	1	0
AWRI796_1899	VPS62	0.196	1	0	AWRI796_4769	RBD2	0.171	1	0
AWRI796_2110	BCD1	0.196	1	0	AWRI796_4931	ALD6	0.171	1	0
AWRI796_2262	SCH9	0.196	1	0	AWRI796_5140	RPC82	0.171	1	0
AWRI796_3680	VBA1	0.196	1	0	AWRI796_0783	PST2	0.17	1	0
AWRI796_0980	HSP78	0.195	1	0	AWRI796_2146	LAM4	0.17	1	0
AWRI796_2040	RPL8A	0.195	1	0	AWRI796_2320	POR2	0.17	1	0
AWRI796_2250	EGD2	0.195	1	0	AWRI796_4959	ERG10	0.17	1	0
AWRI796_2419	PAN1	0.195	1	0	AWRI796_4181	LST8	0.169	1	0
AWRI796_3395	KAP95	0.195	1	0	AWRI796_4900	MSY1	0.169	1	0
AWRI796_4464	YOR062C	0.195	1	0	AWRI796_4969	IRC15	0.169	1	0
AWRI796_0363	YBR220C	0.194	1	0	AWRI796_0914	CDC1	0.168	1	0
AWRI796_0696	RPP1A	0.194	1	0	AWRI796_1743	ALG13	0.168	1	0
AWRI796_4573	SPR1	0.194	1	0	AWRI796_3753	MME1	0.168	1	0
AWRI796_0029	FUN12	0.193	1	0	AWRI796_1621	IME4	0.167	1	0
AWRI796_0202	SCO1	0.193	1	0	AWRI796_3985	SLA2	0.167	1	0
AWRI796_2388	BCY1	0.193	1	0	AWRI796_3176	FMP25	0.166	1	0
AWRI796_2541	PRM10	0.193	1	0	AWRI796_3600	YML002W	0.166	1	0
AWRI796_3321	YEF3	0.193	1	0	AWRI796_4551	YRR1	0.166	1	0
AWRI796_4331	DUF1	0.193	1	0	AWRI796_5016	GLN1	0.166	1	0
AWRI796_0594	ACK1	0.192	1	0	AWRI796_5042	SPE3	0.166	1	0
AWRI796_4921	UBP16	0.192	1	0	AWRI796_1928	ERG1	0.165	1	0
AWRI796_5117	TIF3	0.192	1	0	AWRI796_2465	NUC1	0.165	1	0
AWRI796_0919	CCT6	0.191	1	0	AWRI796_2771	SAC1	0.165	1	0
AWRI796_2640	GPI14	0.191	1	0	AWRI796_2776	EMC3	0.165	1	0
AWRI796_2954	PAP1	0.191	1	0	AWRI796_3177	BOS1	0.165	1	0
AWRI796_3148	STU2	0.191	1	0	AWRI796_3887	ATM1	0.165	1	0

AWRI796 Gene ID	Gene Name	log_2 Fold Change	Adj. *p* -value	Score	AWRI796 Gene ID	Gene Name	log_2 Fold Change	Adj. *p* -value	Score
AWRI796_4599	DSC3	0.165	1	0	AWRI796_1943	XKS1	0.146	1	0
AWRI796_1868	PCP1	0.164	1	0	AWRI796_2397	RPB3	0.146	1	0
AWRI796_3477	FPR4	0.164	1	0	AWRI796_2687	NPA3	0.146	1	0
AWRI796_1481	MIL1	0.163	1	0	AWRI796_2774	STE6	0.146	1	0
AWRI796_1760	PIB2	0.163	1	0	AWRI796_4231	LYS9	0.146	1	0
AWRI796_1892	YGR130C	0.163	1	0	AWRI796_0147	NCL1	0.145	1	0
AWRI796_2089	DED81	0.163	1	0	AWRI796_0595	TRM8	0.145	1	0
AWRI796_2163	SFB3	0.163	1	0	AWRI796_1823	SCM4	0.145	1	0
AWRI796_3297	CCC1	0.163	1	0	AWRI796_3169	MEF1	0.145	1	0
AWRI796_3632	EIS1	0.163	1	0	AWRI796_5005	EAF3	0.145	1	0
AWRI796_4671	SLY41	0.163	1	0	AWRI796_0340	RIM2	0.144	1	0
AWRI796_0358	MET8	0.162	1	0	AWRI796_0484	YCR007C	0.144	1	0
AWRI796_0641	YDL144C	0.162	1	0	AWRI796_0620	UGA3	0.144	1	0
AWRI796_1568	ADH4	0.162	1	0	AWRI796_1297	BIM1	0.144	1	0
AWRI796_2946	LAC1	0.162	1	0	AWRI796_1993	ENO1	0.144	1	0
AWRI796_5115	SGV1	0.162	1	0	AWRI796_2154	RPF1	0.144	1	0
AWRI796_0353	KTR3	0.161	1	0	AWRI796_2251	MDM31	0.144	1	0
AWRI796_0659	UBP1	0.161	1	0	AWRI796_3852	YMR262W	0.144	1	0
AWRI796_2794	MTR2	0.161	1	0	AWRI796_4280	NOP8	0.144	1	0
AWRI796_3449	VPS36	0.161	1	0	AWRI796_0633	MSH5	0.143	1	0
AWRI796_4232	BRE5	0.161	1	0	AWRI796_1422	SCC4	0.143	1	0
AWRI796_0399	TAE1	0.16	1	0	AWRI796_1998	TNA1	0.143	1	0
AWRI796_0917	UPS3	0.16	1	0	AWRI796_2135	DYS1	0.143	1	0
AWRI796_1563	COS12	0.16	1	0	AWRI796_2826	AVT3	0.143	1	0
AWRI796_2023	BIO2	0.16	1	0	AWRI796_3150	FRE8	0.143	1	0
AWRI796_2577	MPM1	0.16	1	0	AWRI796_3545	TEM1	0.143	1	0
AWRI796_2650	GEA1	0.16	1	0	AWRI796_1625	TPN1	0.142	1	0
AWRI796_4665	BUD7	0.16	1	0	AWRI796_2454	AAD4	0.142	1	0
AWRI796_1469	RGD2	0.159	1	0	AWRI796_2956	YKR005C	0.141	1	0
AWRI796_2060	RPS20	0.159	1	0	AWRI796_3886	ADE4	0.141	1	0
AWRI796_3493	TUB3	0.159	1	0	AWRI796_4071	SRV2	0.141	1	0
AWRI796_3918	KRE1	0.159	1	0	AWRI796_4490	TMA46	0.141	1	0
AWRI796_4180	SIS1	0.159	1	0	AWRI796_0192	OLA1	0.14	1	0
AWRI796_2188	ANS1	0.158	1	0	AWRI796_1462	YPR204W	0.14	1	0
AWRI796_2375	MET30	0.158	1	0	AWRI796_2115	YHR045W	0.14	1	0
AWRI796_4911	ELP3	0.158	1	0	AWRI796_3747	YMR160W	0.14	1	0
AWRI796_1781	ERG26	0.157	1	0	AWRI796_1011	MHR1	0.139	1	0
AWRI796_2136	RRP4	0.157	1	0	AWRI796_3948	CUS2	0.139	1	0
AWRI796_2323	COX5B	0.157	1	0	AWRI796_4230	MSO1	0.139	1	0
AWRI796_3097	PSR1	0.157	1	0	AWRI796_4461	LPL1	0.139	1	0
AWRI796_3650	STV1	0.157	1	0	AWRI796_5030	SEC8	0.139	1	0
AWRI796_3775	SGS1	0.157	1	0	AWRI796_0661	YFH1	0.138	1	0
AWRI796_0805	TGL2	0.156	1	0	AWRI796_0780	VPS54	0.138	1	0
AWRI796_0866	SAC6	0.156	1	0	AWRI796_1054	MRP1	0.138	1	0
AWRI796_2333	SGA1	0.156	1	0	AWRI796_1059	YPQ2	0.138	1	0
AWRI796_2553	KHA1	0.156	1	0	AWRI796_1298	AFG3	0.138	1	0
AWRI796_3031	PRP16	0.156	1	0	AWRI796_2748	RPS4B	0.138	1	0
AWRI796_4341	MDM20	0.156	1	0	AWRI796_2779	EAP1	0.138	1	0
AWRI796_4374	NOP12	0.156	1	0	AWRI796_2982	DAL80	0.138	1	0
AWRI796_4650	RDL1	0.156	1	0	AWRI796_3159	MNL2	0.138	1	0
AWRI796_0764	SOK1	0.155	1	0	AWRI796_3227	PDC5	0.138	1	0
AWRI796_3752	PAH1	0.155	1	0	AWRI796_3973	FOL1	0.138	1	0
AWRI796_4124	IMP4	0.155	1	0	AWRI796_0825	VPS41	0.137	1	0
AWRI796_4142	MSG5	0.155	1	0	AWRI796_0857	TRM1	0.137	1	0
AWRI796_4859	PXA1	0.155	1	0	AWRI796_1542	QCR6	0.137	1	0
AWRI796_0053	SWC3	0.154	1	0	AWRI796_3937	CLA4	0.137	1	0
AWRI796_1948	PMT6	0.154	1	0	AWRI796_4197	PHO91	0.137	1	0
AWRI796_2180	TOM71	0.154	1	0	AWRI796_0083	SEA4	0.136	1	0
AWRI796_3005	TIF1	0.154	1	0	AWRI796_0321	NPL4	0.136	1	0
AWRI796_4068	MEP2	0.154	1	0	AWRI796_0635	RPC53	0.136	1	0
AWRI796_4556	GLN4	0.154	1	0	AWRI796_1378	PRS2	0.136	1	0
AWRI796_4896	FMP30	0.154	1	0	AWRI796_2157	MSR1	0.136	1	0
AWRI796_0047	PSK1	0.153	1	0	AWRI796_2580	LAS21	0.136	1	0
AWRI796_0066	BUD14	0.153	1	0	AWRI796_2622	NOP9	0.136	1	0
AWRI796_1049	YDR338C	0.153	1	0	AWRI796_2701	JSN1	0.136	1	0
AWRI796_2679	RPA12	0.153	1	0	AWRI796_2004	FOL2	0.135	1	0
AWRI796_4413	RRP6	0.153	1	0	AWRI796_4053	CBK1	0.135	1	0
AWRI796_1202	SPS1	0.152	1	0	AWRI796_4808	HRR25	0.135	1	0
AWRI796_1222	DLD3	0.152	1	0	AWRI796_4856	YPL150W	0.135	1	0
AWRI796_1489	BST1	0.152	1	0	AWRI796_4904	NOG1	0.135	1	0
AWRI796_1740	TYW3	0.152	1	0	AWRI796_4949	YPL039W	0.135	1	0
AWRI796_3399	YLR352W	0.152	1	0	AWRI796_0779	NSI1	0.134	1	0
AWRI796_3506	COQ5	0.152	1	0	AWRI796_2523	YJL132W	0.134	1	0
AWRI796_3684	AIP1	0.152	1	0	AWRI796_4136	NOP2	0.134	1	0
AWRI796_4106	PHO23	0.152	1	0	AWRI796_0323	SMY2	0.133	1	0
AWRI796_0786	ARO3	0.151	1	0	AWRI796_1142	UTP6	0.133	1	0
AWRI796_1249	CYC7	0.151	1	0	AWRI796_1405	LCP5	0.133	1	0
AWRI796_2068	STE20	0.151	1	0	AWRI796_1510	DEG1	0.133	1	0
AWRI796_2338	LYS12	0.151	1	0	AWRI796_3298	UTP13	0.133	1	0
AWRI796_2576	YJL068C	0.151	1	0	AWRI796_3615	SEC59	0.133	1	0
AWRI796_2692	MIR1	0.151	1	0	AWRI796_3890	UBP15	0.133	1	0
AWRI796_3071	ENT4	0.151	1	0	AWRI796_3993	YNL234W	0.133	1	0
AWRI796_3410	MDM30	0.151	1	0	AWRI796_4717	PDE2	0.133	1	0
AWRI796_4363	AIM39	0.151	1	0	AWRI796_0201	CSG2	0.132	1	0
AWRI796_2077	ERG11	0.15	1	0	AWRI796_0403	REI1	0.132	1	0
AWRI796_2230	NMD3	0.15	1	0	AWRI796_0776	FAL1	0.132	1	0
AWRI796_2409	YIA6	0.15	1	0	AWRI796_1005	RTT103	0.132	1	0
AWRI796_2552	BCK1	0.15	1	0	AWRI796_2226	CDC23	0.132	1	0
AWRI796_2912	DCW1	0.15	1	0	AWRI796_2390	SSM4	0.132	1	0
AWRI796_2987	KAE1	0.15	1	0	AWRI796_1182	PUF6	0.131	1	0
AWRI796_1269	NPP2	0.149	1	0	AWRI796_1909	RSR1	0.131	1	0
AWRI796_1474	FET5	0.149	1	0	AWRI796_1951	PCT1	0.131	1	0
AWRI796_3526	TUB1	0.149	1	0	AWRI796_2517	RPB4	0.131	1	0
AWRI796_0521	RSC6	0.148	1	0	AWRI796_2927	TCD2	0.131	1	0
AWRI796_0535	SSK22	0.148	1	0	AWRI796_4112	RHO2	0.131	1	0
AWRI796_1545	RSC8	0.148	1	0	AWRI796_4216	ABZ1	0.131	1	0
AWRI796_3026	RPF2	0.148	1	0	AWRI796_1016	CFT1	0.13	1	0
AWRI796_3217	YPS3	0.148	1	0	AWRI796_1244	IES6	0.13	1	0
AWRI796_4771	HUT1	0.148	1	0	AWRI796_2837	YKL133C	0.13	1	0
AWRI796_2114	DOG1	0.147	1	0	AWRI796_4525	VPS17	0.13	1	0
AWRI796_2424	STS1	0.147	1	0	AWRI796_0107	SSA3	0.129	1	0
AWRI796_2479	SWE1	0.147	1	0	AWRI796_1281	IRC22	0.129	1	0
AWRI796_4581	MRM1	0.147	1	0	AWRI796_1406	VFA1	0.129	1	0
AWRI796_4917	ATP4	0.147	1	0	AWRI796_1684	COQ8	0.129	1	0
AWRI796_5128	DPB2	0.147	1	0	AWRI796_1925	YIP1	0.129	1	0
AWRI796_0533	CPR4	0.146	1	0	AWRI796_3614	CLU1	0.129	1	0
AWRI796_0870	CCW12	0.146	1	0	AWRI796_4468	MSA1	0.129	1	0

AWRI796 Gene ID	Gene Name	log_2 Fold Change	Adj. *p* -value	Score	AWRI796 Gene ID	Gene Name	log_2 Fold Change	Adj. *p* -value	Score
AWRI796_0227	YBR063C	0.128	1	0	AWRI796_4463	CKA2	0.111	1	0
AWRI796_0354	FTH1	0.128	1	0	AWRI796_4482	TGL5	0.111	1	0
AWRI796_0993	DON1	0.128	1	0	AWRI796_0415	SAF1	0.11	1	0
AWRI796_1744	RIM8	0.128	1	0	AWRI796_1512	NIC96	0.11	1	0
AWRI796_2203	CHS7	0.128	1	0	AWRI796_1529	AWRI796_1529	0.11	1	0
AWRI796_2221	YAP1801	0.128	1	0	AWRI796_2046	RIM101	0.11	1	0
AWRI796_2496	TPK1	0.128	1	0	AWRI796_2433	SEC11	0.11	1	0
AWRI796_2668	OSM1	0.128	1	0	AWRI796_1538	PTR3	0.109	1	0
AWRI796_4964	RAD1	0.128	1	0	AWRI796_1840	ROM1	0.109	1	0
AWRI796_1524	CMK1	0.127	1	0	AWRI796_2376	PIG2	0.109	1	0
AWRI796_2001	SAY1	0.127	1	0	AWRI796_2870	YJU3	0.109	1	0
AWRI796_3832	YMR252C	0.127	1	0	AWRI796_4649	YOR283W	0.109	1	0
AWRI796_0314	TOS1	0.126	1	0	AWRI796_5108	PIN3	0.109	1	0
AWRI796_1132	PPZ2	0.126	1	0	AWRI796_0728	SIR2	0.108	1	0
AWRI796_1315	EDC2	0.126	1	0	AWRI796_0848	YDR109C	0.108	1	0
AWRI796_2080	TDA3	0.126	1	0	AWRI796_1707	SPC105	0.108	1	0
AWRI796_2192	YHR131C	0.126	1	0	AWRI796_1867	MDR1	0.108	1	0
AWRI796_2362	EFM4	0.126	1	0	AWRI796_2245	GPI16	0.108	1	0
AWRI796_5139	SKI3	0.126	1	0	AWRI796_3009	LAS1	0.108	1	0
AWRI796_1637	ROK1	0.125	1	0	AWRI796_3125	YEH2	0.108	1	0
AWRI796_3431	ART10	0.125	1	0	AWRI796_0072	UIP3	0.107	1	0
AWRI796_4562	HEM15	0.125	1	0	AWRI796_0566	GYP7	0.107	1	0
AWRI796_1018	CPR5	0.124	1	0	AWRI796_2562	ALY2	0.107	1	0
AWRI796_1245	YEL043W	0.124	1	0	AWRI796_3216	YPS1	0.107	1	0
AWRI796_1628	GTS1	0.124	1	0	AWRI796_3322	SSP120	0.107	1	0
AWRI796_3870	GPI12	0.124	1	0	AWRI796_3458	TDA5	0.107	1	0
AWRI796_4037	IPI3	0.124	1	0	AWRI796_3785	RAD14	0.107	1	0
AWRI796_4684	PRO2	0.124	1	0	AWRI796_4251	PDR18	0.107	1	0
AWRI796_5048	OPY2	0.124	1	0	AWRI796_4629	RPT4	0.107	1	0
AWRI796_1144	PPN1	0.123	1	0	AWRI796_0946	GTB1	0.106	1	0
AWRI796_2772	TRP3	0.123	1	0	AWRI796_5214	YCR102C	0.106	1	0
AWRI796_2792	PXA2	0.123	1	0	AWRI796_0419	YBR284W	0.105	1	0
AWRI796_3316	MAP1	0.123	1	0	AWRI796_0652	CDC53	0.105	1	0
AWRI796_3356	GSP1	0.123	1	0	AWRI796_0753	PTC1	0.105	1	0
AWRI796_3073	GRC3	0.122	1	0	AWRI796_1069	ESF1	0.105	1	0
AWRI796_3742	YMR155W	0.122	1	0	AWRI796_2654	RAD26	0.105	1	0
AWRI796_3799	GAS3	0.122	1	0	AWRI796_3713	PKR1	0.105	1	0
AWRI796_4781	SSO1	0.122	1	0	AWRI796_3796	EFR3	0.105	1	0
AWRI796_0101	ALG3	0.121	1	0	AWRI796_1537	CDC14	0.104	1	0
AWRI796_0379	ERT1	0.121	1	0	AWRI796_2021	ERV29	0.104	1	0
AWRI796_2386	CKA1	0.121	1	0	AWRI796_2293	SSL2	0.104	1	0
AWRI796_0309	ICS2	0.12	1	0	AWRI796_2473	UBP12	0.104	1	0
AWRI796_1240	RML2	0.12	1	0	AWRI796_2985	CAF4	0.104	1	0
AWRI796_4908	RLM1	0.12	1	0	AWRI796_3465	TSR2	0.104	1	0
AWRI796_5129	BET2	0.12	1	0	AWRI796_4208	MPP6	0.104	1	0
AWRI796_0390	SPO23	0.119	1	0	AWRI796_4215	PPG1	0.104	1	0
AWRI796_1539	MET10	0.119	1	0	AWRI796_4977	RQC2	0.104	1	0
AWRI796_2657	GEF1	0.119	1	0	AWRI796_0122	TOD6	0.103	1	0
AWRI796_4149	YNL046W	0.119	1	0	AWRI796_0311	IFA38	0.103	1	0
AWRI796_4666	RAX1	0.119	1	0	AWRI796_0699	MDH3	0.103	1	0
AWRI796_5017	VMA13	0.119	1	0	AWRI796_1007	SRP101	0.103	1	0
AWRI796_1426	UBP3	0.118	1	0	AWRI796_1445	RAD3	0.103	1	0
AWRI796_1543	PHO4	0.118	1	0	AWRI796_1626	YGL185C	0.103	1	0
AWRI796_1751	PNC1	0.118	1	0	AWRI796_2308	STH1	0.103	1	0
AWRI796_1762	ALK1	0.118	1	0	AWRI796_2997	TRK2	0.103	1	0
AWRI796_1813	CAX4	0.118	1	0	AWRI796_3264	SWI6	0.103	1	0
AWRI796_2132	RRP3	0.118	1	0	AWRI796_4218	ARC35	0.103	1	0
AWRI796_2844	RRN3	0.118	1	0	AWRI796_4550	PNS1	0.103	1	0
AWRI796_3972	SIP3	0.118	1	0	AWRI796_4639	FSF1	0.103	1	0
AWRI796_4606	MKK1	0.118	1	0	AWRI796_0038	DRS2	0.102	1	0
AWRI796_5014	HTS1	0.118	1	0	AWRI796_1646	AIM14	0.102	1	0
AWRI796_5237	AIF1	0.118	1	0	AWRI796_1681	NAB2	0.102	1	0
AWRI796_0149	PIM1	0.117	1	0	AWRI796_2801	COY1	0.102	1	0
AWRI796_0489	PGK1	0.117	1	0	AWRI796_2810	KKQ8	0.102	1	0
AWRI796_1225	HPA3	0.117	1	0	AWRI796_3039	MLP1	0.102	1	0
AWRI796_1663	HUL5	0.117	1	0	AWRI796_4424	YOR012W	0.102	1	0
AWRI796_3113	PAM18	0.117	1	0	AWRI796_4968	CTF19	0.102	1	0
AWRI796_3497	YML119W	0.117	1	0	AWRI796_5118	MMS1	0.102	1	0
AWRI796_4716	VTS1	0.117	1	0	AWRI796_0520	YCR051W	0.101	1	0
AWRI796_4840	MRX4	0.117	1	0	AWRI796_0663	CYK3	0.101	1	0
AWRI796_0171	COQ1	0.116	1	0	AWRI796_1020	PMT7	0.101	1	0
AWRI796_2767	URA1	0.116	1	0	AWRI796_1038	YSP2	0.101	1	0
AWRI796_4054	YGP1	0.116	1	0	AWRI796_2276	YIL161W	0.101	1	0
AWRI796_4266	IMA4	0.116	1	0	AWRI796_2700	GRR1	0.101	1	0
AWRI796_4894	SYH1	0.116	1	0	AWRI796_4519	IAH1	0.101	1	0
AWRI796_1483	HAC1	0.115	1	0	AWRI796_0118	SHP1	0.1	1	0
AWRI796_1788	ECT1	0.115	1	0	AWRI796_0342	AIM4	0.1	1	0
AWRI796_2050	SNF6	0.115	1	0	AWRI796_1507	VTC2	0.1	1	0
AWRI796_2751	BAT2	0.115	1	0	AWRI796_1551	DUG1	0.1	1	0
AWRI796_4376	RPP2A	0.115	1	0	AWRI796_1779	CDH1	0.1	1	0
AWRI796_4686	MYO2	0.115	1	0	AWRI796_2145	IRE1	0.1	1	0
AWRI796_4779	VMA11	0.115	1	0	AWRI796_2932	CDC16	0.1	1	0
AWRI796_3673	SEC14	0.114	1	0	AWRI796_3035	PXL1	0.1	1	0
AWRI796_3795	DML1	0.114	1	0	AWRI796_4314	WSC3	0.1	1	0
AWRI796_4007	YNL217W	0.114	1	0	AWRI796_4799	THI6	0.1	1	0
AWRI796_4411	IZH2	0.114	1	0	AWRI796_0086	ECM21	0.099	1	0
AWRI796_4657	YOR292C	0.114	1	0	AWRI796_0410	CHK1	0.099	1	0
AWRI796_0407	EFM2	0.113	1	0	AWRI796_0742	GPD1	0.099	1	0
AWRI796_0508	PHO87	0.113	1	0	AWRI796_1789	SEC9	0.099	1	0
AWRI796_0889	HOM2	0.113	1	0	AWRI796_2497	YJL163C	0.099	1	0
AWRI796_0960	FMN1	0.113	1	0	AWRI796_3457	TUS1	0.099	1	0
AWRI796_1166	PEX29	0.113	1	0	AWRI796_3750	INP2	0.099	1	0
AWRI796_4381	OPI10	0.113	1	0	AWRI796_3892	FKS3	0.099	1	0
AWRI796_5079	RGC1	0.113	1	0	AWRI796_0838	GRX3	0.098	1	0
AWRI796_0367	YBR225W	0.112	1	0	AWRI796_0974	BTT1	0.098	1	0
AWRI796_0686	PMT5	0.112	1	0	AWRI796_1336	HIS1	0.098	1	0
AWRI796_1235	POL5	0.112	1	0	AWRI796_2069	MRP4	0.098	1	0
AWRI796_1944	SKI6	0.112	1	0	AWRI796_2129	RPP1	0.098	1	0
AWRI796_3054	GTT2	0.112	1	0	AWRI796_2655	HUL4	0.098	1	0
AWRI796_3198	ICT1	0.112	1	0	AWRI796_3662	AVO2	0.098	1	0
AWRI796_3237	RMP1	0.112	1	0	AWRI796_4761	BBP1	0.098	1	0
AWRI796_3617	ERG5	0.112	1	0	AWRI796_4774	HSP82	0.098	1	0
AWRI796_4594	RFC1	0.112	1	0	AWRI796_1756	SCW11	0.097	1	0
AWRI796_1154	SPP41	0.111	1	0	AWRI796_3710	ASI1	0.097	1	0
AWRI796_3273	UPS1	0.111	1	0	AWRI796_4552	DDP1	0.097	1	0
AWRI796_3281	MSS51	0.111	1	0	AWRI796_4600	RPB8	0.097	1	0
AWRI796_3983	VPS75	0.111	1	0	AWRI796_4719	PRE10	0.097	1	0

AWRI796 Gene ID	Gene Name	$\log_2$ Fold Change	Adj. p -value	Score	AWRI796 Gene ID	Gene Name	$\log_2$ Fold Change	Adj. p -value	Score
AWRI796_5202	YRF1-7	0.097	1	0	AWRI796_4163	HDA1	0.08	1	0
AWRI796_1595	VRG4	0.096	1	0	AWRI796_5061	ASR1	0.08	1	0
AWRI796_3435	AFG2	0.096	1	0	AWRI796_5268	FLP1	0.08	1	0
AWRI796_4755	FUM1	0.096	1	0	AWRI796_1610	SPT16	0.079	1	0
AWRI796_0271	RAD16	0.095	1	0	AWRI796_1945	FYV8	0.079	1	0
AWRI796_1791	YGR012W	0.095	1	0	AWRI796_4099	LEU4	0.079	1	0
AWRI796_1901	SKN1	0.095	1	0	AWRI796_4184	PET8	0.079	1	0
AWRI796_2312	POG1	0.095	1	0	AWRI796_4453	RAT1	0.079	1	0
AWRI796_3124	PSR2	0.095	1	0	AWRI796_0628	DHH1	0.078	1	0
AWRI796_3420	CSR1	0.095	1	0	AWRI796_1923	PSD2	0.078	1	0
AWRI796_4212	YNR029C	0.095	1	0	AWRI796_3478	HMG2	0.078	1	0
AWRI796_4219	MRPS12	0.095	1	0	AWRI796_0746	CDC7	0.077	1	0
AWRI796_4834	NIP100	0.095	1	0	AWRI796_1242	AWRI796_1242	0.077	1	0
AWRI796_4943	CAM1	0.095	1	0	AWRI796_1382	SSA4	0.077	1	0
AWRI796_1333	HOM3	0.094	1	0	AWRI796_2764	COS9	0.077	1	0
AWRI796_2790	CNB1	0.094	1	0	AWRI796_3416	STP3	0.077	1	0
AWRI796_3575	USA1	0.094	1	0	AWRI796_1252	ANP1	0.076	1	0
AWRI796_4306	PTH4	0.094	1	0	AWRI796_1434	BUR6	0.076	1	0
AWRI796_4617	DGA1	0.094	1	0	AWRI796_2594	UBX6	0.076	1	0
AWRI796_4683	LDB19	0.094	1	0	AWRI796_2734	STR2	0.076	1	0
AWRI796_0143	PET9	0.093	1	0	AWRI796_3087	KNS1	0.076	1	0
AWRI796_0332	YPC1	0.093	1	0	AWRI796_3377	MMS22	0.076	1	0
AWRI796_0637	NOP14	0.093	1	0	AWRI796_4664	MBF1	0.076	1	0
AWRI796_1045	SWR1	0.093	1	0	AWRI796_0859	KIN1	0.075	1	0
AWRI796_1330	TPA1	0.093	1	0	AWRI796_1851	GCD2	0.075	1	0
AWRI796_2055	OPI1	0.093	1	0	AWRI796_3387	SGD1	0.075	1	0
AWRI796_2237	AWRI796_2237	0.093	1	0	AWRI796_3964	PIK1	0.075	1	0
AWRI796_2619	CCT3	0.093	1	0	AWRI796_2261	MNL1	0.074	1	0
AWRI796_2966	MIC60	0.093	1	0	AWRI796_3324	MCP2	0.074	1	0
AWRI796_4204	ATP23	0.093	1	0	AWRI796_3741	RIM13	0.074	1	0
AWRI796_0042	FUN26	0.092	1	0	AWRI796_4213	ALG12	0.074	1	0
AWRI796_0110	AST1	0.092	1	0	AWRI796_4604	WTM2	0.074	1	0
AWRI796_0840	TVP15	0.092	1	0	AWRI796_0505	FEN1	0.074	1	0
AWRI796_1698	RPL28	0.092	1	0	AWRI796_0135	APL3	0.073	1	0
AWRI796_2414	SGN1	0.092	1	0	AWRI796_0718	MCH1	0.073	1	0
AWRI796_5146	SGE1	0.092	1	0	AWRI796_2104	PIH1	0.073	1	0
AWRI796_0806	MAK21	0.091	1	0	AWRI796_2144	YHR078W	0.073	1	0
AWRI796_1519	GCN20	0.091	1	0	AWRI796_2259	YHR202W	0.073	1	0
AWRI796_2172	GGA2	0.091	1	0	AWRI796_2378	CBR1	0.073	1	0
AWRI796_2770	DOA1	0.091	1	0	AWRI796_3182	EMP70	0.073	1	0
AWRI796_2818	APE2	0.091	1	0	AWRI796_4238	BIO4	0.073	1	0
AWRI796_4370	PSK2	0.091	1	0	AWRI796_4783	USV1	0.073	1	0
AWRI796_1897	TPO2	0.09	1	0	AWRI796_4797	YPL216W	0.073	1	0
AWRI796_2949	AUR1	0.09	1	0	AWRI796_1250	UTR4	0.072	1	0
AWRI796_3235	DPH6	0.09	1	0	AWRI796_1589	TAN1	0.072	1	0
AWRI796_4815	APL5	0.09	1	0	AWRI796_1757	CWH41	0.072	1	0
AWRI796_0556	YCR099C	0.089	1	0	AWRI796_2019	BGL2	0.072	1	0
AWRI796_2096	RPN1	0.089	1	0	AWRI796_2199	ARO9	0.072	1	0
AWRI796_2420	EGH1	0.089	1	0	AWRI796_3991	YTP1	0.072	1	0
AWRI796_2717	CPA2	0.089	1	0	AWRI796_0693	YDL086W	0.071	1	0
AWRI796_3105	DNM1	0.089	1	0	AWRI796_0892	ACL4	0.071	1	0
AWRI796_4108	APP1	0.089	1	0	AWRI796_3532	CPR3	0.071	1	0
AWRI796_0529	HCM1	0.088	1	0	AWRI796_4869	ODC1	0.071	1	0
AWRI796_0578	DTD1	0.088	1	0	AWRI796_0392	DUT1	0.07	1	0
AWRI796_2234	FMO1	0.088	1	0	AWRI796_0849	FOB1	0.07	1	0
AWRI796_3134	RPL15A	0.088	1	0	AWRI796_0904	SUP35	0.07	1	0
AWRI796_3542	ERV41	0.088	1	0	AWRI796_0574	WHI4	0.069	1	0
AWRI796_4198	YNR014W	0.088	1	0	AWRI796_1301	GPA2	0.069	1	0
AWRI796_1937	TFG1	0.087	1	0	AWRI796_1554	BNA6	0.069	1	0
AWRI796_3817	RNA1	0.087	1	0	AWRI796_2339	RSM25	0.069	1	0
AWRI796_3833	YMR253C	0.087	1	0	AWRI796_2636	TDH2	0.069	1	0
AWRI796_4359	YOL057W	0.087	1	0	AWRI796_3598	GLO1	0.069	1	0
AWRI796_5026	ATG11	0.087	1	0	AWRI796_3989	LAP3	0.069	1	0
AWRI796_5152	AWRI796_5152	0.087	1	0	AWRI796_4459	NOB1	0.069	1	0
AWRI796_2474	ELO1	0.086	1	0	AWRI796_4473	SGO1	0.069	1	0
AWRI796_3419	SEC61	0.086	1	0	AWRI796_4530	RUP1	0.069	1	0
AWRI796_3544	ORC1	0.086	1	0	AWRI796_0279	PTC4	0.068	1	0
AWRI796_4682	PMT3	0.086	1	0	AWRI796_0671	YDL109C	0.068	1	0
AWRI796_5004	SDD4	0.086	1	0	AWRI796_0968	MNN10	0.068	1	0
AWRI796_0357	NGR1	0.085	1	0	AWRI796_1120	ARO80	0.068	1	0
AWRI796_0791	YDR042C	0.085	1	0	AWRI796_1826	YGR054W	0.068	1	0
AWRI796_0828	RRP8	0.085	1	0	AWRI796_2379	PKP1	0.068	1	0
AWRI796_1478	TUB2	0.085	1	0	AWRI796_2710	RSM26	0.068	1	0
AWRI796_3402	ILV5	0.085	1	0	AWRI796_3861	SCS7	0.068	1	0
AWRI796_3789	PFK2	0.085	1	0	AWRI796_4049	BNI5	0.068	1	0
AWRI796_4724	RPS12	0.085	1	0	AWRI796_4288	BSC6	0.068	1	0
AWRI796_5019	TIP41	0.085	1	0	AWRI796_0183	YBR016W	0.067	1	0
AWRI796_1088	EFT2	0.084	1	0	AWRI796_1869	GTF1	0.067	1	0
AWRI796_2078	YHR007C-A	0.084	1	0	AWRI796_1983	LSC2	0.067	1	0
AWRI796_2133	SSF1	0.084	1	0	AWRI796_2461	YJL213W	0.067	1	0
AWRI796_2823	MCR1	0.084	1	0	AWRI796_3348	NNT1	0.067	1	0
AWRI796_3063	LDB18	0.084	1	0	AWRI796_4310	SHR5	0.067	1	0
AWRI796_0296	SUP45	0.083	1	0	AWRI796_0093	MAP2	0.066	1	0
AWRI796_2403	MNT3	0.083	1	0	AWRI796_0653	LYS21	0.066	1	0
AWRI796_2457	DAK2	0.083	1	0	AWRI796_0740	RTK1	0.066	1	0
AWRI796_4901	PNG1	0.083	1	0	AWRI796_1056	YPS7	0.066	1	0
AWRI796_0288	CKS1	0.082	1	0	AWRI796_2024	IMA1	0.066	1	0
AWRI796_0445	YCL049C	0.082	1	0	AWRI796_2065	ETP1	0.066	1	0
AWRI796_0855	APC4	0.082	1	0	AWRI796_2566	SCP160	0.066	1	0
AWRI796_1599	NIF3	0.082	1	0	AWRI796_3226	CKI1	0.066	1	0
AWRI796_3376	BUD6	0.082	1	0	AWRI796_3265	TOS4	0.066	1	0
AWRI796_4780	NSL1	0.082	1	0	AWRI796_3825	ZRC1	0.066	1	0
AWRI796_4838	DAP1	0.082	1	0	AWRI796_4129	RPL16B	0.066	1	0
AWRI796_0060	TFC3	0.081	1	0	AWRI796_4152	BOP3	0.066	1	0
AWRI796_0345	YBR197C	0.081	1	0	AWRI796_2518	YUR1	0.065	1	0
AWRI796_1629	ATG1	0.081	1	0	AWRI796_2880	RRP14	0.065	1	0
AWRI796_2042	GOS1	0.081	1	0	AWRI796_2976	GCN3	0.065	1	0
AWRI796_2883	SMY1	0.081	1	0	AWRI796_3579	YML6	0.065	1	0
AWRI796_4002	SSU72	0.081	1	0	AWRI796_4156	GPI15	0.065	1	0
AWRI796_0051	DEP1	0.08	1	0	AWRI796_4814	OXR1	0.065	1	0
AWRI796_0808	LCB2	0.08	1	0	AWRI796_4898	ATG21	0.065	1	0
AWRI796_0885	GIR2	0.08	1	0	AWRI796_5060	NVJ2	0.065	1	0
AWRI796_2317	PRM5	0.08	1	0	AWRI796_0336	GDT1	0.064	1	0
AWRI796_2510	RPA34	0.08	1	0	AWRI796_2673	YJR056C	0.064	1	0
AWRI796_2960	FOX2	0.08	1	0	AWRI796_3501	VAN1	0.064	1	0
AWRI796_3114	RLP24	0.08	1	0	AWRI796_3589	TRM9	0.064	1	0
AWRI796_3540	POB3	0.08	1	0	AWRI796_3638	CCS1	0.064	1	0

AWRI796 Gene ID	Gene Name	log_2 Fold Change	Adj. *p* -value	Score	AWRI796 Gene ID	Gene Name	log_2 Fold Change	Adj. *p* -value	Score
AWRI796_3692	MUB1	0.064	1	0	AWRI796_1591	SAP4	0.05	1	0
AWRI796_3749	DNF3	0.064	1	0	AWRI796_1700	SEH1	0.05	1	0
AWRI796_3804	ERG8	0.064	1	0	AWRI796_2659	NUP85	0.05	1	0
AWRI796_4765	ATG41	0.064	1	0	AWRI796_3045	SIR1	0.05	1	0
AWRI796_4882	DBP1	0.064	1	0	AWRI796_3527	YML083C	0.05	1	0
AWRI796_0193	ETR1	0.063	1	0	AWRI796_4091	DMA2	0.05	1	0
AWRI796_2081	DIA4	0.063	1	0	AWRI796_4909	YPL088W	0.05	1	0
AWRI796_2134	HTD2	0.063	1	0	AWRI796_0088	BNA4	0.049	1	0
AWRI796_2629	MPP10	0.063	1	0	AWRI796_0412	PPS1	0.049	1	0
AWRI796_3120	BRE2	0.063	1	0	AWRI796_0765	TRP1	0.049	1	0
AWRI796_3160	SHM2	0.063	1	0	AWRI796_4328	MSH2	0.049	1	0
AWRI796_4913	BRO1	0.063	1	0	AWRI796_4626	TRE2	0.049	1	0
AWRI796_0307	CNS1	0.062	1	0	AWRI796_0270	CYC8	0.048	1	0
AWRI796_0547	ABP1	0.062	1	0	AWRI796_0475	SGF29	0.048	1	0
AWRI796_0584	NOP6	0.062	1	0	AWRI796_1286	YND1	0.048	1	0
AWRI796_1358	MRX1	0.062	1	0	AWRI796_1622	CDC55	0.048	1	0
AWRI796_2340	YIL092W	0.062	1	0	AWRI796_3452	URA4	0.048	1	0
AWRI796_2499	FMP33	0.062	1	0	AWRI796_4674	DGK1	0.048	1	0
AWRI796_2916	VPS24	0.062	1	0	AWRI796_4807	PGC1	0.048	1	0
AWRI796_4183	HRB1	0.062	1	0	AWRI796_0008	ECM1	0.047	1	0
AWRI796_4284	PPM2	0.062	1	0	AWRI796_0478	LDB16	0.047	1	0
AWRI796_4322	COQ3	0.062	1	0	AWRI796_0544	TUP1	0.047	1	0
AWRI796_4585	NOC2	0.062	1	0	AWRI796_0658	YDL124W	0.047	1	0
AWRI796_4694	ALA1	0.062	1	0	AWRI796_1775	PMA1	0.047	1	0
AWRI796_0040	LTE1	0.061	1	0	AWRI796_1793	MSB2	0.047	1	0
AWRI796_0473	BUD3	0.061	1	0	AWRI796_2412	INP51	0.047	1	0
AWRI796_0532	ATG15	0.061	1	0	AWRI796_2785	MIA40	0.047	1	0
AWRI796_0925	REF2	0.061	1	0	AWRI796_2895	YET1	0.047	1	0
AWRI796_1084	YRA1	0.061	1	0	AWRI796_4828	TCO89	0.047	1	0
AWRI796_1163	YDR476C	0.061	1	0	AWRI796_5126	VPS4	0.047	1	0
AWRI796_2579	MRPL8	0.061	1	0	AWRI796_0409	UBX7	0.046	1	0
AWRI796_3147	PDC1	0.061	1	0	AWRI796_0497	YCR023C	0.046	1	0
AWRI796_4009	IES2	0.061	1	0	AWRI796_0588	CWC2	0.046	1	0
AWRI796_4270_71	AWRI796_4270_71	0.061	1	0	AWRI796_1004	NSE3	0.046	1	0
AWRI796_4736	FIT2	0.061	1	0	AWRI796_1085	RPP2B	0.046	1	0
AWRI796_4897	ELP4	0.061	1	0	AWRI796_1431	YER156C	0.046	1	0
AWRI796_0394	MTC4	0.06	1	0	AWRI796_1965	CRM1	0.046	1	0
AWRI796_0611	YDL180W	0.06	1	0	AWRI796_2176	APE4	0.046	1	0
AWRI796_1425	SPI1	0.06	1	0	AWRI796_2178	DMA1	0.046	1	0
AWRI796_1672	SNT2	0.06	1	0	AWRI796_2648	BNA1	0.046	1	0
AWRI796_2092	MYO1	0.06	1	0	AWRI796_3373	CDC3	0.046	1	0
AWRI796_2131	SSZ1	0.06	1	0	AWRI796_4220	DBP6	0.046	1	0
AWRI796_2165	GEP4	0.06	1	0	AWRI796_4571	MSB1	0.046	1	0
AWRI796_3389	RPP0	0.06	1	0	AWRI796_4864	MKK2	0.046	1	0
AWRI796_3488	ERO1	0.06	1	0	AWRI796_1392	BOI2	0.045	1	0
AWRI796_4282	RIB4	0.06	1	0	AWRI796_1454	ISC10	0.045	1	0
AWRI796_4994	SUT2	0.06	1	0	AWRI796_1847	YGR079W	0.045	1	0
AWRI796_0090	MRX3	0.059	1	0	AWRI796_2415	MPH1	0.045	1	0
AWRI796_0938	GCD6	0.059	1	0	AWRI796_2611	VPS53	0.045	1	0
AWRI796_1975	PHO81	0.059	1	0	AWRI796_3510	URA5	0.045	1	0
AWRI796_3404	RSC2	0.059	1	0	AWRI796_4205	YNR021W	0.045	1	0
AWRI796_4547	PUP1	0.059	1	0	AWRI796_0877	SAN1	0.044	1	0
AWRI796_0383	ALG7	0.058	1	0	AWRI796_1493	GAT1	0.044	1	0
AWRI796_1572	RTG2	0.058	1	0	AWRI796_2038	VMR1	0.044	1	0
AWRI796_2151	IPI1	0.058	1	0	AWRI796_2207	MRPL6	0.044	1	0
AWRI796_3344	YSH1	0.058	1	0	AWRI796_2843	YPK1	0.044	1	0
AWRI796_3944	RFC3	0.058	1	0	AWRI796_3136	RAD5	0.044	1	0
AWRI796_3956	MET2	0.058	1	0	AWRI796_3797	CEF1	0.044	1	0
AWRI796_4749	PLC1	0.058	1	0	AWRI796_4121	NIS1	0.044	1	0
AWRI796_0260	EXO84	0.057	1	0	AWRI796_4734	RDR1	0.044	1	0
AWRI796_0382	YBR242W	0.057	1	0	AWRI796_4855	PRP46	0.044	1	0
AWRI796_2171	CDC12	0.057	1	0	AWRI796_0373	PBP2	0.043	1	0
AWRI796_2702	BUD4	0.057	1	0	AWRI796_0665	IWR1	0.043	1	0
AWRI796_2754	DAN4	0.057	1	0	AWRI796_1075	VPS74	0.043	1	0
AWRI796_1066	TFC6	0.056	1	0	AWRI796_3818	TAF9	0.043	1	0
AWRI796_1620	HOS2	0.056	1	0	AWRI796_4305	PAP2	0.043	1	0
AWRI796_2811	TPK3	0.056	1	0	AWRI796_1175	PAC11	0.042	1	0
AWRI796_3091	DPS1	0.056	1	0	AWRI796_1875	CLD1	0.042	1	0
AWRI796_3121	PML1	0.056	1	0	AWRI796_2319	NUP159	0.042	1	0
AWRI796_3199	ERG27	0.056	1	0	AWRI796_2537	MDV1	0.042	1	0
AWRI796_3798	SCJ1	0.056	1	0	AWRI796_3077	GPI13	0.042	1	0
AWRI796_5168	AWRI796_5168	0.056	1	0	AWRI796_3214	YLR118C	0.042	1	0
AWRI796_0292	YBR139W	0.055	1	0	AWRI796_3283	HMX1	0.042	1	0
AWRI796_0936	MSS4	0.055	1	0	AWRI796_3319	IRC20	0.042	1	0
AWRI796_1319	HVG1	0.055	1	0	AWRI796_3678	SEG1	0.042	1	0
AWRI796_3822	CUS1	0.055	1	0	AWRI796_3911	RPD3	0.042	1	0
AWRI796_3865	DSK2	0.055	1	0	AWRI796_4140	POR1	0.042	1	0
AWRI796_4865	UME1	0.055	1	0	AWRI796_5024	MSF1	0.042	1	0
AWRI796_0162	HIR1	0.054	1	0	AWRI796_0343	MSI1	0.041	1	0
AWRI796_0881	EKI1	0.054	1	0	AWRI796_2022	ZUO1	0.041	1	0
AWRI796_0991	CCC2	0.054	1	0	AWRI796_4397	CMK2	0.041	1	0
AWRI796_1305	YAT2	0.054	1	0	AWRI796_0036	FRT2	0.04	1	0
AWRI796_1745	RNA15	0.054	1	0	AWRI796_0326	ECM31	0.04	1	0
AWRI796_4545	ISN1	0.054	1	0	AWRI796_0372	SWC5	0.04	1	0
AWRI796_0457	LSB5	0.053	1	0	AWRI796_0613	DLD2	0.04	1	0
AWRI796_1008	SSD1	0.053	1	0	AWRI796_1459	AWRI796_1459	0.04	1	0
AWRI796_1105	RPB7	0.053	1	0	AWRI796_1799	YGR021W	0.04	1	0
AWRI796_2897	YKL063C	0.053	1	0	AWRI796_2257	RPN10	0.04	1	0
AWRI796_4264	ENB1	0.053	1	0	AWRI796_2290	ATG32	0.04	1	0
AWRI796_0161	ALK2	0.052	1	0	AWRI796_3867	PRM15	0.04	1	0
AWRI796_0209	TCM62	0.052	1	0	AWRI796_4244	YNR063W	0.04	1	0
AWRI796_0954	IVY1	0.052	1	0	AWRI796_5020	TIF5	0.04	1	0
AWRI796_1616	EMP24	0.052	1	0	AWRI796_5161	AWRI796_5161	0.04	1	0
AWRI796_1919	MRPS35	0.052	1	0	AWRI796_1092	SAC7	0.039	1	0
AWRI796_3004	GLG1	0.052	1	0	AWRI796_2633	POL31	0.039	1	0
AWRI796_3971	DSL1	0.052	1	0	AWRI796_0657	CDC48	0.038	1	0
AWRI796_0113	SEF1	0.051	1	0	AWRI796_0891	SSY1	0.038	1	0
AWRI796_0957	RTN1	0.051	1	0	AWRI796_1314	ZRG8	0.038	1	0
AWRI796_1255	SPF1	0.051	1	0	AWRI796_2082	VPS29	0.038	1	0
AWRI796_1866	TEL2	0.051	1	0	AWRI796_2361	RNR3	0.038	1	0
AWRI796_2316	RHO3	0.051	1	0	AWRI796_3040	ESL2	0.038	1	0
AWRI796_2516	YAK1	0.051	1	0	AWRI796_5056	ASA1	0.038	1	0
AWRI796_2825	SDH1	0.051	1	0	AWRI796_1905	NAT2	0.037	1	0
AWRI796_3006	UTP30	0.051	1	0	AWRI796_2141	PPE1	0.037	1	0
AWRI796_4034	UBP10	0.051	1	0	AWRI796_3959	TOF1	0.037	1	0
AWRI796_0982	SWM1	0.05	1	0	AWRI796_4412	PHO80	0.037	1	0
AWRI796_1366	ILV1	0.05	1	0	AWRI796_4764	YAH1	0.037	1	0

AWRI796 Gene ID	Gene Name	$\log_2$ Fold Change	Adj. p-value	Score	AWRI796 Gene ID	Gene Name	$\log_2$ Fold Change	Adj. p-value	Score
AWRI796_2098	YHI9	0.036	1	0	AWRI796_3479	LEU3	0.022	1	0
AWRI796_2288	MLP2	0.036	1	0	AWRI796_3626	MRPL3	0.022	1	0
AWRI796_2740	MET5	0.036	1	0	AWRI796_5066	RPL11A	0.022	1	0
AWRI796_2833	CTK1	0.036	1	0	AWRI796_1449	TMT1	0.021	1	0
AWRI796_3591	ERV25	0.036	1	0	AWRI796_3129	UBR2	0.021	1	0
AWRI796_3616	BUD22	0.036	1	0	AWRI796_3500	ATR1	0.021	1	0
AWRI796_3927	ZIM17	0.036	1	0	AWRI796_4207	SNF12	0.021	1	0
AWRI796_4570	TUF1	0.036	1	0	AWRI796_4498	RAS1	0.021	1	0
AWRI796_2048	YHL026C	0.035	1	0	AWRI796_4827	CTI6	0.021	1	0
AWRI796_4227	TRM112	0.035	1	0	AWRI796_4854	RRD2	0.021	1	0
AWRI796_0132	ERD2	0.034	1	0	AWRI796_2324	HPM1	0.02	1	0
AWRI796_0269	YSA1	0.034	1	0	AWRI796_2713	SOD1	0.02	1	0
AWRI796_2149	SAM35	0.034	1	0	AWRI796_3051	AYT1	0.02	1	0
AWRI796_2174	ERP5	0.034	1	0	AWRI796_3115	TEN1	0.02	1	0
AWRI796_2427	YIR014W	0.034	1	0	AWRI796_3511	SEC65	0.02	1	0
AWRI796_2532	ALB1	0.034	1	0	AWRI796_3551	SML1	0.02	1	0
AWRI796_3017	DRE2	0.034	1	0	AWRI796_3934	RPS19B	0.02	1	0
AWRI796_3029	HBS1	0.034	1	0	AWRI796_4047	FMP41	0.02	1	0
AWRI796_3353	COQ11	0.034	1	0	AWRI796_4058	NSG2	0.02	1	0
AWRI796_4918	GPI2	0.034	1	0	AWRI796_4507	CEX1	0.02	1	0
AWRI796_0444	APA1	0.033	1	0	AWRI796_4936	LGE1	0.02	1	0
AWRI796_0651	SRF1	0.033	1	0	AWRI796_1079	ARH1	0.019	1	0
AWRI796_1709	NBP35	0.033	1	0	AWRI796_3241	YLR149C	0.019	1	0
AWRI796_2328	MOB1	0.033	1	0	AWRI796_3561	GSF2	0.019	1	0
AWRI796_3062	FRE6	0.033	1	0	AWRI796_4372	NTG2	0.019	1	0
AWRI796_3286	SEC13	0.033	1	0	AWRI796_4907	RPS6B	0.019	1	0
AWRI796_3333	RED1	0.033	1	0	AWRI796_5081	YPR117W	0.019	1	0
AWRI796_3787	TOM40	0.033	1	0	AWRI796_0798	TPI1	0.018	1	0
AWRI796_0971	YDR248C	0.032	1	0	AWRI796_0856	VBA4	0.018	1	0
AWRI796_1199	EUG1	0.032	1	0	AWRI796_1473	LAM5	0.018	1	0
AWRI796_1262	YEL023C	0.032	1	0	AWRI796_2478	RPS22A	0.018	1	0
AWRI796_1828	RSC1	0.032	1	0	AWRI796_2696	YJR084W	0.018	1	0
AWRI796_3189	XDJ1	0.032	1	0	AWRI796_0463	RNQ1	0.017	1	0
AWRI796_3200	APC9	0.032	1	0	AWRI796_2970	VPS51	0.017	1	0
AWRI796_3530	DUS1	0.032	1	0	AWRI796_3104	RTT109	0.017	1	0
AWRI796_3889	ADH2	0.032	1	0	AWRI796_3897	GLC8	0.017	1	0
AWRI796_4092	YNL115C	0.032	1	0	AWRI796_4920	YTA6	0.017	1	0
AWRI796_4435	HST3	0.032	1	0	AWRI796_0402	TSC10	0.016	1	0
AWRI796_4005	ALG9	0.031	1	0	AWRI796_0569	PTP1	0.016	1	0
AWRI796_4751	DIM1	0.031	1	0	AWRI796_0852	MRX14	0.016	1	0
AWRI796_4885	HOS3	0.031	1	0	AWRI796_1439	PAB1	0.016	1	0
AWRI796_0255	PBY1	0.03	1	0	AWRI796_1645	YIP5	0.016	1	0
AWRI796_0294	BMT2	0.03	1	0	AWRI796_2150	STE12	0.016	1	0
AWRI796_0377	PRP5	0.03	1	0	AWRI796_3665	TVP18	0.016	1	0
AWRI796_0844	TMS1	0.03	1	0	AWRI796_5170	AWRI796_5170	0.016	1	0
AWRI796_2494	ERG20	0.03	1	0	AWRI796_0545	CSM1	0.015	1	0
AWRI796_2554	TOK1	0.03	1	0	AWRI796_1257	BUD16	0.015	1	0
AWRI796_4514	RIO1	0.03	1	0	AWRI796_1264	URA3	0.015	1	0
AWRI796_4870	RDS2	0.03	1	0	AWRI796_2130	PAN5	0.015	1	0
AWRI796_0127	PSY4	0.029	1	0	AWRI796_2581	NUP82	0.015	1	0
AWRI796_0935	UME6	0.029	1	0	AWRI796_2726	ATP2	0.015	1	0
AWRI796_2882	VMA5	0.029	1	0	AWRI796_3318	ERF2	0.015	1	0
AWRI796_2930	URA6	0.029	1	0	AWRI796_0716	MBP1	0.014	1	0
AWRI796_4151	YIP3	0.029	1	0	AWRI796_1436	RAD4	0.014	1	0
AWRI796_4260	YIR042C	0.029	1	0	AWRI796_1888	YGR126W	0.014	1	0
AWRI796_4668	ISW2	0.029	1	0	AWRI796_2239	YHR182W	0.014	1	0
AWRI796_4925	YPL068C	0.029	1	0	AWRI796_2247	ERG9	0.014	1	0
AWRI796_1395	RPL23B	0.028	1	0	AWRI796_2838	RMA1	0.014	1	0
AWRI796_1669	RPL1B	0.028	1	0	AWRI796_3810	TAF7	0.014	1	0
AWRI796_1864	ASK10	0.028	1	0	AWRI796_4122	APJ1	0.014	1	0
AWRI796_2212	SPO12	0.028	1	0	AWRI796_4182	MRP7	0.014	1	0
AWRI796_2344	AVT7	0.028	1	0	AWRI796_5103	YPR147C	0.014	1	0
AWRI796_3487	YML131W	0.028	1	0	AWRI796_0953	PCF11	0.013	1	0
AWRI796_0615	YDL176W	0.027	1	0	AWRI796_1588	SEC15	0.013	1	0
AWRI796_1812	YGR035C	0.027	1	0	AWRI796_1961	RTA1	0.013	1	0
AWRI796_2627	OST1	0.027	1	0	AWRI796_2301	FLX1	0.013	1	0
AWRI796_4330	MPD2	0.027	1	0	AWRI796_3827	COA6	0.013	1	0
AWRI796_4408	RPB11	0.027	1	0	AWRI796_4414	ALG6	0.013	1	0
AWRI796_4549	MTR10	0.027	1	0	AWRI796_0581	RRI1	0.012	1	0
AWRI796_0089	BRN1	0.026	1	0	AWRI796_1006	HRQ1	0.012	1	0
AWRI796_0453	ATG22	0.026	1	0	AWRI796_1237	MAK10	0.012	1	0
AWRI796_1091	RVS167	0.026	1	0	AWRI796_2047	AWRI796_2047	0.012	1	0
AWRI796_1596	SDT1	0.026	1	0	AWRI796_2707	YJR098C	0.012	1	0
AWRI796_2318	HIS5	0.026	1	0	AWRI796_3127	SDO1	0.012	1	0
AWRI796_2514	YJL144W	0.026	1	0	AWRI796_3654	SEN15	0.012	1	0
AWRI796_3398	NIT3	0.026	1	0	AWRI796_3931	MRPS18	0.012	1	0
AWRI796_3849	TRM732	0.026	1	0	AWRI796_5099	TAZ1	0.012	1	0
AWRI796_3949	MRPL10	0.026	1	0	AWRI796_0301	ARA1	0.011	1	0
AWRI796_4241	FRE4	0.026	1	0	AWRI796_0320	SSE2	0.011	1	0
AWRI796_5046	LTP1	0.026	1	0	AWRI796_0401	YPT10	0.011	1	0
AWRI796_5123	JIP5	0.026	1	0	AWRI796_0738	MPS1	0.011	1	0
AWRI796_0097	RPL23A	0.025	1	0	AWRI796_0760	YRB1	0.011	1	0
AWRI796_1532	ROG3	0.025	1	0	AWRI796_1326	SPO73	0.011	1	0
AWRI796_1583	CSE1	0.025	1	0	AWRI796_2399	FAF1	0.011	1	0
AWRI796_2585	IKS1	0.025	1	0	AWRI796_2508	SNA3	0.011	1	0
AWRI796_3225	USB1	0.025	1	0	AWRI796_3335	PDR8	0.011	1	0
AWRI796_4669	RRG7	0.025	1	0	AWRI796_3658	AEP1	0.011	1	0
AWRI796_1102	URH1	0.024	1	0	AWRI796_3955	CAF120	0.011	1	0
AWRI796_1348	RRT13	0.024	1	0	AWRI796_4421	TIR4	0.011	1	0
AWRI796_1548	SAP155	0.024	1	0	AWRI796_4458	VHS3	0.011	1	0
AWRI796_1796	YGR017W	0.024	1	0	AWRI796_4497	CRC1	0.011	1	0
AWRI796_1999	APL6	0.024	1	0	AWRI796_4589	MGM1	0.011	1	0
AWRI796_3271	PEX13	0.024	1	0	AWRI796_0164	LDB7	0.01	1	0
AWRI796_4470	VPS5	0.024	1	0	AWRI796_0758	RMD1	0.01	1	0
AWRI796_4630	GCD1	0.024	1	0	AWRI796_0834	RLI1	0.01	1	0
AWRI796_0735	DBP10	0.023	1	0	AWRI796_1876	YGR111W	0.01	1	0
AWRI796_1268	GTT3	0.023	1	0	AWRI796_2731	VPS70	0.01	1	0
AWRI796_1963	GPI1	0.023	1	0	AWRI796_2943	CCE1	0.01	1	0
AWRI796_2076	STP2	0.023	1	0	AWRI796_3032	OMA1	0.01	1	0
AWRI796_4993	HAA1	0.023	1	0	AWRI796_4247	YNR066C	0.01	1	0
AWRI796_5034	ARO7	0.023	1	0	AWRI796_4654	YOR289W	0.01	1	0
AWRI796_0117	YEL1	0.022	1	0	AWRI796_5006	YME1	0.01	1	0
AWRI796_0175	DSF2	0.022	1	0	AWRI796_0888	RPA14	0.009	1	0
AWRI796_1146	GUK1	0.022	1	0	AWRI796_3249	PUS5	0.009	1	0
AWRI796_1726	NPY1	0.022	1	0	AWRI796_3635	IMP2	0.009	1	0
AWRI796_2778	LOS1	0.022	1	0	AWRI796_4221	ZRG17	0.009	1	0
AWRI796_2991	SHB17	0.022	1	0	AWRI796_4299	HRP1	0.009	1	0

AWRI796 Gene ID	Gene Name	log_2 Fold Change	Adj. *p* -value	Score	AWRI796 Gene ID	Gene Name	log_2 Fold Change	Adj. *p* -value	Score
AWRI796_4492	CMR2	0.009	1	0	AWRI796_5150	HSP33	-0.005	1	0
AWRI796_4714	SNX3	0.009	1	0	AWRI796_1082	RGA2	-0.006	1	0
AWRI796_0317	TYR1	0.008	1	0	AWRI796_1535	HIS2	-0.006	1	0
AWRI796_1037	YCG1	0.008	1	0	AWRI796_1593	VID30	-0.006	1	0
AWRI796_1367	AIM10	0.008	1	0	AWRI796_1753	MIG1	-0.006	1	0
AWRI796_1697	VPS73	0.008	1	0	AWRI796_1924	MSM1	-0.006	1	0
AWRI796_1723	HSF1	0.008	1	0	AWRI796_2142	PTC7	-0.006	1	0
AWRI796_1818	NQM1	0.008	1	0	AWRI796_2169	YPT35	-0.006	1	0
AWRI796_2678	NTA1	0.008	1	0	AWRI796_2236	STB5	-0.006	1	0
AWRI796_2783	PEX1	0.008	1	0	AWRI796_3853	SAP30	-0.006	1	0
AWRI796_2928	GPX1	0.008	1	0	AWRI796_4623	NAT5	-0.006	1	0
AWRI796_3907	AWRI796_3907	0.008	1	0	AWRI796_0253	PHO3	-0.007	1	0
AWRI796_4304	MSN1	0.008	1	0	AWRI796_0277	MRPL36	-0.007	1	0
AWRI796_0589	NHP2	0.007	1	0	AWRI796_0325	SWD3	-0.007	1	0
AWRI796_2183	MSH1	0.007	1	0	AWRI796_0446	SPS22	-0.007	1	0
AWRI796_3278	PBA1	0.007	1	0	AWRI796_1452	PDA1	-0.007	1	0
AWRI796_3724	ERG29	0.007	1	0	AWRI796_3346	YLR283W	-0.007	1	0
AWRI796_3828	FAA4	0.007	1	0	AWRI796_0224	ORC2	-0.008	1	0
AWRI796_4621	TUM1	0.007	1	0	AWRI796_0416	DUG2	-0.008	1	0
AWRI796_4710	SOG2	0.007	1	0	AWRI796_0858	DPB4	-0.008	1	0
AWRI796_1307	CHO1	0.006	1	0	AWRI796_0932	COQ4	-0.008	1	0
AWRI796_2762	MCH2	0.006	1	0	AWRI796_2216	LIN1	-0.008	1	0
AWRI796_3581	APT1	0.006	1	0	AWRI796_2671	KCH1	-0.008	1	0
AWRI796_4233	POP2	0.006	1	0	AWRI796_2852	APN1	-0.008	1	0
AWRI796_5025	TAH18	0.006	1	0	AWRI796_3675	ISF1	-0.008	1	0
AWRI796_0826	PDC2	0.005	1	0	AWRI796_4661	YOR296W	-0.008	1	0
AWRI796_0966	PRP28	0.005	1	0	AWRI796_5071	YTH1	-0.008	1	0
AWRI796_1061	TRP4	0.005	1	0	AWRI796_0603	ARF1	-0.009	1	0
AWRI796_2807	EBP2	0.005	1	0	AWRI796_0792	NRG1	-0.009	1	0
AWRI796_3208	CCW12	0.005	1	0	AWRI796_2351	YIL077C	-0.009	1	0
AWRI796_3220	APC2	0.005	1	0	AWRI796_2777	ADD66	-0.009	1	0
AWRI796_4387	MIM1	0.005	1	0	AWRI796_3253	APS1	-0.009	1	0
AWRI796_0687	SRP14	0.004	1	0	AWRI796_4891	YPL109C	-0.009	1	0
AWRI796_1033	ASP1	0.004	1	0	AWRI796_0259	FES1	-0.01	1	0
AWRI796_1208	CAB1	0.004	1	0	AWRI796_0948	CRF1	-0.01	1	0
AWRI796_1386	GLE2	0.004	1	0	AWRI796_2057	YHL018W	-0.01	1	0
AWRI796_1418	DDI1	0.004	1	0	AWRI796_3210	AVL9	-0.01	1	0
AWRI796_1632	YGL176C	0.004	1	0	AWRI796_4015	YNL208W	-0.01	1	0
AWRI796_2718	YMR1	0.004	1	0	AWRI796_4102	AVT4	-0.01	1	0
AWRI796_2996	FMP46	0.004	1	0	AWRI796_0376	ABD1	-0.011	1	0
AWRI796_3236	ACF2	0.004	1	0	AWRI796_0528	BUD31	-0.011	1	0
AWRI796_3917	LEM3	0.004	1	0	AWRI796_0642	CCT4	-0.011	1	0
AWRI796_4467	CYT1	0.004	1	0	AWRI796_0727	PRP11	-0.011	1	0
AWRI796_5172	PAU6	0.004	1	0	AWRI796_1316	ARB1	-0.011	1	0
AWRI796_1737	SDS23	0.003	1	0	AWRI796_1486	CAF16	-0.011	1	0
AWRI796_1767	KAP122	0.003	1	0	AWRI796_2125	MED6	-0.011	1	0
AWRI796_2725	JHD2	0.003	1	0	AWRI796_3427	REH1	-0.011	1	0
AWRI796_4348	HST1	0.003	1	0	AWRI796_4817	RSA1	-0.011	1	0
AWRI796_0364	PDB1	0.002	1	0	AWRI796_5068	FHL1	-0.011	1	0
AWRI796_1263	GEA2	0.002	1	0	AWRI796_0606	PPH22	-0.012	1	0
AWRI796_1959	ZPR1	0.002	1	0	AWRI796_1226	SIT1	-0.012	1	0
AWRI796_4366	GSH2	0.002	1	0	AWRI796_3428	STE23	-0.012	1	0
AWRI796_1280	WBP1	0.001	1	0	AWRI796_3505	BUL2	-0.012	1	0
AWRI796_3294	CPR6	0.001	1	0	AWRI796_3668	SDD2	-0.012	1	0
AWRI796_3507	ZDS2	0.001	1	0	AWRI796_5216	COS3	-0.012	1	0
AWRI796_4647	FSH3	0.001	1	0	AWRI796_1060	TRR1	-0.013	1	0
AWRI796_4978	CHL1	0.001	1	0	AWRI796_1152	MRPL28	-0.013	1	0
AWRI796_0810	RPS13	0	1	0	AWRI796_1853	RPL11B	-0.013	1	0
AWRI796_1534	LSB3	0	1	0	AWRI796_1962	RSM27	-0.013	1	0
AWRI796_3304	ECM22	0	1	0	AWRI796_3168	FYV7	-0.013	1	0
AWRI796_4762	HFI1	0	1	0	AWRI796_3407	STE11	-0.013	1	0
AWRI796_0196	RKM3	-0.001	1	0	AWRI796_4390	TSR4	-0.013	1	0
AWRI796_0312	CDC28	-0.001	1	0	AWRI796_4394	YOL019W	-0.013	1	0
AWRI796_0541	SRB8	-0.001	1	0	AWRI796_1615	MCM6	-0.014	1	0
AWRI796_0710	UBC9	-0.001	1	0	AWRI796_2513	SFH5	-0.014	1	0
AWRI796_1343	CEM1	-0.001	1	0	AWRI796_2719	YJR111C	-0.014	1	0
AWRI796_2506	VPS35	-0.001	1	0	AWRI796_4146	SFB2	-0.014	1	0
AWRI796_2529	GCD14	-0.001	1	0	AWRI796_4466	YNG1	-0.014	1	0
AWRI796_2720	NNF1	-0.001	1	0	AWRI796_0208	QDR3	-0.015	1	0
AWRI796_2876	CAB3	-0.001	1	0	AWRI796_0422	YBR287W	-0.015	1	0
AWRI796_4789	MMT2	-0.001	1	0	AWRI796_0724	SIT4	-0.015	1	0
AWRI796_0751	APC11	-0.002	1	0	AWRI796_1387	FLO8	-0.015	1	0
AWRI796_2722	TDA4	-0.002	1	0	AWRI796_1941	TDH3	-0.015	1	0
AWRI796_3044	SKG1	-0.002	1	0	AWRI796_0012	ACS1	-0.016	1	0
AWRI796_3381	YLR326W	-0.002	1	0	AWRI796_0669	RRP42	-0.016	1	0
AWRI796_4316	ITR2	-0.002	1	0	AWRI796_1396	SHO1	-0.016	1	0
AWRI796_4385	YAP7	-0.002	1	0	AWRI796_1477	YPT1	-0.016	1	0
AWRI796_4906	GLR1	-0.002	1	0	AWRI796_2000	BUD32	-0.016	1	0
AWRI796_4941	MNN9	-0.002	1	0	AWRI796_2067	YHL008C	-0.016	1	0
AWRI796_0160	YBL010C	-0.003	1	0	AWRI796_2877	CYT2	-0.016	1	0
AWRI796_0256	YBR096W	-0.003	1	0	AWRI796_3782	CIK1	-0.016	1	0
AWRI796_0605	RBS1	-0.003	1	0	AWRI796_3811	MTF1	-0.016	1	0
AWRI796_1973	PHB2	-0.003	1	0	AWRI796_4109	YPT53	-0.016	1	0
AWRI796_1995	GND2	-0.003	1	0	AWRI796_4115	MKT1	-0.016	1	0
AWRI796_2432	MRS1	-0.003	1	0	AWRI796_5021	PUF2	-0.016	1	0
AWRI796_2643	ESS1	-0.003	1	0	AWRI796_0305	RIB7	-0.017	1	0
AWRI796_3008	TFA2	-0.003	1	0	AWRI796_0562	GUD1	-0.017	1	0
AWRI796_3664	MOT3	-0.003	1	0	AWRI796_1081	LSM6	-0.017	1	0
AWRI796_4199	SMM1	-0.003	1	0	AWRI796_1451	BMH1	-0.017	1	0
AWRI796_5189	IMD2	-0.003	1	0	AWRI796_1835	SPT4	-0.017	1	0
AWRI796_0782	RAD28	-0.004	1	0	AWRI796_2463	PEX2	-0.017	1	0
AWRI796_2229	DBP8	-0.004	1	0	AWRI796_3342	MCM5	-0.017	1	0
AWRI796_3549	OGG1	-0.004	1	0	AWRI796_3587	PPZ1	-0.017	1	0
AWRI796_4294	VPS68	-0.004	1	0	AWRI796_4958	SUV3	-0.017	1	0
AWRI796_1131	PPM1	-0.005	1	0	AWRI796_4967	VTC3	-0.017	1	0
AWRI796_2108	RRF1	-0.005	1	0	AWRI796_0013	FLC2	-0.018	1	0
AWRI796_2360	YIL067C	-0.005	1	0	AWRI796_0559	AAD4	-0.018	1	0
AWRI796_2848	OAC1	-0.005	1	0	AWRI796_1353	TDA2	-0.018	1	0
AWRI796_2911	ANR2	-0.005	1	0	AWRI796_1608	MIG2	-0.018	1	0
AWRI796_3495	GTR1	-0.005	1	0	AWRI796_1750	OCH1	-0.018	1	0
AWRI796_3699	ILV2	-0.005	1	0	AWRI796_1786	TFG2	-0.018	1	0
AWRI796_3896	YMR310C	-0.005	1	0	AWRI796_1787	PRP18	-0.018	1	0
AWRI796_4045	APC1	-0.005	1	0	AWRI796_2697	YJR085C	-0.018	1	0
AWRI796_4082	FAR11	-0.005	1	0	AWRI796_2866	MTC2	-0.018	1	0
AWRI796_4344	THP1	-0.005	1	0	AWRI796_0226	YBR062C	-0.019	1	0
AWRI796_4388	LAG2	-0.005	1	0	AWRI796_0831	RRP1	-0.019	1	0
AWRI796_4956	PHO85	-0.005	1	0	AWRI796_0900	STB3	-0.019	1	0

AWRI796 Gene ID	Gene Name	log_2 Fold Change	Adj. *p* -value	Score	AWRI796 Gene ID	Gene Name	log_2 Fold Change	Adj. *p* -value	Score
AWRI796_1109	ADE8	-0.019	1	0	AWRI796_4168	SAM50	-0.031	1	0
AWRI796_1174	RIB3	-0.019	1	0	AWRI796_0992	GLO2	-0.032	1	0
AWRI796_2745	YJR142W	-0.019	1	0	AWRI796_1213	PAD1	-0.032	1	0
AWRI796_3016	YKR070W	-0.019	1	0	AWRI796_1376	SHC1	-0.032	1	0
AWRI796_3642	ARG80	-0.019	1	0	AWRI796_1540	SMC2	-0.032	1	0
AWRI796_0391	MRPS5	-0.02	1	0	AWRI796_2220	PEX18	-0.032	1	0
AWRI796_0845	ARP10	-0.02	1	0	AWRI796_2387	CAP2	-0.032	1	0
AWRI796_2011	RTT102	-0.02	1	0	AWRI796_3244	YLR152C	-0.032	1	0
AWRI796_2730	ENT3	-0.02	1	0	AWRI796_3622	FMS1	-0.032	1	0
AWRI796_4999	TIF6	-0.02	1	0	AWRI796_3755	CEP3	-0.032	1	0
AWRI796_5098	LOA1	-0.02	1	0	AWRI796_4279	CTR9	-0.032	1	0
AWRI796_0439	PRD1	-0.021	1	0	AWRI796_4727	NDD1	-0.032	1	0
AWRI796_0557	YCR100C	-0.021	1	0	AWRI796_4942	DIG1	-0.032	1	0
AWRI796_1399	YER121W	-0.021	1	0	AWRI796_4946	SSN3	-0.032	1	0
AWRI796_1871	SRB5	-0.021	1	0	AWRI796_0264	PHO88	-0.033	1	0
AWRI796_4851	KIP2	-0.021	1	0	AWRI796_0324	UMP1	-0.033	1	0
AWRI796_0472	DCC1	-0.022	1	0	AWRI796_0501	FEN2	-0.033	1	0
AWRI796_0667	ATG20	-0.022	1	0	AWRI796_0908	NGG1	-0.033	1	0
AWRI796_1068	CDC40	-0.022	1	0	AWRI796_1229	NPR2	-0.033	1	0
AWRI796_1968	HSV2	-0.022	1	0	AWRI796_1687	SNF4	-0.033	1	0
AWRI796_2185	CIA2	-0.022	1	0	AWRI796_2755	DAL5	-0.033	1	0
AWRI796_3015	MET1	-0.022	1	0	AWRI796_3509	PML39	-0.033	1	0
AWRI796_3351	MEC3	-0.022	1	0	AWRI796_0181	GRX7	-0.034	1	0
AWRI796_3727	PSO2	-0.022	1	0	AWRI796_1855	PDC6	-0.034	1	0
AWRI796_3765	CTL1	-0.022	1	0	AWRI796_3019	AIM29	-0.034	1	0
AWRI796_4866	SPP1	-0.022	1	0	AWRI796_1032	SWA2	-0.035	1	0
AWRI796_4884	IDI1	-0.022	1	0	AWRI796_1423	SPT15	-0.035	1	0
AWRI796_0176	FLR1	-0.023	1	0	AWRI796_2521	LCB3	-0.035	1	0
AWRI796_1127	TIF35	-0.023	1	0	AWRI796_3242	STM1	-0.035	1	0
AWRI796_1308	GAL83	-0.023	1	0	AWRI796_3268	MDL1	-0.035	1	0
AWRI796_1843	PRP38	-0.023	1	0	AWRI796_3270	MMR1	-0.035	1	0
AWRI796_2197	YCK1	-0.023	1	0	AWRI796_3434	VPS33	-0.035	1	0
AWRI796_2373	NEO1	-0.023	1	0	AWRI796_4006	MGS1	-0.035	1	0
AWRI796_3967	YIF1	-0.023	1	0	AWRI796_0173	RCR1	-0.036	1	0
AWRI796_4103	MIC27	-0.023	1	0	AWRI796_0225	TRM7	-0.036	1	0
AWRI796_4947	MRX11	-0.023	1	0	AWRI796_0289	MEC1	-0.036	1	0
AWRI796_0023	CDC24	-0.024	1	0	AWRI796_0344	PGI1	-0.036	1	0
AWRI796_1335	GIP2	-0.024	1	0	AWRI796_0722	KNH1	-0.036	1	0
AWRI796_1546	IRC5	-0.024	1	0	AWRI796_1640	PMR1	-0.036	1	0
AWRI796_1734	PKP2	-0.024	1	0	AWRI796_2052	NPR3	-0.036	1	0
AWRI796_2122	CIC1	-0.024	1	0	AWRI796_2100	RRM3	-0.036	1	0
AWRI796_3856	RSN1	-0.024	1	0	AWRI796_2232	SPC97	-0.036	1	0
AWRI796_4000	SQS1	-0.024	1	0	AWRI796_2235	YHR177W	-0.036	1	0
AWRI796_0245	UBC4	-0.025	1	0	AWRI796_2436	MND2	-0.036	1	0
AWRI796_1090	YDR387C	-0.025	1	0	AWRI796_2854	ABF1	-0.036	1	0
AWRI796_1218	YDR541C	-0.025	1	0	AWRI796_4300	SMF1	-0.036	1	0
AWRI796_1306	GCD11	-0.025	1	0	AWRI796_0056	FUN14	-0.037	1	0
AWRI796_1798	VMA7	-0.025	1	0	AWRI796_0366	TDP1	-0.037	1	0
AWRI796_2531	MTC1	-0.025	1	0	AWRI796_1266	MMS21	-0.037	1	0
AWRI796_2644	TES1	-0.025	1	0	AWRI796_1350	MOT2	-0.037	1	0
AWRI796_3816	RNH1	-0.025	1	0	AWRI796_2014	CWC22	-0.037	1	0
AWRI796_3850	TIF11	-0.025	1	0	AWRI796_2079	SOD2	-0.037	1	0
AWRI796_0240	SLM4	-0.026	1	0	AWRI796_2416	AIM21	-0.037	1	0
AWRI796_0715	YDL057W	-0.026	1	0	AWRI796_2665	CYC1	-0.037	1	0
AWRI796_1113	RRP17	-0.026	1	0	AWRI796_2874	CUE2	-0.037	1	0
AWRI796_1411	GLC7	-0.026	1	0	AWRI796_3439	SFP1	-0.037	1	0
AWRI796_1714	GUP1	-0.026	1	0	AWRI796_4004	ADE12	-0.037	1	0
AWRI796_1893	PHB1	-0.026	1	0	AWRI796_4057	IGO1	-0.037	1	0
AWRI796_3466	ECM30	-0.026	1	0	AWRI796_4093	RPC19	-0.037	1	0
AWRI796_3539	DAK1	-0.026	1	0	AWRI796_5057	SUA7	-0.037	1	0
AWRI796_4659	RRS1	-0.026	1	0	AWRI796_0103	PET112	-0.038	1	0
AWRI796_1374	PUP3	-0.027	1	0	AWRI796_0151	RFT1	-0.038	1	0
AWRI796_1412	YER134C	-0.027	1	0	AWRI796_1236	RPL12A	-0.038	1	0
AWRI796_1820	TAM41	-0.027	1	0	AWRI796_1774	LEU1	-0.038	1	0
AWRI796_2485	ATG27	-0.027	1	0	AWRI796_2547	GSH1	-0.038	1	0
AWRI796_3010	OAF3	-0.027	1	0	AWRI796_3139	MLH2	-0.038	1	0
AWRI796_4405	COQ10	-0.027	1	0	AWRI796_3582	UNG1	-0.038	1	0
AWRI796_0714	USO1	-0.028	1	0	AWRI796_3860	RRN9	-0.038	1	0
AWRI796_0752	RPT2	-0.028	1	0	AWRI796_4518	CAT5	-0.038	1	0
AWRI796_0967	PEX5	-0.028	1	0	AWRI796_4620	CLP1	-0.038	1	0
AWRI796_1706	PAN2	-0.028	1	0	AWRI796_0261	SIF2	-0.039	1	0
AWRI796_2389	ULP2	-0.028	1	0	AWRI796_0498	SLM5	-0.039	1	0
AWRI796_2747	MGM101	-0.028	1	0	AWRI796_0811	RRG1	-0.039	1	0
AWRI796_2817	RCN1	-0.028	1	0	AWRI796_0905	ARG82	-0.039	1	0
AWRI796_2887	MUD2	-0.028	1	0	AWRI796_3201	CDC45	-0.039	1	0
AWRI796_3430	CCW14	-0.028	1	0	AWRI796_3567	YMD8	-0.039	1	0
AWRI796_3740	NUP53	-0.028	1	0	AWRI796_3998	JJJ1	-0.039	1	0
AWRI796_3807	UBP8	-0.028	1	0	AWRI796_4957	TRM44	-0.039	1	0
AWRI796_5246	YNL284C-A	-0.028	1	0	AWRI796_0322	SEC66	-0.04	1	0
AWRI796_1044	RQC1	-0.029	1	0	AWRI796_0664	NUP84	-0.04	1	0
AWRI796_1095	SPT3	-0.029	1	0	AWRI796_0986	AKR1	-0.04	1	0
AWRI796_1715	SCY1	-0.029	1	0	AWRI796_1918	GTR2	-0.04	1	0
AWRI796_2986	SPC34	-0.029	1	0	AWRI796_2170	TRR2	-0.04	1	0
AWRI796_3792	ERG12	-0.029	1	0	AWRI796_2828	RPC25	-0.04	1	0
AWRI796_3932	BXI1	-0.029	1	0	AWRI796_3142	RIC1	-0.04	1	0
AWRI796_4938	KTR6	-0.029	1	0	AWRI796_3411	SSQ1	-0.04	1	0
AWRI796_0014	OAF1	-0.03	1	0	AWRI796_3734	TIF34	-0.04	1	0
AWRI796_0890	SAC3	-0.03	1	0	AWRI796_4910	YDC1	-0.04	1	0
AWRI796_1003	INM2	-0.03	1	0	AWRI796_5109	NCA2	-0.04	1	0
AWRI796_1093	UBA2	-0.03	1	0	AWRI796_0075	YAT1	-0.041	1	0
AWRI796_1704	TOS8	-0.03	1	0	AWRI796_1393	SPR6	-0.041	1	0
AWRI796_2788	ACP1	-0.03	1	0	AWRI796_2106	BRL1	-0.041	1	0
AWRI796_3311	LIP2	-0.03	1	0	AWRI796_2314	QDR1	-0.041	1	0
AWRI796_3464	CNA1	-0.03	1	0	AWRI796_3712	RPL15B	-0.041	1	0
AWRI796_3706	MGR3	-0.03	1	0	AWRI796_4805	RKM1	-0.041	1	0
AWRI796_4472	NRT1	-0.03	1	0	AWRI796_1605	VAM7	-0.042	1	0
AWRI796_5067	PRE2	-0.03	1	0	AWRI796_2307	MET18	-0.042	1	0
AWRI796_0134	MRPL16	-0.031	1	0	AWRI796_3130	SNF7	-0.042	1	0
AWRI796_0867	FIN1	-0.031	1	0	AWRI796_3313	CSC1	-0.042	1	0
AWRI796_1310	SMB1	-0.031	1	0	AWRI796_4616	ESA1	-0.042	1	0
AWRI796_1860	DBF2	-0.031	1	0	AWRI796_4880	TFB2	-0.042	1	0
AWRI796_2621	VTC4	-0.031	1	0	AWRI796_4953	YPL034W	-0.042	1	0
AWRI796_2709	AIM25	-0.031	1	0	AWRI796_5073	YPR109W	-0.042	1	0
AWRI796_2998	YKR051W	-0.031	1	0	AWRI796_0092	RPL32	-0.043	1	0
AWRI796_3072	PRP19	-0.031	1	0	AWRI796_0962	SEC26	-0.043	1	0
AWRI796_3558	GAL80	-0.031	1	0	AWRI796_1327	SAP1	-0.043	1	0
AWRI796_3942	PUS4	-0.031	1	0	AWRI796_1441	BCK2	-0.043	1	0

AWRI796 Gene ID	Gene Name	log_2 Fold Change	Adj. *p* -value	Score	AWRI796 Gene ID	Gene Name	log_2 Fold Change	Adj. *p* -value	Score
AWRI796_1981	PFK1	-0.043	1	0	AWRI796_3112	NSE1	-0.059	1	0
AWRI796_2527	PBS2	-0.043	1	0	AWRI796_3940	RIM21	-0.059	1	0
AWRI796_2556	GWT1	-0.043	1	0	AWRI796_4841	REV3	-0.059	1	0
AWRI796_4930	TIM50	-0.043	1	0	AWRI796_1200	URC2	-0.06	1	0
AWRI796_1013	ATP5	-0.044	1	0	AWRI796_1304	PRO3	-0.06	1	0
AWRI796_1470	FMP32	-0.044	1	0	AWRI796_1770	PDR1	-0.06	1	0
AWRI796_2936	SWD2	-0.044	1	0	AWRI796_2417	DJP1	-0.06	1	0
AWRI796_4391	DIS3	-0.044	1	0	AWRI796_2631	SAG1	-0.06	1	0
AWRI796_4578	LIP5	-0.044	1	0	AWRI796_3400	BUD8	-0.06	1	0
AWRI796_4627	CDC31	-0.044	1	0	AWRI796_4165	FAP1	-0.06	1	0
AWRI796_2595	RTT101	-0.045	1	0	AWRI796_5065	SNT309	-0.06	1	0
AWRI796_2903	NUP120	-0.045	1	0	AWRI796_1034	MRPL35	-0.061	1	0
AWRI796_3066	RPL8B	-0.045	1	0	AWRI796_1852	MRP13	-0.061	1	0
AWRI796_3228	SLX4	-0.045	1	0	AWRI796_2294	CCT2	-0.061	1	0
AWRI796_3315	GPN3	-0.045	1	0	AWRI796_2300	VHS2	-0.061	1	0
AWRI796_3522	PRE8	-0.045	1	0	AWRI796_2803	LST4	-0.061	1	0
AWRI796_4141	VAC7	-0.045	1	0	AWRI796_3901	YMR315W	-0.061	1	0
AWRI796_4431	HSP10	-0.045	1	0	AWRI796_4172	SIW14	-0.061	1	0
AWRI796_4489	PTC5	-0.045	1	0	AWRI796_4375	RPS15	-0.061	1	0
AWRI796_5116	ORC4	-0.045	1	0	AWRI796_4816	DDC1	-0.061	1	0
AWRI796_0141	HEK2	-0.046	1	0	AWRI796_5002	MCM4	-0.061	1	0
AWRI796_1624	COX4	-0.046	1	0	AWRI796_0807	YDR061W	-0.062	1	0
AWRI796_3203	SEN2	-0.046	1	0	AWRI796_0883A	NUM1	-0.062	1	0
AWRI796_3874	NGL2	-0.046	1	0	AWRI796_1485	CAK1	-0.062	1	0
AWRI796_3902	DIA1	-0.046	1	0	AWRI796_2528	SPT10	-0.062	1	0
AWRI796_4095	CYB5	-0.046	1	0	AWRI796_4097	YAF9	-0.062	1	0
AWRI796_4249	YNR068C	-0.046	1	0	AWRI796_4508	AZF1	-0.062	1	0
AWRI796_1580	YGL242C	-0.047	1	0	AWRI796_5138	MLC2	-0.062	1	0
AWRI796_2464	CBP1	-0.047	1	0	AWRI796_0374	ARC40	-0.063	1	0
AWRI796_2865	UTP11	-0.047	1	0	AWRI796_1790	NMA2	-0.063	1	0
AWRI796_3397	ORM2	-0.047	1	0	AWRI796_3213	CLF1	-0.063	1	0
AWRI796_3498	NGL3	-0.047	1	0	AWRI796_3371	MRPL15	-0.063	1	0
AWRI796_3634	RCH1	-0.047	1	0	AWRI796_3588	TAF11	-0.063	1	0
AWRI796_3690	ATP25	-0.047	1	0	AWRI796_4117	SAL1	-0.063	1	0
AWRI796_0310	AMN1	-0.048	1	0	AWRI796_4134	YDJ1	-0.063	1	0
AWRI796_1832	ERG25	-0.048	1	0	AWRI796_5106	SUE1	-0.063	1	0
AWRI796_2992	UIP5	-0.048	1	0	AWRI796_2244	IKI1	-0.064	1	0
AWRI796_3733	NDE1	-0.048	1	0	AWRI796_3140	YLR036C	-0.064	1	0
AWRI796_4400	HRD1	-0.048	1	0	AWRI796_3280	COQ9	-0.064	1	0
AWRI796_5063	YPR097W	-0.048	1	0	AWRI796_4603	MCP1	-0.064	1	0
AWRI796_1609	SIP2	-0.049	1	0	AWRI796_1584	HAP2	-0.065	1	0
AWRI796_4048	SKO1	-0.049	1	0	AWRI796_3037	SRP40	-0.065	1	0
AWRI796_4452	STD1	-0.049	1	0	AWRI796_3757	ALD2	-0.065	1	0
AWRI796_4809	TPK2	-0.049	1	0	AWRI796_3922	PFS2	-0.065	1	0
AWRI796_0778	SES1	-0.05	1	0	AWRI796_3974	GIS2	-0.065	1	0
AWRI796_1055	PAL1	-0.05	1	0	AWRI796_4123	MKS1	-0.065	1	0
AWRI796_1365	GET2	-0.05	1	0	AWRI796_4352	MET22	-0.065	1	0
AWRI796_1381	RPS8B	-0.05	1	0	AWRI796_4546	NFI1	-0.065	1	0
AWRI796_1764	CKB1	-0.05	1	0	AWRI796_4835	MRPL40	-0.065	1	0
AWRI796_2391	YNL284C-B	-0.05	1	0	AWRI796_0299	RTC2	-0.066	1	0
AWRI796_2563	TAX4	-0.05	1	0	AWRI796_0526	TAH1	-0.066	1	0
AWRI796_3111	SSK1	-0.05	1	0	AWRI796_0963	YDR239C	-0.066	1	0
AWRI796_4935	SUR1	-0.05	1	0	AWRI796_1302	RPN3	-0.066	1	0
AWRI796_5137	PZF1	-0.05	1	0	AWRI796_2515	TIM17	-0.066	1	0
AWRI796_1724	AFT1	-0.051	1	0	AWRI796_4644	CAF20	-0.066	1	0
AWRI796_1727	SGF73	-0.051	1	0	AWRI796_4883	MRP51	-0.066	1	0
AWRI796_1977	MIC26	-0.051	1	0	AWRI796_5035	JID1	-0.066	1	0
AWRI796_2252	NVJ1	-0.051	1	0	AWRI796_5159	AWRI796_5159	-0.066	1	0
AWRI796_2327	PFK26	-0.051	1	0	AWRI796_1752	YGL036W	-0.067	1	0
AWRI796_3943	MID1	-0.051	1	0	AWRI796_1986	CPD1	-0.067	1	0
AWRI796_4488	VPS21	-0.051	1	0	AWRI796_2352	SEC28	-0.067	1	0
AWRI796_0119	PTH2	-0.052	1	0	AWRI796_4196	URK1	-0.067	1	0
AWRI796_0303	APD1	-0.052	1	0	AWRI796_5059	YPR089W	-0.067	1	0
AWRI796_1523	IOC3	-0.052	1	0	AWRI796_0996	RNH202	-0.068	1	0
AWRI796_1695	MLC1	-0.052	1	0	AWRI796_1895	CAF130	-0.068	1	0
AWRI796_1942	PDX1	-0.052	1	0	AWRI796_2382	TED1	-0.068	1	0
AWRI796_2533	RPE1	-0.052	1	0	AWRI796_3266	EMG1	-0.068	1	0
AWRI796_0507	RBK1	-0.053	1	0	AWRI796_3423	SMC6	-0.068	1	0
AWRI796_0538	FUB1	-0.053	1	0	AWRI796_3694	YMR102C	-0.068	1	0
AWRI796_2967	HEL1	-0.053	1	0	AWRI796_4018	SPS18	-0.068	1	0
AWRI796_3310	FAR10	-0.053	1	0	AWRI796_4040	RPS3	-0.068	1	0
AWRI796_4044	MDG1	-0.053	1	0	AWRI796_4538	SPP2	-0.068	1	0
AWRI796_4283	RRP40	-0.053	1	0	AWRI796_5074	RPC40	-0.068	1	0
AWRI796_4989	AIM45	-0.053	1	0	AWRI796_0672	KIN28	-0.069	1	0
AWRI796_1896	LSB1	-0.054	1	0	AWRI796_0943	RAD9	-0.069	1	0
AWRI796_1913	CHO2	-0.054	1	0	AWRI796_1015	PRO1	-0.069	1	0
AWRI796_3534	WAR1	-0.054	1	0	AWRI796_1674	RSM23	-0.069	1	0
AWRI796_4823	MF(ALPHA)1	-0.054	1	0	AWRI796_4608	KIN4	-0.069	1	0
AWRI796_0341	MED8	-0.055	1	0	AWRI796_0494	MAK32	-0.07	1	0
AWRI796_0737	ARP2	-0.055	1	0	AWRI796_0747	TSC13	-0.07	1	0
AWRI796_3165	ENV10	-0.055	1	0	AWRI796_1471	SEC53	-0.07	1	0
AWRI796_4041	MRPL22	-0.055	1	0	AWRI796_1972	SMI1	-0.07	1	0
AWRI796_4478	BUD21	-0.055	1	0	AWRI796_3737	SWP1	-0.07	1	0
AWRI796_0237	RDH54	-0.056	1	0	AWRI796_0085	SFT2	-0.071	1	0
AWRI796_0843	SPO71	-0.056	1	0	AWRI796_0485	SAT4	-0.071	1	0
AWRI796_1241	FRD1	-0.056	1	0	AWRI796_0627	ENT1	-0.071	1	0
AWRI796_1987	SOL4	-0.056	1	0	AWRI796_0907	RSM24	-0.071	1	0
AWRI796_2348	CAB2	-0.056	1	0	AWRI796_2587	YJL055W	-0.071	1	0
AWRI796_4301	RPS19A	-0.056	1	0	AWRI796_3979	RAD50	-0.071	1	0
AWRI796_0018	AIM1	-0.057	1	0	AWRI796_0146	RRN10	-0.072	1	0
AWRI796_0676	QRI7	-0.057	1	0	AWRI796_0139	STU1	-0.073	1	0
AWRI796_1400	GLO3	-0.057	1	0	AWRI796_0573	SHS1	-0.073	1	0
AWRI796_3826	YMR244W	-0.057	1	0	AWRI796_0691	ASM4	-0.073	1	0
AWRI796_4361	THI20	-0.057	1	0	AWRI796_1448	GRX4	-0.073	1	0
AWRI796_4533	LSC1	-0.057	1	0	AWRI796_2851	PRR1	-0.073	1	0
AWRI796_4775	YAR1	-0.057	1	0	AWRI796_2935	RAM2	-0.073	1	0
AWRI796_4777	ENV7	-0.057	1	0	AWRI796_3859	TMA23	-0.073	1	0
AWRI796_1180	RSM28	-0.058	1	0	AWRI796_0365	PCS60	-0.074	1	0
AWRI796_1597	COG1	-0.058	1	0	AWRI796_0522	THR4	-0.074	1	0
AWRI796_3858	PRP24	-0.058	1	0	AWRI796_1686	CDC20	-0.074	1	0
AWRI796_1039	SKP1	-0.059	1	0	AWRI796_3378	SFH1	-0.074	1	0
AWRI796_1380	AST2	-0.059	1	0	AWRI796_3819	BCH1	-0.074	1	0
AWRI796_1555	RMD8	-0.059	1	0	AWRI796_3821	RNT1	-0.074	1	0
AWRI796_2208	IMP3	-0.059	1	0	AWRI796_4031	SRP1	-0.074	1	0
AWRI796_2487	SWI3	-0.059	1	0	AWRI796_4609	DFR1	-0.074	1	0
AWRI796_2544	PAM16	-0.059	1	0	AWRI796_0067	ADE1	-0.075	1	0
AWRI796_2977	BCH2	-0.059	1	0	AWRI796_0622	SFA1	-0.075	1	0

AWRI796 Gene ID	Gene Name	$\log_2$ Fold Change	Adj. p-value	Score	AWRI796 Gene ID	Gene Name	$\log_2$ Fold Change	Adj. p-value	Score
AWRI796_1256	ECM10	-0.075	1	0	AWRI796_0700	VAM6	-0.091	1	0
AWRI796_1332	JHD1	-0.075	1	0	AWRI796_1204	RBA50	-0.091	1	0
AWRI796_2477	SOP4	-0.075	1	0	AWRI796_1274	GCN4	-0.091	1	0
AWRI796_2669	RAD7	-0.075	1	0	AWRI796_1938	HGH1	-0.091	1	0
AWRI796_2690	HOC1	-0.075	1	0	AWRI796_2964	YPT52	-0.091	1	0
AWRI796_4903	SEC62	-0.075	1	0	AWRI796_3994	BNI4	-0.091	1	0
AWRI796_0087	ATP1	-0.076	1	0	AWRI796_4010	PEX17	-0.091	1	0
AWRI796_0802	PST1	-0.076	1	0	AWRI796_4064	PGA2	-0.091	1	0
AWRI796_2051	RIM4	-0.076	1	0	AWRI796_4130	FKH2	-0.091	1	0
AWRI796_2353	RPN2	-0.076	1	0	AWRI796_4275	DCP1	-0.091	1	0
AWRI796_4338	REX4	-0.076	1	0	AWRI796_4485	OST3	-0.091	1	0
AWRI796_0688	UBX3	-0.077	1	0	AWRI796_4537	MDM32	-0.091	1	0
AWRI796_0989	CIA1	-0.077	1	0	AWRI796_0010	GPB2	-0.092	1	0
AWRI796_1035	PEP7	-0.077	1	0	AWRI796_0629	STE7	-0.092	1	0
AWRI796_1497	MDJ1	-0.077	1	0	AWRI796_1205	HLR1	-0.092	1	0
AWRI796_2598	GYP6	-0.077	1	0	AWRI796_1673	CEG1	-0.092	1	0
AWRI796_2618	YJL016W	-0.077	1	0	AWRI796_1842	UPF3	-0.092	1	0
AWRI796_2968	YKR018C	-0.077	1	0	AWRI796_2470	ECM25	-0.092	1	0
AWRI796_0987	PEX10	-0.078	1	0	AWRI796_2821	GPM1	-0.092	1	0
AWRI796_2195	NSG1	-0.078	1	0	AWRI796_4137	ARP5	-0.092	1	0
AWRI796_2434	DAL81	-0.078	1	0	AWRI796_4483	WHI5	-0.092	1	0
AWRI796_3187	GAA1	-0.078	1	0	AWRI796_4793	RPL1A	-0.092	1	0
AWRI796_3282	QRI5	-0.078	1	0	AWRI796_5130	PRP4	-0.092	1	0
AWRI796_3552	CMP2	-0.078	1	0	AWRI796_0772	KCS1	-0.093	1	0
AWRI796_3644	IOC4	-0.078	1	0	AWRI796_0830	AFR1	-0.093	1	0
AWRI796_5107	URN1	-0.078	1	0	AWRI796_1097	RPT3	-0.093	1	0
AWRI796_0032	POP5	-0.079	1	0	AWRI796_1145	TSA2	-0.093	1	0
AWRI796_0131	PRE7	-0.079	1	0	AWRI796_1738	OLE1	-0.093	1	0
AWRI796_1641	CUP2	-0.079	1	0	AWRI796_2044	OCA5	-0.093	1	0
AWRI796_1725	MNP1	-0.079	1	0	AWRI796_2482	MNN11	-0.093	1	0
AWRI796_3386	NUP2	-0.079	1	0	AWRI796_3240	PEP3	-0.093	1	0
AWRI796_3405	ADE13	-0.079	1	0	AWRI796_3293	CDC123	-0.093	1	0
AWRI796_0824	PET100	-0.08	1	0	AWRI796_3476	VMA6	-0.093	1	0
AWRI796_0836	GIS1	-0.08	1	0	AWRI796_4038	YNL181W	-0.093	1	0
AWRI796_0863	SWF1	-0.08	1	0	AWRI796_4051	IBD2	-0.093	1	0
AWRI796_2623	CCT8	-0.08	1	0	AWRI796_4074	FPR1	-0.093	1	0
AWRI796_2749	RPS4A	-0.08	1	0	AWRI796_4382	SIL1	-0.093	1	0
AWRI796_2901	MPE1	-0.08	1	0	AWRI796_5077	PIS1	-0.093	1	0
AWRI796_2973	YKR023W	-0.08	1	0	AWRI796_0797	VMS1	-0.094	1	0
AWRI796_3030	MRPL20	-0.08	1	0	AWRI796_0978	CTA1	-0.094	1	0
AWRI796_1070	KEI1	-0.081	1	0	AWRI796_1138	SSN2	-0.094	1	0
AWRI796_3085	HIF1	-0.081	1	0	AWRI796_1294	PRP22	-0.094	1	0
AWRI796_3649	STB2	-0.081	1	0	AWRI796_1487	GYP8	-0.094	1	0
AWRI796_4239	BIO3	-0.081	1	0	AWRI796_3099	LMO1	-0.094	1	0
AWRI796_4494	RKI1	-0.081	1	0	AWRI796_3669	RCO1	-0.094	1	0
AWRI796_5028	NHP6A	-0.081	1	0	AWRI796_4079	CPT1	-0.094	1	0
AWRI796_5070	ISR1	-0.081	1	0	AWRI796_4554	SEY1	-0.094	1	0
AWRI796_1801	MTL1	-0.082	1	0	AWRI796_4804	IPL1	-0.094	1	0
AWRI796_2181	ORC6	-0.082	1	0	AWRI796_5223	ENA2	-0.094	1	0
AWRI796_2918	PTM1	-0.082	1	0	AWRI796_0285	CCZ1	-0.095	1	0
AWRI796_3336	BOP2	-0.082	1	0	AWRI796_0708	IDP1	-0.095	1	0
AWRI796_0525	YIH1	-0.083	1	0	AWRI796_1151	TFB3	-0.095	1	0
AWRI796_1581	KAP114	-0.083	1	0	AWRI796_2184	LSM12	-0.095	1	0
AWRI796_1794	YGR015C	-0.083	1	0	AWRI796_2715	ECM27	-0.095	1	0
AWRI796_2072	OSH7	-0.083	1	0	AWRI796_3442	YLR407W	-0.095	1	0
AWRI796_2538	CCT7	-0.083	1	0	AWRI796_3762	MMT1	-0.095	1	0
AWRI796_2819	RSM22	-0.083	1	0	AWRI796_3970	LTO1	-0.095	1	0
AWRI796_3243	PCD1	-0.083	1	0	AWRI796_0868	YDR131C	-0.096	1	0
AWRI796_3728	CIN4	-0.083	1	0	AWRI796_1457	TOG1	-0.096	1	0
AWRI796_4178	IDP3	-0.083	1	0	AWRI796_1668	MRM2	-0.096	1	0
AWRI796_4380	MSE1	-0.083	1	0	AWRI796_2606	TAD2	-0.096	1	0
AWRI796_4871	COX11	-0.083	1	0	AWRI796_2607	KAR2	-0.096	1	0
AWRI796_0450	PDI1	-0.084	1	0	AWRI796_2738	MCM22	-0.096	1	0
AWRI796_0512	MATALPHA1	-0.084	1	0	AWRI796_2999	MRS4	-0.096	1	0
AWRI796_1074	CTS2	-0.084	1	0	AWRI796_3153	FCF2	-0.096	1	0
AWRI796_1260	YEL025C	-0.084	1	0	AWRI796_4290	MED7	-0.096	1	0
AWRI796_3211	CFT2	-0.084	1	0	AWRI796_4648	PLP2	-0.096	1	0
AWRI796_4584	GEP3	-0.084	1	0	AWRI796_0431	MAL33	-0.097	1	0
AWRI796_0275	MUD1	-0.085	1	0	AWRI796_0625	CDC36	-0.097	1	0
AWRI796_0969	TRS23	-0.085	1	0	AWRI796_0861	YDR124W	-0.097	1	0
AWRI796_1660	ROG1	-0.085	1	0	AWRI796_1631	MPT5	-0.097	1	0
AWRI796_3303	ADY4	-0.085	1	0	AWRI796_1728	ALG2	-0.097	1	0
AWRI796_3406	DCR2	-0.085	1	0	AWRI796_2952	MET14	-0.097	1	0
AWRI796_0034	GIP4	-0.086	1	0	AWRI796_4434	AHC1	-0.097	1	0
AWRI796_0650	PPH21	-0.086	1	0	AWRI796_4487	YVC1	-0.097	1	0
AWRI796_1927	CBP4	-0.086	1	0	AWRI796_4637	PAC1	-0.097	1	0
AWRI796_4565	SYC1	-0.086	1	0	AWRI796_4886	BEM3	-0.097	1	0
AWRI796_1047	MRX8	-0.087	1	0	AWRI796_5027	MAK3	-0.097	1	0
AWRI796_1172	VPS72	-0.087	1	0	AWRI796_0148	MCM2	-0.098	1	0
AWRI796_1652	LYS5	-0.087	1	0	AWRI796_0330	RPS6B	-0.098	1	0
AWRI796_2493	SET2	-0.087	1	0	AWRI796_0624	FAP7	-0.098	1	0
AWRI796_4645	HEM4	-0.087	1	0	AWRI796_1354	VTC1	-0.098	1	0
AWRI796_4829	PPQ1	-0.087	1	0	AWRI796_1550	IRC6	-0.098	1	0
AWRI796_1736	GEP7	-0.088	1	0	AWRI796_2304	FKH1	-0.098	1	0
AWRI796_1780	ERP6	-0.088	1	0	AWRI796_3758	EAR1	-0.098	1	0
AWRI796_1989	YGR250C	-0.088	1	0	AWRI796_3871	AEP2	-0.098	1	0
AWRI796_2693	BNA2	-0.088	1	0	AWRI796_4416	UTP23	-0.098	1	0
AWRI796_2859	AAT1	-0.088	1	0	AWRI796_5044	YPR071W	-0.098	1	0
AWRI796_4531	SFL1	-0.088	1	0	AWRI796_1467	SWP82	-0.099	1	0
AWRI796_5232	HSP33	-0.088	1	0	AWRI796_2781	MNN4	-0.099	1	0
AWRI796_0033	PRP45	-0.089	1	0	AWRI796_3116	LOT6	-0.099	1	0
AWRI796_0158	FMT1	-0.089	1	0	AWRI796_3759	HOT1	-0.099	1	0
AWRI796_1902	THI4	-0.089	1	0	AWRI796_4553	GET4	-0.099	1	0
AWRI796_2765	SRY1	-0.089	1	0	AWRI796_5124	BSP1	-0.099	1	0
AWRI796_3338	DCS1	-0.089	1	0	AWRI796_0114	PRX1	-0.1	1	0
AWRI796_3702	YMR111C	-0.089	1	0	AWRI796_0872	RGP1	-0.1	1	0
AWRI796_3899	TGL3	-0.089	1	0	AWRI796_1206	QCR7	-0.1	1	0
AWRI796_4513	RTC5	-0.089	1	0	AWRI796_1894	PEX4	-0.1	1	0
AWRI796_4622	TMA16	-0.089	1	0	AWRI796_2364	ARC15	-0.1	1	0
AWRI796_0939	TCP1	-0.09	1	0	AWRI796_2551	MRPL49	-0.1	1	0
AWRI796_1111	STE14	-0.09	1	0	AWRI796_3279	YKE2	-0.1	1	0
AWRI796_2189	YHR127W	-0.09	1	0	AWRI796_0438	KRR1	-0.101	1	0
AWRI796_2369	GPP1	-0.09	1	0	AWRI796_0572	GCS1	-0.101	1	0
AWRI796_2879	MDH1	-0.09	1	0	AWRI796_1073	DXO1	-0.101	1	0
AWRI796_4451	DBP5	-0.09	1	0	AWRI796_1104	DIT1	-0.101	1	0
AWRI796_4471	GYP1	-0.09	1	0	AWRI796_1169	CWC21	-0.101	1	0
AWRI796_0199	HMT1	-0.091	1	0	AWRI796_1978	YGR237C	-0.101	1	0

AWRI796 Gene ID	Gene Name	$\log_2$ Fold Change	Adj. p-value	Score	AWRI796 Gene ID	Gene Name	$\log_2$ Fold Change	Adj. p-value	Score
AWRI796_2483	YJL181W	-0.101	1	0	AWRI796_1717	MPC1	-0.115	1	0
AWRI796_0071	YAR023C	-0.102	1	0	AWRI796_2099	SLT2	-0.115	1	0
AWRI796_0514	YCR043C	-0.102	1	0	AWRI796_3815	TRI1	-0.115	1	0
AWRI796_0599	ASF2	-0.102	1	0	AWRI796_0207	CST26	-0.116	1	0
AWRI796_0886	ENT5	-0.102	1	0	AWRI796_0250	IST2	-0.116	1	0
AWRI796_1130	GPI17	-0.102	1	0	AWRI796_1053	SVF1	-0.116	1	0
AWRI796_1283	NOP16	-0.102	1	0	AWRI796_1057	ATP22	-0.116	1	0
AWRI796_1340	PCL6	-0.102	1	0	AWRI796_1388	KAP123	-0.116	1	0
AWRI796_2674	CDC8	-0.102	1	0	AWRI796_2400	VID28	-0.116	1	0
AWRI796_3068	ATG10	-0.102	1	0	AWRI796_2733	EFM3	-0.116	1	0
AWRI796_3219	YLR126C	-0.102	1	0	AWRI796_3290	TUB4	-0.116	1	0
AWRI796_3284	ENT2	-0.102	1	0	AWRI796_3300	UCC1	-0.116	1	0
AWRI796_3997	URE2	-0.102	1	0	AWRI796_0654	YDL129W	-0.117	1	0
AWRI796_4289	PFK27	-0.102	1	0	AWRI796_2392	EMC5	-0.117	1	0
AWRI796_4379	SMC5	-0.102	1	0	AWRI796_2894	YNK1	-0.117	1	0
AWRI796_1861	DRN1	-0.103	1	0	AWRI796_3084	POM33	-0.117	1	0
AWRI796_2209	SKG6	-0.103	1	0	AWRI796_3403	ATG33	-0.117	1	0
AWRI796_2804	ZRT3	-0.103	1	0	AWRI796_3820	DFG5	-0.117	1	0
AWRI796_2971	ALY1	-0.103	1	0	AWRI796_3885	DYN3	-0.117	1	0
AWRI796_3502	TAF8	-0.103	1	0	AWRI796_4500	PIN2	-0.117	1	0
AWRI796_3689	MTG1	-0.103	1	0	AWRI796_0150	HAP3	-0.118	1	0
AWRI796_1058	SBE2	-0.104	1	0	AWRI796_1705	VPS45	-0.118	1	0
AWRI796_2573	ARG2	-0.104	1	0	AWRI796_3473	ECM7	-0.118	1	0
AWRI796_2847	DGR2	-0.104	1	0	AWRI796_0801	CDC34	-0.119	1	0
AWRI796_3103	SFI1	-0.104	1	0	AWRI796_0821	RAD55	-0.119	1	0
AWRI796_4327	SPO21	-0.104	1	0	AWRI796_1849	SLX9	-0.119	1	0
AWRI796_1178	IZH1	-0.105	1	0	AWRI796_2839	SHE2	-0.119	1	0
AWRI796_1713	LCL3	-0.105	1	0	AWRI796_3784	ROT1	-0.119	1	0
AWRI796_1811	RPL26B	-0.105	1	0	AWRI796_4143	COX5A	-0.119	1	0
AWRI796_1974	NAS6	-0.105	1	0	AWRI796_4420	SLG1	-0.119	1	0
AWRI796_3580	NSE5	-0.105	1	0	AWRI796_4988	YPR003C	-0.119	1	0
AWRI796_4023	WHI3	-0.105	1	0	AWRI796_0750	GRX6	-0.12	1	0
AWRI796_4169	CRZ1	-0.105	1	0	AWRI796_0775	DAS2	-0.12	1	0
AWRI796_4308	MSB4	-0.105	1	0	AWRI796_0979	RKM4	-0.12	1	0
AWRI796_4914	SEN54	-0.105	1	0	AWRI796_4065	ALF1	-0.12	1	0
AWRI796_4951	EGD1	-0.105	1	0	AWRI796_4426	RTS1	-0.12	1	0
AWRI796_0243	SEC18	-0.106	1	0	AWRI796_0371	OM14	-0.121	1	0
AWRI796_0832	SLU7	-0.106	1	0	AWRI796_0393	TRS20	-0.121	1	0
AWRI796_0899	CDC37	-0.106	1	0	AWRI796_0604	UFD2	-0.121	1	0
AWRI796_3221	DCN1	-0.106	1	0	AWRI796_0837	MSH6	-0.121	1	0
AWRI796_3508	YML108W	-0.106	1	0	AWRI796_0893	NBP2	-0.121	1	0
AWRI796_3915	PFA3	-0.106	1	0	AWRI796_1782	EFM5	-0.121	1	0
AWRI796_3954	PRM1	-0.106	1	0	AWRI796_2305	ASG1	-0.121	1	0
AWRI796_4457	TMC1	-0.106	1	0	AWRI796_3194	IOC2	-0.121	1	0
AWRI796_1239	VMA8	-0.107	1	0	AWRI796_3875	DSS1	-0.121	1	0
AWRI796_1288	PAC2	-0.107	1	0	AWRI796_5064	MRPL51	-0.121	1	0
AWRI796_3936	TRF5	-0.107	1	0	AWRI796_5082	MRI1	-0.121	1	0
AWRI796_4206	MRPL50	-0.107	1	0	AWRI796_0862	ECM18	-0.122	1	0
AWRI796_0063	SWD1	-0.108	1	0	AWRI796_2211	MTC6	-0.122	1	0
AWRI796_0368	MCX1	-0.108	1	0	AWRI796_2227	THP2	-0.122	1	0
AWRI796_0369	SLX1	-0.108	1	0	AWRI796_2260	RPS4B	-0.122	1	0
AWRI796_0470	LEU2	-0.108	1	0	AWRI796_4702	TYE7	-0.122	1	0
AWRI796_0923	NUP42	-0.108	1	0	AWRI796_4818	PRM3	-0.122	1	0
AWRI796_1284	PMI40	-0.108	1	0	AWRI796_0347	KTR4	-0.123	1	0
AWRI796_1514	RPN11	-0.108	1	0	AWRI796_1476	ACT1	-0.123	1	0
AWRI796_2218	KEL1	-0.108	1	0	AWRI796_2950	MRP17	-0.123	1	0
AWRI796_2975	RPC37	-0.108	1	0	AWRI796_3166	SPC3	-0.123	1	0
AWRI796_3185	SMC4	-0.108	1	0	AWRI796_3250	SEC10	-0.123	1	0
AWRI796_4050	YNL165W	-0.108	1	0	AWRI796_5033	YMC1	-0.123	1	0
AWRI796_4128	LAT1	-0.108	1	0	AWRI796_0425	BSD2	-0.124	1	0
AWRI796_0136	YBL036C	-0.109	1	0	AWRI796_0565	YPD1	-0.124	1	0
AWRI796_0804	YOS9	-0.109	1	0	AWRI796_1556	PRE4	-0.124	1	0
AWRI796_0869	YDR132C	-0.109	1	0	AWRI796_2613	RNR2	-0.124	1	0
AWRI796_2036	CBP2	-0.109	1	0	AWRI796_2921	TUL1	-0.124	1	0
AWRI796_2219	TDA11	-0.109	1	0	AWRI796_2948	BYE1	-0.124	1	0
AWRI796_2359	SEC6	-0.109	1	0	AWRI796_3772	YMR187C	-0.124	1	0
AWRI796_2363	YRB2	-0.109	1	0	AWRI796_3854	CUE1	-0.124	1	0
AWRI796_4340	BRX1	-0.109	1	0	AWRI796_4430	YOR019W	-0.124	1	0
AWRI796_0895	SEC1	-0.11	1	0	AWRI796_4895	MSD1	-0.124	1	0
AWRI796_1176	SLD5	-0.11	1	0	AWRI796_5164	AWRI796_5164	-0.124	1	0
AWRI796_1289	SEC3	-0.11	1	0	AWRI796_0278	TFC1	-0.125	1	0
AWRI796_1696	ARC1	-0.11	1	0	AWRI796_1160	TRS31	-0.125	1	0
AWRI796_2039	SBP1	-0.11	1	0	AWRI796_3033	TVP38	-0.125	1	0
AWRI796_3475	YLR446W	-0.11	1	0	AWRI796_3620	YMR018W	-0.125	1	0
AWRI796_3554	SPC2	-0.11	1	0	AWRI796_4756	YPL260W	-0.125	1	0
AWRI796_4113	TOP2	-0.11	1	0	AWRI796_0111	PRS4	-0.126	1	0
AWRI796_0030	MTW1	-0.111	1	0	AWRI796_0339	RPL21A	-0.126	1	0
AWRI796_0610	LYS20	-0.111	1	0	AWRI796_2355	SPO22	-0.126	1	0
AWRI796_0675	NSE4	-0.111	1	0	AWRI796_2658	URB2	-0.126	1	0
AWRI796_0829	TVP23	-0.111	1	0	AWRI796_2863	HSL1	-0.126	1	0
AWRI796_1682	GPG1	-0.111	1	0	AWRI796_2871	MBR1	-0.126	1	0
AWRI796_1773	MPO1	-0.111	1	0	AWRI796_2969	IRS4	-0.126	1	0
AWRI796_2938	ATP7	-0.111	1	0	AWRI796_4516	LEO1	-0.126	1	0
AWRI796_2951	DID4	-0.111	1	0	AWRI796_0055	SPO7	-0.127	1	0
AWRI796_4417	DNL4	-0.111	1	0	AWRI796_1118	RAD30	-0.127	1	0
AWRI796_4822	POS5	-0.111	1	0	AWRI796_1293	PRE1	-0.127	1	0
AWRI796_5227	AWRI796_5227	-0.111	1	0	AWRI796_2809	MRPL38	-0.127	1	0
AWRI796_0211	ZTA1	-0.112	1	0	AWRI796_3003	TRM2	-0.127	1	0
AWRI796_0456	GRX1	-0.112	1	0	AWRI796_3251	RPS31	-0.127	1	0
AWRI796_0725	FAD1	-0.112	1	0	AWRI796_4596	RCN2	-0.127	1	0
AWRI796_1186	PLM2	-0.112	1	0	AWRI796_4833	SPT14	-0.127	1	0
AWRI796_1258	VMA3	-0.112	1	0	AWRI796_0585	SHR3	-0.128	1	0
AWRI796_2739	TTI2	-0.112	1	0	AWRI796_1509	SPB4	-0.128	1	0
AWRI796_3863	RCE1	-0.112	1	0	AWRI796_2685	HAM1	-0.128	1	0
AWRI796_4757	APM1	-0.112	1	0	AWRI796_3296	MSC3	-0.128	1	0
AWRI796_2800	RPL17A	-0.113	1	0	AWRI796_3429	ECM19	-0.128	1	0
AWRI796_4857	ATG5	-0.113	1	0	AWRI796_4515	GCY1	-0.128	1	0
AWRI796_4991	ICL2	-0.113	1	0	AWRI796_4801	PUS1	-0.128	1	0
AWRI796_0112	UBP13	-0.114	1	0	AWRI796_0125	SEC17	-0.129	1	0
AWRI796_1078	BCS1	-0.114	1	0	AWRI796_0736	PRP9	-0.129	1	0
AWRI796_1675	CWC23	-0.114	1	0	AWRI796_0809	AIM7	-0.129	1	0
AWRI796_3432	ATP10	-0.114	1	0	AWRI796_1108	TRS120	-0.129	1	0
AWRI796_3984	SUI1	-0.114	1	0	AWRI796_2578	DLS1	-0.129	1	0
AWRI796_4139	OCA2	-0.114	1	0	AWRI796_2805	TPO5	-0.129	1	0
AWRI796_4860	NOP53	-0.114	1	0	AWRI796_2812	MCD4	-0.129	1	0
AWRI796_0404	MRPL37	-0.115	1	0	AWRI796_3808	MRE11	-0.129	1	0
AWRI796_1511	LOC1	-0.115	1	0	AWRI796_4981	AEP3	-0.129	1	0

AWRI796 Gene ID	Gene Name	$\log_2$ Fold Change	Adj. p-value	Score	AWRI796 Gene ID	Gene Name	$\log_2$ Fold Change	Adj. p-value	Score
AWRI796_5032	BRR1	-0.129	1	0	AWRI796_5010	APL4	-0.143	1	0
AWRI796_5217	DDI2	-0.129	1	0	AWRI796_1955	CIR1	-0.144	1	0
AWRI796_0799	DET1	-0.13	1	0	AWRI796_2012	RNH70	-0.144	1	0
AWRI796_1040	PEX3	-0.13	1	0	AWRI796_2570	SMC3	-0.144	1	0
AWRI796_1165	SNM1	-0.13	1	0	AWRI796_2775	CBT1	-0.144	1	0
AWRI796_1276	YEA6	-0.13	1	0	AWRI796_3302	BUR2	-0.144	1	0
AWRI796_1576	PDE1	-0.13	1	0	AWRI796_3683	NPL6	-0.144	1	0
AWRI796_1966	TOS2	-0.13	1	0	AWRI796_4164	RCM1	-0.144	1	0
AWRI796_2287	MCM10	-0.13	1	0	AWRI796_4613	MET7	-0.144	1	0
AWRI796_3011	PAM17	-0.13	1	0	AWRI796_4720	PIP2	-0.144	1	0
AWRI796_3480	SST2	-0.13	1	0	AWRI796_0814	DOS2	-0.145	1	0
AWRI796_3969	ORC5	-0.13	1	0	AWRI796_1063	CNL1	-0.145	1	0
AWRI796_5266	REP1	-0.13	1	0	AWRI796_2302	RPL16A	-0.145	1	0
AWRI796_0152	APN2	-0.131	1	0	AWRI796_2336	BMT5	-0.145	1	0
AWRI796_0563	AIM6	-0.131	1	0	AWRI796_2614	RRN7	-0.145	1	0
AWRI796_1147	NHX1	-0.131	1	0	AWRI796_3132	AAT2	-0.145	1	0
AWRI796_1401	YCK3	-0.131	1	0	AWRI796_4830	CBC2	-0.145	1	0
AWRI796_2013	CAB4	-0.131	1	0	AWRI796_0926	CAB5	-0.146	1	0
AWRI796_2947	CAP1	-0.131	1	0	AWRI796_1125	BNA7	-0.146	1	0
AWRI796_2958	MEH1	-0.131	1	0	AWRI796_2410	EPS1	-0.146	1	0
AWRI796_0222	UBP14	-0.132	1	0	AWRI796_2953	VPS1	-0.146	1	0
AWRI796_0649	RDI1	-0.132	1	0	AWRI796_3401	TAL1	-0.146	1	0
AWRI796_1578	RTF1	-0.132	1	0	AWRI796_3512	MDM1	-0.146	1	0
AWRI796_1763	GET1	-0.132	1	0	AWRI796_4966	ULP1	-0.146	1	0
AWRI796_2610	MAD2	-0.132	1	0	AWRI796_4990	HAL1	-0.146	1	0
AWRI796_2641	YJR015W	-0.132	1	0	AWRI796_1653	PEX14	-0.147	1	0
AWRI796_2906	DEF1	-0.132	1	0	AWRI796_1785	PEX31	-0.147	1	0
AWRI796_3492	PGA3	-0.132	1	0	AWRI796_3156	OSW2	-0.147	1	0
AWRI796_3857	PPA2	-0.132	1	0	AWRI796_4711	MSC6	-0.147	1	0
AWRI796_4634	RBL2	-0.132	1	0	AWRI796_0471	NFS1	-0.148	1	0
AWRI796_0500	RHB1	-0.133	1	0	AWRI796_0586	YDL211C	-0.148	1	0
AWRI796_5055	YPR084W	-0.133	1	0	AWRI796_0800	DBF4	-0.148	1	0
AWRI796_1227	AVT2	-0.134	1	0	AWRI796_0887	CPR1	-0.148	1	0
AWRI796_1331	RSM18	-0.134	1	0	AWRI796_2683	YAE1	-0.148	1	0
AWRI796_1630	TOS3	-0.134	1	0	AWRI796_3193	GIS3	-0.148	1	0
AWRI796_2175	UBA4	-0.134	1	0	AWRI796_3913	MDJ2	-0.148	1	0
AWRI796_2462	OPT1	-0.134	1	0	AWRI796_4324	RFC4	-0.148	1	0
AWRI796_4776	SUI3	-0.134	1	0	AWRI796_4715	HAP5	-0.148	1	0
AWRI796_5043	MED1	-0.134	1	0	AWRI796_0062	ERP1	-0.149	1	0
AWRI796_0385	ISW1	-0.135	1	0	AWRI796_0180	YBR013C	-0.149	1	0
AWRI796_0506	RRP43	-0.135	1	0	AWRI796_1409	RPS26B	-0.149	1	0
AWRI796_4014	SSB2	-0.135	1	0	AWRI796_3515	CUE4	-0.149	1	0
AWRI796_5119	RHO1	-0.135	1	0	AWRI796_3754	MLH1	-0.149	1	0
AWRI796_0091	ROX3	-0.136	1	0	AWRI796_4346	NBA1	-0.149	1	0
AWRI796_0426	CTP1	-0.136	1	0	AWRI796_4928	VPS28	-0.149	1	0
AWRI796_1071	YPR1	-0.136	1	0	AWRI796_5052	GRS2	-0.149	1	0
AWRI796_1114	ERD1	-0.136	1	0	AWRI796_0084	RTG3	-0.15	1	0
AWRI796_3485	GAB1	-0.136	1	0	AWRI796_0553	CDC50	-0.15	1	0
AWRI796_3536	FPR3	-0.136	1	0	AWRI796_0785	LYS14	-0.15	1	0
AWRI796_3735	YMR147W	-0.136	1	0	AWRI796_1043	IRC3	-0.15	1	0
AWRI796_0204	ATP3	-0.137	1	0	AWRI796_2662	SSC1	-0.15	1	0
AWRI796_0386	RRT2	-0.137	1	0	AWRI796_3337	SEC22	-0.15	1	0
AWRI796_0614	YDL177C	-0.137	1	0	AWRI796_3370	ATG39	-0.15	1	0
AWRI796_1012	SUR2	-0.137	1	0	AWRI796_3704	FOL3	-0.15	1	0
AWRI796_1029	OMS1	-0.137	1	0	AWRI796_3977	MRPL17	-0.15	1	0
AWRI796_1749	YGL039W	-0.137	1	0	AWRI796_5090	ANT1	-0.15	1	0
AWRI796_2010	TAF1	-0.137	1	0	AWRI796_0590	GLE1	-0.151	1	0
AWRI796_3456	SPP382	-0.137	1	0	AWRI796_1442	CCA1	-0.151	1	0
AWRI796_3834	PET111	-0.137	1	0	AWRI796_3651	BUB2	-0.151	1	0
AWRI796_4313	YOL107W	-0.137	1	0	AWRI796_4502	RGS2	-0.151	1	0
AWRI796_4523	ORT1	-0.137	1	0	AWRI796_5244	YNL284C-B	-0.151	1	0
AWRI796_4561	ALE1	-0.137	1	0	AWRI796_0405	SDH8	-0.152	1	0
AWRI796_0138	POL12	-0.138	1	0	AWRI796_0876	PEX7	-0.152	1	0
AWRI796_0440	KAR4	-0.138	1	0	AWRI796_1234	HAT2	-0.152	1	0
AWRI796_4119	EOS1	-0.138	1	0	AWRI796_2586	ZAP1	-0.152	1	0
AWRI796_4211	CPR8	-0.138	1	0	AWRI796_4447	CKB2	-0.152	1	0
AWRI796_4691	VMA4	-0.138	1	0	AWRI796_4560	MED4	-0.152	1	0
AWRI796_4767	GAL4	-0.138	1	0	AWRI796_4929	CWC27	-0.152	1	0
AWRI796_5041	HOS1	-0.138	1	0	AWRI796_4975	TAF3	-0.152	1	0
AWRI796_0221	MUM2	-0.139	1	0	AWRI796_0414	PAF1	-0.153	1	0
AWRI796_0531	SED4	-0.139	1	0	AWRI796_0648	ARF2	-0.153	1	0
AWRI796_0997	RRP45	-0.139	1	0	AWRI796_3546	RPS1B	-0.153	1	0
AWRI796_1153	STP1	-0.139	1	0	AWRI796_4422	TIR2	-0.153	1	0
AWRI796_1623	RPS26A	-0.139	1	0	AWRI796_0021	PTA1	-0.154	1	0
AWRI796_1690	TAF6	-0.139	1	0	AWRI796_0109	RPS8A	-0.154	1	0
AWRI796_2645	REC107	-0.139	1	0	AWRI796_0813	OCA6	-0.154	1	0
AWRI796_2698	EMC2	-0.139	1	0	AWRI796_0839	BMH2	-0.154	1	0
AWRI796_1129	NPL3	-0.14	1	0	AWRI796_1041	UBX5	-0.154	1	0
AWRI796_1676	SOH1	-0.14	1	0	AWRI796_2923	TTI1	-0.154	1	0
AWRI796_3681	YTA12	-0.14	1	0	AWRI796_3426	VAC14	-0.154	1	0
AWRI796_4347	NUF2	-0.14	1	0	AWRI796_5182	YNL284C-B	-0.154	1	0
AWRI796_4419	SGT2	-0.14	1	0	AWRI796_0073	YAR028W	-0.155	1	0
AWRI796_0769	PSF1	-0.141	1	0	AWRI796_0153	POP8	-0.155	1	0
AWRI796_2453	THI13	-0.141	1	0	AWRI796_0537	ERS1	-0.155	1	0
AWRI796_2486	RPL17B	-0.141	1	0	AWRI796_1080	ATP17	-0.155	1	0
AWRI796_3590	UBX2	-0.141	1	0	AWRI796_1742	RPT6	-0.155	1	0
AWRI796_0417	MRPL27	-0.142	1	0	AWRI796_1754	RPL24A	-0.155	1	0
AWRI796_0481	CDC10	-0.142	1	0	AWRI796_2505	FBP26	-0.155	1	0
AWRI796_0874	MTQ2	-0.142	1	0	AWRI796_2831	SDH3	-0.155	1	0
AWRI796_1285	FMP52	-0.142	1	0	AWRI796_2885	YKL077W	-0.155	1	0
AWRI796_1906	RPL24B	-0.142	1	0	AWRI796_3328	YLR257W	-0.155	1	0
AWRI796_2588	TIM54	-0.142	1	0	AWRI796_3385	RPS25B	-0.155	1	0
AWRI796_3717	SAS2	-0.142	1	0	AWRI796_3625	MSS1	-0.155	1	0
AWRI796_3729	RIM11	-0.142	1	0	AWRI796_3920	YNL320W	-0.155	1	0
AWRI796_4512	RPT5	-0.142	1	0	AWRI796_4191	ATG3	-0.155	1	0
AWRI796_4672	SNU66	-0.142	1	0	AWRI796_5072	RPN7	-0.155	1	0
AWRI796_4970	SWI1	-0.142	1	0	AWRI796_2205	DCD1	-0.156	1	0
AWRI796_0959	PRP42	-0.143	1	0	AWRI796_2246	PTH1	-0.156	1	0
AWRI796_2152	NAM8	-0.143	1	0	AWRI796_2691	CDC11	-0.156	1	0
AWRI796_2196	WSS1	-0.143	1	0	AWRI796_4404	MDM12	-0.156	1	0
AWRI796_2297	TPM2	-0.143	1	0	AWRI796_0328	FZO1	-0.157	1	0
AWRI796_2422	MSL1	-0.143	1	0	AWRI796_0701	RXT3	-0.157	1	0
AWRI796_3372	SPH1	-0.143	1	0	AWRI796_1190	GMC1	-0.157	1	0
AWRI796_3392	GAS2	-0.143	1	0	AWRI796_1359	ICP55	-0.157	1	0
AWRI796_3459	MAG2	-0.143	1	0	AWRI796_3317	CDD1	-0.157	1	0
AWRI796_3610	ADI1	-0.143	1	0	AWRI796_3450	CDC73	-0.157	1	0
AWRI796_4692	MRS2	-0.143	1	0	AWRI796_4474	CDC21	-0.157	1	0

AWRI796 Gene ID	Gene Name	log_2 Fold Change	Adj. *p* -value	Score	AWRI796 Gene ID	Gene Name	log_2 Fold Change	Adj. *p* -value	Score
AWRI796_5093	SPN1	-0.157	1	0	AWRI796_2343	YIL089W	-0.174	1	0
AWRI796_0882	KGD2	-0.158	1	0	AWRI796_2845	SSH4	-0.174	1	0
AWRI796_1644	SUT1	-0.158	1	0	AWRI796_3350	YLR287C	-0.174	1	0
AWRI796_1802	THG1	-0.158	1	0	AWRI796_4795	SAR1	-0.174	1	0
AWRI796_3056	JLP1	-0.158	1	0	AWRI796_0177	HHF1	-0.175	1	0
AWRI796_4056	PGA1	-0.158	1	0	AWRI796_1170	KRE2	-0.175	1	0
AWRI796_0973	PAM1	-0.159	1	0	AWRI796_1253	HYP2	-0.175	1	0
AWRI796_2329	SLM1	-0.159	1	0	AWRI796_1389	SWI4	-0.175	1	0
AWRI796_3384	MID2	-0.159	1	0	AWRI796_1413	GDI1	-0.175	1	0
AWRI796_3691	YMR099C	-0.159	1	0	AWRI796_2917	NFU1	-0.175	1	0
AWRI796_4159	YNL035C	-0.159	1	0	AWRI796_4088	NCS2	-0.175	1	0
AWRI796_4759	YPL257W	-0.159	1	0	AWRI796_4171	HHT2	-0.175	1	0
AWRI796_0016	GEM1	-0.16	1	0	AWRI796_0298	MRPS9	-0.176	1	0
AWRI796_0990	MSW1	-0.16	1	0	AWRI796_0360	HPC2	-0.176	1	0
AWRI796_1443	RPH1	-0.16	1	0	AWRI796_1094	YDR391C	-0.176	1	0
AWRI796_2255	AIM18	-0.16	1	0	AWRI796_1272	UBC8	-0.176	1	0
AWRI796_2900	FBA1	-0.16	1	0	AWRI796_2522	MRS3	-0.176	1	0
AWRI796_3441	DUS4	-0.161	1	0	AWRI796_2727	IBA57	-0.176	1	0
AWRI796_3773	MRPS17	-0.161	1	0	AWRI796_3631	RSF1	-0.176	1	0
AWRI796_1117	RPL12B	-0.162	1	0	AWRI796_3701	HFD1	-0.176	1	0
AWRI796_1184	SEC20	-0.162	1	0	AWRI796_4291	HRT1	-0.176	1	0
AWRI796_1207	APA2	-0.162	1	0	AWRI796_4785	CET1	-0.176	1	0
AWRI796_1212	STL1	-0.162	1	0	AWRI796_0061	NUP60	-0.177	1	0
AWRI796_1642	YRB30	-0.162	1	0	AWRI796_1194	SDH7	-0.177	1	0
AWRI796_1778	RPN14	-0.162	1	0	AWRI796_2684	RFC2	-0.177	1	0
AWRI796_1877	SHY1	-0.162	1	0	AWRI796_2820	SRP102	-0.177	1	0
AWRI796_2296	REV7	-0.162	1	0	AWRI796_3100	MMM1	-0.177	1	0
AWRI796_4177	YNL010W	-0.162	1	0	AWRI796_0213	RPS11B	-0.178	1	0
AWRI796_4360	GPM3	-0.162	1	0	AWRI796_2677	YJR061W	-0.178	1	0
AWRI796_4632	GPN2	-0.162	1	0	AWRI796_2706	YJR096W	-0.178	1	0
AWRI796_0316	ARL1	-0.163	1	0	AWRI796_2761	YKL222C	-0.178	1	0
AWRI796_2210	PEX28	-0.163	1	0	AWRI796_2878	SRX1	-0.178	1	0
AWRI796_2634	SUI2	-0.163	1	0	AWRI796_2937	HCS1	-0.178	1	0
AWRI796_2703	FIP1	-0.163	1	0	AWRI796_4276	SPT20	-0.178	1	0
AWRI796_3167	PET309	-0.163	1	0	AWRI796_4922	YPL071C	-0.178	1	0
AWRI796_3518	VPS9	-0.163	1	0	AWRI796_0985	DIN7	-0.179	1	0
AWRI796_3876	HSH155	-0.163	1	0	AWRI796_1328	CAJ1	-0.179	1	0
AWRI796_3910	AAD14	-0.163	1	0	AWRI796_1804	RPS25A	-0.179	1	0
AWRI796_4803	SRP72	-0.163	1	0	AWRI796_3178	SIC1	-0.179	1	0
AWRI796_1516	YFR006W	-0.164	1	0	AWRI796_3393	YLR345W	-0.179	1	0
AWRI796_4114	TCB2	-0.164	1	0	AWRI796_5120	MRP2	-0.179	1	0
AWRI796_4874	TBF1	-0.164	1	0	AWRI796_5149	ARR3	-0.179	1	0
AWRI796_0754	MED2	-0.165	1	0	AWRI796_1733	YBP2	-0.18	1	0
AWRI796_0965	AMD2	-0.165	1	0	AWRI796_1810	TIM21	-0.18	1	0
AWRI796_1232	PCM1	-0.165	1	0	AWRI796_1822	UFD1	-0.18	1	0
AWRI796_1433	YER158C	-0.165	1	0	AWRI796_0460	RRP7	-0.181	1	0
AWRI796_1834	COX18	-0.165	1	0	AWRI796_0976	CHL4	-0.181	1	0
AWRI796_2345	AIM19	-0.165	1	0	AWRI796_1651	CDC43	-0.181	1	0
AWRI796_2535	NCA3	-0.165	1	0	AWRI796_2280	COA1	-0.181	1	0
AWRI796_3161	REX2	-0.165	1	0	AWRI796_2347	SDS3	-0.181	1	0
AWRI796_4448	GLO4	-0.165	1	0	AWRI796_2574	YJL070C	-0.181	1	0
AWRI796_0423	APM3	-0.166	1	0	AWRI796_2875	MIF2	-0.181	1	0
AWRI796_1694	RMD9	-0.166	1	0	AWRI796_4971	HST2	-0.181	1	0
AWRI796_1859	PRP31	-0.166	1	0	AWRI796_0254	PHO5	-0.182	1	0
AWRI796_2056	APM2	-0.166	1	0	AWRI796_1960	SLI1	-0.182	1	0
AWRI796_2194	IGO2	-0.166	1	0	AWRI796_2827	RPT1	-0.182	1	0
AWRI796_4462	SLD7	-0.166	1	0	AWRI796_4377	PRE6	-0.182	1	0
AWRI796_4499	OST2	-0.166	1	0	AWRI796_4432	SFM1	-0.182	1	0
AWRI796_0739	MRX9	-0.167	1	0	AWRI796_4477	RTS2	-0.182	1	0
AWRI796_3055	YLL058W	-0.167	1	0	AWRI796_5023	MCM16	-0.182	1	0
AWRI796_3192	NYV1	-0.167	1	0	AWRI796_0191	SCO2	-0.183	1	0
AWRI796_3343	DBP9	-0.167	1	0	AWRI796_1417	MAG1	-0.183	1	0
AWRI796_3481	RIF2	-0.167	1	0	AWRI796_1506	SEC4	-0.183	1	0
AWRI796_4008	RAP1	-0.167	1	0	AWRI796_1607	YPT32	-0.183	1	0
AWRI796_0909	UBC1	-0.168	1	0	AWRI796_2446	YIR035C	-0.183	1	0
AWRI796_1670	PCL10	-0.168	1	0	AWRI796_3131	SED5	-0.183	1	0
AWRI796_1784	CUL3	-0.168	1	0	AWRI796_3736	OSW5	-0.183	1	0
AWRI796_1882	COG2	-0.168	1	0	AWRI796_5197	COS3	-0.183	1	0
AWRI796_1922	PUS6	-0.168	1	0	AWRI796_0644	BPL1	-0.184	1	0
AWRI796_3238	SPE4	-0.168	1	0	AWRI796_0773	YDR018C	-0.184	1	0
AWRI796_4469	ALG8	-0.168	1	0	AWRI796_1520	UBP6	-0.184	1	0
AWRI796_4819	YPL191C	-0.168	1	0	AWRI796_1521	MIC19	-0.184	1	0
AWRI796_5003	AGC1	-0.168	1	0	AWRI796_3574	RCF1	-0.184	1	0
AWRI796_0338	NTC20	-0.169	1	0	AWRI796_3873	YKU70	-0.184	1	0
AWRI796_1027	RAD34	-0.169	1	0	AWRI796_4548	PET123	-0.184	1	0
AWRI796_1856	CTT1	-0.169	1	0	AWRI796_4569	GSP2	-0.184	1	0
AWRI796_2249	LNP1	-0.169	1	0	AWRI796_0458	MXR2	-0.185	1	0
AWRI796_2635	MHO1	-0.17	1	0	AWRI796_1357A	YER076C	-0.185	1	0
AWRI796_2699	BIR1	-0.17	1	0	AWRI796_1661	MRF1	-0.185	1	0
AWRI796_2869	YJU2	-0.17	1	0	AWRI796_2191	ARP1	-0.185	1	0
AWRI796_3756	ALD3	-0.17	1	0	AWRI796_2406	DOT5	-0.185	1	0
AWRI796_4297	TRM13	-0.17	1	0	AWRI796_2512	IDS2	-0.185	1	0
AWRI796_0049	NTG1	-0.171	1	0	AWRI796_2550	SAP185	-0.185	1	0
AWRI796_0189	POA1	-0.171	1	0	AWRI796_3720	YMR130W	-0.185	1	0
AWRI796_0380	THI2	-0.171	1	0	AWRI796_4398	IRC10	-0.185	1	0
AWRI796_1150	PFA5	-0.171	1	0	AWRI796_2126	FYV4	-0.186	1	0
AWRI796_2835	APL2	-0.171	1	0	AWRI796_4944	VPS16	-0.186	1	0
AWRI796_3730	SIP5	-0.171	1	0	AWRI796_0476	ILV6	-0.187	1	0
AWRI796_4354	APM4	-0.171	1	0	AWRI796_0523	CTR86	-0.187	1	0
AWRI796_4740	PHR1	-0.171	1	0	AWRI796_1517	YFH7	-0.187	1	0
AWRI796_5104	YPR148C	-0.171	1	0	AWRI796_1841	ENV11	-0.187	1	0
AWRI796_1582	DOC1	-0.172	1	0	AWRI796_2530	LSM1	-0.187	1	0
AWRI796_1947	YPP1	-0.172	1	0	AWRI796_0094	MRP21	-0.188	1	0
AWRI796_2371	PCL7	-0.172	1	0	AWRI796_0124	PIN4	-0.188	1	0
AWRI796_2742	HOM6	-0.172	1	0	AWRI796_0384	GPX2	-0.188	1	0
AWRI796_4309	MDY2	-0.172	1	0	AWRI796_3646	CSM3	-0.188	1	0
AWRI796_0099	BOI1	-0.173	1	0	AWRI796_3809	YMR226C	-0.188	1	0
AWRI796_0297	ADH5	-0.173	1	0	AWRI796_4026	YNL194C	-0.188	1	0
AWRI796_0517	IMG1	-0.173	1	0	AWRI796_0681	BUG1	-0.189	1	0
AWRI796_0704	YET3	-0.173	1	0	AWRI796_0906	HMO1	-0.189	1	0
AWRI796_1321	YEN1	-0.173	1	0	AWRI796_1106	MRP20	-0.189	1	0
AWRI796_2186	EPT1	-0.173	1	0	AWRI796_1188	LPP1	-0.189	1	0
AWRI796_2536	ASF1	-0.173	1	0	AWRI796_2534	PHO86	-0.189	1	0
AWRI796_2549	CHS6	-0.173	1	0	AWRI796_2676	CBF1	-0.189	1	0
AWRI796_3568	YML037C	-0.173	1	0	AWRI796_2929	PAN3	-0.189	1	0
AWRI796_0678	POL3	-0.174	1	0	AWRI796_3711	ADE17	-0.189	1	0
AWRI796_1161	PRP3	-0.174	1	0	AWRI796_4610	HES1	-0.189	1	0

AWRI796 Gene ID	Gene Name	log_2 Fold Change	Adj. *p* -value	Score	AWRI796 Gene ID	Gene Name	log_2 Fold Change	Adj. *p* -value	Score
AWRI796_5012	NTO1	-0.189	1	0	AWRI796_3453	RPN13	-0.202	1	0
AWRI796_1042	GPI8	-0.19	1	0	AWRI796_3483	PDP3	-0.202	1	0
AWRI796_1398	SCS2	-0.19	1	0	AWRI796_4845	YPL162C	-0.202	1	0
AWRI796_1654	NUT1	-0.19	1	0	AWRI796_0080	MIX23	-0.203	1	0
AWRI796_1772	SCL1	-0.19	1	0	AWRI796_0334	MBA1	-0.203	1	0
AWRI796_1836	VHT1	-0.19	1	0	AWRI796_1317	PHM8	-0.203	1	0
AWRI796_1932	RNR4	-0.19	1	0	AWRI796_1702	USE1	-0.203	1	0
AWRI796_2385	CST6	-0.19	1	0	AWRI796_3287	PNP1	-0.203	1	0
AWRI796_2444	MGA2	-0.19	1	0	AWRI796_3288	CLB4	-0.203	1	0
AWRI796_4410	PFA4	-0.19	1	0	AWRI796_3923	ATP11	-0.203	1	0
AWRI796_4427	ERP4	-0.19	1	0	AWRI796_3976	TEX1	-0.203	1	0
AWRI796_4501	VAM3	-0.19	1	0	AWRI796_4440	HMS1	-0.203	1	0
AWRI796_0398	RGD1	-0.191	1	0	AWRI796_4568	SER1	-0.203	1	0
AWRI796_0703	AHK1	-0.191	1	0	AWRI796_5054	MDM36	-0.203	1	0
AWRI796_0794	RPC11	-0.191	1	0	AWRI796_0349	DER1	-0.204	1	0
AWRI796_1879	SPT6	-0.191	1	0	AWRI796_1992	PUP2	-0.204	1	0
AWRI796_1920	TRS65	-0.191	1	0	AWRI796_1996	MTM1	-0.204	1	0
AWRI796_2816	KDX1	-0.191	1	0	AWRI796_3748	HLJ1	-0.204	1	0
AWRI796_4226	PET494	-0.191	1	0	AWRI796_4772	SRP68	-0.204	1	0
AWRI796_5039	UBA3	-0.191	1	0	AWRI796_4924	BTS1	-0.204	1	0
AWRI796_0194	YPK3	-0.192	1	0	AWRI796_5136	ATG13	-0.204	1	0
AWRI796_0268	ALG1	-0.192	1	0	AWRI796_0469	KCC4	-0.205	1	0
AWRI796_0818	SNF11	-0.192	1	0	AWRI796_0755	ATP16	-0.205	1	0
AWRI796_0920	SLY1	-0.192	1	0	AWRI796_1291	YER010C	-0.205	1	0
AWRI796_1574	RMR1	-0.192	1	0	AWRI796_0549	YCR090C	-0.206	1	0
AWRI796_3472	SIR3	-0.192	1	0	AWRI796_0695	SUB2	-0.206	1	0
AWRI796_4429	ROD1	-0.192	1	0	AWRI796_2653	PET191	-0.206	1	0
AWRI796_1156	PKH3	-0.193	1	0	AWRI796_3824	RPL20A	-0.206	1	0
AWRI796_2383	NOT3	-0.193	1	0	AWRI796_3872	RIT1	-0.206	1	0
AWRI796_3571	SRC1	-0.193	1	0	AWRI796_4396	ESC8	-0.206	1	0
AWRI796_3667	IRC21	-0.193	1	0	AWRI796_0019	YAL044W-A	-0.207	1	0
AWRI796_4524	YOR131C	-0.193	1	0	AWRI796_0228	ECM2	-0.207	1	0
AWRI796_0048	TPD3	-0.194	1	0	AWRI796_0894	CWC15	-0.207	1	0
AWRI796_0098	YBL086C	-0.194	1	0	AWRI796_1339	PET117	-0.207	1	0
AWRI796_0206	FAT1	-0.194	1	0	AWRI796_1815	KSS1	-0.207	1	0
AWRI796_2572	PSF2	-0.194	1	0	AWRI796_3110	SSL1	-0.207	1	0
AWRI796_3224	ACE2	-0.194	1	0	AWRI796_4881	VPS30	-0.207	1	0
AWRI796_3305	CDC42	-0.194	1	0	AWRI796_4926	YPL067C	-0.207	1	0
AWRI796_3655	SAM37	-0.194	1	0	AWRI796_1320	GLN3	-0.208	1	0
AWRI796_4217	SOL1	-0.194	1	0	AWRI796_2365	SNP1	-0.208	1	0
AWRI796_4662	TIM18	-0.194	1	0	AWRI796_2555	SRS2	-0.208	1	0
AWRI796_5018	ERV2	-0.194	1	0	AWRI796_2560	TRL1	-0.208	1	0
AWRI796_1592	SHE10	-0.195	1	0	AWRI796_3771	HSC82	-0.208	1	0
AWRI796_1845	PEX8	-0.195	1	0	AWRI796_4449	CUE5	-0.208	1	0
AWRI796_2689	MOG1	-0.195	1	0	AWRI796_4843	MLH3	-0.208	1	0
AWRI796_3533	BET5	-0.195	1	0	AWRI796_0643	CRD1	-0.209	1	0
AWRI796_4104	OCA1	-0.195	1	0	AWRI796_0726	MTF2	-0.209	1	0
AWRI796_4658	RPS10A	-0.195	1	0	AWRI796_1247	YEF1	-0.209	1	0
AWRI796_5053	DIB1	-0.195	1	0	AWRI796_1729	MRH4	-0.209	1	0
AWRI796_0319	PEX32	-0.196	1	0	AWRI796_3323	SYM1	-0.209	1	0
AWRI796_0884	CTH1	-0.196	1	0	AWRI796_4189	SWM2	-0.209	1	0
AWRI796_1025	SSF2	-0.196	1	0	AWRI796_4916	RPL21B	-0.209	1	0
AWRI796_1181	VPS3	-0.196	1	0	AWRI796_0492	YCR016W	-0.21	1	0
AWRI796_1379	UBC6	-0.196	1	0	AWRI796_0683	RPN6	-0.21	1	0
AWRI796_2630	MRX12	-0.196	1	0	AWRI796_1600	FRA2	-0.21	1	0
AWRI796_3437	BDF1	-0.196	1	0	AWRI796_2143	NMD2	-0.21	1	0
AWRI796_3605	TAF4	-0.196	1	0	AWRI796_2215	LAM1	-0.21	1	0
AWRI796_3624	UBC7	-0.196	1	0	AWRI796_4162	ARK1	-0.21	1	0
AWRI796_3777	GYL1	-0.196	1	0	AWRI796_5148	ARR2	-0.21	1	0
AWRI796_4972	CIP1	-0.196	1	0	AWRI796_0057	ERP2	-0.211	1	0
AWRI796_0682	SNU23	-0.197	1	0	AWRI796_3215	SRN2	-0.211	1	0
AWRI796_1157	TLG1	-0.197	1	0	AWRI796_3451	YLR419W	-0.211	1	0
AWRI796_1346	VHR2	-0.197	1	0	AWRI796_3556	YML053C	-0.211	1	0
AWRI796_1807	POP6	-0.197	1	0	AWRI796_2263	SKN7	-0.212	1	0
AWRI796_2121	COX6	-0.197	1	0	AWRI796_2448	GTT1	-0.212	1	0
AWRI796_2557	DPB11	-0.197	1	0	AWRI796_2615	PET130	-0.212	1	0
AWRI796_2649	YJR030C	-0.197	1	0	AWRI796_2728	RPS5	-0.212	1	0
AWRI796_2955	OSH6	-0.197	1	0	AWRI796_2926	TFA1	-0.212	1	0
AWRI796_2994	PET10	-0.197	1	0	AWRI796_3256	IDP2	-0.212	1	0
AWRI796_4035	MRPL19	-0.197	1	0	AWRI796_3577	YOX1	-0.212	1	0
AWRI796_0560	LRG1	-0.198	1	0	AWRI796_4098	INP52	-0.212	1	0
AWRI796_1179	MZM1	-0.198	1	0	AWRI796_4185	DOM34	-0.212	1	0
AWRI796_1570	FZF1	-0.198	1	0	AWRI796_0246	TEC1	-0.213	1	0
AWRI796_2200	YHR138C	-0.198	1	0	AWRI796_0542	AHC2	-0.213	1	0
AWRI796_3648	FAR3	-0.198	1	0	AWRI796_1357B	YER076C	-0.213	1	0
AWRI796_3760	DDR48	-0.198	1	0	AWRI796_1468	EMP47	-0.213	1	0
AWRI796_4367	RRT8	-0.198	1	0	AWRI796_2413	YIL001W	-0.213	1	0
AWRI796_4933	GRX5	-0.198	1	0	AWRI796_3075	IRC19	-0.213	1	0
AWRI796_0232	BAP2	-0.199	1	0	AWRI796_4987	PDH1	-0.213	1	0
AWRI796_0576	FMP45	-0.199	1	0	AWRI796_0479	PGS1	-0.214	1	0
AWRI796_2377	AGE2	-0.199	1	0	AWRI796_0702	BRE1	-0.214	1	0
AWRI796_3957	BOR1	-0.199	1	0	AWRI796_0854	TMA64	-0.214	1	0
AWRI796_4588	NPT1	-0.199	1	0	AWRI796_0897	SEC5	-0.214	1	0
AWRI796_4593	RUD3	-0.199	1	0	AWRI796_1907	YGR149W	-0.214	1	0
AWRI796_0251	RFC5	-0.2	1	0	AWRI796_1956	SER2	-0.214	1	0
AWRI796_0719	PBP4	-0.2	1	0	AWRI796_1976	YHB1	-0.214	1	0
AWRI796_1549	ERJ5	-0.2	1	0	AWRI796_2061	YLF2	-0.214	1	0
AWRI796_1816	BUD9	-0.2	1	0	AWRI796_3409	GRX8	-0.214	1	0
AWRI796_2857	SLD2	-0.2	1	0	AWRI796_4532	ARP8	-0.214	1	0
AWRI796_3928	STB1	-0.2	1	0	AWRI796_4539	SMP3	-0.214	1	0
AWRI796_3966	PDR17	-0.2	1	0	AWRI796_4939	OAZ1	-0.214	1	0
AWRI796_0632	CLB3	-0.201	1	0	AWRI796_5040	ISA2	-0.214	1	0
AWRI796_0873	HPR1	-0.201	1	0	AWRI796_5075	DBF20	-0.214	1	0
AWRI796_3640	YET2	-0.201	1	0	AWRI796_0361	YBP1	-0.215	1	0
AWRI796_3686	CTF13	-0.201	1	0	AWRI796_0898	TAF10	-0.215	1	0
AWRI796_3725	GID8	-0.201	1	0	AWRI796_3715	STO1	-0.215	1	0
AWRI796_3779	ICY1	-0.201	1	0	AWRI796_3975	RTC4	-0.215	1	0
AWRI796_4336	ATG19	-0.201	1	0	AWRI796_4229	YNR048W	-0.215	1	0
AWRI796_4496	KTR1	-0.201	1	0	AWRI796_4437	STI1	-0.215	1	0
AWRI796_5100	KAR3	-0.201	1	0	AWRI796_0350	MCM7	-0.216	1	0
AWRI796_5125	YPR172W	-0.201	1	0	AWRI796_2168	GRE3	-0.216	1	0
AWRI796_0575	HBT1	-0.202	1	0	AWRI796_2609	BET4	-0.216	1	0
AWRI796_1338	HMF1	-0.202	1	0	AWRI796_3202	LCL2	-0.216	1	0
AWRI796_1372	MET6	-0.202	1	0	AWRI796_0026	CDC19	-0.217	1	0
AWRI796_1432	COG3	-0.202	1	0	AWRI796_0618	PAR32	-0.217	1	0
AWRI796_2639	YJR012C	-0.202	1	0	AWRI796_3446	BER1	-0.217	1	0
AWRI796_2913	PRI2	-0.202	1	0	AWRI796_4120	TPM1	-0.217	1	0

AWRI796 Gene ID	Gene Name	log_2 Fold Change	Adj. *p* -value	Score	AWRI796 Gene ID	Gene Name	log_2 Fold Change	Adj. *p* -value	Score
AWRI796_4597	MCT1	-0.217	1	0	AWRI796_4976	RET3	-0.237	1	0
AWRI796_0486	RVS161	-0.218	1	0	AWRI796_0927	CBS2	-0.238	1	0
AWRI796_1122	CAD1	-0.218	1	0	AWRI796_2380	GVP36	-0.238	1	0
AWRI796_1290	NTF2	-0.218	1	0	AWRI796_2855	KTI12	-0.238	1	0
AWRI796_1848	TWF1	-0.218	1	0	AWRI796_3531	YML079W	-0.238	1	0
AWRI796_2334	FMC1	-0.218	1	0	AWRI796_3643	MCM1	-0.238	1	0
AWRI796_2509	DAS1	-0.218	1	0	AWRI796_3995	PDR16	-0.238	1	0
AWRI796_3234	PUT1	-0.218	1	0	AWRI796_4303	RRI2	-0.238	1	0
AWRI796_0741	DIA3	-0.219	1	0	AWRI796_0352	LDH1	-0.239	1	0
AWRI796_2248	CTF8	-0.219	1	0	AWRI796_2941	ARC19	-0.239	1	0
AWRI796_2565	ARP4	-0.219	1	0	AWRI796_3440	SEI1	-0.239	1	0
AWRI796_2647	MDE1	-0.219	1	0	AWRI796_0602	NUS1	-0.24	1	0
AWRI796_3262	SAM1	-0.219	1	0	AWRI796_0621	UGX2	-0.24	1	0
AWRI796_0179	IPP1	-0.22	1	0	AWRI796_1048	MRPS28	-0.24	1	0
AWRI796_0853	MRPL1	-0.22	1	0	AWRI796_2757	YJR154W	-0.24	1	0
AWRI796_1024	TFB1	-0.22	1	0	AWRI796_3357	ATP14	-0.24	1	0
AWRI796_2006	HUA1	-0.22	1	0	AWRI796_3980	MPA43	-0.24	1	0
AWRI796_2066	YAP3	-0.22	1	0	AWRI796_4222	YNR040W	-0.24	1	0
AWRI796_2310	AYR1	-0.22	1	0	AWRI796_0961	MRPL7	-0.241	1	0
AWRI796_3108	CMS1	-0.22	1	0	AWRI796_1028	IPK1	-0.241	1	0
AWRI796_4073	EAF7	-0.22	1	0	AWRI796_3947	SEC21	-0.241	1	0
AWRI796_4973	MRPS16	-0.22	1	0	AWRI796_4326	YPQ1	-0.241	1	0
AWRI796_5086	AXL1	-0.22	1	0	AWRI796_4675	RPL20B	-0.241	1	0
AWRI796_0880	SWI5	-0.221	1	0	AWRI796_4899	INA17	-0.241	1	0
AWRI796_0928	RKM2	-0.221	1	0	AWRI796_1067	ESC2	-0.242	1	0
AWRI796_2231	ATG7	-0.221	1	0	AWRI796_1167	DIG2	-0.242	1	0
AWRI796_2467	YJL206C	-0.221	1	0	AWRI796_1914	MTR3	-0.242	1	0
AWRI796_2596	AIM22	-0.221	1	0	AWRI796_2213	SPO16	-0.242	1	0
AWRI796_4332	AWRI796_4332	-0.221	1	0	AWRI796_2850	SBA1	-0.242	1	0
AWRI796_2468	RCY1	-0.222	1	0	AWRI796_4125	MLF3	-0.242	1	0
AWRI796_2694	AIM24	-0.222	1	0	AWRI796_4932	MFM1	-0.242	1	0
AWRI796_0054	MDM10	-0.223	1	0	AWRI796_0950	HTA1	-0.243	1	0
AWRI796_0690	NUR1	-0.223	1	0	AWRI796_0558	YCR101C	-0.244	1	0
AWRI796_1957	TRX2	-0.223	1	0	AWRI796_1590	EMC4	-0.244	1	0
AWRI796_2421	PRI1	-0.223	1	0	AWRI796_1765	JAC1	-0.244	1	0
AWRI796_2942	PRP40	-0.223	1	0	AWRI796_1797	UGA1	-0.244	1	0
AWRI796_3275	NMT1	-0.223	1	0	AWRI796_2028	COS8	-0.244	1	0
AWRI796_4118	PMS1	-0.223	1	0	AWRI796_2695	EAF6	-0.244	1	0
AWRI796_0095	AVT5	-0.224	1	0	AWRI796_3471	RPS1A	-0.244	1	0
AWRI796_1133	GPI19	-0.224	1	0	AWRI796_4072	NAM9	-0.244	1	0
AWRI796_1649	ARI1	-0.224	1	0	AWRI796_4979	TFC8	-0.244	1	0
AWRI796_1665	FLC3	-0.224	1	0	AWRI796_0803	EMC10	-0.245	1	0
AWRI796_2270	AWRI796_2270	-0.224	1	0	AWRI796_3425	SWC7	-0.245	1	0
AWRI796_2888	LHS1	-0.224	1	0	AWRI796_4259	MAN2	-0.245	1	0
AWRI796_3314	ARV1	-0.224	1	0	AWRI796_4679	FAA1	-0.245	1	0
AWRI796_3524	UFO1	-0.224	1	0	AWRI796_4846	BEM4	-0.245	1	0
AWRI796_1499	IES1	-0.225	1	0	AWRI796_0706	BDF2	-0.246	1	0
AWRI796_3672	CTF18	-0.225	1	0	AWRI796_1135	LRS4	-0.246	1	0
AWRI796_4522	AFI1	-0.225	1	0	AWRI796_1544	CDC26	-0.246	1	0
AWRI796_0011	PEX22	-0.226	1	0	AWRI796_1971	DIE2	-0.246	1	0
AWRI796_1693	YGL108C	-0.226	1	0	AWRI796_2381	APQ12	-0.246	1	0
AWRI796_3731	RPL13B	-0.226	1	0	AWRI796_2902	TOA2	-0.246	1	0
AWRI796_4557	LCB4	-0.226	1	0	AWRI796_2983	DID2	-0.246	1	0
AWRI796_4580	BFR1	-0.226	1	0	AWRI796_3595	YAP1	-0.246	1	0
AWRI796_4985	HAT1	-0.226	1	0	AWRI796_3627	PEX12	-0.246	1	0
AWRI796_0596	MGT1	-0.227	1	0	AWRI796_0220	YBR056W	-0.247	1	0
AWRI796_1187	SAM2	-0.227	1	0	AWRI796_2435	INA22	-0.247	1	0
AWRI796_1455	FMP10	-0.227	1	0	AWRI796_2872	BUD2	-0.247	1	0
AWRI796_3082	PAU17	-0.227	1	0	AWRI796_3722	JLP2	-0.247	1	0
AWRI796_0487	ADY2	-0.228	1	0	AWRI796_0064	RFA1	-0.248	1	0
AWRI796_0761	RCR2	-0.228	1	0	AWRI796_0313	CSH1	-0.248	1	0
AWRI796_1747	YGL041W-A	-0.228	1	0	AWRI796_1490	EPL1	-0.248	1	0
AWRI796_2337	PRK1	-0.228	1	0	AWRI796_2853	RAD27	-0.248	1	0
AWRI796_3352	GUF1	-0.228	1	0	AWRI796_3126	IRC25	-0.248	1	0
AWRI796_3361	EXG1	-0.228	1	0	AWRI796_3366	CDA1	-0.248	1	0
AWRI796_3520	GIM5	-0.228	1	0	AWRI796_4788	YPL225W	-0.248	1	0
AWRI796_4794	PCL8	-0.228	1	0	AWRI796_0282	ATG14	-0.249	1	0
AWRI796_1547	OSW7	-0.229	1	0	AWRI796_0721	LHP1	-0.249	1	0
AWRI796_3996	ELA1	-0.229	1	0	AWRI796_0816	PAA1	-0.249	1	0
AWRI796_5007	CCL1	-0.229	1	0	AWRI796_1031	MCM21	-0.249	1	0
AWRI796_1991	GCN5	-0.23	1	0	AWRI796_1980	PEX21	-0.249	1	0
AWRI796_3848	AWRI796_3848	-0.23	1	0	AWRI796_3572	RAD52	-0.249	1	0
AWRI796_4055	ASI2	-0.23	1	0	AWRI796_3618	SOK2	-0.249	1	0
AWRI796_4798	CBP3	-0.23	1	0	AWRI796_4307	SKM1	-0.249	1	0
AWRI796_4982	LSP1	-0.23	1	0	AWRI796_4687	SNC2	-0.249	1	0
AWRI796_2898	MSN4	-0.231	1	0	AWRI796_2429	MET28	-0.25	1	0
AWRI796_4225	AGA1	-0.231	1	0	AWRI796_3412	ARC18	-0.25	1	0
AWRI796_1552	YFR045W	-0.232	1	0	AWRI796_5088	YLH47	-0.25	1	0
AWRI796_3566	VPS71	-0.232	1	0	AWRI796_3547	MFT1	-0.251	1	0
AWRI796_4601	ISU2	-0.232	1	0	AWRI796_4105	RAS2	-0.251	1	0
AWRI796_1010	HDA2	-0.233	1	0	AWRI796_4286	CDC33	-0.251	1	0
AWRI796_2430	YAP5	-0.233	1	0	AWRI796_4879	RNY1	-0.251	1	0
AWRI796_2601	NSP1	-0.233	1	0	AWRI796_1746	DST1	-0.252	1	0
AWRI796_2711	VPS25	-0.233	1	0	AWRI796_1934	TIM13	-0.252	1	0
AWRI796_3636	MIH1	-0.233	1	0	AWRI796_4878	SPC29	-0.252	1	0
AWRI796_3744	AIM36	-0.233	1	0	AWRI796_0709	PEX19	-0.253	1	0
AWRI796_4510	TRS33	-0.233	1	0	AWRI796_0820	PPH3	-0.253	1	0
AWRI796_1639	SUA5	-0.234	1	0	AWRI796_1019	YDR306C	-0.253	1	0
AWRI796_1908	CCM1	-0.234	1	0	AWRI796_3656	RNA14	-0.253	1	0
AWRI796_3355	SEC72	-0.235	1	0	AWRI796_4145	YNL050C	-0.253	1	0
AWRI796_3597	TRM12	-0.235	1	0	AWRI796_4194	CSE2	-0.253	1	0
AWRI796_4681	GNT1	-0.235	1	0	AWRI796_4723	RAD17	-0.253	1	0
AWRI796_0348	BEM1	-0.236	1	0	AWRI796_5188	PHO12	-0.253	1	0
AWRI796_1604	SKI8	-0.236	1	0	AWRI796_0922	HST4	-0.254	1	0
AWRI796_1838	YGR067C	-0.236	1	0	AWRI796_1739	ERV14	-0.254	1	0
AWRI796_1939	BUB1	-0.236	1	0	AWRI796_2173	CTM1	-0.254	1	0
AWRI796_2372	DFG10	-0.236	1	0	AWRI796_5001	RLF2	-0.254	1	0
AWRI796_2795	ASH1	-0.236	1	0	AWRI796_1223	DSF1	-0.256	1	0
AWRI796_2892	YKL069W	-0.236	1	0	AWRI796_1296	FAA2	-0.256	1	0
AWRI796_2989	YKR041W	-0.236	1	0	AWRI796_1444	ADK2	-0.256	1	0
AWRI796_3621	STB4	-0.236	1	0	AWRI796_2599	YJL043W	-0.256	1	0
AWRI796_3946	CAF40	-0.236	1	0	AWRI796_3358	YLR297W	-0.256	1	0
AWRI796_4386	MDM38	-0.236	1	0	AWRI796_3382	NMA1	-0.256	1	0
AWRI796_4962	SKS1	-0.236	1	0	AWRI796_3768	SSO2	-0.256	1	0
AWRI796_0397	YBR259W	-0.237	1	0	AWRI796_4076	FYV6	-0.256	1	0
AWRI796_1173	VPS60	-0.237	1	0	AWRI796_4651	RDL2	-0.256	1	0
AWRI796_4323	HMI1	-0.237	1	0	AWRI796_0680	GET3	-0.257	1	0

AWRI796 Gene ID	Gene Name	log_2 Fold Change	Adj. *p* -value	Score	AWRI796 Gene ID	Gene Name	log_2 Fold Change	Adj. *p* -value	Score
AWRI796_1558	RPN12	-0.257	1	0	AWRI796_4940	ARL3	-0.277	1	0
AWRI796_2423	DSN1	-0.257	1	0	AWRI796_0429	PCA1	-0.278	1	0
AWRI796_2744	YJR141W	-0.257	1	0	AWRI796_0777	CIS1	-0.278	1	0
AWRI796_4019	SPS19	-0.257	1	0	AWRI796_0915	PLP1	-0.278	1	0
AWRI796_4535	ELG1	-0.257	1	0	AWRI796_2539	GZF3	-0.278	1	0
AWRI796_5031	TFB4	-0.257	1	0	AWRI796_5147	ARR1	-0.278	1	0
AWRI796_1460	YER187W	-0.258	1	0	AWRI796_0579	YDL218W	-0.279	1	0
AWRI796_1825	YGR053C	-0.258	1	0	AWRI796_0689	RAM1	-0.279	1	0
AWRI796_1911	CYS4	-0.258	1	0	AWRI796_0762	RAD57	-0.279	1	0
AWRI796_4436	BUB3	-0.258	1	0	AWRI796_3930	MCK1	-0.279	1	0
AWRI796_1158	SDC1	-0.259	1	0	AWRI796_4619	APC5	-0.279	1	0
AWRI796_1659	TIP20	-0.259	1	0	AWRI796_4635	PNT1	-0.279	1	0
AWRI796_0427	VBA2	-0.26	1	0	AWRI796_5249	SNO2	-0.279	1	0
AWRI796_0543	TRX3	-0.26	1	0	AWRI796_4444	PEP12	-0.28	1	0
AWRI796_1261	RIP1	-0.26	1	0	AWRI796_5094	MSS18	-0.28	1	0
AWRI796_1424	PEA2	-0.26	1	0	AWRI796_1472	OTU1	-0.281	1	0
AWRI796_2408	NAS2	-0.26	1	0	AWRI796_1480	MOB2	-0.281	1	0
AWRI796_3601	YPT7	-0.26	1	0	AWRI796_2849	VPH2	-0.281	1	0
AWRI796_0636	ATG9	-0.261	1	0	AWRI796_3289	ATG38	-0.281	1	0
AWRI796_0951	ADK1	-0.261	1	0	AWRI796_4154	YNL040W	-0.281	1	0
AWRI796_2035	EFM1	-0.261	1	0	AWRI796_4157	IDH1	-0.281	1	0
AWRI796_2273	YIL165C	-0.261	1	0	AWRI796_4748	KAR9	-0.281	1	0
AWRI796_2484	ATP12	-0.261	1	0	AWRI796_1303	SRB4	-0.282	1	0
AWRI796_3170	XYL2	-0.261	1	0	AWRI796_2402	BAR1	-0.282	1	0
AWRI796_3383	CHS5	-0.261	1	0	AWRI796_2737	SGM1	-0.282	1	0
AWRI796_4395	TLG2	-0.261	1	0	AWRI796_4148	SLM2	-0.282	1	0
AWRI796_4542	ATG40	-0.261	1	0	AWRI796_4712	GDS1	-0.282	1	0
AWRI796_4544	SLP1	-0.261	1	0	AWRI796_1662	GPI10	-0.283	1	0
AWRI796_0879	TAF12	-0.262	1	0	AWRI796_2591	IRC8	-0.283	1	0
AWRI796_1215	FDC1	-0.262	1	0	AWRI796_4176	YNL011C	-0.283	1	0
AWRI796_0430	PHO89	-0.263	1	0	AWRI796_4633	DSE3	-0.283	1	0
AWRI796_3924	DAL82	-0.263	1	0	AWRI796_4831	CUP9	-0.283	1	0
AWRI796_0267	CMD1	-0.264	1	0	AWRI796_0447	POF1	-0.284	1	0
AWRI796_1311	CHZ1	-0.264	1	0	AWRI796_3630	FAR8	-0.284	1	0
AWRI796_3776	SPG5	-0.264	1	0	AWRI796_2147	LRP1	-0.285	1	0
AWRI796_4263	CSS3	-0.264	1	0	AWRI796_3069	SDH2	-0.285	1	0
AWRI796_4428	PET127	-0.264	1	0	AWRI796_5231	FEX1	-0.285	1	0
AWRI796_4480	DIA2	-0.264	1	0	AWRI796_0015	AIM2	-0.286	1	0
AWRI796_4892	YPL107W	-0.264	1	0	AWRI796_2469	PRP21	-0.286	1	0
AWRI796_1990	NOP19	-0.265	1	0	AWRI796_4707	MNE1	-0.286	1	0
AWRI796_3421	CTF3	-0.265	1	0	AWRI796_0660	YDL121C	-0.287	1	0
AWRI796_3494	PHO84	-0.265	1	0	AWRI796_0749	SLX5	-0.287	1	0
AWRI796_0165	PDR3	-0.266	1	0	AWRI796_1334	PIC2	-0.287	1	0
AWRI796_0564	PHO13	-0.266	1	0	AWRI796_1878	DAM1	-0.287	1	0
AWRI796_0692	LUC7	-0.266	1	0	AWRI796_4017	RTT106	-0.287	1	0
AWRI796_1185	LCD1	-0.266	1	0	AWRI796_0913	SAS4	-0.288	1	0
AWRI796_5085	THI22	-0.266	1	0	AWRI796_3184	ARP6	-0.288	1	0
AWRI796_0815	DOA4	-0.267	1	0	AWRI796_3191	SUL2	-0.288	1	0
AWRI796_1872	VOA1	-0.267	1	0	AWRI796_3205	REX3	-0.288	1	0
AWRI796_2520	GLG2	-0.267	1	0	AWRI796_3247	MAS1	-0.288	1	0
AWRI796_5207	COS3	-0.267	1	0	AWRI796_5121	MET16	-0.288	1	0
AWRI796_0462	BIK1	-0.268	1	0	AWRI796_5131	HDA3	-0.288	1	0
AWRI796_0931	RAV2	-0.268	1	0	AWRI796_4274	GRE2	-0.289	1	0
AWRI796_0964	SNU56	-0.268	1	0	AWRI796_4927	RGL1	-0.289	1	0
AWRI796_1579	TAD1	-0.268	1	0	AWRI796_0656	PCL2	-0.29	1	0
AWRI796_2127	VMA22	-0.268	1	0	AWRI796_0591	YDL206W	-0.291	1	0
AWRI796_2441	DCG1	-0.268	1	0	AWRI796_3766	YMR181C	-0.291	1	0
AWRI796_3152	YLR050C	-0.268	1	0	AWRI796_0290	YBR137W	-0.292	1	0
AWRI796_3548	PIF1	-0.268	1	0	AWRI796_0631	CMR1	-0.292	1	0
AWRI796_3709	SHH3	-0.268	1	0	AWRI796_1456	FAU1	-0.292	1	0
AWRI796_4493	ARF3	-0.268	1	0	AWRI796_1814	ORM1	-0.292	1	0
AWRI796_0972	YDR249C	-0.269	1	0	AWRI796_1954	MVB12	-0.292	1	0
AWRI796_1076	FRQ1	-0.269	1	0	AWRI796_3661	UBX4	-0.292	1	0
AWRI796_2062	OTU2	-0.269	1	0	AWRI796_4824	UIP4	-0.292	1	0
AWRI796_3745	MRPS8	-0.269	1	0	AWRI796_1921	YGR168C	-0.293	1	0
AWRI796_4763	VIK1	-0.269	1	0	AWRI796_3080	ISA1	-0.293	1	0
AWRI796_0717	PSA1	-0.27	1	0	AWRI796_3486	COS3	-0.293	1	0
AWRI796_0851	PDS1	-0.27	1	0	AWRI796_5165	AWRI796_5165	-0.293	1	0
AWRI796_1415	EMP65	-0.27	1	0	AWRI796_1721	MPS2	-0.294	1	0
AWRI796_2589	PEP8	-0.27	1	0	AWRI796_4445	CYC2	-0.294	1	0
AWRI796_2681	ARP3	-0.27	1	0	AWRI796_5127	YPR174C	-0.294	1	0
AWRI796_3417	PSY3	-0.27	1	0	AWRI796_0356	AME1	-0.295	1	0
AWRI796_4029	DUG3	-0.27	1	0	AWRI796_1515	SAD1	-0.295	1	0
AWRI796_4062	INN1	-0.27	1	0	AWRI796_4660	UAF30	-0.295	1	0
AWRI796_4335	ATG34	-0.27	1	0	AWRI796_5122	NUT2	-0.295	1	0
AWRI796_5132	AOS1	-0.27	1	0	AWRI796_0413	DPB3	-0.296	1	0
AWRI796_0265	IML3	-0.271	1	0	AWRI796_1191	GIN4	-0.296	1	0
AWRI796_1716	YGL082W	-0.271	1	0	AWRI796_2087	YSC83	-0.296	1	0
AWRI796_3093	EMC6	-0.271	1	0	AWRI796_2315	RPI1	-0.296	1	0
AWRI796_3490	RSC9	-0.271	1	0	AWRI796_3196	HRT3	-0.296	1	0
AWRI796_4080	NRK1	-0.271	1	0	AWRI796_4506	YOR111W	-0.296	1	0
AWRI796_1159	UGO1	-0.272	1	0	AWRI796_5179	YLR410W-B	-0.296	1	0
AWRI796_2846	SRP21	-0.272	1	0	AWRI796_0304	SPP381	-0.297	1	0
AWRI796_3592	RAD33	-0.272	1	0	AWRI796_2084	SPO13	-0.298	1	0
AWRI796_3770	RTP1	-0.272	1	0	AWRI796_3781	VTI1	-0.298	1	0
AWRI796_4083	SPC98	-0.272	1	0	AWRI796_3813	PEP5	-0.298	1	0
AWRI796_0679	DUN1	-0.273	1	0	AWRI796_0302	TBS1	-0.299	1	0
AWRI796_0120	PTC3	-0.274	1	0	AWRI796_2071	HSE1	-0.299	1	0
AWRI796_1064	GGA1	-0.274	1	0	AWRI796_2401	SNL1	-0.299	1	0
AWRI796_1618	DSD1	-0.274	1	0	AWRI796_3146	TRX1	-0.299	1	0
AWRI796_2285	YIL152W	-0.274	1	0	AWRI796_0145	YBL028C	-0.3	1	0
AWRI796_0952	SIR4	-0.275	1	0	AWRI796_0827	STN1	-0.3	1	0
AWRI796_3295	COA4	-0.275	1	0	AWRI796_0929	VPS64	-0.3	1	0
AWRI796_3880	HER2	-0.275	1	0	AWRI796_1777	COG7	-0.3	1	0
AWRI796_4278	PSF3	-0.275	1	0	AWRI796_1916	RTS3	-0.3	1	0
AWRI796_4678	COT1	-0.275	1	0	AWRI796_2354	SER33	-0.3	1	0
AWRI796_5245	YOL103W-B	-0.275	1	0	AWRI796_0677	QRI1	-0.302	1	0
AWRI796_1002	YDR286C	-0.276	1	0	AWRI796_2724	ILM1	-0.302	1	0
AWRI796_2651	CPR7	-0.276	1	0	AWRI796_3197	CHA4	-0.302	1	0
AWRI796_2723	STE24	-0.276	1	0	AWRI796_4984	SNF8	-0.302	1	0
AWRI796_0284	SHE3	-0.277	1	0	AWRI796_1594	MTC3	-0.303	1	0
AWRI796_0442	PBN1	-0.277	1	0	AWRI796_1710	LIF1	-0.303	1	0
AWRI796_0757	NHP10	-0.277	1	0	AWRI796_2198	SPL2	-0.303	1	0
AWRI796_3484	NBP1	-0.277	1	0	AWRI796_3088	AWRI796_3088	-0.303	1	0
AWRI796_3629	TAP42	-0.277	1	0	AWRI796_4786	ALG5	-0.303	1	0
AWRI796_4096	YNL108C	-0.277	1	0	AWRI796_3462	ATG23	-0.304	1	0
AWRI796_4443	SHE4	-0.277	1	0	AWRI796_3916	FIG4	-0.304	1	0

AWRI796 Gene ID	Gene Name	log_2 Fold Change	Adj. *p* -value	Score	AWRI796 Gene ID	Gene Name	log_2 Fold Change	Adj. *p* -value	Score
AWRI796_4534	THI80	-0.304	1	0	AWRI796_5037	YPR063C	-0.332	1	0
AWRI796_4773	IQG1	-0.304	1	0	AWRI796_2910	ELM1	-0.333	1	0
AWRI796_0003	FLO5	-0.305	1	0	AWRI796_4371	PEX15	-0.334	1	0
AWRI796_2858	YKL107W	-0.305	1	0	AWRI796_0554	OCA4	-0.335	1	0
AWRI796_3339	CMG1	-0.305	1	0	AWRI796_1414	RTR1	-0.335	1	0
AWRI796_0396	POP4	-0.306	1	0	AWRI796_3059	YLL054C	-0.335	1	0
AWRI796_2593	CHM7	-0.306	1	0	AWRI796_3379	CWC24	-0.335	1	0
AWRI796_2814	PIR3	-0.306	1	0	AWRI796_0670	TMA17	-0.336	1	0
AWRI796_4365	GAL11	-0.306	1	0	AWRI796_1755	CGR1	-0.336	1	0
AWRI796_4587	PTP2	-0.306	1	0	AWRI796_1931	OKP1	-0.336	1	0
AWRI796_4758	THI21	-0.307	1	0	AWRI796_4081	TEP1	-0.336	1	0
AWRI796_0315	EXO5	-0.308	1	0	AWRI796_4179	ASI3	-0.336	1	0
AWRI796_0443	LRE1	-0.308	1	0	AWRI796_4190	VPS27	-0.336	1	0
AWRI796_0638	RPN5	-0.308	1	0	AWRI796_1898	CBF2	-0.337	1	0
AWRI796_1062	SPC110	-0.308	1	0	AWRI796_4540	MRPL23	-0.337	1	0
AWRI796_4439	DFG16	-0.308	1	0	AWRI796_4643	RIM20	-0.337	1	0
AWRI796_0945	MFB1	-0.309	1	0	AWRI796_2519	TIF2	-0.338	1	0
AWRI796_2856	HAP4	-0.309	1	0	AWRI796_2074	NEM1	-0.339	1	0
AWRI796_3898	ELP6	-0.309	1	0	AWRI796_1513	YPI1	-0.34	1	0
AWRI796_4153	COG6	-0.309	1	0	AWRI796_0017	SPC72	-0.341	1	0
AWRI796_5084	CLB5	-0.309	1	0	AWRI796_1072	XRS2	-0.341	1	0
AWRI796_0234	ALG14	-0.31	1	0	AWRI796_2959	RSC4	-0.341	1	0
AWRI796_2503	FAR1	-0.31	1	0	AWRI796_5112	CUR1	-0.341	1	0
AWRI796_4373	NGL1	-0.31	1	0	AWRI796_0999	MRX10	-0.342	1	0
AWRI796_0509	BUD5	-0.311	1	0	AWRI796_1979	KEL2	-0.342	1	0
AWRI796_2542	IME2	-0.311	1	0	AWRI796_2632	APL1	-0.342	1	0
AWRI796_2769	YRA2	-0.311	1	0	AWRI796_2864	YPF1	-0.342	1	0
AWRI796_2791	HYM1	-0.311	1	0	AWRI796_4401	HTZ1	-0.342	1	0
AWRI796_4961	AWRI796_4961	-0.311	1	0	AWRI796_4476	SKI7	-0.342	1	0
AWRI796_2886	YKL075C	-0.312	1	0	AWRI796_1267	EAF5	-0.344	1	0
AWRI796_2924	IXR1	-0.312	1	0	AWRI796_3363	MET17	-0.344	1	0
AWRI796_3491	ERG13	-0.312	1	0	AWRI796_4127	RNH201	-0.344	1	0
AWRI796_3965	IST1	-0.312	1	0	AWRI796_4607	MGE1	-0.344	1	0
AWRI796_4242	YNR061C	-0.312	1	0	AWRI796_0933	MSC2	-0.345	1	0
AWRI796_4351	INP54	-0.312	1	0	AWRI796_3641	ARA2	-0.345	1	0
AWRI796_4800	LEA1	-0.312	1	0	AWRI796_4059	CUZ1	-0.345	1	0
AWRI796_1196	SLF1	-0.313	1	0	AWRI796_4317	TPT1	-0.346	1	0
AWRI796_5092	NAT3	-0.313	1	0	AWRI796_2070	LAG1	-0.347	1	0
AWRI796_0335	PCH2	-0.314	1	0	AWRI796_2418	IST3	-0.347	1	0
AWRI796_3585	YML018C	-0.314	1	0	AWRI796_3960	SEC2	-0.347	1	0
AWRI796_4812	YPL199C	-0.314	1	0	AWRI796_4572	IES4	-0.347	1	0
AWRI796_1361	AIM9	-0.315	1	0	AWRI796_3541	ITT1	-0.348	1	0
AWRI796_3359	YHC1	-0.315	1	0	AWRI796_0490	POL4	-0.349	1	0
AWRI796_4853	RAD53	-0.315	1	0	AWRI796_1022	GIC2	-0.349	1	0
AWRI796_0308	SLI15	-0.316	1	0	AWRI796_1648	RCK1	-0.349	1	0
AWRI796_4708	MEK1	-0.316	1	0	AWRI796_0115	KIP1	-0.35	1	0
AWRI796_4728	NUD1	-0.316	1	0	AWRI796_1021	SRB7	-0.35	1	0
AWRI796_0437	MRC1	-0.317	1	0	AWRI796_1689	SLD3	-0.35	1	0
AWRI796_0784	MRH1	-0.317	1	0	AWRI796_1783	SWC4	-0.35	1	0
AWRI796_1712	MAD1	-0.317	1	0	AWRI796_3181	SRL2	-0.35	1	0
AWRI796_1803	YGR026W	-0.317	1	0	AWRI796_3307	EST1	-0.35	1	0
AWRI796_4277	PEX11	-0.317	1	0	AWRI796_3563	PRP39	-0.35	1	0
AWRI796_4528	IDH2	-0.317	1	0	AWRI796_4012	VID27	-0.35	1	0
AWRI796_4722	SCP1	-0.317	1	0	AWRI796_2206	CRP1	-0.351	1	0
AWRI796_1318	KRE29	-0.318	1	0	AWRI796_2356	HOP1	-0.351	1	0
AWRI796_2272	YIL166C	-0.318	1	0	AWRI796_3716	DLT1	-0.351	1	0
AWRI796_0744	RPN4	-0.319	1	0	AWRI796_3962	ALP1	-0.351	1	0
AWRI796_1447	RAD24	-0.319	1	0	AWRI796_4126	MSK1	-0.351	1	0
AWRI796_2972	NTR2	-0.319	1	0	AWRI796_1149	HEH2	-0.352	1	0
AWRI796_3102	ORC3	-0.319	1	0	AWRI796_2824	DBR1	-0.352	1	0
AWRI796_3671	VPS20	-0.319	1	0	AWRI796_3151	YLR049C	-0.352	1	0
AWRI796_0763	MAF1	-0.32	1	0	AWRI796_3326	NDL1	-0.352	1	0
AWRI796_4030	YNL190W	-0.32	1	0	AWRI796_4087	TOM70	-0.352	1	0
AWRI796_4362	PSH1	-0.32	1	0	AWRI796_4628	HNT3	-0.352	1	0
AWRI796_5105	NCE102	-0.32	1	0	AWRI796_4863	FRK1	-0.352	1	0
AWRI796_5183	YOL103W-B	-0.32	1	0	AWRI796_1453	DMC1	-0.353	1	0
AWRI796_0050	SYN8	-0.321	1	0	AWRI796_3057	YLL056C	-0.353	1	0
AWRI796_0842	STE5	-0.321	1	0	AWRI796_3576	TSA1	-0.353	1	0
AWRI796_2842	PGM1	-0.321	1	0	AWRI796_0420	YBR285W	-0.354	1	0
AWRI796_2979	SET3	-0.321	1	0	AWRI796_0731	BSC1	-0.354	1	0
AWRI796_3751	MSS11	-0.321	1	0	AWRI796_3523	RPM2	-0.354	1	0
AWRI796_4042	TDA7	-0.321	1	0	AWRI796_0241	ECM33	-0.355	1	0
AWRI796_4591	SAS5	-0.321	1	0	AWRI796_0902	YDR170W-A	-0.355	1	0
AWRI796_0609	YDL183C	-0.322	1	0	AWRI796_1171	VPS52	-0.355	1	0
AWRI796_2832	TGL1	-0.322	1	0	AWRI796_1880	YGR117C	-0.355	1	0
AWRI796_0823	SHU2	-0.323	1	0	AWRI796_2584	BIT61	-0.355	1	0
AWRI796_2708	YUH1	-0.323	1	0	AWRI796_1536	ECO1	-0.356	1	0
AWRI796_2931	YKL023W	-0.323	1	0	AWRI796_3639	SUB1	-0.356	1	0
AWRI796_3239	SMD3	-0.323	1	0	AWRI796_4861	KES1	-0.356	1	0
AWRI796_3805	YMR221C	-0.323	1	0	AWRI796_3538	COG8	-0.357	1	0
AWRI796_5253	RDS1	-0.323	1	0	AWRI796_0930	SPC19	-0.359	1	0
AWRI796_1718	KXD1	-0.325	1	0	AWRI796_0233	TAT1	-0.36	1	0
AWRI796_3331	LCB5	-0.325	1	0	AWRI796_1627	STR3	-0.36	1	0
AWRI796_4252	YNR071C	-0.325	1	0	AWRI796_1817	MTE1	-0.36	1	0
AWRI796_4836	COX10	-0.325	1	0	AWRI796_3603	MIX17	-0.36	1	0
AWRI796_5045	NOT5	-0.325	1	0	AWRI796_2498	JJJ2	-0.361	1	0
AWRI796_1193	SMT3	-0.326	1	0	AWRI796_4116	END3	-0.361	1	0
AWRI796_4144	COG5	-0.326	1	0	AWRI796_1408	COM2	-0.362	1	0
AWRI796_0291	YBR138C	-0.327	1	0	AWRI796_1732	DUO1	-0.362	1	0
AWRI796_1435	SPT2	-0.327	1	0	AWRI796_3014	BET3	-0.362	1	0
AWRI796_2661	VPS55	-0.327	1	0	AWRI796_0100	CDC27	-0.363	1	0
AWRI796_3623	MAC1	-0.327	1	0	AWRI796_1634	BUD13	-0.365	1	0
AWRI796_4611	YOR238W	-0.327	1	0	AWRI796_3999	CNM67	-0.365	1	0
AWRI796_0408	HSM3	-0.328	1	0	AWRI796_4590	STE4	-0.365	1	0
AWRI796_0142	SHE1	-0.329	1	0	AWRI796_0459	STE50	-0.366	1	0
AWRI796_2266	CRG1	-0.329	1	0	AWRI796_2667	ISY1	-0.366	1	0
AWRI796_2830	MRP8	-0.329	1	0	AWRI796_4160	YNL034W	-0.366	1	0
AWRI796_4992	REC8	-0.329	1	0	AWRI796_4709	TFB6	-0.366	1	0
AWRI796_0258	MMS4	-0.33	1	0	AWRI796_0860	INO2	-0.367	1	0
AWRI796_1017	RSC3	-0.33	1	0	AWRI796_2394	YIL024C	-0.367	1	0
AWRI796_1518	FAR7	-0.33	1	0	AWRI796_2787	SDS22	-0.367	1	0
AWRI796_2571	JEM1	-0.33	1	0	AWRI796_4479	ATX2	-0.367	1	0
AWRI796_2957	MRPL13	-0.33	1	0	AWRI796_4577	SLK19	-0.367	1	0
AWRI796_3743	TPP1	-0.33	1	0	AWRI796_0630	YDL157C	-0.368	1	0
AWRI796_4167	SSN8	-0.33	1	0	AWRI796_1671	ITC1	-0.368	1	0
AWRI796_0281	VMA2	-0.331	1	0	AWRI796_2620	MAD3	-0.368	1	0
AWRI796_3703	MED11	-0.332	1	0	AWRI796_1844	MRPL25	-0.369	1	0

AWRI796 Gene ID	Gene Name	log_2 Fold Change	Adj. *p* -value	Score	AWRI796 Gene ID	Gene Name	log_2 Fold Change	Adj. *p* -value	Score
AWRI796_3504	CTK3	-0.369	1	0	AWRI796_0911	NVJ3	-0.411	1	0
AWRI796_0037	SAW1	-0.37	1	0	AWRI796_1394	SLX8	-0.411	1	0
AWRI796_1865	ESP1	-0.37	1	0	AWRI796_3933	YPT11	-0.411	1	0
AWRI796_2638	YJR011C	-0.37	1	0	AWRI796_1383	RTT105	-0.413	1	0
AWRI796_2836	OCT1	-0.37	1	0	AWRI796_2335	FYV10	-0.414	1	0
AWRI796_1488	STE2	-0.371	1	0	AWRI796_2524	AIM23	-0.414	1	0
AWRI796_2267	YHR210C	-0.371	1	0	AWRI796_1101	HPT1	-0.415	1	0
AWRI796_0123	SAS3	-0.372	1	0	AWRI796_0994	BSC2	-0.416	1	0
AWRI796_4090	MLS1	-0.372	1	0	AWRI796_3778	MRPL24	-0.416	1	0
AWRI796_4475	UFE1	-0.372	1	0	AWRI796_4011	RRG9	-0.417	1	0
AWRI796_1345	THO1	-0.373	1	0	AWRI796_0555	GIT1	-0.418	1	0
AWRI796_4389	IFM1	-0.373	1	0	AWRI796_2890	YKL071W	-0.418	1	0
AWRI796_4680	HSH49	-0.373	1	0	AWRI796_0981	YAP6	-0.42	1	0
AWRI796_2784	YKT6	-0.374	1	0	AWRI796_0674	PHO2	-0.421	0.981777	0
AWRI796_3604	MVP1	-0.375	1	0	AWRI796_0912	SCC2	-0.421	1	0
AWRI796_3705	YMR114C	-0.375	1	0	AWRI796_2187	NDT80	-0.421	1	0
AWRI796_0975	MET32	-0.377	1	0	AWRI796_3659	KAR5	-0.421	1	0
AWRI796_4100	MET4	-0.377	1	0	AWRI796_3418	FBP1	-0.422	1	0
AWRI796_4955	SVL3	-0.377	1	0	AWRI796_5144	YPR196W	-0.423	1	0
AWRI796_5087	CTR1	-0.377	1	0	AWRI796_2558	SIP4	-0.424	1	0
AWRI796_0318	POP7	-0.378	1	0	AWRI796_4312	INO4	-0.424	1	0
AWRI796_1313	FIR1	-0.378	1	0	AWRI796_4295	YGK3	-0.425	0.816423	0
AWRI796_3002	RHO4	-0.378	1	0	AWRI796_1203	AGE1	-0.426	0.748436	0
AWRI796_4036	NPR1	-0.378	1	0	AWRI796_2455	AGP3	-0.426	1	0
AWRI796_4875	HHO1	-0.378	1	0	AWRI796_4245	YNR064C	-0.426	1	0
AWRI796_2179	COX23	-0.379	1	0	AWRI796_2939	PUT3	-0.427	1	0
AWRI796_2292	NDC80	-0.379	1	0	AWRI796_1805	MSP1	-0.428	0.709651	0
AWRI796_4867	GIP3	-0.379	1	0	AWRI796_2511	MRX5	-0.428	1	0
AWRI796_1089	MUS81	-0.38	1	0	AWRI796_3229	TIS11	-0.429	1	0
AWRI796_1390	LSM4	-0.38	1	0	AWRI796_3248	SHH4	-0.43	0.920426	0
AWRI796_5095	CTF4	-0.38	1	0	AWRI796_0582	GDH2	-0.431	0.468841	0
AWRI796_1360	YER079W	-0.381	1	0	AWRI796_1123	SNX41	-0.432	0.838525	0
AWRI796_3246	RNH203	-0.381	1	0	AWRI796_4078	TOM22	-0.432	0.929287	0
AWRI796_3769	ADD37	-0.381	1	0	AWRI796_4563	MPC54	-0.432	1	0
AWRI796_1136	DOT1	-0.382	1	0	AWRI796_3332	YPT6	-0.434	0.71729	0
AWRI796_3190	GEP5	-0.382	1	0	AWRI796_2033	YHL042W	-0.435	1	0
AWRI796_3028	DAD2	-0.383	1	0	AWRI796_3607	AWRI796_3607	-0.435	1	0
AWRI796_1850	TOM20	-0.384	1	0	AWRI796_3408	NMD4	-0.436	1	0
AWRI796_3038	PTR2	-0.385	1	0	AWRI796_5267	REP2	-0.438	0.715224	0
AWRI796_3347	ECI1	-0.385	1	0	AWRI796_1504	SMC1	-0.439	0.665738	0
AWRI796_4937	LEE1	-0.385	1	0	AWRI796_3036	SRL3	-0.439	1	0
AWRI796_0655	VCX1	-0.386	1	0	AWRI796_0329	DTR1	-0.441	1	0
AWRI796_2815	YKL162C	-0.386	1	0	AWRI796_3368	IMH1	-0.441	0.534392	0
AWRI796_0924	MSS116	-0.387	1	0	AWRI796_0333	YBR184W	-0.444	1	0
AWRI796_1821	TFC4	-0.387	1	0	AWRI796_2962	YKR011C	-0.444	0.699282	0
AWRI796_1830	PEF1	-0.387	1	0	AWRI796_5000	DSS4	-0.445	1	0
AWRI796_3788	INP1	-0.387	1	0	AWRI796_3364	ACO1	-0.446	0.535651	0
AWRI796_2915	SPC42	-0.388	1	0	AWRI796_1985	BRF1	-0.447	0.428319	0
AWRI796_3666	ABF2	-0.388	1	0	AWRI796_3086	SPA2	-0.448	0.278208	0
AWRI796_4292	YOL131W	-0.388	1	0	AWRI796_2475	CDC6	-0.449	0.877099	0
AWRI796_0331	SMP1	-0.389	1	0	AWRI796_2481	ATG36	-0.449	0.828033	0
AWRI796_0646	SCM3	-0.389	1	0	AWRI796_2617	MPS3	-0.449	0.621808	0
AWRI796_1735	RAD6	-0.389	1	0	AWRI796_3076	YLL032C	-0.451	0.467757	0
AWRI796_2303	CSM2	-0.389	1	0	AWRI796_0210	GIP1	-0.452	0.670663	0
AWRI796_2561	EXO70	-0.389	1	0	AWRI796_1322	MXR1	-0.452	0.417917	0
AWRI796_3252	UPS2	-0.389	1	0	AWRI796_0790	RSM10	-0.453	0.253784	0
AWRI796_3415	VID22	-0.389	1	0	AWRI796_3154	IES3	-0.453	1	0
AWRI796_1026	PIB1	-0.39	1	0	AWRI796_4923	MUK1	-0.453	0.323065	0
AWRI796_0283	OPY1	-0.391	1	0	AWRI796_4631	RPN8	-0.454	0.378139	0
AWRI796_0198	EDS1	-0.392	1	0	AWRI796_1633	SAE2	-0.456	1	0
AWRI796_2241	SSP1	-0.392	1	0	AWRI796_3137	RSC58	-0.456	0.486132	0
AWRI796_2274	NIT1	-0.392	1	0	AWRI796_4240	MNT4	-0.456	0.266345	0
AWRI796_2786	MST1	-0.392	1	0	AWRI796_3660	SOV1	-0.457	0.286351	0
AWRI796_3263	VTA1	-0.392	1	0	AWRI796_1910	GTO1	-0.458	0.189786	0
AWRI796_4505	TFC7	-0.392	1	0	AWRI796_0337	AWRI796_0337	-0.46	1	0
AWRI796_1857	NNF2	-0.393	1	0	AWRI796_3814	FUS2	-0.46	0.934274	0
AWRI796_2156	YNG2	-0.394	1	0	AWRI796_3926	SKP2	-0.46	0.198533	0
AWRI796_3599	YML003W	-0.395	1	0	AWRI796_3637	MSN2	-0.461	0.180551	0
AWRI796_3708	SPC24	-0.395	1	0	AWRI796_0850	ALT2	-0.462	0.27149	0
AWRI796_3877	ABZ2	-0.396	1	0	AWRI796_0847	TRS85	-0.463	0.158011	0
AWRI796_3164	PER33	-0.398	1	0	AWRI796_5194	COS7	-0.463	0.183422	0
AWRI796_4850	PRM4	-0.398	1	0	AWRI796_2545	GSM1	-0.465	0.114261	0
AWRI796_0984	YDR262W	-0.399	1	0	AWRI796_4349	RTG1	-0.467	0.336	0
AWRI796_1795	YGR016W	-0.399	1	0	AWRI796_0495	PET18	-0.47	0.189786	0
AWRI796_2834	CMC1	-0.399	1	0	AWRI796_0587	UGA4	-0.471	0.35127	0
AWRI796_0846	TMN2	-0.401	1	0	AWRI796_0673	MSS2	-0.473	0.16451	0
AWRI796_1230	CIN8	-0.401	1	0	AWRI796_0713	RAD59	-0.473	0.466597	0
AWRI796_3340	YCS4	-0.401	1	0	AWRI796_1086	NKP1	-0.473	0.129153	0
AWRI796_0105	ATG8	-0.402	1	0	AWRI796_0214	REB1	-0.474	0.050633	0
AWRI796_0707	CBS1	-0.402	1	0	AWRI796_3739	YIM1	-0.476	0.08006	0
AWRI796_4250	BSC5	-0.402	1	0	AWRI796_2037	MUP3	-0.477	0.105831	0
AWRI796_4329	HAL9	-0.402	1	0	AWRI796_4032	KAR1	-0.477	0.340527	0
AWRI796_5225	RSC30	-0.402	1	0	AWRI796_2909	CSE4	-0.48	0.072352	0
AWRI796_2891	YKL070W	-0.404	1	0	AWRI796_4311	ZEO1	-0.48	0.14794	0
AWRI796_3559	AIM32	-0.404	1	0	AWRI796_2672	HIT1	-0.483	0.28633	0
AWRI796_3687	SNO1	-0.404	1	0	AWRI796_3023	YKR078W	-0.484	0.328566	0
AWRI796_4175	SPO1	-0.404	1	0	AWRI796_0436	VAC17	-0.486	0.131206	0
AWRI796_2358	MAM33	-0.405	1	0	AWRI796_2980	GMH1	-0.486	0.632939	0
AWRI796_3301	YLR225C	-0.405	1	0	AWRI796_4784	YPL229W	-0.488	0.217029	0
AWRI796_3596	GIS4	-0.405	1	0	AWRI796_4790	GRE1	-0.489	0.319727	0
AWRI796_3682	YMR090W	-0.405	1	0	AWRI796_1220	YEL073C	-0.492	0.979922	0
AWRI796_3726	GAT2	-0.405	1	0	AWRI796_4423	AUS1	-0.492	0.061083	0
AWRI796_0787	EHD3	-0.406	1	0	AWRI796_2075	GPA1	-0.493	0.189159	0
AWRI796_1731	PYC1	-0.406	1	0	AWRI796_3698	SPG4	-0.493	0.044515	-1
AWRI796_0230	AWRI796_0230	-0.407	1	0	AWRI796_1829	LST7	-0.494	0.125244	0
AWRI796_1647	YGL159W	-0.407	1	0	AWRI796_1124	RPN9	-0.495	0.094225	0
AWRI796_2393	IRR1	-0.407	1	0	AWRI796_0770	RAD61	-0.496	0.087688	0
AWRI796_0178	HHT1	-0.408	1	0	AWRI796_1221	RMD6	-0.497	0.045503	-1
AWRI796_2439	DAL4	-0.408	1	0	AWRI796_2123	RSC30	-0.497	0.01823	-1
AWRI796_4027	YNL193W	-0.408	1	0	AWRI796_5069	COG4	-0.497	0.039632	-1
AWRI796_2543	SET4	-0.409	1	0	AWRI796_4345	SDH5	-0.499	0.027096	-1
AWRI796_2625	CTK2	-0.409	1	0	AWRI796_4810	AFT2	-0.499	0.027096	-1
AWRI796_3764	SPT21	-0.409	1	0	AWRI796_5184	YNL284C-A	-0.501	0.664532	0
AWRI796_0174	UGA2	-0.41	1	0	AWRI796_2582	BNA3	-0.504	0.084086	0
AWRI796_3584	OST6	-0.41	1	0	AWRI796_2605	SNX4	-0.507	0.017166	-1
AWRI796_3881	JNM1	-0.41	1	0	AWRI796_1567	MNT2	-0.511	0.019525	-1
AWRI796_4555	SWT1	-0.41	1	0	AWRI796_2802	STE3	-0.512	0.349035	0

AWRI796 Gene ID	Gene Name	log_2 Fold Change	Adj. *p* -value	Score
AWRI796_5163	AWRI796_5163	-0.512	0.151927	0
AWRI796_2914	PHD1	-0.514	0.159962	0
AWRI796_2660	POL32	-0.516	0.186218	0
AWRI796_0910	CSN9	-0.518	0.133639	0
AWRI796_3155	YLR053C	-0.518	0.02508	-1
AWRI796_3135	YLR030W	-0.519	0.052916	0
AWRI796_4509	YOR114W	-0.52	0.062835	0
AWRI796_2489	RFA3	-0.524	0.018505	-1
AWRI796_2053	SPO11	-0.525	0.523722	0
AWRI796_0212	FMP23	-0.527	0.020327	-1
AWRI796_0771	HED1	-0.527	0.523678	0
AWRI796_2295	AXL2	-0.527	0.016379	-1
AWRI796_3207	AHP1	-0.528	0.551449	0
AWRI796_3245	ACS2	-0.53	0.039159	-1
AWRI796_4706	CIN1	-0.53	0.01968	-1
AWRI796_4750	ACM1	-0.53	0.27149	0
AWRI796_2357	PCI8	-0.534	0.137441	0
AWRI796_1209	KRE28	-0.535	0.175397	0
AWRI796_0027	YAL037W	-0.536	0.015263	-1
AWRI796_3489	MSC1	-0.537	0.007361	-1
AWRI796_0998	PHM6	-0.538	0.006341	-1
AWRI796_1356	PTP3	-0.539	0.050633	0
AWRI796_0435	CHA1	-0.54	0.007852	-1
AWRI796_0949	HTB1	-0.541	0.036087	-1
AWRI796_0185	GAL7	-0.543	0.045655	-1
AWRI796_4703	REV1	-0.543	0.045655	-1
AWRI796_4433	YOR022C	-0.544	0.010209	-1
AWRI796_0530	RAD18	-0.552	0.037903	-1
AWRI796_4460	ASE1	-0.552	0.001968	-1
AWRI796_1189	PSP1	-0.555	0.001184	-1
AWRI796_5254	AAD3	-0.555	0.007255	-1
AWRI796_1216	IRC4	-0.56	0.18346	0
AWRI796_0065	SEN34	-0.561	0.008701	-1
AWRI796_0252	POL30	-0.562	0.020552	-1
AWRI796_1819	RME1	-0.563	0.000825	-1
AWRI796_3882	YMR295C	-0.566	0.00406	-1
AWRI796_2670	BFA1	-0.569	0.048402	-1
AWRI796_4296	MDH2	-0.57	0.016343	-1
AWRI796_0977	RMD5	-0.573	0.000825	-1
AWRI796_3619	SPO20	-0.579	1	0
AWRI796_0218	YRO2	-0.587	0.0013	-1
AWRI796_3455	ATG17	-0.593	0.001116	-1
AWRI796_2217	REC104	-0.595	0.0706	0
AWRI796_1001	ZIP1	-0.602	0.005723	-1
AWRI796_3746	ATG16	-0.602	0.005336	-1
AWRI796_4066	YNL146W	-0.606	0.022802	-1
AWRI796_3693	SRT1	-0.612	0.057732	0
AWRI796_1970	AMA1	-0.613	0.016832	-1
AWRI796_3109	THI73	-0.614	0.000125	-1
AWRI796_2214	RTT107	-0.615	0.00095	-1
AWRI796_1553	CNN1	-0.616	0.000731	-1
AWRI796_5178	YOR343W-B	-0.617	0.005408	-1
AWRI796_1533	PES4	-0.628	0.065204	0
AWRI796_3613	YDR210W-B	-0.629	0.050633	0
AWRI796_0155	FUS3	-0.643	0.015286	-1
AWRI796_2899	BLI1	-0.644	0.000351	-1
AWRI796_0593	RTN2	-0.663	0.000181	-1
AWRI796_3041	PCK1	-0.667	0.001633	-1
AWRI796_3375	EST2	-0.668	8.30E-05	-1
AWRI796_3341	PIG1	-0.677	0.00095	-1
AWRI796_5180	YOR192C-A	-0.679	0.042947	-1
AWRI796_0551	MSH3	-0.685	0.000351	-1
AWRI796_4576	PEX27	-0.696	0.000283	-1
AWRI796_1498	HSP12	-0.701	0.000163	-1
AWRI796_2646	LSM8	-0.721	0.000637	-1
AWRI796_3688	SNZ1	-0.721	7.00E-05	-1
AWRI796_1279	GIM4	-0.723	4.30E-05	-1
AWRI796_5177	YOR343W-A	-0.723	0.009878	-1
AWRI796_1884	YGR122W	-0.726	3.10E-05	-1
AWRI796_1277	VAB2	-0.731	0.002214	-1
AWRI796_4667	CPA1	-0.731	0.000152	-1
AWRI796_4039	RHO5	-0.738	0.001026	-1
AWRI796_1347	ICL1	-0.74	4.90E-05	-1
AWRI796_4261	COS3	-0.75	0.011501	-1
AWRI796_3206	YLR108C	-0.752	7.00E-06	-1
AWRI796_0666	YDL114W	-0.769	0.005858	-1
AWRI796_4721	YOR365C	-0.773	0.005408	-1
AWRI796_0235	YBR071W	-0.8	6.40E-05	-1
AWRI796_3670	PDS5	-0.82	1.30E-05	-1
AWRI796_2705	SFC1	-0.823	1.20E-05	-1
AWRI796_3058	YCT1	-0.831	5.60E-05	-1
AWRI796_2032	ECM34	-0.833	0.008183	-1
AWRI796_4868	ISU1	-0.897	6.40E-05	-1
AWRI796_0002	SEO1	-0.907	0.001633	-1
AWRI796_3144	AFB1	-0.911	0.004012	-1
AWRI796_3394	CIS1	-0.934	2.90E-05	-1
AWRI796_5038	ROX1	-0.994	0.000366	-1
AWRI796_4438	CIN5	-0.996	0	-1
AWRI796_1508	MSH4	-1.018	6.40E-05	-1
AWRI796_2704	IME1	-1.028	4.00E-06	-1
AWRI796_0947	YDR222W	-1.064	0	-1
AWRI796_0129	ECM13	-1.191	1.00E-06	-1
AWRI796_1837	YGR066C	-1.217	0	-1
AWRI796_1077	PHO92	-1.495	3.60E-05	-1
AWRI796_4158	NCE103	-1.722	0	-1

Bibliography

Adams, A., Gottschling, D. E., Kaiser, C. A., and Stearns, T. (1998). *Methods in Yeast Genetics: A Cold Spring Harbor Laboratory Course Manual, 1997 Edition*. Cold Spring Harbor Laboratory Press, New York.

Albuquerque, P. and Casadevall, A. (2012). Quorum sensing in fungi – a review. *Medical Mycology*, 50(4):337–345.

Andreottola, G., Foladori, P., Nardelli, P., and Denicolo, A. (2005). Treatment of winery wastewater in a full-scale fixed bed biofilm reactor. *Water Science and Technology*, 51(1):71–79.

Antonangelo, A. T. B. F., Alonso, D. P., Ribolla, P. E. M., and Colombi, D. (2013). Microsatellite marker-based assessment of the biodiversity of native bioethanol yeast strains. *Yeast*, 30(8):307–317.

Azzolini, M., Fedrizzi, B., Tosi, E., Finato, F., Vagnoli, P., Scrinzi, C., and Zapparoli, G. (2012). Effects of *Torulaspora delbrueckii* and *Saccharomyces cerevisiae* mixed cultures on fermentation and aroma of Amarone wine. *European Food Research and Technology*, 235(2):303–313.

Barabási, A.-L. and Oltvai, Z. N. (2004). Network biology: understanding the cell's functional organization. *Nature Reviews Genetics*, 5(2):101–113.

Bardi, L., Crivelli, C., and Marzona, M. (1998). Esterase activity and release of ethyl esters of medium-chain fatty acids by *Saccharomyces cerevisiae* during anaerobic growth. *Canadian Journal of Microbiology*, 44(12):1171–1176.

Barrales, R. R., Jimenez, J., and Ibeas, J. I. (2008). Identification of novel activation mechanisms for *FLO11* regulation in *Saccharomyces cerevisiae*. *Genetics*, 178(1):145–156.

Bauer, F. F. and Pretorius, I. S. (2000). Yeast stress response and fermentation efficiency: how to survive the making of wine - a review. *South African Journal for Enology and Viticulture*, 21:27–51.

Beese, S. E., Negishi, T., Levin, D. E., Boulton, V., Wagle, M., and der Does, C. V. (2009). Identification of positive regulators of the yeast Fps1 glycerol channel. *PLOS Genetics*, 5(11):e1000738.

Bell, S.-J. and Henschke, P. A. (2005). Implications of nitrogen nutrition for grapes, fermentation and wine. *Australian Journal of Grape and Wine Research*, 11(3):242–295.

Binder, B. J., Sundstrom, J. F., Gardner, J. M., Jiranek, V., and Oliver, S. G. (2015). Quantifying two-dimensional filamentous and invasive growth spatial patterns in yeast colonies. *PLOS Computational Biology*, 11(2):e1004070.

Blackstone, E. and Roth, M. B. (2007). Suspended animation-like state protects mice from lethal hypoxia. *Shock*, 27(4):370–372.

Blanco, P., Orriols, I., and Losada, A. (2011). Survival of commercial yeasts in the winery environment and their prevalence during spontaneous fermentations. *Journal of Industrial Microbiology and Biotechnology*, 38(1):235–239.

Bojsen, R. K., Andersen, K. S., and Regenberg, B. (2012). *Saccharomyces cerevisiae* – a model to uncover molecular mechanisms for yeast biofilm biology. *FEMS Immunology and Medical Microbiology*, 65(2):169–182.

Bokulich, N. A., Ohta, M., Richardson, P. M., and Mills, D. A. (2013). Monitoring seasonal changes in winery-resident microbiota. *PLOS ONE*, 8(6):e66437.

Bokulich, N. A., Thorngate, J. H., Richardson, P. M., and Mills, D. A. (2014). Microbial biogeography of wine grapes is conditioned by cultivar, vintage, and climate. *Proceedings of the National Academy of Sciences of the United States of America*, 111(1):E139–E148.

Booher, R. N., Deshaies, R. J., and Kirschner, M. W. (1993). Properties of *Saccharomyces cerevisiae* wee1 and its differential regulation of $p34^{CDC28}$ in response to G_1 and G_2 cyclins. *The EMBO Journal*, 12(9):3417–3426.

Borneman, A. R., Desany, B. A., Riches, D., Affourtit, J. P., Forgan, A. H., Pretorius, I. S., Egholm, M., and Chambers, P. J. (2011). Whole-genome comparison reveals novel genetic elements that characterize the genome of industrial strains of *Saccharomyces cerevisiae*. *PLOS Genetics*, 7(2):e1001287.

Borneman, A. R., Forgan, A. H., Kolouchova, R., Fraser, J. A., and Schmidt, S. A. (2016). Whole genome comparison reveals high levels of inbreeding and strain redundancy across the spectrum of commercial wine strains of *Saccharomyces cerevisiae*. *G3: Genes, Genomes, Genetics*, 6(4):957–971.

Borneman, A. R., Forgan, A. H., Pretorius, I. S., and Chambers, P. J. (2008). Comparative genome analysis of a *Saccharomyces cerevisiae* wine strain. *FEMS Yeast Research*, 8(7):1185–1195.

Braus, G. H., Grundmann, O., Brückner, S., and Mösch, H.-U. (2003). Amino acid starvation and Gcn4p regulate adhesive growth and *FLO11* gene expression in *Saccharomyces cerevisiae*. *Molecular Biology of the Cell*, 14(10):4272–4284.

Brown, J. A., Sherlock, G., Myers, C. L., Burrows, N. M., Deng, C., Wu, H. I., McCann, K. E., Troyanskaya, O. G., and Brown, J. M. (2006). Global analysis of gene function in yeast by quantitative phenotypic profiling. *Molecular Systems Biology*, 2:2006.0001.

Brückner, S. and Mösch, H.-U. (2012). Choosing the right lifestyle: adhesion and development in *Saccharomyces cerevisiae*. *FEMS Microbiology Reviews*, 36(1):25–58.

Busturia, A. and Lagunas, R. (1986). Catabolite inactivation of the glucose transport system in *Saccharomyces cerevisiae*. *Microbiology*, 132(2):379–385.

Calderone, A., Castagnoli, L., and Cesareni, G. (2013). mentha: a resource for browsing integrated protein-interaction networks. *Nature Methods*, 10(8):690–691.

Campbell, K., Vowinckel, J., and Ralser, M. (2016). Cell-to-cell heterogeneity emerges as consequence of metabolic cooperation in a synthetic yeast community. *Biotechnology Journal*, 11(9):1169–1178.

Carmack, M., Moore, M. B., and Balis, M. E. (1950). The structure of the antihemorrhagic sodium bisulfite addition product of 2-Methyl-1,4-naphthoquinone (Menadione)[1]. *Journal of the American Chemical Society*, 72(2):844–847.

Carrozza, M. J., Florens, L., Swanson, S. K., Shia, W.-J., Anderson, S., Yates, J., Washburn, M. P., and Workman, J. L. (2005). Stable incorporation of sequence specific repressors Ash1 and Ume6 into the Rpd3L complex. *Biochimica et Biophysica Acta (BBA) - Gene Structure and Expression*, 1731(2):77–87.

Casalone, E., Barberio, C., Cappellini, L., and Polsinelli, M. (2005). Characterization of *Saccharomyces cerevisiae* natural populations for pseudohyphal growth and colony morphology. *Research in Microbiology*, 156(2):191–200.

Chant, J. and Pringle, J. R. (1995). Patterns of bud-site selection in the yeast *Saccharomyces cerevisiae*. *The Journal of Cell Biology*, 129(3):751–765.

Chavel, C. A., Caccamise, L. M., Li, B., and Cullen, P. J. (2014). Global Regulation of a Differentiation MAPK Pathway in Yeast. *Genetics*, 198(3):1309–1328.

Chen, H. and Fink, G. R. (2006). Feedback control of morphogenesis in fungi by aromatic alcohols. *Genes & Development*, 20(9):1150–1161.

Chen, H., Fujita, M., Feng, Q., Clardy, J., and Fink, G. R. (2004). Tyrosol is a quorum-sensing molecule in *Candida albicans*. *Proceedings of the National Academy of Sciences of the United States of America*, 101(14):5048–5052.

Chen, L., Noorbakhsh, J., Adams, R. M., Samaniego-Evans, J., Agollah, G., Nevozhay, D., Kuzdzal-Fick, J., Mehta, P., and Balázsi, G. (2014). Two-dimensionality of yeast colony expansion accompanied by pattern formation. *PLOS Computational Biology*, 10(12):e1003979.

Christiaens, J. F., Franco, L. M., Cools, T. L., De Meester, L., Michiels, J., Wenseleers, T., Hassan, B. A., Yaksi, E., and Verstrepen, K. J. (2014). The fungal aroma gene *ATF1* promotes dispersal of yeast cells through insect vectors. *Cell Reports*, 9(2):425–432.

Ciani, M., Comitini, F., Mannazzu, I., and Domizio, P. (2010). Controlled mixed culture fermentation: a new perspective on the use of non-*Saccharomyces* yeasts in winemaking. *FEMS Yeast Research*, 10(2):123–133.

Ciani, M., Mannazzu, I., Marinangeli, P., Clementi, F., and Martini, A. (2004). Contribution of winery-resident *Saccharomyces cerevisiae* strains to spontaneous grape must fermentation. *Antonie van Leeuwenhoek*, 85(2):159–164.

Clamens, T., Rosay, T., Crépin, A., Grandjean, T., Kentache, T., Hardouin, J., Bortolotti, P., Neidig, A., Mooij, M., Hillion, M., Vieillard, J., Cosette, P., Overhage, J., O'Gara, F., Bouffartigues, E., Dufour, A., Chevalier, S., Guery, B., Cornelis, P., Feuilloley, M. G. J., and Lesouhaitier, O. (2017). The aliphatic amidase AmiE is involved in regulation of *Pseudomonas aeruginosa* virulence. *Scientific Reports*, 7:41178.

Codon, A. C., Gasent-Ramirez, J. M., and Benitez, T. (1995). Factors which affect the frequency of sporulation and tetrad formation in *Saccharomyces cerevisiae* baker's yeasts. *Applied and Environment Microbiology*, 61(2):630–638.

Comitini, F., Gobbi, M., Domizio, P., Romani, C., Lencioni, L., Mannazzu, I., and Ciani, M. (2011). Selected non-*Saccharomyces* wine yeasts in controlled multistarter fermentations with *Saccharomyces cerevisiae*. *Food Microbiology*, 28(5):873–882.

Cook, J. G., Bardwell, L., and Thorner, J. (1997). Inhibitory and activating functions for MAPK Kss1 in the *S. cerevisiae* filamentous-growth signalling pathway. *Nature*, 390(6655):85–88.

Corbacho, I., Teixidó, F., Velázquez, R., Hernández, L. M., and Olivero, I. (2011). Standard YPD, even supplemented with extra nutrients, does not always compensate growth defects of *Saccharomyces cerevisiae* auxotrophic strains. *Antonie van Leeuwenhoek*, 99(3):591–600.

Cordente, A. G., Heinrich, A., Pretorius, I. S., and Swiegers, J. H. (2009). Isolation of sulfite reductase variants of a commercial wine yeast with significantly reduced hydrogen sulfide production. *FEMS Yeast Research*, 9(3):446–459.

Cordero-Bueso, G., Arroyo, T., Serrano, A., and Valero, E. (2011). Remanence and survival of commercial yeast in different ecological niches of the vineyard. *FEMS Microbiology Ecology*, 77(2):429–437.

Costanzo, M., Baryshnikova, A., Bellay, J., Kim, Y., Spear, E. D., Sevier, C. S., Ding, H., Koh, J. L., Toufighi, K., Mostafavi, S., Prinz, J., St. Onge, R. P., VanderSluis, B., Makhnevych, T., Vizeacoumar, F. J., Alizadeh, S., Bahr, S., Brost, R. L., Chen, Y., Cokol, M., Deshpande, R., Li, Z., Lin, Z.-Y., Liang, W., Marback, M., Paw, J., San

Luis, B.-J., Shuteriqi, E., Tong, A. H. Y., van Dyk, N., Wallace, I. M., Whitney, J. A., Weirauch, M. T., Zhong, G., Zhu, H., Houry, W. A., Brudno, M., Ragibizadeh, S., Papp, B., Pál, C., Roth, F. P., Giaever, G., Nislow, C., Troyanskaya, O. G., Bussey, H., Bader, G. D., Gingras, A.-C., Morris, Q. D., Kim, P. M., Kaiser, C. A., Myers, C. L., Andrews, B. J., and Boone, C. (2010). The genetic landscape of a cell. *Science*, 327(5964):425–431.

Costerton, J. W., Lewandowski, Z., Caldwell, D. E., Korber, D. R., and Lappin-Scott, H. M. (1995). Microbial biofilms. *Annual Review of Microbiology*, 49(1):711–745.

Cottier, F. and Mühlschlegel, F. A. (2011). Communication in fungi. *International Journal of Microbiology*, 2012:351832.

Cullen, P. J. and Sprague, G. F. (2000). Glucose depletion causes haploid invasive growth in yeast. *Proceedings of the National Academy of Sciences of the United States of America*, 97(25):13619–13624.

Cullen, P. J. and Sprague, G. F. (2002). The roles of bud-site-selection proteins during haploid invasive growth in yeast. *Molecular Biology of the Cell*, 13:2990–3004.

Cullen, P. J. and Sprague, G. F. (2012). The regulation of filamentous growth in yeast. *Genetics*, 190(1):23–49.

Cutler, N. S., Pan, X., Heitman, J., and Cardenas, M. E. (2001). The TOR signal transduction cascade controls cellular differentiation in response to nutrients. *Molecular Biology of the Cell*, 12(12):4103–4113.

Davis-Hanna, A., Piispanen, A. E., Stateva, L. I., and Hogan, D. A. (2008). Farnesol and dodecanol effects on the *Candida albicans* Ras1-cAMP signalling pathway and the regulation of morphogenesis. *Molecular Microbiology*, 67(1):47–62.

Dickinson, J. R. (1994). Irreversible formation of pseudohyphae by haploid *Saccharomyces cerevisiae*. *FEMS Microbiology Letters*, 119(1–2):99–103.

Dickinson, J. R. (1996). 'Fusel' alcohols induce hyphal-like extensions and pseudohyphal formation in yeasts. *Microbiology*, 142(6):1391–1397.

Dikicioglu, D., Dunn, W. B., Kell, D. B., Kirdar, B., and Oliver, S. G. (2012). Short- and long-term dynamic responses of the metabolic network and gene expression in yeast to a transient change in the nutrient environment. *Molecular BioSystems*, 8(6):1760–1774.

Dikicioglu, D., Karabekmez, E., Rash, B., Pir, P., Kirdar, B., and Oliver, S. G. (2011). How yeast re-programmes its transcriptional profile in response to different nutrient impulses. *BMC Systems Biology*, 5(1):148.

Divol, B., du Toit, M., and Duckitt, E. (2012). Surviving in the presence of sulphur dioxide: strategies developed by wine yeasts. *Applied Microbiology and Biotechnology*, 95(3):601–613.

Doeller, J. E., Isbell, T. S., Benavides, G., Koenitzer, J., Patel, H., Patel, R. P., Lancaster, J. R., Darley-Usmar, V. M., and Kraus, D. W. (2005). Polarographic measurement of hydrogen sulfide production and consumption by mammalian tissues. *Analytical Biochemistry*, 341(1):40–51.

Domitrovic, T., Kozlov, G., Freire, J. C. G., Masuda, C. A., Almeida, M. d. S., Montero-Lomeli, M., Atella, G. C., Matta-Camacho, E., Gehring, K., and Kurtenbach, E. (2010). Structural and functional study of Yer067w, a new protein involved in yeast metabolism control and drug resistance. *PLOS ONE*, 5(6):e11163.

Dowell, R. D., Ryan, O., Jansen, A., Cheung, D., Agarwala, S., Danford, T., Bernstein, D. A., Rolfe, P. A., Heisler, L. E., Chin, B., Nislow, C., Giaever, G., Phillips, P. C., Fink, G. R., Gifford, D. K., and Boone, C. (2010). Genotype to phenotype: a complex problem. *Science*, 328(5977):469.

Elshorbagy, A. K., Valdivia-Garcia, M., Mattocks, D. A. L., Plummer, J. D., Orentreich, D. S., Orentreich, N., Refsum, H., and Perrone, C. E. (2013). Effect of taurine and N-acetylcysteine on methionine restriction-mediated adiposity resistance. *Metabolism: Clinical & Experimental*, 62(4):509–517.

Finn, R. D., Coggill, P., Eberhardt, R. Y., Eddy, S. R., Mistry, J., Mitchell, A. L., Potter, S. C., Punta, M., Qureshi, M., Sangrador-Vegas, A., Salazar, G. A., Tate, J., and Bateman, A. (2016). The Pfam protein families database: towards a more sustainable future. *Nucleic Acids Research*, 44(D1):D279–D285.

Fleet, G. and Heard, G. (1993). Yeasts: growth during fermentation. In Fleet, G., editor, *Wine Microbiology and Biotechnology*, pages 27–75. Harwood Academic Publishers, Chur, Switzerland.

Francis, I. L. and Newton, J. L. (2005). Determining wine aroma from compositional data. *Australian Journal of Grape and Wine Research*, 11(2):114–126.

Furne, J., Saeed, A., and Levitt, M. D. (2008). Whole tissue hydrogen sulfide concentrations are orders of magnitude lower than presently accepted values. *American Journal of Physiology - Regulatory, Integrative and Comparative Physiology*, 295(5):R1479–R1485.

Gardner, J. M., Poole, K., and Jiranek, V. (2002). Practical significance of relative assimilable nitrogen requirements of yeast: a preliminary study of fermentation performance and liberation of H_2S. *Australian Journal of Grape and Wine Research*, 8(3):175–179.

Gasch, A. P., Spellman, P. T., Kao, C. M., Carmel-Harel, O., Eisen, M. B., Storz, G., Botstein, D., and Brown, P. O. (2000). Genomic expression programs in the response of yeast cells to environmental changes. *Molecular Biology of the Cell*, 11(12):4241–4257.

Gayevskiy, V. and Goddard, M. R. (2012). Geographic delineations of yeast communities and populations associated with vines and wines in New Zealand. *The ISME Journal*, 6(7):1281–1290.

Gietz, R. D. and Schiestl, R. H. (2007). High-efficiency yeast transformation using the LiAc/SS carrier DNA/PEG method. *Nature Protocols*, 2(1):31–34.

Gimeno, C. J., Ljungdahl, P. O., Styles, C. A., and Fink, G. R. (1992). Unipolar cell divisions in the yeast *S. cerevisiae* lead to filamentous growth: Regulation by starvation and RAS. *Cell*, 68(6):1077–1090.

Gladfelter, A. S., Kozubowski, L., Zyla, T. R., and Lew, D. J. (2005). Interplay between septin organization, cell cycle and cell shape in yeast. *Journal of Cell Science*, 118(8):1617–1628.

Gladfelter, A. S., Zyla, T. R., and Lew, D. J. (2004). Genetic interactions among regulators of septin organization. *Eukaryotic Cell*, 3(4):847–854.

Gobbi, M., Comitini, F., Domizio, P., Romani, C., Lencioni, L., Mannazzu, I., and Ciani, M. (2013). *Lachancea thermotolerans* and *Saccharomyces cerevisiae* in simultaneous and sequential co-fermentation: A strategy to enhance acidity and improve the overall quality of wine. *Food Microbiology*, 33(2):271–281.

Goddard, M. R., Anfang, N., Tang, R., Gardner, R. C., and Jun, C. (2010). A distinct population of *Saccharomyces cerevisiae* in New Zealand: evidence for local dispersal by insects and human-aided global dispersal in oak barrels. *Environmental Microbiology*, 12(1):63–73.

Gori, K., Knudsen, P. B., Nielsen, K. F., Arneborg, N., and Jespersen, L. (2011). Alcohol-based quorum sensing plays a role in adhesion and sliding motility of the yeast *Debaryomyces hansenii*. *FEMS Yeast Research*, 11(8):643–652.

Granek, J. A. and Magwene, P. M. (2010). Environmental and genetic determinants of colony morphology in yeast. *PLOS Genetics*, 6(1):e1000823.

Granek, J. A., Murray, D., Kayrkçi, Ö., and Magwene, P. M. (2013). The genetic architecture of biofilm formation in a clinical isolate of *Saccharomyces cerevisiae*. *Genetics*, 193(2):587–600.

Grüning, N.-M., Lehrach, H., and Ralser, M. (2010). Regulatory crosstalk of the metabolic network. *Trends in Biochemical Sciences*, 35(4):220–227.

Guo, B., Styles, C. A., Feng, Q., and Fink, G. R. (2000). A *Saccharomyces* gene family involved in invasive growth, cell-cell adhesion, and mating. *Proceedings of the National Academy of Sciences of the United States of America*, 97(22):12158–12163.

Hall, B., Durall, D. M., and Stanley, G. (2011). Population dynamics of *Saccharomyces cerevisiae* during spontaneous fermentation at a British Columbia winery. *American Journal of Enology and Viticulture*, 62(1):66–72.

Halme, A., Bumgarner, S., Styles, C., and Fink, G. R. (2004). Genetic and epigenetic regulation of the *FLO* gene family generates cell-surface variation in yeast. *Cell*, 116(3):405–415.

Harashima, T. and Heitman, J. (2002). The Gα protein Gpa2 controls yeast differentiation by interacting with Kelch repeat proteins that mimic Gβ subunits. *Molecular Cell*, 10(1):163–173.

Harkins, H. A., Pagé, N., Schenkman, L. R., De Virgilio, C., Shaw, S., Bussey, H., and Pringle, J. R. (2001). Bud8p and Bud9p, proteins that may mark the sites for bipolar budding in yeast. *Molecular Biology of the Cell*, 12(8):2497–2518.

Hasan, F., Xess, I., Wang, X., Jain, N., and Fries, B. C. (2009). Biofilm formation in clinical *Candida* isolates and its association with virulence. *Microbes and Infection*, 11(8–9):753–761.

Hazelwood, L. A., Daran, J.-M., van Maris, A. J. A., Pronk, J. T., and Dickinson, J. R. (2008). The Ehrlich pathway for fusel alcohol production: a century of research on *Saccharomyces cerevisiae* metabolism. *Applied and Environmental Microbiology*, 74(8):2259–2266.

He, X., Li, S., and Kaminskyj, S. G. W. (2014). Using *Aspergillus nidulans* to identify antifungal drug resistance mutations. *Eukaryotic Cell*, 13(2):288–294.

Henke, J. M. and Bassler, B. L. (2004). Bacterial social engagements. *Trends in Cell Biology*, 14(11):648–656.

Hess, D. C., Myers, C. L., Huttenhower, C., Hibbs, M. A., Hayes, A. P., Paw, J., Clore, J. J., Mendoza, R. M., Luis, B. S., Nislow, C., Giaever, G., Costanzo, M., Troyanskaya, O. G., and Caudy, A. A. (2009). Computationally driven, quantitative experiments discover genes required for mitochondrial biogenesis. *PLOS Genetics*, 5(3):e1000407.

Hine, C. and Mitchell, J. R. (2015). Calorie restriction and methionine restriction in control of endogenous hydrogen sulfide production by the transsulfuration pathway. *Experimental Gerontology*, 68:26–32.

Hinze, H. and Holzer, H. (1986). Analysis of the energy metabolism after incubation of *Saccharomyces cerevisiae* with sulfite or nitrite. *Archives of Microbiology*, 145(1):27–31.

Homoto, S. and Izawa, S. (2016). Effects of severe ethanol stress on septin-localization and morphology of *Saccharomyces cerevisiae*. In *14th International Congress on Yeasts Program & Abstracts*, page 250.

Honigberg, S. M. (2011). Cell signals, cell contacts, and the organization of yeast communities. *Eukaryotic Cell*, 10(4):466–473.

Hope, E. A. and Dunham, M. J. (2014). Ploidy-regulated variation in biofilm-related phenotypes in natural isolates of *Saccharomyces cerevisiae*. *G3: Genes, Genomes, Genetics*, 4(9):1773–1786.

Hornby, J. M., Jensen, E. C., Lisec, A. D., Tasto, J. J., Jahnke, B., Shoemaker, R., Dussault, P., and Nickerson, K. W. (2001). Quorum sensing in the dimorphic fungus *Candida albicans* is mediated by farnesol. *Applied and Environmental Microbiology*, 67(7):2982–2992.

Hurles, M. E., Matisoo-Smith, E., Gray, R. D., and Penny, D. (2003). Untangling Oceanic settlement: the edge of the knowable. *Trends in Ecology & Evolution*, 18(10):531–540.

Hwang, G.-W., Furuchi, T., and Naganuma, A. (2007). Ubiquitin-conjugating enzyme Cdc34 mediates cadmium resistance in budding yeast through ubiquitination of the transcription factor Met4. *Biochemical & Biophysical Research Communications*, 363(3):873–878.

Iranon, N. N. and Miller, D. L. (2012). Interactions between oxygen homeostasis, food availability, and hydrogen sulfide signaling. *Frontiers in Genetics*, 3:257.

Iraqui, I., Vissers, S., André, B., and Urrestarazu, A. (1999). Transcriptional induction by aromatic amino acids in *Saccharomyces cerevisiae*. *Molecular and Cellular Biology*, 19(5):3360–3371.

Jia, X., He, W., Murchie, A. I. H., and Chen, D. (2011). The global transcriptional response of fission yeast to hydrogen sulfide. *PLOS ONE*, 6(12):e28275.

Jin, R., Dobry, C. J., McCown, P. J., and Kumar, A. (2008). Large-scale analysis of yeast filamentous growth by systematic gene disruption and overexpression. *Molecular Biology of the Cell*, 19(1):284–296.

Jiranek, V., Langridge, P., and Henschke, P. A. (1995). Regulation of hydrogen sulfide liberation in wine-producing *Saccharomyces cerevisiae* strains by assimilable nitrogen. *Applied and Environmental Microbiology*, 61(2):461–467.

John Hopkins School of Medicine (1999). Quick DAPI staining of yeast.

Johnson, C., Kweon, H. K., Sheidy, D., Shively, C. A., Mellacheruvu, D., Nesvizhskii, A. I., Andrews, P. C., and Kumar, A. (2014). The yeast Sks1p kinase signaling network regulates pseudohyphal growth and glucose response. *PLOS Genetics*, 10(3):e1004183.

Johnson, J. E. and Johnson, F. B. (2014). Methionine restriction activates the retrograde response and confers both stress tolerance and lifespan extension to yeast, mouse and human cells. *PLOS ONE*, 9(5):e97729.

Johnson, J. W., Fisher, J. F., and Mobashery, S. (2013). Bacterial cell-wall recycling. *Annals of the New York Academy of Sciences*, 1277(1):54–75.

Karunanithi, S., Joshi, J., Chavel, C., Birkaya, B., Grell, L., and Cullen, P. J. (2012). Regulation of mat responses by a differentiation MAPK pathway in *Saccharomyces cerevisiae*. *PLOS ONE*, 7(4):e32294.

Klis, F. M., Boorsma, A., and De Groot, P. W. J. (2006). Cell wall construction in *Saccharomyces cerevisiae*. *Yeast*, 23(3):185–202.

Knight, S., Klaere, S., Fedrizzi, B., Goddard, M. R., and Querol, A. (2015). Regional microbial signatures positively correlate with differential wine phenotypes: evidence for a microbial aspect to terroir. *Scientific Reports*, 5(1):14233.

Koh, J. L. Y., Ding, H., Costanzo, M., Baryshnikova, A., Toufighi, K., Bader, G. D., Myers, C. L., Andrews, B. J., and Boone, C. (2010). DRYGIN: a database of quantitative genetic interaction networks in yeast. *Nucleic Acids Research*, 38(Database issue):D502–D507.

Kron, S. J., Styles, C. A., and Fink, G. R. (1994). Symmetric cell division in pseudohyphae of the yeast *Saccharomyces cerevisiae*. *Molecular Biology of the Cell*, 5(9):1003–1022.

Kubota, S., Takeo, I., Kume, K., Kanai, M., Shitamukai, A., Mizunuma, M., Miyakawa, T., Shimoi, H., Iefuji, H., and Hirata, D. (2004). Effect of ethanol on cell growth of budding yeast: genes that are important for cell growth in the presence of ethanol. *Bioscience, Biotechnology, and Biochemistry*, 68(4):968–972.

Kuchin, S., Vyas, V. K., and Carlson, M. (2002). Snf1 protein kinase and the repressors Nrg1 and Nrg2 regulate *FLO11*, haploid invasive growth, and diploid pseudohyphal differentiation. *Molecular and Cellular Biology*, 22(12):3994–4000.

Kuthan, M., Devaux, F., Janderová, B., Slaninová, I., Jacq, C., and Palková, Z. (2003). Domestication of wild *Saccharomyces cerevisiae* is accompanied by changes in gene expression and colony morphology. *Molecular Microbiology*, 47(3):745–754.

Lafuente, M. J., Gancedo, C., Jauniaux, J.-C., and Gancedo, J. M. (2000). Mth1 receives the signal given by the glucose sensors Snf3 and Rgt2 in *Saccharomyces cerevisiae*. *Molecular Microbiology*, 35(1):161–172.

Lambrechts, M. and Bauer, F. (1996). Muc1, a mucin-like protein that is regulated by Mss10, is critical for pseudohyphal differentiation in yeast. *Proceedings of the National Academy of Sciences of the United States of America*, 93(16):8419–8424.

Law, C. W., Chen, Y., Shi, W., and Smyth, G. K. (2014). voom: precision weights unlock linear model analysis tools for RNA-seq read counts. *Genome Biology*, 15(2):R29.

Lees, E. K., Król, E., Grant, L., Shearer, K., Wyse, C., Moncur, E., Bykowska, A. S., Mody, N., Gettys, T. W., and Delibegovic, M. (2014). Methionine restriction restores a younger metabolic phenotype in adult mice with alterations in fibroblast growth factor 21. *Aging Cell*, 13(5):817–827.

Liao, Y., Smyth, G. K., and Shi, W. (2013). The Subread aligner: fast, accurate and scalable read mapping by seed-and-vote. *Nucleic Acids Research*, 41(10):e108.

Lilly, M., Bauer, F. F., Lambrechts, M. G., Swiegers, J. H., Cozzolino, D., and Pretorius, I. S. (2006). The effect of increased yeast alcohol acetyltransferase and esterase activity on the flavour profiles of wine and distillates. *Yeast*, 23(9):641–659.

Linderholm, A. L., Findleton, C. L., Kumar, G., Hong, Y., and Bisson, L. F. (2008). Identification of genes affecting hydrogen sulfide formation in *Saccharomyces cerevisiae*. *Applied and Environmental Microbiology*, 74(5):1418–1427.

Litzinger, S., Duckworth, A., Nitzsche, K., Risinger, C., Wittmann, V., and Mayer, C. (2010). Muropeptide rescue in *Bacillus subtilis* involves sequential hydrolysis by β-*N*-acetylglucosaminidase and *N*-acetylmuramyl-L-alanine amidase. *Journal of Bacteriology*, 192(12):3132–3143.

Liu, H., Styles, C. A., and Fink, G. R. (1993). Elements of the yeast pheromone response pathway required for filamentous growth of diploids. *Science*, 262(5140):1741–1744.

Liu, H., Styles, C. A., and Fink, G. R. (1996). *Saccharomyces cerevisiae* S288C has a mutation in *FLO8*, a gene required for filamentous growth. *Genetics*, 144(3):967–978.

Liu, Z. and Butow, R. A. (2006). Mitochondrial retrograde signaling. *Annual Review of Genetics*, 40:159–185.

Lloyd, D. (2006). Hydrogen sulfide: clandestine microbial messenger? *Trends in Microbiology*, 14(10):456–462.

Lo, W. S. and Dranginis, A. M. (1998). The cell surface flocculin Flo11 is required for pseudohyphae formation and invasion by *Saccharomyces cerevisiae*. *Molecular Biology of the Cell*, 9(1):161–171.

Lõoke, M., Kristjuhan, K., and Kristjuhan, A. (2011). Extraction of genomic DNA from yeasts for PCR-based applications. *BioTechniques*, 50(5):325–328.

Lorenz, M. C., Cutler, N. S., and Heitman, J. (2000). Characterization of alcohol-induced filamentous growth in *Saccharomyces cerevisiae*. *Molecular Biology of the Cell*, 11(1):183–199.

Lorenz, M. C. and Heitman, J. (1998). Regulators of pseudohyphal differentiation in *Saccharomyces cerevisiae* identified through multicopy suppressor analysis in ammonium permease mutant strains. *Genetics*, 150(4):1443–1457.

Luyten, K., Riou, C., and Blondin, B. (2002). The hexose transporters of *Saccharomyces cerevisiae* play different roles during enological fermentation. *Yeast*, 19(8):713–726.

Malandra, L., Wolfaardt, G., Zietsman, A., and Viljoen-Bloom, M. (2003). Microbiology of a biological contactor for winery wastewater treatment. *Water Research*, 37(17):4125–4134.

Mannheim, B. (1989). D-glucose/d-fructose. In *Methods of Biochemical Analysis and Food Analysis*, pages 50–55. Boehringer Mannheim.

Martineau, C. N., Beckerich, J. M., and Kabani, M. (2007). Flo11p-independent control of "mat" formation by Hsp70 molecular chaperones and nucleotide exchange factors in yeast. *Genetics*, 177(3):1679–1689.

Martineau, C. N., Melki, R., and Kabani, M. (2010). Swa2p-dependent clathrin dynamics is critical for Flo11p processing and 'Mat' formation in the yeast *Saccharomyces cerevisiae*. *FEBS Letters*, 584(6):1149–1155.

Martínez, A., Torello, S., and Kolter, R. (1999). Sliding motility in Mycobacteria. *Journal of Bacteriology*, 181(23):7331–7338.

Martínez, P., Pérez Rodríguez, L., and Benítez, T. (1997). Velum formation by flor yeasts isolated from sherry wine. *American Journal of Enology and Viticulture*, 48(1):55–62.

Martini, A. (1993). Origin and domestication of the wine yeast *Saccharomyces cerevisiae*. *Journal of Wine Research*, 4(3):165–176.

Martiniuk, J. T., Pacheco, B., Russell, G., Tong, S., Backstrom, I., and Measday, V. (2016). Impact of commercial strain use on *Saccharomyces cerevisiae* population structure and dynamics in Pinot Noir vineyards and spontaneous fermentations of a Canadian winery. *PLOS ONE*, 11(8):1–19.

Matsushita, M. and Fujikawa, H. (1990). Diffusion-limited growth in bacterial colony formation. *Physica A: Statistical Mechanics and its Applications*, 168(1):498–506.

McCarthy, D. J. and Smyth, G. K. (2009). Testing significance relative to a fold-change threshold is a TREAT. *Bioinformatics*, 25(6):765–771.

Miller, D. L. and Roth, M. B. (2007). Hydrogen sulfide increases thermotolerance and lifespan in *Caenorhabditis elegans*. *Proceedings of the National Academy of Sciences of the United States of America*, 104(51):20618–20622.

Miller, M. B. and Bassler, B. L. (2001). Quorum sensing in bacteria. *Annual Review of Microbiology*, 55(1):165–199.

Miller, R. A., Buehner, G., Chang, Y., Harper, J. M., Sigler, R., and Smith-Wheelock, M. (2005). Methionine-deficient diet extends mouse lifespan, slows immune and lens aging, alters glucose, T4, IGF-I and insulin levels, and increases hepatocyte MIF levels and stress resistance. *Aging Cell*, 4(3):119–125.

Mitchell, A., Chang, H.-Y., Daugherty, L., Fraser, M., Hunter, S., Lopez, R., McAnulla, C., McMenamin, C., Nuka, G., Pesseat, S., Sangrador-Vegas, A., Scheremetjew, M., Rato, C., Yong, S.-Y., Bateman, A., Punta, M., Attwood, T. K., Sigrist, C. J. A., Redaschi, N., Rivoire, C., Xenarios, I., Kahn, D., Guyot, D., Bork, P., Letunic, I., Gough, J., Oates, M., Haft, D., Huang, H., Natale, D. A., Wu, C. H., Orengo, C.,

Sillitoe, I., Mi, H., Thomas, P. D., and Finn, R. D. (2015). The InterPro protein families database: the classification resource after 15 years. *Nucleic Acids Research*, 43(Database issue):D213–D221.

Mortimer, R. and Polsinelli, M. (1999). On the origins of wine yeast. *Research in Microbiology*, 150(3):199–204.

Murray, D. B., Klevecz, R. R., and Lloyd, D. (2003). Generation and maintenance of synchrony in *Saccharomyces cerevisiae* continuous culture. *Experimental Cell Research*, 287(1):10–15.

Niederberger, P., Miozzari, G., and Hotte, R. (1981). Biological role of the general control of amino acid biosynthesis in *Saccharomyces cerevisiae*. *Molecular and Cellular Biology*, 1(7):584–593.

Ochiai, S., Yasumoto, S., Morohoshi, T., and Ikeda, T. (2014). AmiE, a novel *N*-acylhomoserine lactone acylase belonging to the amidase family, from the activated-sludge isolate *Acinetobacter* sp. strain Ooi24. *Applied and Environmental Microbiology*, 80(22):6919–6925.

Octavio, L. M., Gedeon, K., and Maheshri, N. (2009). Epigenetic and conventional regulation is distributed among activators of *FLO11* allowing tuning of population-level heterogeneity in its expression. *PLOS Genetics*, 5(10):e1000673.

Oliveira, R., Lages, F., Silva-Graça, M., and Lucas, C. (2003). Fps1p channel is the mediator of the major part of glycerol passive diffusion in *Saccharomyces cerevisiae*: artefacts and re-definitions. *Biochimica et Biophysica Acta (BBA) - Biomembranes*, 1613(1):57–71.

Olson, K. R. (2012). Mitochondrial adaptations to utilize hydrogen sulfide for energy and signaling. *Journal of Comparative Physiology B*, 182(7):881–897.

Olson, K. R. and Whitfield, N. L. (2010). Hydrogen sulfide and oxygen sensing in the cardiovascular system. *Antioxidants & Redox Signaling*, 12(10):1219–1234.

Olson, K. R., Whitfield, N. L., Bearden, S. E., St Leger, J., Nilson, E., Gao, Y., and Madden, J. A. (2010). Hypoxic pulmonary vasodilation: a paradigm shift with a hydrogen sulfide mechanism. *American Journal of Physiology - Regulatory, Integrative and Comparative Physiology*, 298(1):R51–R60.

O'Toole, G., Kaplan, H. B., and Kolter, R. (2000). Biofilm formation as microbial development. *Annual Review of Microbiology*, 54(1):49–79.

Palecek, S. P., Parikh, A. S., and Kron, S. J. (2000). Genetic analysis reveals that *FLO11* upregulation and cell polarization independently regulate invasive growth in *Saccharomyces cerevisiae*. *Genetics*, 156(3):1005–1023.

Palecek, S. P., Parikh, A. S., and Kron, S. J. (2002). Sensing, signalling and integrating physical processes during *Saccharomyces cerevisiae* invasive and filamentous growth. *Microbiology*, 148(4):893–907.

Palková, Z., Janderová, B., Gabriel, J., Zikánová, B., Pospísek, M., and Forstová, J. (1997). Ammonia mediates communication between yeast colonies. *Nature*, 390(6659):532–536.

Palková, Z. and Váchová, L. (2006). Life within a community: benefit to yeast long-term survival. *FEMS Microbiology Reviews*, 30(5):806–824.

Palková, Z., Wilkinson, D., and Váchová, L. (2014). Aging and differentiation in yeast populations: elders with different properties and functions. *FEMS Yeast Research*, 14(1):96–108.

Palma, M., Madeira, S. C., Mendes-Ferreira, A., and Sá-Correia, I. (2012). Impact of assimilable nitrogen availability in glucose uptake kinetics in *Saccharomyces cerevisiae* during alcoholic fermentation. *Microbial Cell Factories*, 11:99.

Pan, X. and Heitman, J. (2002). Protein kinase A operates a molecular switch that governs yeast pseudohyphal differentiation. *Molecular and Cellular Biology*, 22(12):3981–3993.

Park, H. and Hwang, Y.-S. (2008). Genome-wide transcriptional responses to sulfite in *Saccharomyces cerevisiae*. *Journal of Microbiology*, 46(5):542–548.

Park, H.-O. and Bi, E. (2007). Central roles of small GTPases in the development of cell polarity in yeast and beyond. *Microbiology and Molecular Biology Reviews*, 71(1):48–96.

Parsek, M. R. and Singh, P. K. (2003). Bacterial biofilms: an emerging link to disease pathogenesis. *Annual Reviews in Microbiology*, 57(1):677–701.

Pinto, C., Pinho, D., Cardoso, R., Custódio, V., Fernandes, J., Sousa, S., Pinheiro, M., Egas, C., and Gomes, A. C. (2015). Wine fermentation microbiome: A landscape from different Portuguese wine appellations. *Frontiers in Microbiology*, 6:905.

Plaisance, E. P., Greenway, F. L., Boudreau, A., Hill, K. L., Johnson, W. D., Krajcik, R. A., Perrone, C. E., Orentreich, N., Cefalu, W. T., and Gettys, T. W. (2011). Dietary methionine restriction increases fat oxidation in obese adults with metabolic syndrome. *The Journal of Clinical Endocrinology & Metabolism*, 96(5):E836–E840.

Porman, A. M., Alby, K., Hirakawa, M. P., and Bennett, R. J. (2011). Discovery of a phenotypic switch regulating sexual mating in the opportunistic fungal pathogen *Candida tropicalis*. *Proceedings of the National Academy of Sciences of the United States of America*, 108(52):21158–21163.

Preibisch, S., Saalfeld, S., and Tomancak, P. (2009). Globally optimal stitching of tiled 3D microscopic image acquisitions. *Bioinformatics*, 25(11):1463–1465.

Pretorius, I. S., van der Westhuizen, T. J., and Augustyn, O. P. H. (1999). Yeast biodiversity in vineyards and wineries and its importance to the South African wine industry. *South African Journal of Enology and Viticulture*, 20(2):61–74.

Pruyne, D. and Bretscher, A. (2000). Polarization of cell growth in yeast. *Journal of Cell Science*, 113:365–375.

Querol, A., Barrio, E., and Ramón, D. (1994). Population dynamics of natural *Saccharomyces* strains during wine fermentation. *International Journal of Food Microbiology*, 21(4):315–323.

Ramage, G., Saville, S. P., Thomas, D. P., and López-Ribot, J. L. (2005). *Candida* biofilms: an update. *Eukaryotic Cell*, 4(4):633–638.

Rankine, B. C. and Pocock, K. F. (1969). Influence of yeast strain on binding of sulphur dioxide in wines, and on its formation during fermentation. *Journal of the Science of Food and Agriculture*, 20(2):104–109.

Recht, J., Martínez, A., Torello, S., and Kolter, R. (2000). Genetic analysis of sliding motility in *Mycobacterium smegmatis*. *Journal of Bacteriology*, 182(15):4348–4351.

Regenberg, B., Hanghøj, K. E., Andersen, K. S., and Boomsma, J. J. (2016). Clonal yeast biofilms can reap competitive advantages through cell differentiation without being obligatorily multicellular. *Proceedings of the Royal Society B - Biological Sciences*, 283(1842):20161303.

Rep, M., Krantz, M., Thevelein, J. M., and Hohmann, S. (2000). The transcriptional response of *Saccharomyces cerevisiae* to osmotic shock. *The Journal of Biological Chemistry*, 275(12):8290–8300.

Reynolds, T. B. (2006). The Opi1p transcription factor affects expression of *FLO11*, mat formation, and invasive growth in *Saccharomyces cerevisiae*. *Eukaryotic cell*, 5(8):1266–1275.

Reynolds, T. B. and Fink, G. R. (2001). Bakers' yeast, a model for fungal biofilm formation. *Science*, 291(5505):878–881.

Reynolds, T. B., Jansen, A., Peng, X., and Fink, G. R. (2008). Mat formation in *Saccharomyces cerevisiae* requires nutrient and pH gradients. *Eukaryotic Cell*, 7(1):122–130.

Ritchie, M. E., Phipson, B., Wu, D., Hu, Y., Law, C. W., Shi, W., and Smyth, G. K. (2015). *limma* powers differential expression analyses for RNA-sequencing and microarray studies. *Nucleic Acids Research*, 43(7):e47.

Roberts, R. L. and Fink, G. R. (1994). Elements of a single MAP kinase cascade in *Saccharomyces cerevisiae* mediate two developmental programs in the same cell type: mating and invasive growth. *Genes & Development*, 8(24):2974–2985.

Robertson, L. S. and Fink, G. R. (1998). The three yeast A kinases have specific signaling functions in pseudohyphal growth. *Proceedings of the National Academy of Sciences of the United States of America*, 95(23):13783–13787.

Rodriguez, M. E., Orozco, H., Cantoral, J. M., Matallana, E., and Aranda, A. (2014). Acetyltransferase *SAS2* and sirtuin *SIR2*, respectively, control flocculation and biofilm formation in wine yeast. *FEMS Yeast Research*, 14(6):845–857.

Rossouw, D., Bagheri, B., Setati, M. E., and Bauer, F. F. (2015). Co-flocculation of yeast species, a new mechanism to govern population dynamics in microbial ecosystems. *PLOS ONE*, 10(8):e0136249.

Rupp, S., Summers, E., Lo, H. J., Madhani, H., and Fink, G. (1999). MAP kinase and cAMP filamentation signaling pathways converge on the unusually large promoter of the yeast *FLO11* gene. *The EMBO Journal*, 18(5):1257–1269.

Ryan, M., Bridge, P., Smith, D., and Jeffries, P. (2002). Phenotypic degeneration occurs during sector formation in *Metarhizium anisopliae*. *Journal of Applied Microbiology*, 93(1):163–168.

Ryan, O., Shapiro, R. S., Kurat, C. F., Mayhew, D., Baryshnikova, A., Chin, B., Lin, Z.-Y., Cox, M. J., Vizeacoumar, F., Cheung, D., Bahr, S., Tsui, K., Tebbji, F., Sellam, A., Istel, F., Schwarzmüller, T., Reynolds, T. B., Kuchler, K., Gifford, D. K., Whiteway, M., Giaever, G., Nislow, C., Costanzo, M., Gingras, A.-C., Mitra, R. D., Andrews, B., Fink, G. R., Cowen, L. E., and Boone, C. (2012). Global gene deletion analysis exploring yeast filamentous growth. *Science*, 337(6100):1353–1356.

Rytka, J. (1975). Positive selection of general amino acid permease mutants in *Saccharomyces cerevisiae*. *Journal of Bacteriology*, 121(2):562–570.

Saerens, S. M. G., Delvaux, F. R., Verstrepen, K. J., and Thevelein, J. M. (2010). Production and biological function of volatile esters in *Saccharomyces cerevisiae*. *Microbial Biotechnology*, 3(2):165–177.

Saerens, S. M. G., Verstrepen, K. J., Van Laere, S. D. M., Voet, A. R. D., Van Dijck, P., Delvaux, F. R., and Thevelein, J. M. (2006). The *Saccharomyces cerevisiae EHT1* and *EEB1* genes encode novel enzymes with medium-chain fatty acid ethyl ester synthesis and hydrolysis capacity. *The Journal of Biological Chemistry*, 281(7):4446–4456.

Sarode, N., Davis, S. E., Tams, R. N., and Reynolds, T. B. (2014). The Wsc1p cell wall signaling protein controls biofilm (mat) formation independently of Flo11p in *Saccharomyces cerevisiae*. *G3: Genes, Genomes, Genetics*, 4(2):199–207.

Sarode, N., Miracle, B., Peng, X., Ryan, O., and Reynolds, T. B. (2011). Vacuolar protein sorting genes regulate mat formation in *Saccharomyces cerevisiae* by Flo11p-dependent and -independent mechanisms. *Eukaryotic Cell*, 10(11):1516–1526.

Sato, T., Watanabe, T., Mikami, T., and Matsumoto, T. (2004). Farnesol, a morphogenetic autoregulatory substance in the dimorphic fungus *Candida albicans*, inhibits hyphae growth through suppression of a mitogen-activated protein kinase cascade. *Biological and Pharmaceutical Bulletin*, 27(5):751–752.

Saveanu, C., Bienvenu, D., Namane, A., Gleizes, P.-E., Gas, N., Jacquier, A., and Fromont-Racine, M. (2001). Nog2p, a putative GTPase associated with pre-60S subunits and required for late 60S maturation steps. *The EMBO Journal*, 20(22):6475–6484.

Schimz, K.-L. (1980). The effect of sulfite on the yeast *Saccharomyces cerevisiae*. *Archives of Microbiology*, 125(1–2):89–95.

Schimz, K.-L. and Holzer, H. (1979). Rapid decrease of ATP content in intact cells of *Saccharomyces cerevisiae* after incubation with low concentrations of sulfite. *Archives of Microbiology*, 121(3):225–229.

Schindelin, J., Arganda-Carreras, I., Frise, E., Kaynig, V., Longair, M., Pietzsch, T., Preibisch, S., Rueden, C., Saalfeld, S., Schmid, B., Tinevez, J.-Y., White, D. J., Hartenstein, V., Eliceiri, K., Tomancak, P., and Cardona, A. (2012). Fiji: an open-source platform for biological-image analysis. *Nature Methods*, 9(7):676–682.

Scholl, C. M., Morgan, S. C., Stone, M. L., Tantikachornkiat, M., Neuner, M., and Durall, D. M. (2016). Composition of *Saccharomyces cerevisiae* strains in spontaneous fermentations of Pinot Noir and Chardonnay. *Australian Journal of Grape and Wine Research*, 22(3):384–390.

Selvaraju, K., Gowsalya, R., Vijayakumar, R., and Nachiappan, V. (2016). *MGL2/YMR210w* encodes a monoacylglycerol lipase in *Saccharomyces cerevisiae*. *FEBS Letters*, 590(8):1174–1186.

Sengupta, N., Vinod, P. K., and Venkatesh, K. V. (2007). Crosstalk between cAMP-PKA and MAP kinase pathways is a key regulatory design necessary to regulate *FLO11* expression. *Biophysical Chemistry*, 125(1):59–71.

Shannon, P., Markiel, A., Ozier, O., Baliga, N. S., Wang, J. T., Ramage, D., Amin, N., Schwikowski, B., and Ideker, T. (2003). Cytoscape: a software environment for integrated models of biomolecular interaction networks. *Genome Research*, 13(11):2498–2504.

Shively, C. A., Eckwahl, M. J., Dobry, C. J., Mellacheruvu, D., Nesvizhskii, A., and Kumar, A. (2013). Genetic networks inducing invasive growth in *Saccharomyces cerevisiae* identified through systematic genome-wide overexpression. *Genetics*, 193(4):1297–1310.

Sidari, R., Caridi, A., and Howell, K. S. (2014). Wild *Saccharomyces cerevisiae* strains display biofilm-like morphology in contact with polyphenols from grapes and wine. *International Journal of Food Microbiology*, 189:146–152.

Simpson-Lavy, K. J., Sajman, J., Zenvirth, D., and Brandeis, M. (2009). APC/C^{Cdh1} specific degradation of Hsl1 and Clb2 is required for proper stress responses of *S. cerevisiae*. *Cell Cycle*, 8(18):3006–3012.

Singh, A. and Sherman, F. (1974). Characteristics and relationships of mercury-resistant mutants and methionine auxotrophs of yeast. *Journal of Bacteriology*, 118(3):911–918.

Sohn, H.-Y., Murray, D. B., and Kuriyama, H. (2000). Ultradian oscillation of *Saccharomyces cerevisiae* during aerobic continuous culture: hydrogen sulphide mediates population synchrony. *Yeast*, 16(13):1185–1190.

Štovíček, V., Váchová, L., Begany, M., Wilkinson, D., and Palková, Z. (2014). Global changes in gene expression associated with phenotypic switching of wild yeast. *BMC Genomics*, 15(1):1–16.

Štovíček, V., Váchová, L., Kuthan, M., and Palková, Z. (2010). General factors important for the formation of structured biofilm-like yeast colonies. *Fungal Genetics and Biology*, 47(12):1012–1022.

Sperandio, V., Torres, A. G., and Kaper, J. B. (2002). Quorum sensing *Escherichia coli* regulators B and C (QseBC): a novel two-component regulatory system involved in the regulation of flagella and motility by quorum sensing in *E. coli*. *Molecular Microbiology*, 43(3):809–821.

Stefanini, I., Dapporto, L., Legras, J.-L., Calabretta, A., Di Paola, M., De Filippo, C., Viola, R., Capretti, P., Polsinelli, M., Turillazzi, S., and Cavalieri, D. (2012). Role of social wasps in *Saccharomyces cerevisiae* ecology and evolution. *Proceedings of the National Academy of Sciences of the United States of America*, 109(33):13398–13403.

Supek, F., Bošnjak, M., Škunca, N., and Šmuc, T. (2011). REVIGO summarizes and visualizes long lists of gene ontology terms. *PLOS ONE*, 6(7):e21800.

Swiegers, J. H., Bartowsky, E. J., Henschke, P. A., and Pretorius, I. S. (2005). Yeast and bacterial modulation of wine aroma and flavour. *Australian Journal of Grape and Wine Research*, 11(2):139–173.

Swiegers, J. H. and Pretorius, I. S. (2005). Yeast Modulation of Wine Flavor. In Laskin, A., Bennett, J., and Gadd, G., editors, *Advances in Applied Microbiology*, pages 131–175. Elsevier, New York, USA, vol. 57 edition.

Tamas, M. J., Luyten, K., Sutherland, F. C. W., Hernandez, A., Albertyn, J., Valadi, H., Li, H., Prior, B. A., Kilian, S. G., Ramos, J., Gustafsson, L., Thevelein, J. M., and Hohmann, S. (1999). Fps1p controls the accumulation and release of the compatible solute glycerol in yeast osmoregulation. *Molecular Microbiology*, 31(4):1087–1104.

Taylor, S., Wakem, M., Dijkman, G., Alsarraj, M., and Nguyen, M. (2015). A practical approach to RT-qPCR - publishing data that conform to the MIQE Guidelines. Technical report, Bio-Rad Laboratories, Inc., Hercule, CA.

Teixeira, M. C., Monteiro, P. T., Guerreiro, J. F., Gonçalves, J. P., Mira, N. P., dos Santos, S. C., Cabrito, T. R., Palma, M., Costa, C., Francisco, A. P., Madeira, S. C., Oliveira, A. L., Freitas, A. T., and Sá-Correia, I. (2014). The YEASTRACT database: an upgraded information system for the analysis of gene and genomic transcription regulation in *Saccharomyces cerevisiae*. *Nucleic Acids Research*, 42(Database issue):D161–D166.

Teste, M.-A., Duquenne, M., François, J. M., and Parrou, J.-L. (2009). Validation of reference genes for quantitative expression analysis by real-time RT-PCR in *Saccharomyces cerevisiae*. *BMC Molecular Biology*, 10:99.

Thévenaz, P. and Unser, M. (2007). User-friendly semiautomated assembly of accurate image mosaics in microscopy. *Microscopy Research and Technique*, 70(2):135–146.

Thomas, D. and Surdin-Kerjan, Y. (1997). Metabolism of sulfur amino acids in *Saccharomyces cerevisiae*. *Microbiology and Molecular Biology Reviews*, 61(4):503–532.

Thurston, P. A., Quain, D. E., and Tubb, R. S. (1982). Lipid metabolism and the regulation of volatile ester synthesis in *Saccharomyces cerevisiae*. *Journal of the Institute of Brewing*, 88(2):90–94.

Trapnell, C., Pachter, L., and Salzberg, S. L. (2009). TopHat: discovering splice junctions with RNA-Seq. *Bioinformatics*, 25(9):1105–1111.

Váchová, L., Štoví, V., Hlaváček, O., Chernyavskiy, O., Štěpánek, L., Kubínová, L., and Palková, Z. (2011). Flo11p, drug efflux pumps, and the extracellular matrix cooperate to form biofilm yeast colonies. *Journal of Cell Biology*, 194(5):679–687.

Valero, E., Cambon, B., Schuller, D., Casal, M., and Dequin, S. (2007). Biodiversity of *Saccharomyces* yeast strains from grape berries of wine-producing areas using starter commercial yeasts. *FEMS Yeast Research*, 7(2):317–329.

Valero, E., Schuller, D., Cambon, B., Casal, M., and Dequin, S. (2005). Dissemination and survival of commercial wine yeast in the vineyard: A large-scale, three-years study. *FEMS Yeast Research*, 5(10):959–969.

Van der Westhuizen, T. J., Augustyn, O. P. H., and Pretorius, I. S. (2000). Geographical distribution of indigenous *Saccharomyces cerevisiae* strains isolated from vineyards in the coastal regions of the Western Cape in South Africa. *South African Journal of Enology and Viticulture*, 21(1):3–9.

Van Mulders, S. E., Christianen, E., Saerens, S. M. G., Daenen, L., Verbelen, P. J., Willaert, R., Verstrepen, K. J., and Delvaux, F. R. (2009). Phenotypic diversity of Flo protein family-mediated adhesion in *Saccharomyces cerevisiae*. *FEMS Yeast Research*, 9(2):178–190.

Vandesompele, J., De Preter, K., Pattyn, F., Poppe, B., Van Roy, N., De Paepe, A., and Speleman, F. (2002). Accurate normalization of real-time quantitative RT-PCR

data by geometric averaging of multiple internal control genes. *Genome Biology*, 3(7):research0034.1–research0034.11.

Verstrepen, K. J., Derdelinckx, G., Verachtert, H., and Delvaux, F. R. (2003). Yeast flocculation: what brewers should know. *Applied Microbiology and Biotechnology*, 61(3):197–205.

Vyas, V. K., Kuchin, S., Berkey, C. D., and Carlson, M. (2003). Snf1 kinases with different β-subunit isoforms play distinct roles in regulating haploid invasive growth. *Molecular and Cellular Biology*, 23(4):1341–1348.

Wach, A., Brachat, A., Pöhlmann, R., and Philippsen, P. (1994). New heterologous modules for classical or PCR-based gene disruptions in *Saccharomyces cerevisiae*. *Yeast*, 10(13):1793–1808.

Walker, M., Gardner, J., Vystavelova, A., McBryde, C., Lopes, M., and Jiranek, V. (2003). Application of the reuseable, *KanMX* selectable marker to industrial yeast: construction and evaluation of heterothallic wine strains of *Saccharomyces cerevisiae*, possessing minimal foreign dna sequences. *FEMS Yeast Research*, 4(3):339–347.

Wang, X. D., Bohlscheid, J. C., and Edwards, C. G. (2003). Fermentative activity and production of volatile compounds by *Saccharomyces* grown in synthetic grape juice media deficient in assimilable nitrogen and/or pantothenic acid. *Journal of Applied Microbiology*, 94(3):349–359.

White, H. E., Orlova, E. V., Chen, S., Wang, L., Ignatiou, A., Gowen, B., Stromer, T., Franzmann, T. M., Haslbeck, M., Buchner, J., and Saibil, H. R. (2006). Multiple distinct assemblies reveal conformational flexibility in the small heat shock protein Hsp26. *Structure*, 14(7):1197–1204.

Wiame, J.-M., Grenson, M., and Ars, H. N. (1985). Nitrogen catabolite repression in yeasts and filamentous fungi. *Advances in Microbial Physiology*, 26:1–88.

Winzeler, E. A., Shoemaker, D. D., Astromoff, A., Liang, H., Anderson, K., Andre, B., Bangham, R., Benito, R., Boeke, J. D., Bussey, H., Chu, A. M., Connelly, C., Davis, K., Dietrich, F., Dow, S. W., El Bakkoury, M., Foury, F., Friend, S. H., Gentalen, E., Giaever, G., Hegemann, J. H., Jones, T., Laub, M., Liao, H., Liebundguth, N., Lockhart, D. J., Lucau-Danila, A., Lussier, M., M'Rabet, N., Menard, P., Mittmann, M., Pai, C., Rebischung, C., Revuelta, J. L., Riles, L., Roberts, C. J., Ross-MacDonald, P., Scherens, B., Snyder, M., Sookhai-Mahadeo, S., Storms, R. K., Véronneau, S., Voet, M., Volckaert, G., Ward, T. R., Wysocki, R., Yen, G. S., Yu, K., Zimmermann, K., Philippsen, P., Johnston, M., and Davis, R. W. (1999). Functional characterization of the *S. cerevisiae* genome by gene deletion and parallel analysis. *Science*, 285(5429):901–906.

Wuster, A. and Babu, M. M. (2010). Transcriptional control of the quorum sensing response in yeast. *Molecular BioSystems*, 6(1):134–141.

Youk, H. and Lim, W. A. (2014). Secreting and sensing the same molecule allows cells to achieve versatile social behaviors. *Science*, 343(6171):1242782.

Young, M. D., Wakefield, M. J., Smyth, G. K., and Oshlack, A. (2010). Gene ontology analysis for RNA-seq: accounting for selection bias. *Genome Biology*, 11(2):R14.

Zara, G., Zara, S., Pinna, C., Marceddu, S., and Budroni, M. (2009). *FLO11* gene length and transcriptional level affect biofilm-forming ability of wild flor strains of *Saccharomyces cerevisiae*. *Microbiology*, 155(12):3838–3846.

Zara, S., Bakalinsky, A. T., Zara, G., Pirino, G., Demontis, M. A., and Budroni, M. (2005). *FLO11*-based model for air-liquid interfacial biofilm formation by *Saccharomyces cerevisiae*. *Applied and Environmental Microbiology*, 71(6):2934–2939.

Zotenko, E., Mestre, J., O'Leary, D. P., and Przytycka, T. M. (2008). Why do hubs in the yeast protein interaction network tend to be essential: reexamining the connection between the network topology and essentiality. *PLOS Computational Biology*, 4(8):e1000140.

Zupan, J. and Raspor, P. (2010). Invasive growth of *Saccharomyces cerevisiae* depends on environmental triggers: a quantitative model. *Yeast*, 27(4):217–228.